3-17-1989

Pixel-by-pixel reduction of atmospheric haze effects in multispectral digital imagery of water

John W. Francis

PIXEL-BY-PIXEL REDUCTION OF ATMOSPHERIC HAZE EFFECTS IN MULTISPECTRAL DIGITAL IMAGERY OF WATER

by

John Francis

A thesis submitted in partial fulfillment
of the requirements for the degree of
Master of Science
at the
Center For Imaging Science
of the
Rochester Institute of Technology

March 17, 1989

Signature of the Author John Francis
Center for Imaging Science

Accepted By P. Mounuli 4-19-89
Coordinator, M. S. Degree Program

College of Graphic Arts and Photography
Rochester Institute of Technology
Rochester, New York

CERTIFICATE OF APPROVAL

M. S. DEGREE THESIS

The M. S. Thesis of John W. Francis
has been examined and approved
by the thesis committee
as satisfactory for the thesis requirement
of the
Master of Science degree

Dr. John R. Schott, Thesis Advisor

Dr Willem Brouwer

Mr. Carl Salvaggio

3/17/89
Date

THESIS RELEASE FORM

Rochester Institute of Technology
College of Graphic Arts and Photography

Title of Thesis: **Pixel-By-Pixel Reduction of Atmospheric Haze Effects in Multispectral Digital Imagery of Water**

I, John W. Francis, hereby grant permission to the Wallace Memorial Library of R. I. T. to reproduce this thesis in whole or part. Any reproduction will not be for commercial use or profit.

Date 3/17/89

Pixel-By-Pixel Reduction of
Atmospheric Haze Effects in Multispectral
Digital Imagery of Water

By

John W. Francis

Submitted to the
Center For Imaging Science
in partial fulfillment of the requirements
for the Master of Science degree
at the Rochester Institute of Technology

ABSTRACT

A study is described in which the effects of the atmosphere on a remotely sensed, multispectral image of water are reduced in a spatially varying manner. The near zero IR reflectance of a water body is used to compute the atmospheric path transmittance and atmospheric path radiance on a pixel-by-pixel basis for a LANDSAT-5 Thematic Mapper image of Lake Ontario. TM Band 4 (0.76-0.90μm) image radiance measures are used to define the atmospheric path radiance. Radiosonde data and the LOWTRAN 6 atmospheric model are used to compute the equivalent atmospheric effects for the spectral regions corresponding to the visible wavelength Thematic Mapper image bands on a pixel specific basis. The pixel-by-pixel correction technique is shown to provide a useful reduction of atmospheric effects and to significantly reduce the uncertainty in the image derived measurement of water reflectance.

Acknowledgements

The author wishes to thank the many people who provided input and support for this work. In particular the author is thankful for the patience of his parents, John and Marjorie, who never really understood why this thesis work had to take so long to complete. Gratitude is also due to the author's advisor, Dr. John R. Schott, who also couldn't understand why this thesis took so long, for his helpfulness and advice throughout the author's academic career. Thanks also to the other members of the thesis committee, Dr. Willem Brouwer and Mr. Carl Salvaggio for their direction and review of this work.

Special thanks are due to the following people: Ms. Carolyn Kitchen, Mr. Steve Schultz, Mr. Tim Gallagher, Mr. Rolando Raqueno, Mr. Bernie Brower, Ms. Marcia Murray and Ms. Pam Schott. Each provided a myriad of assistance to the author during the course of this work and their efforts are very sincerely appreciated.

Dedication

This work is dedicated to the author's parents, John and Marjorie Francis, who's hopes and support made it possible.

Table Of Contents

List of Figures ix

List of Tables. xii

1.0 Introduction and Overview 1

1.1 History of Earth Surface Remote Sensing 3

1.2 Remote Sensing of Water Resources 8

1.2.1 Spectral Characteristics of Water 15

1.3 The Atmosphere - Composition and Radiative Transfer 18

1.3.1 The Equation of Radiative Transfer 20

1.4 Modeling Atmospheric Radiative Transfer 28

1.5 Atmospheric Radiation Propagation Model: LOWTRAN 6 36

1.6 The LANDSAT Satellite Series and the Thematic Mapper 40

1.6.1 The Thematic Mapper Imaging System 42

1.6.2 Processing LANDSAT TM Data 46

2.0 Experimental 48

2.1 Image Selection 48

2.1.1 Image Data Reformatting 57

2.1.2 Ancillary Scene Data Acquisition 60

2.2 LANDSAT-5 TM Image Water Region Segmentation 60

2.3 Modeling of Atmospheric Effects 75

2.3.1 Simplification of the Equation of Radiative Transfer 75

2.3.2 Preparation of the LOWTRAN 6 Atmospheric Model 77

2.3.2.1 Software Development and Modification 77

2.3.2.2 Atmospheric Model Control Point 79

2.3.3 Theory of Spatially Varying Haze Phenomena 82

2.3.4 Creation of the Atmospheric Correction Look-Up Tables 87

2.3.5 Utility of the TM Band 4 Image For Determining Atmospheric Upwelling Radiance 89

2.4 Image Processing For Pixel-By-Pixel Atmospheric Haze Reduction 92

3.0 Results 96

3.1 Verification of the Utility of the TM Band 4 Image for Determining Atmospheric Upwelling Radiance 96

3.2 Examination of the Corrected Image Data 99

3.2.1 Comparison of Atmospheric Corrections Using Several Values of the Henyey-Greenstein Asymmetry Parameter 101

3.2.2 Application of the Pixel-By-Pixel Atmospheric Correction Technique to a Second Image 117

3.3 Quantitative Algorithm Performance Analysis 122

3.3.1 Comparison of Surface Measurements of Visibility to LOWTRAN 6 Derived Values of Meteorological Range 124

3.3.2 Examination of Computed Water Reflectance 125

3.3.3 Reduction of Water Body Reflectance Estimate Error Using the Pixel-By-Pixel Atmospheric Correction Technique 131

4.0 Conclusions and Recommendations 135

5.0 References 137

6.0 Appendices 142

6.1 Appendix A - Example LOWTRAN 6 Run 143

6.2 Appendix B - Spectral Response of the LANDSAT-4 TM and LANDSAT-5 TM Reflected Energy Sensors 158

6.3 Appendix C - LANDSAT TM Tape Reading and Format Programs 161

6.4 Appendix D - LANDSAT TM Ancillary Scene Data Acquisition Program 170

6.5 Appendix E - Image Thresholding and Masking Programs 175

6.6 Appendix F - Atmospheric Modeling Programs 184

6.7 Appendix G - Atmospheric Correction Programs 216

List of Figures

Figure 1.2.1-1	Transmittance Through 10 m of Water	16
Figure 1.2.1-2	Reflectance of Clear and Turbid Water	17
Figure 1.2.1-3	Spectral Reflectance of Ocean Water With High and Low Chlorophyll-a Concentration	17
Figure 1.3.1-1	Earth-Sun-Sensor Coordinate System	25
Figure 1.6-1	Layout of LANDSAT Thematic Mapper	44
Figure 1.6-2	Thematic Mapper Optical System	45
Figure 1.6-3	Format of 1600 BPI TM Image CCT	47
Figure 2.1-1	True Color Image of 22 June 1984 Lake Ontario Scene	49
Figure 2.1-2	TM Band 1 Image of the 22 June 1984 Lake Ontario Scene	50
Figure 2.1-3	TM Band 2 Image of the 22 June 1984 Lake Ontario Scene	50
Figure 2.1-4	TM Band 3 Image of the 22 June 1984 Lake Ontario Scene	51
Figure 2.1-5	TM Band 4 Image of the 22 June 1984 Lake Ontario Scene	51
Figure 2.1-6	TM Band 5 Image of the 22 June 1984 Lake Ontario Scene	52
Figure 2.1-7	TM Band 6 Image of the 22 June 1984 Lake Ontario Scene	52
Figure 2.1-8	TM Band 7 Image of the 22 June 1984 Lake Ontario Scene	53
Figure 2.1-9	True Color Image of 25 May 1985 Lake Ontario Scene	54
Figure 2.1-10	TM Band 1 Image of the 25 May 1985 Lake Ontario Scene	55
Figure 2.1-11	TM Band 2 Image of the 25 May 1985 Lake Ontario Scene	55
Figure 2.1-12	TM Band 3 Image of the 25 May 1985 Lake Ontario Scene	56
Figure 2.1-13	TM Band 4 Image of the 25 May 1985 Lake Ontario Scene	56
Figure 2.1.1-1	Construction of a Full Image From Two Image Quadrants	58
Figure 2.2-1	Water Region Mask Creation	65
Figure 2.2-2	TM Band 1 Water Radiance Histogram (22 June 1984 Image)	66
Figure 2.2-3	TM Band 2 Water Radiance Histogram (22 June 1984 Image)	67
Figure 2.2-4	TM Band 3 Water Radiance Histogram (22 June 1984 Image)	68
Figure 2.2-5	TM Band 4 Water Radiance Histogram (22 June 1984 Image)	69
Figure 2.2-6	TM Band 5 Water Radiance Histogram (22 June 1984 Image)	70

Figure 2.2-7	TM Band 1 Water Radiance Histogram (25 May 1985 Image)	71
Figure 2.2-8	TM Band 2 Water Radiance Histogram (25 May 1985 Image)	72
Figure 2.2-9	TM Band 3 Water Radiance Histogram (25 May 1985 Image)	73
Figure 2.2-10	TM Band 4 Water Radiance Histogram (25 May 1985 Image)	74
Figure 2.3.3-1	LOWTRAN 6 and Henyey-Greenstein Aerosol Scattering Phase Functions	86
Figure 2.3.4-1	Creation of the Atmospheric Correction Look-Up Tables	88
Figure 2.4-1	Flow Chart for Program CORRECT_ATMOS	93
Figure 3.1-1	22 June 1984 TM Band 4 Water Pseudoreflectance Histogram	97
Figure 3.1-2	22 June 1984 TM Band 5 Water Pseudoreflectance Histogram	98
Figure 3.2.1-1	TM Band 1 Corrected Water Image Using 0.10 for the Henyey-Greenstein Asymmetry Parameter (22 June 1984)	107
Figure 3.2.1-2	TM Band 2 Corrected Water Image Using 0.10 for the Henyey-Greenstein Asymmetry Parameter (22 June 1984)	108
Figure 3.2.1-3	TM Band 3 Corrected Water Image Using 0.10 for the Henyey-Greenstein Asymmetry Parameter (22 June 1984)	109
Figure 3.2.1-4	TM Band 1 Corrected Water Image Using 0.15 for the Henyey-Greenstein Asymmetry Parameter (22 June 1984)	110
Figure 3.2.1-5	TM Band 2 Corrected Water Image Using 0.15 for the Henyey-Greenstein Asymmetry Parameter (22 June 1984)	111
Figure 3.2.1-6	TM Band 3 Corrected Water Image Using 0.15 for the Henyey-Greenstein Asymmetry Parameter (22 June 1984)	112
Figure 3.2.1-7	TM Band 1 Corrected Water Image Using 0.20 for the Henyey-Greenstein Asymmetry Parameter (22 June 1984)	113
Figure 3.2.1-8	TM Band 2 Corrected Water Image Using 0.20 for the Henyey-Greenstein Asymmetry Parameter (22 June 1984)	114
Figure 3.2.1-9	TM Band 3 Corrected Water Image Using 0.20 for the Henyey-Greenstein Asymmetry Parameter (22 June 1984)	115
Figure 3.2.2-1	TM Band 1 of the 25 May 1985 Lake Ontario Scene Processed Using a Henyey-Greenstein Asymmetry Parameter of 0.15	119
Figure 3.2.2-2	TM Band 2 of the 25 May 1985 Lake Ontario Scene Processed Using a Henyey-Greenstein Asymmetry Parameter of 0.15	120
Figure 3.2.2-3	TM Band 3 of the 25 May 1985 Lake Ontario Scene Processed Using a Henyey-Greenstein Asymmetry Parameter of 0.15	121
Figure 3.3-1	Map of Surface Weather Monitoring Station Locations	123
Figure 3.3.2-1	TM Band 1 Corrected Water Reflectance Histogram Using 0.15 for the Henyey-Greenstein Asymmetry Parameter (22 June 1984)	127

Figure 3.3.2-2 TM Band 2 Corrected Water Reflectance Histogram Using 0.15 for the Henyey-Greenstein Asymmetry Parameter (22 June 1984) 128

Figure 3.3.2-3 TM Band 3 Corrected Water Reflectance Histogram Using 0.15 for the Henyey-Greenstein Asymmetry Parameter (22 June 1984) 129

Figure 3.3.2-4 Lake Ontario Spectral Signature 130

List of Tables

Table 2.1.2-1	Imaging Geometry and Acquisition Data	61
Table 2.1.2-2	Spectral Band Calibration Data	62
Table 2.3.2.2-1	Radiosonde Data for the 22 June 1984 Scene	80
Table 2.3.2.2-2	Radiosonde Data for the 25 May 1985 Scene	81
Table 2.3.5-1	LOWTRAN Sun and Sky Illumination to Compute TM Band 4 and TM Band 5 Water Pseudoreflectance	91
Table 3.2.1-1	Atmospheric Correction Look-Up Table Using Henyey-Greenstein Asymmetry Parameter of 0.10	103
Table 3.2.1-2	Atmospheric Correction Look-Up Table Using Henyey-Greenstein Asymmetry Parameter of 0.15	104
Table 3.2.1-3	Atmospheric Correction Look-Up Table Using Henyey-Greenstein Asymmetry Parameter of 0.20	105
Table 3.3-1	LOWTRAN 6 Meteorological Range Data, Surface Visibility and TM Band 4 Water Image Count Values	124
Table 3.3.2-1	LOWTRAN Sun and Sky Illumination to Compute Corrected Water Reflectance	126

1.0 Introduction and Overview

The synoptic view of the Earth provided by modern satellite imaging systems provides a great deal of Earth resource information. Quantitative use of this resource information requires, however, that the atmospheric effects on such imagery be accurately compensated. Unfortunately, to date there are no atmospheric correction methods available that are able to compensate for the spatial variability of atmospheric effects on wide-expanse satellite imagery. A new technique is presented here that may be able to compensate for the spatially variable effects of the atmosphere on remotely sensed multispectral imagery of water.

Water reflects minimal radiation in the near-IR spectral region. Any radiance observed in a near-IR image of water can be considered to be due solely to the atmosphere and, as such, is a direct measurement of the atmospheric upwelling path radiance in that spectral band.

A model estimate of the same atmospheric upwelling path radiance can be made using the LOWTRAN 6 atmospheric model. By suitable adjustment of the LOWTRAN 6 input parameters, to reflect the prevailing atmospheric conditions, a match can be made between the atmospheric upwelling path radiance modeled by LOWTRAN 6 and that observed in the near-IR image data. Once a match has been made, the LOWTRAN 6 input parameters effectively describe the state of the atmosphere at that point in the image. These same inputs can then be used to determine the atmospheric effects for any other spectral band.

The LANDSAT Thematic Mapper (TM) imagery consists of seven registered multispectral image bands. Using each pixel of its near-IR image (TM Band 4) to estimate a value of the atmospheric upwelling path radiance at a water location, along

with matched model output from LOWTRAN 6, allows a pixel-by-pixel atmospheric correction to be performed on the TM visible spectral band images (Bands 1, 2 and 3).

It is hoped that successful use of such a technique could provide an increase in the utility of wide-expanse imagery of water bodies for water quality monitoring.

1.1 History of Earth Surface Remote Sensing

The most common and useful method of obtaining remote sensing data is by observation of the Earth's surface from within or outside the earth's atmosphere. Aerial remote sensing was born in 1858 when a French photographer, Gaspard Felix Tournachon, more commonly known as "Nadar", assembled his cumbersome photographic apparatus in a hot-air balloon and produced the world's first aerial photograph.[1] The view of Paris provided by the 80 meter high platform of Nadar's balloon sparked an immediate interest in balloon photography, and the technique flourished for the remainder of the 19th century.[2] About 1882, as an extension of their use for obtaining meteorological data, kites were used to obtain aerial photography. The most famous example of kite photography was produced on April 18, 1906 by G.R. Lawrence.[3] On that day he hoisted a gigantic camera, capable of producing 1.4 x 2.4m negatives, to an altitude of 600 meters using a kite, and photographed the aftermath of the great San Francisco earthquake. Even carrier pigeons were seriously considered for use in obtaining aerial photographs at the beginning of the 20th century.[4]

Because obtaining airphoto's from pigeons, balloons, and kites is risky, and produces uncertain results, systematic regular exploitation of aerial photographs had to wait for the development of the airplane. The first airplane to be used as a camera platform was piloted, appropriately enough, by Wilbur Wright. On April 24, 1909 a motion picture photographer accompanied Wright on a flight over Centocelli, Italy.[5,6] From that time, the combination of airplane and camera produced the new technology of airphoto interpretation, the first step toward modern remote sensing. The first, and perhaps the most straightforward, application of the new technology of airphoto interpretation was to the field of cartography. As early as 1913 the utility of

airphotos for producing maps was described.[7] The use of airphotos for cartography was at first laborious and time consuming. During the 1920's, however, several optical devices were developed to aid the cartographers.[8] The Zeiss Stereoplanigraph of 1923 greatly increased the use of airphotos for cartography. By the 1950's, with the development of orthophotos and the orthoscope, the use of airphotos for cartography and updating had become routine.

Although the military intelligence value of aerial photographs was at first slow to be realized, much of the technology of airphoto interpretation came as an outgrowth of military development. Late in the course of World War I British intelligence agents monitored enemy movements in German held areas using airphotos made by British pilots using hand held cameras.[9,10] The intelligence information exploited from the airphotos assisted in the eventual defeat of the German army, and firmly established airphoto reconnissance as a military tool. After World War I the military need for aerial photography waned, but during the late thirties the Germans, ironically, made extensive use of airphotos for military intelligence use. From the beginning of World War II in September of 1939 to May 1940, the German forces produced an extensive set of airphotos of the Western Front.[11] Their photographs of military installations and transportation facilities accounted for much of the success of the German Western offensive in the spring of 1940.

As the use of aerial photography for reconnissance became widespread, counter-measures were developed. Items of military sensitivity were covered with materials painted to look like vegetation, thus making those items undetectable in airphotos. Such countermeasures led to counter-counter measures and in 1942 the Eastman Kodak Co. developed "Camouflage Detection" false-color infrared sensitive film.[12,13,14] By coloring red any ground features having a high IR reflectance, as live

vegetation does, photointerpreters could easily detect items painted to look like vegetation. Because of the extreme usefulness of the "Camouflage Detection" Film in resource analysis, the development of false-color infrared sensitive film marks a milestone in the development of aerial remote sensing and earth resource monitoring technology.

During the between-war years of the 1920's and 1930's and the post World War II years many scientific and commercial uses for airphotos were found. During the 1930's the U.S. Forestry Service monitored much of the country's timber reserve using airphotos. The U.S. Geological Survey began using airphotos for producing topographical maps, and the Tennessee Valley Authority used airphotos for resource planning purposes.[15] By the 1960's numerous works had been published on how airphoto interpretation could be applied to the earth sciences.[16]

The use of aerial photography for earth resource monitoring took a large step forward with the development of quantitative radiometric measurement made from photographs. Colwell (1965)[17] did early work on measurement of vegetation stress and disease using measurements made with false-color infrared film. Numerous works have since been published on quantitative radiometry done using aerial photographs and the correlation to earth resource metrics.

Sensor technology developments enabled the development of solid state imagers. In 1954 the USAF Strategic Air Command sponsored a program to develop a long-wave and microwave Side Looking Airborne Radar (SLAR) imaging system.[18] By the late 1950's synthetic aperture SLAR imaging had been developed.[19]

The ultimate synoptic view of the earth, that from space, was achieved in 1960 with the launch of the TIROS I meteorological satellite. The infrared television imaging package aboard this satellite provided the first systematic observation of

earth from an orbital platform.[20] The utility of orbital earth photography was demonstrated by 70mm photographs made from an unmanned MA-4 Mercury spacecraft. The photographs enabled mapping of several thousand square miles of the Sahara Desert.[21] Development of an earth imaging system in permanent orbit for earth surface observation took a great step forward with the S065 Multispectral Terrain Photography experiment, carried out in 1969 aboard Apollo 9. This experiment proved the feasibility and value of multispectral imaging of the earth's surface for resource studies.[22] The results of the S065 experiment led directly to the development of the first Earth Resources Technology Satellite (ERTS-1). ERTS-1 was launched on July 23, 1972, the first orbital imaging system designed specifically to collect earth surface resource data.[23] The ERTS-1 satellite carried three acquisition systems, (1) a multispectral return-beam vidicon (RBV) television system imaging in the blue-green, green-yellow, and red-infrared spectral bands,[24] designated bands 1, 2, and 3, (2) a Multispectral Scanning System (MSS) operating in the 0.5-0.6μm, 0.6-0.7μm, 0.7-0.8μm and 0.8-1.1μm spectral regions and designated band 4, 5, 6, and 7, and (3) an environmental data collection system that relayed ground-based data to ground receiving stations.[25,26,27] As of January 1975 the ERTS satellite program was renamed the LANDSAT program.[25]

A second LANDSAT satellite (LANDSAT-2) was launched on January 22, 1975, and LANDSAT-3 was launched on March 5, 1978.[25,26] LANDSAT 1, 2, and 3 all carried similar sensing packages with the exception of a fifth, thermal-infrared, channel carried on the MSS aboard LANDSAT-3.[27]

The data from the LANDSAT Multispectral Scanner Systems has probably been studied more thoroughly and by more investigators than any other aircraft or space imaging system. A natural outgrowth of such intense study is the identification of system limitations. The most obvious limitation of the MSS is the 80-meter ground

projected instantaneous field of view (IFOV), limiting the spatial resolution of the imagery. A more subtle system limitation is that the spectral channels do not coincide well with specific earth surface absorption bands. A new sensor package, the Thematic Mapper (TM), was designed to alleviate these problems.[28]

The first TM sensor package was flown aboard the LANDSAT-4 satellite launched on December 14, 1981.[29] The ground projected IFOV of the TM sensor was reduced to 30 meters. This increase in spatial resolution lead to more accurate values for the radiance from agricultural areas.[30] The number of spectral channels on the TM sensor was increased to 7 over the 4 channels of the MSS, and the spectral passbands filtered to better coincide with specific earth surface spectral features (See Section 1.6). The TM sensor package also provided improved radiometric quantization and interband pixel registration.[31]

SPOT, a French space program similar to LANDSAT, launched its own earth resources satellite on Feb 22, 1986 from Kourou, French Guianna using an Ariane-1 rocket.[32] The SPOT system can image in a panchromatic mode, from 0.51-0.73μm, with a 10-meter ground projected IFOV, and in a multispectral mode with a 20-meter ground projected IFOV. The multispectral mode consists of a green channel (0.5-0.59μm), a red channel (0.61-0.68μm), and a near-infrared channel (0.79-0.89μm).[33] In addition to having improved spatial resolution over TM, the SPOT system is also capable of pointing up to 26 degrees from nadir.[34] This permits increased frequency of ground feature coverage, and the capability to acquire stereo images.

1.2 Remote Sensing of Water Resources

Water is undoubtably one of the earth's most important resources. The use of water by mankind encompasses just about all aspects of daily life. Common uses of water resources include, but are, of course, not limited to: drinking, irrigation for food production, industrial manufacturing, power generation and recreation. Water is also an abundant earth resource, comprising some 70% of the earth's surface. The bulk of the earth's water, about 97%, is found in the oceans. Of the remaining 3%, most is frozen at the poles. Only about 1/2 of 1% of the earth's water supply is available to the rivers, lakes, streams, ponds and reservoirs of the world. The coastal and inland waters upon which mankind daily depend are not as plentiful as one may at first think. It is not surprising, therefore, that much attention is being placed on monitoring and improving the quality of the world's water resources.[35]

The social and economic benefits of a systematic monitoring of water quality are obvious. As world population increases, the stress on available water resources will also increase, and water quality preservation will become ever more important. The techniques of modern remote sensing, particularly satellite-based remote sensing, are particularly well suited to the water quality monitoring problem. The synoptic and multi-temporal nature of satellite imagery make it ideal for use in an operational water quality monitoring system.

To date, remote sensing technology has been applied to water resource monitoring, in one of three distinct ways:[36]

1) Qualitative observations from airborne or spaceborne imagery are used as a guide for making *in-situ* measurements or to interpolate between *in-situ* observations.

2) Remote imagery has been used to define and delineate bodies of water.

3) Quantitative estimation of the hydrological parameters, of a water body are made directly from remotely sensed imagery.

Item 3 above holds the greatest potential for the use of remote sensing data for water quality monitoring and it is the aim of the research described here to aid in obtaining useful quantitative remotely sensed data.

Use of remotely sensed imagery for analysis of water quality is, of course, limited to monitoring those quality parameters that alter the optical properties of the water surface. Although this may at first seem to be a severe restriction on the utility of remote sensing techniques, much work has been done to show that several important water quality parameters do indeed manifest themselves as changes in the optical properties of the water body under study.[37] Items such as: concentration of suspended solids, dissolved organics, and chlorophyll-a concentration are important measures of water quality and do change the optical properties of the water body in which they are suspended in a predictable manner.[37,38] It should be noted that some water quality parameters of interest such as dissolved gas concentration (eg. oxygen, nitrogen, CO_2), dissolved inorganics (eg. sodium chloride), and acidity do not directly produce predictable changes in the spectral characteristics of a water body and can not be directly measured from remotely sensed imagery.[39]

The early use of airborne or spaceborne imagery for water quality monitoring consisted almost entirely of supplementing ground-based measurements. This is still true to a large extent today. Johnson (1980)[40] presented an early review of the capabilities of measurement of water quality using remotely sensed imagery. Johnson's data indicated that ground-based measurements of chlorophyll-a concentration (a primary indicator of water quality) correlate well with Coastal Zone Color Scanner and LANDSAT MSS radiance measurements.[41] He concluded that "...remote sensing measurements provide critical complementary information to

conventional oceanographic measurements..."[42] Later work by Johnson utilized multiple regression techniques to develop quantitative equations to predict chlorophyll-a and suspended solids concentration from airborne imagery data. He discussed the necessity of having both aircraft and shipboard measurements in order to produce quantitative maps, since temporal atmospheric changes preclude the use of regression equations developed for one set of imagery on imagery obtained at a later date. Lillisand *et al* (1983)[44] studied the utility of using LANDSAT data to enable the State of Minnesota to comply with Section 314(a) of the Clean Water Act of 1977. Section 314(a) mandated that each state identify and classify all public freshwater lakes within its borders according to trophic condition. Lillisand and co-workers obtained lake surface measurements concurrent with two LANDSAT overpasses. Although the work showed great utility in assessing lake trophic state, the authors realized that implementation of their approach on a statewide basis would require either tremendous amounts of lake-surface measurements or some means of normalizing temporal atmospheric changes.[45]

Work similar to that of Johnson and Lillisand *et al* was performed by Carpenter and Carpenter (1983).[46] Like Johnson, they used multiple linear regression techniques to predict turbidity and algal pigment concentration from LANDSAT MSS data. The prediction equations were developed using concurrently obtained lake-surface measurements. Although no explicit atmospheric compensation was used, Carpenter and Carpenter attempted to make their prediction equations date-independent by pooling both lake surface and satellite data for several dates, accounting for sun angle differences and developing new global predictor equations.[47] Their results forced them to conclude that their predictions were of limited usefulness when trying to predict the turbidity and algal pigment

concentration of a water body not included in the development of the predictor equations.

The limitations of using regression analysis techniques for remote sensing of water quality parameters was investigated by Whitlock *et al* (1982)[48] Although several recommendations are made by the authors with regard to ground truth collection and statistical rigor, their treatment of the problem is still scene specific because the time-varying atmospheric component had not been considered.

Piech and Schott (1975)[49] enumerated several of the most important reasons for accurate compensation of atmospheric effects in airborne and satellite imagery of water bodies. They state:

1) Bodies of water are usually the darkest objects in a scene, having reflectances of the order of a few percent. Small changes in atmospheric effects could thus be interpreted as significant changes in lake reflectance.

2) Minor variations in the reflectance of a lake (of the order of 0.5 to 1%) can correspond to important physical changes in the lake.

3) A large lake or lake system extends over a broad geographic area within which atmospheric conditions may fluctuate.

4) Accurate measurement of seasonal variations in eutrophication indices are important for limnological analyses.

5) Effects of weather variations on lake parameters are crucial for limnological studies. As a result, aerial surveys cannot wait for ideal weather conditions.

Their investigations utilized a technique developed by Piech and Walker (1974)[50] called the "Scene Color Standard". The technique involves microdensitometry of color film shadow areas to provide an estimate of the ambient atmospheric transmittance and path scattering. Using this technique they were able to illustrate excellent agreement between aircraft obtained measurements of lake reflectance

ratios and similar lake reflectance ratios obtained during a Skylab overpass for several different weather conditions. They also showed good correlation between aircraft derived lake reflectance ratios and surface measurements of several biological parameters.

Other workers have also realized the important influence of the atmosphere on remotely sensed water body radiances, and several other compensation techniques have been developed. Munday (1983)[52] developed what he called a "Chromaticity Analysis" technique to normalize the effects of atmospheric haze in imagery of water made at different times. He used ratio-normalized MSS radiance values, similar to color mixtures on a chromaticity diagram. By moving MSS ratios toward a "standard locus" in a chromaticity diagram, Munday claims to substantially correct for the effect of atmospheric aerosols in imagery of water. Lindall *et al* (1986)[53] extended Munday's technique by including the effects of the sun zenith and azimuth angles on the imagery. Their goal was to minimize the amount of field data required for calibration of imagery by producing a "universal calibration curve" relating measured MSS chromaticity to suspended solids concentration. Although the technique showed moderate success, its use required the assumption of spatially constant atmospheric effects.

Scarpace *et al* (1979)[54] developed a technique for compensation of atmospheric effects similar in nature to that of Piech and Walker. They noticed a systematic change in LANDSAT radiance measured over water for imagery from several dates and attributed that change to differences in atmospheric haze for the several dates. Their technique utilized a simple linear atmospheric radiative transfer model, and used clear lake water as a standard reflector. By assuming that the clear lake water reflects no radiation, (an excellent assumption for the near-IR wavelength bands) an estimate of atmospheric path radiance can be made. No direct estimate of

atmospheric path transmittance could be made using this technique. A normalization factor is defined between the imagery taken on the clearest day and all others. Using no measured ground truth, and lake imagery from several dates, corrected as above, they were able to produce very good predictions of lake trophic state for several Wisconsin lakes. No attempt was made, however, to account for any within-scene atmospheric spatial variations.

Gordon (1978)[55] also made use of imagery of clear lake water within the scene to calibrate for atmospheric effects. He assumes an atmosphere composed of a spectrally selective Rayleigh scattering and spectrally independent aerosol scattering. The component of radiance from a water body image due solely to the atmosphere is computed from knowledge of wavelength, and the aerosol component is calculated by finding the IR radiance from the water body image and subtracting its Rayleigh scattering component. Simulated atmospheric data showed that a significant improvement in water body reflectance determination is possible using this technique. Gordon *et al* (1980)[56] applied this atmospheric calibration technique to CZCS imagery of the Gulf of Mexico. Comparison of CZCS imagery with and without the calibration showed enhancement of eddy-like turbidity patterns that were very difficult to detect on the uncalibrated image. Comparisons of phytoplankton pigment concentration derived from the image to concurrent surface measurements showed only marginal agreement however. Phytoplankton pigment concentration could only be measured to within 0.5 log-concentration units (log [mg/m^3]) using the calibration technique.

Verdin (1985)[57] also recognized the need for atmospheric correction of satellite imagery to be used for water quality studies. By combining a within-scene reflectance standard technique, similar to that of Gordon's, with measurements made by Ahern *et al* (1977)[58], and using an atmospheric radiation propagation model

similar to that developed by Scarpace *et al*, Verdin has provided the most complete treatment of the problem to date. Verdin uses oligotrophic lakes from within the scene as standard reflectors. The lake surface radiance is calculated based on the data of Ahern *et al*. This calculated lake surface radiance, along with the lake surface radiance as measured from a LANDSAT MSS image are input to an atmospheric propagation model created by Turner and Spenser. Additional input to the model is varied until a set of atmospheric parameters are computed that successfully relate the two input radiances based on a fundamental model of atmospheric radiation propagation. The derived atmospheric parameters are used to calibrate image radiance values of other water bodies for atmospheric effects. Use of this technique allowed Verdin to derive a single set of equations to predict chlorophyll-a concentration and secchi disk transparency for seven images taken over a seven year span. The same equations were used for predictions in imagery that had no corresponding surface measurements, thus allowing accurate monitoring of a large reservoir with a minimum of surface sampling. Of course, his use of selected lakes throughout the image to calibrate the image radiance of other lakes again required the assumption of spatially invariant atmospheric effects. The errors associated with such an assumption can not always be considered negligible.

Clearly the modern trend in remote monitoring of water quality is toward increased quantitative measurements using a decreasing surface sampling data set. Much work has been done to show that compensation of atmospheric effects in remote imagery of water has both increased the quality of the quantitative data and reduced the amount of *in situ* measurements required. As this technology advances it will become increasingly important to compensate for the spatial and temporal variations in the atmospheric effects on remote imagery of water. To date, full advantage cannot be taken of the synoptic view of the earth provided by modern

remote sensing techniques. The technology to compensate for the spatial variability of the atmosphere is not very mature. The work presented here is an attempt to address just that issue.

1.2.1 Spectral Characteristics of Natural Waters[37]

As with most earth surface features, the spectral reflectance and transmittance characteristics of water varies with wavelength. This variation is caused not only by the energy interactions with the water molecules but also with any material that is suspended in the water. The spectral reflectance of a water body has been successfully correlated with the concentration of many types of dissolved and otherwise suspended materials.

Relatively clear water reflects little radiation in the near and middle-infrared wavelength bands. Even a very thin layer of water will absorb nearly all the incident radiation in these wavelength regions. This characteristic of water has been put to use for coastal mapping and water body delineation. Very small ponds have been observed on LANDSAT image data in these spectral bands. This characteristic allows bodies of water to be used as a standard reflector for atmospheric calibration for this research.

In the visible wavelength region the radiation/water interactions become more complex. Radiation reflected from a water body can come from the water itself, the bottom of the water body, the surface of the water, or from materials suspended in the water, generally, some combination of all of the above is observed. It has been noted that as the level of turbidity of a water body increases, the reflectance of the water body also increases, and the reflectance peak shifts to longer wavelengths. Radiance measured from imagery made in the 0.6μm to 0.7μm spectral

band has been correlated with turbidity measurements. Algae and chlorophyll concentration has been correlated with blue spectral region measured radiance changes. Figure 1.2.1-1 illustrates the range of spectral reflectance that can be expected from several types of natural water body types. The general decrease in spectral reflectance observed as one moves from from the short wavelength blue region to the longer wavelength red region is characteristic of the water itself. Materials suspended in the water tend to superimpose their spectral reflectance characteristics onto the spectral reflectance characteristics of the water, as illustrated in Figures 1.2.1-2 and 1.2.1-3. For many water quality indicators a change in level causes a quantitative change in the spectral reflectance of the water. It is this level to reflectance correspondence that allows quantitative determination of several water quality parameters from remotely sensed imagery of water.

Of course, as Figures 1.2.1-1, 1.2.1-2 and 1.2.1-3 show, these changes in reflectance are very subtle and require accurate, precise quantitative determination of any confounding effects such as the optical characteristics of the intervening atmosphere. Absolute quantitative determination of water quality using remotely sensed imagery is not possible without such accurate determination.

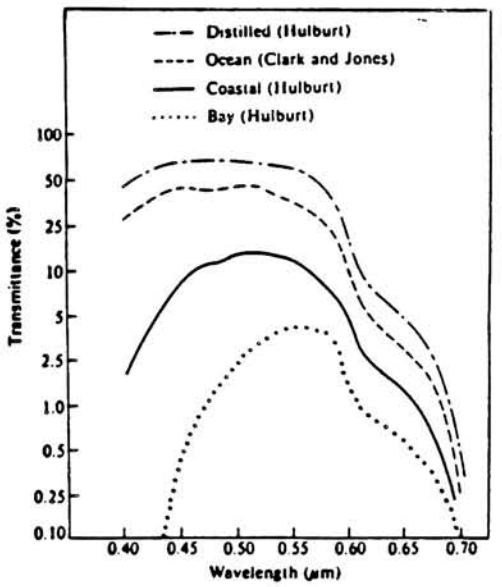

.2.1-1 Transmittance Through
ters Of Water (From Swain[37])

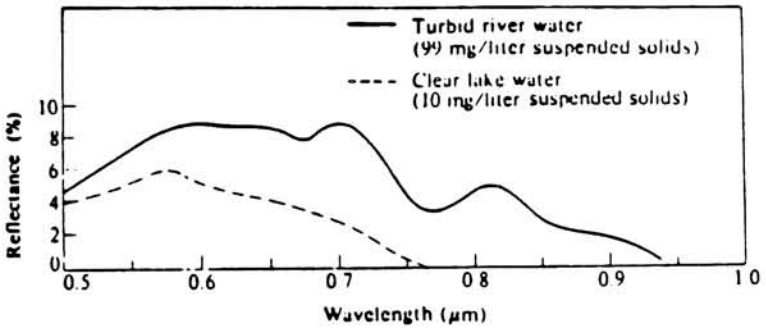

Figure 1.2.1-2 0.5μm-1.0μm
Reflectance Of Turbid And Clear Water (From Swain[37])

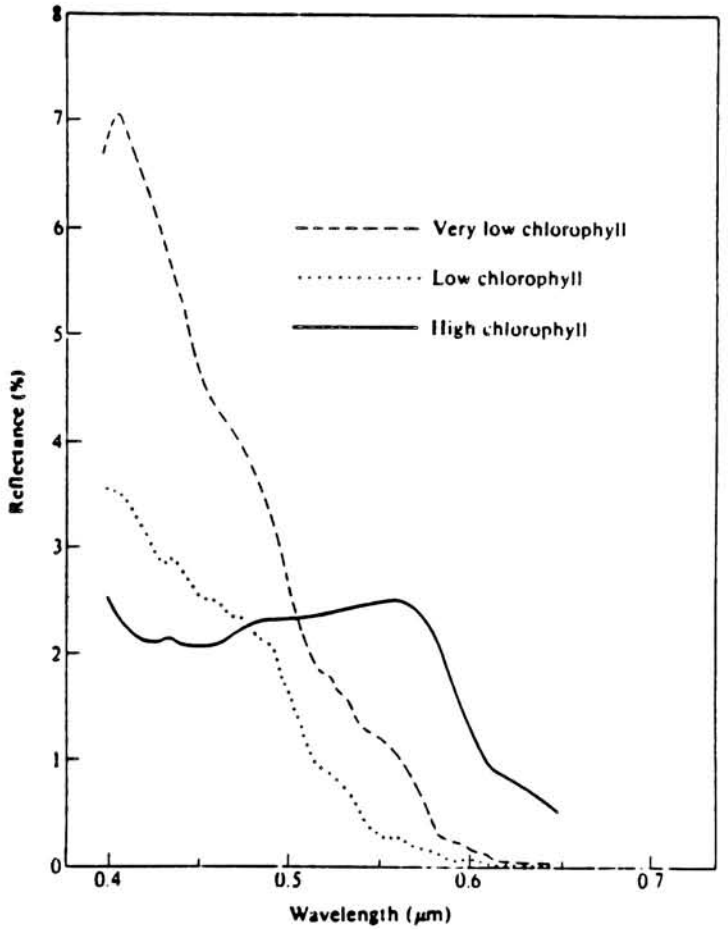

Figure 1.2.1-3 Spectral Reflectance Of Ocean Water
Having High And Low Chlorophtll-a Concentration (From Swain[37])

1.3 The Atmosphere - Composition and Radiative Transfer

Atmospheric air is a mixture of a myriad of substances in all physical states, the principal gases being nitrogen, oxygen, argon, carbon dioxide, and water vapor[59,60] Many other gasses have also been discovered in the earth's atmosphere, such as ozone, hydrogen, and helium, but the concentration of each is insignificant when compared to the principal gases. In addition, suspended particles of both solid and liquid matter are also present and together make up the aerosol content of the atmosphere. Typical of atmospheric aerosols are smoke and dust particles, and products of vapor condensation, originating from both natural and industrial processes.

If all of the water vapor and aerosols of the atmosphere could be removed, a gaseous atmosphere of nearly constant composition would remain. For this reason, many workers in meteorology regard the atmosphere as a mixture of dry air with water vapor and aerosols.

The composition of dry air in the lower atmosphere (<25 km) is more than 99% molecular nitrogen and oxygen. Argon and carbon dioxide compose less than one percent, and trace amounts of the remaining gasses make up what little fraction remains. Both molecular oxygen and nitrogen vary little in percentage with altitude or time. Slight variations in local carbon dioxide concentration have been detected. Carbon dioxide is delivered to the atmosphere by the respiration of animals, and by the combustion of organic compounds, and is used by vegetation for the photosynthesis process. The amount of atmospheric carbon dioxide is lower during the daytime than at night and greater in the winter than summer and spring, because the carbon dioxide requirements of vegetation decrease during these times[60]. A continuous increase in the average carbon dioxide content of the atmosphere has

occurred since 1900. It is probable that this increase is attributable to the tremendous expansion of industry during the 20th century[61].

Water vapor enters the atmosphere by evaporation from the earth's surface. Natural turbulence spreads the water vapor throughout the atmosphere. The maximum water vapor content of the atmosphere is limited. When the partial pressure of water vapor in the atmosphere reaches saturation pressure the water vapor will begin to precipitate back out. The water vapor content of the atmosphere has a significant impact on the processes of absorption, emission, and scattering of radiation. In general, the water vapor content of the atmosphere decreases exponentially with altitude and at altitudes much above 10 km the air is very dry.

Particulate matter in both the solid and liquid state are always present in the atmosphere. These aerosols, so named because the system is indeed a solution with atmospheric air as the solvent, vary greatly in composition and properties. Aerosols play a role in many atmospheric phenomena, including acting as condensation nuclei for cloud, fog and precipitation formation, and making the atmosphere an optically turbid medium. Sources of aerosols include, water in the liquid and solid form, organics such as plant pollen, smoke, volcanic dust, sea-salt particles, and by-products of industrial processes.

Although ozone comprises a very small amount of the earth's atmosphere it is very important to both biological and radiation transfer processes. Ozone is mostly present in a layer about 25 km above the surface[62]. Ozone is a strong absorber of solar radiation, particularly of those wavelengths shorter than 300 nm. The presence of this ozone layer prevents this biologically active energy from reaching the surface, effectively creating a lower limit on the solar spectrum. Because ozone is such an effective absorber of ultraviolet radiation, the temperature of the atmosphere is much

higher at those altitudes than would normally be expected. Formation of atmospheric ozone is thought to be an equilibrium process of photodissociation of oxygen molecules and collisions of excited oxygen atoms. The equilibrium is constantly disrupted, however, leading to a considerable variability of atmospheric ozone content.

1.3.1 The Equation of Radiative Transfer

Chandrasekhar (1960)[63] derived the equation that describes the change in radiance of a monochromatic radiant flux beam as it traverses a turbid medium. This equation is fundamental to atmospheric radiation transfer theory and forms the basis for all models describing the effects of the atmosphere on remotely sensed data.

Chandrasekhar defines a "pencil of radiation" as the amount of radiant energy, dQ , transported across an elemental area dA, in a direction confined to the solid angle $d\omega$, during a time dt.,

$$dQ_\lambda = L_\lambda cos(\theta) d\lambda dA d\omega dt \qquad (1.3.1\text{-}1)$$

where: L is the radiance of the radiation field.

If after traversing a distance ds of a turbid medium, the radiance becomes:

$$L_\lambda + dL_\lambda \qquad (1.3.1\text{-}2)$$

the change in radiance can be expressed as:

$$dL = -K_\lambda \rho L_\lambda ds \qquad (1.3.1\text{-}3)$$

where ρ is the density of the material comprising the medium and $K\rho$ defines the mass extinction coefficient for radiation attenuation of the pencil of radiation caused by both "true absorption" and "scattering" as defined by Van de Hulst (1957)[64]. True

absorption is defined as a permanent loss of radiant energy from the radiation field, scattering defines a loss of radiant energy from the pencil of radiation, that will reappear in the radiation field at some other direction. Therefore,

Extinction = scattering + absorption

Considering a scattering only atmosphere for a moment, a mass scattering coefficient, K' , can be defined such that energy is scattered from a particle having cross sectional area, dA' and height dh' at the rate:

$$dQ\lambda = K'\lambda\rho L\lambda cos(\theta)d\lambda dA d\omega dt dh \qquad (1.3.1\text{-}4)$$

in all directions. The mass of the scattering element can be expressed as:

$$dm = \rho cos(\theta)dA'dh' \qquad (1.3.1\text{-}5)$$

and is substituted into Equation 1.3.1-4 giving:

$$dQ\lambda = K'\lambda L\lambda dm d\lambda d\omega dt \qquad (1.3.1\text{-}6)$$

A function that describes the angular distribution of the scattered radiation can be introduced (called the scattering phase function):

$$dQ\lambda(\omega') = dQ\lambda(\omega)p(\phi)\frac{d\omega'}{4\pi} \qquad (1.3.1\text{-}7)$$

This expression describes the rate at which energy is being scattered by an elemental mass, dm, into the solid angle, $d\omega'$, at an angle ϕ from the solid angle $d\omega$ of the incident pencil of radiation.

For a scattering-only atmosphere, of course:

$$\frac{1}{4\pi}\int_0^{4\pi} p(\phi)d\omega' = 1 \qquad (1.3.1\text{-}8)$$

and for the general case of a true absorbing and scattering atmosphere:

$$\frac{1}{4\pi}\int_{0}^{4\pi} p(\phi)d\omega' = b_0 \leq 1 \qquad (1.3.1\text{-}9)$$

where b_0 represents the fraction of the pencil of radiation lost from scattering and $1\text{-}\ b_0$ represents that fraction having undergone true absorption.

Substitution of Equation 1.3.1-7 into Equation 1.3.1-6 gives:

$$dQ_\lambda(\omega') = K_\lambda L_\lambda(\omega)p(\phi)\frac{d\omega'}{4\pi}\, dm d\lambda d\omega dt \qquad (1.3.1\text{-}10)$$

illustrating the rate at which radiation from direction ω is scattered into the direction ω'. The explicit direction solid angles are included for clarity and the angle between ω and ω' is ϕ. The mass scattering extinction coefficient, $K'\rho_\lambda$, has been replaced by the total mass extinction coefficient, $K\rho_\lambda$, to include both scattering and absorption.

Radiation can also be added to the pencil of radiation by the material that comprises the medium. This added radiation originates as thermal self-emission and radiation scattered in from outside the pencil. For a medium in local thermodynamic equilibrium the thermal self-emission partial source term is defined as:

$$j_\lambda^T = \varepsilon B_\lambda(T) \qquad (1.3.1\text{-}11)$$

where $\varepsilon=(K\rho - K'\rho)$, the true absorption coefficient (also emissivity by Kirchkoff's Law) and $B_\lambda(T)$ is Planck's radiation equation.

For a scattering atmosphere, the scattered-in radiation partial source function is given by:

$$f_{\lambda}^{s} = \frac{1}{4\pi}\int_{0}^{4\pi} p(\phi)\, L(\omega)\, d\omega \qquad (1.3.1\text{-}12)$$

A net source function, $J\lambda(\omega)$, defines the total radiation added to the pencil due to both thermal self-emission and scattering-in:

$$J\lambda(\omega) = \frac{1}{4\pi}\int_{0}^{4\pi} p(\phi)\, L(\omega)\, d\omega + \varepsilon\, B\lambda(T) \qquad (1.3.1\text{-}13)$$

Of course, the net source function does not consider any losses caused by the material comprising the medium.

By counting up gains and losses, the net change in spectral radiance, $dL\lambda$, of a pencil of radiation as it traverses a distance, ds, in a truly absorbing, and scattering medium is given by the differential equation:

$$\frac{-dL\lambda}{K\lambda\,\rho ds} = L\lambda - J\lambda \qquad (1.3.1\text{-}14)$$

solving the differential equation gives:

$$L\lambda(s) = L\lambda(0)\; e^{-\tau\lambda'(s,0)} + \int_{0}^{s} J(0;s')K\lambda\rho e^{-\tau\lambda(s,s')}\, ds' \qquad (1.3.1\text{-}15)$$

where τ'_{λ} is the spectral extinction optical thickness of the medium between points s and s' and is given by:

$$\tau_{\lambda}'(s,s') = \int_{s'}^{s} K\lambda\rho\, ds \qquad (1.3.1\text{-}16)$$

For the case where s is at the top of the atmosphere and the line-of-sight path makes an angle θ with the normal to the surface of the earth, the path transmittance can be expressed as:

$$e^{-\tau'\lambda sec(\theta)} = e^{-\tau'\lambda(s,0)} \qquad (1.3.1\text{-}17)$$

where $\tau\lambda$ is the extinction optical depth of the entire atmosphere along the path normal to the earth's surface. Similarly, a path additive radiance term, $Lu\lambda(\theta)$, can be defined:

$$Lu\lambda(\theta) = \int_0^s J(0;s')K\lambda\rho e^{-\tau\lambda'(s,0)}\, ds' \qquad (1.3.1\text{-}18)$$

Substituting Equations 1.3.1-17 and 1.3.1-18 into Equation 1.3.1-15 gives a simplified equation of radiative transfer:

$$L\lambda(\theta) = L\lambda(0)e^{-\tau\lambda' sec(\theta)} + Lu\lambda(\theta) \qquad (1.3.1\text{-}19)$$

Schott and Henderson-Sellers (1984)[65] use the fixed-coordinate system of Figure 1.3.1-1 to derive an expression essentially identical to that of Equation 1.3.1-19. They derive the following equation to describe the propagation of ground radiance to a remote sensing satellite:

$$L\lambda(\theta,\theta',\phi) = L_r\lambda(\theta,\theta',\phi)e^{-\tau\lambda' sec(\theta)} + L_u\lambda(\theta,\theta',\phi) \qquad (1.3.1\text{-}20)$$

where: θ is the angle between the sensor and normal to the surface
θ' is the source elevation angle relative to the normal to the surface
ϕ is the azimuthal angle between the source and sensor projected onto the surface.

It is clear that Equation 1.3.1-20 is equal to Equation 1.3.1-19 when transformed by a coordinate system rotation. Equation 1.3.1-20 describes only the radiation transfer from a ground feature, through the atmosphere, to the remote sensing platform. They extend this model to a more complete description of radiative transfer by first including a solar illumination term:

$$E_{s\lambda} = E'_{s\lambda} cos(z)\ e^{-\tau_\lambda' sec(z)} \qquad (1.3.1\text{-}21)$$

where: $E'_{s\lambda}$ is the irradiance of the sun onto a plane at the top of the atmosphere, perpendicular to the direction of solar propagation

$E_{s\lambda}$ is the total solar irradiance onto the ground feature.

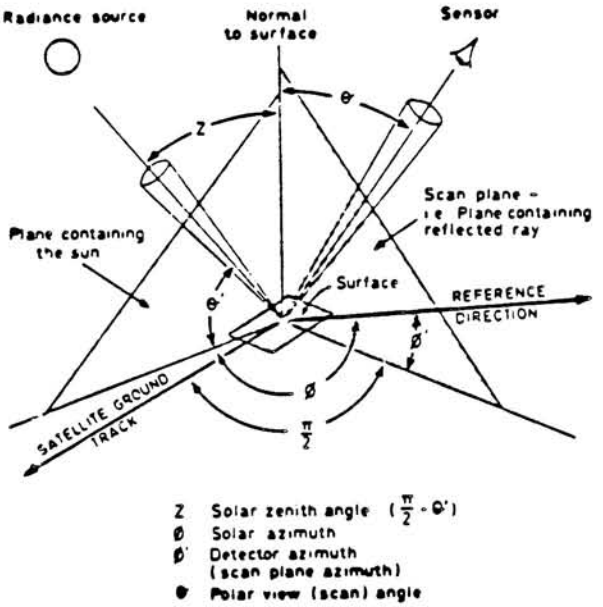

Figure 1.3.1-1

Earth-Sun-Sensor Coordinate System

A sky illumination term is also included in their model. This term is a function of the downwelling solar illumination that has been scattered by the atmosphere. Noting that:

$$dE_\lambda = dL_\lambda d\Omega\ cos(\theta)$$

the sky irradiance onto the ground feature can be written as:

$$E_{\lambda sky} = \int_0^{2\pi} L_{d\lambda}(\theta,\phi) cos(\theta)\ d\Omega \qquad (1.3.1\text{-}22)$$

substituting $d\Omega = sin(\theta)\ d\theta d\phi$

$$E_{\lambda sky} = \int_0^{2\pi} \int_0^{\frac{\pi}{2}} L_{d\lambda}(\theta,\phi)\cos(\theta)\sin(\theta)\, d\theta d\phi \qquad (1.3.1\text{-}23)$$

where: $L_{d\lambda}(\theta,\phi)$ is the radiance downwelled onto the ground feature from the direction (θ,ϕ) as defined above.

Of course, not all of the hemisphere above a ground feature is sky. The radiance onto a ground target from background features (buildings, hills, etc.) adds a component of its own and blocks skylight radiation from that direction. Often relative sky/background shape factors are incorporated into the above sky irradiance model to approximately account for background effects.[66]

The total irradiance onto a ground feature can be approximately expressed as:

$$E_{\lambda G} = E_{s\lambda} + E_{\lambda sky} \qquad (1.3.1\text{-}24)$$

The irradiance reflected from the ground target is:

$$E_{\lambda r}(\theta,\phi) = E_{\lambda G}\, r_{\lambda}(\theta,\phi,\theta',\phi') \qquad (1.3.1\text{-}25)$$

where $r_{\lambda}(\theta,\phi,\theta',\phi')$ is the bidirectional reflectance function for the ground feature. Assuming lambertian target characteristics gives:

$$E_{\lambda r}(\theta,\phi) = E_{\lambda G}\, r_{\lambda} \qquad (1.3.1\text{-}26)$$

The total reflected radiance of a lambertian ground feature is:

$$L_{r\lambda} = \frac{E_{\lambda r}}{\pi} \qquad (1.3.1\text{-}27)$$

A complete expression for the total radiance emitted from a lambertian ground feature must also include the thermal emission of energy from the feature. The thermal emitted radiance dominates the emission for wavelengths longer than about

5μm while the reflected radiance dominates at wavelengths shorter than 3μm. There is significant contribution from both at intermediate wavelengths. The thermal emission radiance, L_B, is a function of the temperature and emissivity of the ground feature and is described by Planck's radiation equation:[67]

$$L_{\lambda B} = \frac{2c^2 h \varepsilon_\lambda}{\lambda^5}\left[e^{\frac{ch}{\lambda k T}} - 1\right]^{-1} \qquad (1.3.1\text{-}28)$$

where:

c is the velocity of light (2.9979250 x 10^8 m/s)
h is the Planck constant (6.626196 x 10^{-34} J s)
T is the absolute temperature of the feature
k is the Boltzman constant (1.380622 x 10^{-23} J/K)
ε_λ is the spectral emissivity of the feature

Therefore, the total radiance emitted from a lambertian ground feature that is illuminated by the sun and sky is:

$$L_{\lambda T} = L_{r\lambda} + L_{\lambda B} \qquad (1.3.1\text{-}29)$$

or

$$L_{\lambda T} = \frac{r_\lambda}{\pi}\left[E'_{s\lambda}\cos(Z)\, e^{-\tau_\lambda' \sec(z)} + \int_0^{2\pi}\int_0^{\frac{\pi}{2}} L_{d\lambda}(\theta,\phi)\cos(\theta)\sin(\theta)\, d\theta\, d\phi \right] + L_{\lambda B} \qquad (1.3.1\text{-}30)$$

Substituting the above into the previous expression gives a total description of the radiative transfer process from sun to ground to remote sensing platform:

$$L_{\lambda(\theta,\theta',\phi)} = \frac{r_{\lambda(\theta,\theta',\phi)}}{\pi}\left[E'_{s\lambda}\cos(Z)\, e^{-\tau_\lambda' \sec(z)} + \int_0^{2\pi}\int_0^{\frac{\pi}{2}} L_{d\lambda}(\theta,\phi)\cos(\theta)\sin(\theta)\, d\theta\, d\phi \right] e^{-\tau_\lambda' \sec(\theta)} + L_{\lambda B}\, e^{-\tau_\lambda' \sec(\theta)} + L_{u\lambda(\theta,\theta',\phi)} \qquad (1.3.1\text{-}31)$$

Most often it is the ground feature reflectance term, that must be determined from the measured radiance data. The other terms in Equation 1.3.1-31 are usually determined from the measurement geometry and by using a model of the atmospheric optical effects based on ambient meteorological conditions.

For satellite imaging of water, the assumption of lambertian water volume reflectance is commonly used but the assumption of lambertian surface reflectance is rarely valid. The air-water interface will cause portions of the solar and sky radiance to be specularly reflected from the surface. The reflectance of the water surface can be computed from Fresnel's equation:

$$r_{spec} = \frac{1}{2}\left\{\frac{sin^2\left[\left(\frac{\pi}{2}-\theta'\right)-\theta''\right]}{sin^2\left[\left(\frac{\pi}{2}-\theta'\right)+\theta''\right]} + \frac{tan^2\left[\left(\frac{\pi}{2}-\theta'\right)-\theta''\right]}{tan^2\left[\left(\frac{\pi}{2}-\theta'\right)+\theta''\right]}\right\} \qquad (1.3.1\text{-}32)$$

Where: θ' is the angle of incidence and

θ'' is the angle of refraction

Equation 1.3.1-31 should be modified to include the specular reflectance of sun irradiance by the surface of the water body when imaging a water surface.

1.4 Modeling Atmospheric Radiative Transfer

Several practical methods for estimating the influence of the atmosphere on remotely sensed data have been developed over the years. Most of these methods are based on the equations of radiative transfer detailed in the previous section. Other methods make use of the stocastic nature of atmospheric radiative transfer and utilize Monte Carlo methods of estimation. Any method of modeling atmospheric radiation transfer must, however, assume some structure for the atmospheric path to be

modeled, decide what atmospheric and meteorological parameters are necessary, and how electromagnetic radiation is affected by those parameters.

Modern models of atmospheric radiation propagation through a vertically inhomogeneous atmosphere usually utilize approximations to the solutions of the equations of radiative transfer by separating the optical effects into several simpler problems. The turbid atmosphere is often divided into an absorption/emission only portion and a scattering only portion.[68,69] The scattering portion of the model is often further divided into separate molecular (or Rayleigh) scattering and aerosol scattering.[70]

LaRocca and Turner[69] have compiled and summarized the details of several atmospheric radiation propagation models. They have classified the models into those that primarily model atmospheric absorption (usually IR wavelength bands) and those that primarily model scattering (usually visible wavelength bands). Of course, all models must account for both mechanisms to some degree. The models are generally optimized for the dominant optical mechanism of the wavelength band for which they were designed.

Models of atmospheric absorption can be divided into two general methods of numerical solution, the so-called line-by-line models and the band models. For the line-by-line models, the absorption line spectra for all the molecules making up the atmospheric path are integrated over the wavelength band of interest. This requires a very large database of molecular absorption parameters, and a very long computation time. Some improvement in computation speed for the line model of Drayson and of Kunde and MaGuire[71] was achieved by using variable width integration techniques. A finer wavelength spacing is used at areas of strong absorption giving increased computation speed without loss of accuracy. Although line models are by

far the most accurate means of calculating atmospheric absorption, they suffer from limitations in addition to long computational times. No line model developed to date is able to accurately model absorption in the water vapor continuum spectral region.[71] Here, the line models must employ the same empirical models that are used by the band models. A much more limiting problem with the line models is their general lack of availability in computer code form. As such, the line models are only used for those remote sensing applications that require very high accuracy estimates of atmospheric transmittance. [78]

The most well known line-by-line atmospheric transmittance model is the FASCOD computer program developed by the Air Force Geophysics Laboratory (AFGL). This program and model contain the most complete set of line data available. The half-width of the absorption lines stored in the FASCOD database are on the order of 1.0nm.[89]

Most remote sensing applications do not require such high accuracy and the band models of atmospheric absorption become attractive alternatives to the cumbersome line models. Most band models use simple functions that approximate the position and strength of molecular absorption lines.[72]

Elsasser[71] developed a model of atmospheric absorption in a wavelength band by allowing a single molecular absorption band to repeat itself periodically throughout the band. A statistical model of absorption within a band has been developed as an extension of the Elsasser model. This model lets the strength of several molecular absorption lines vary according to some underlying statistical distribution. A further extension is the Random Elsasser model where the strength of the absorption lines varies randomly throughout the band and the line position is modeled as a random superposition of the several absorption lines. A quasi-random model has been

proposed by King (1954) and by Wyatt *et al* (1962).[73] This model is said to produce more realistic models of CO_2 and H_2O absorption because the line distribution and strength need not be strictly random or periodic. They divide the wavelength band into several sub-intervals. Models similar to those described above are then used within each sub-interval and the absorption of the band is computed as the average of the sub-interval results.

The band models listed above also suffer from general lack of availability in computer code form, so for practical calculation of atmospheric path absorption or transmittance there exists only two methods generally available. Researchers at the Environmental Research Institute of Michigan (ERIM) have developed what they call the "Aggregate Method"[74,75] and the AFGL has developed the "LOWTRAN" method.[76,77] The Aggregate Method uses a variety of models based on the band models described above. The specific model to be used depends on the wavelength band being modeled and the specific atmospheric constituent for which the absorption is being computed. In all, the Aggregate Method model uses 13 separate models of atmospheric absorption. Although the Aggregate Method model is complex it is not as cumbersome as the line models and offers improved accuracy over any of the above models used alone when a wide spectral band is being modeled. A considerable decrease in complexity can be had, with little loss of accuracy, by using the LOWTRAN method.[78] The simplicity of the LOWTRAN model, along with its ease of use and widespread availability, has made LOWTRAN the most popular atmospheric absorption model.

Unlike any of the models presented thus far, the LOWTRAN method is essentially an empirical model (See Section 1.5). A set of spectral parameters relate the amount of absorber material in the atmospheric path, at standard temperature and pressure (STP), to measured values of atmospheric absorption.[79,80] A profile of

the meteorological conditions along the atmospheric path is used to define the STP amounts of the LOWTRAN absorbers (H_2O, CO_2, O_3,N_2O, CO, CH_4, O_2, HNO_3, and N_2). The absorption due to each absorber is then used to calculate the spectral transmittance of the atmospheric band. Because of its popularity, the LOWTRAN model has been the subject of much study. The model has gone through five major revisions since its inception. The most recent version, LOWTRAN 6, has the ability to compute atmospheric transmittance and path radiance from scattering and emission for any band within the 0.2μm to 25μm spectral region.[81] Because the LOWTRAN 6 model requires input data that is readily available and outputs the desired atmospheric parameters, the LOWTRAN 6 computer program was chosen as the atmospheric model for the research described here (See Appendix A).

Similar to absorption models, models for scattering of radiation by the atmosphere can be divided into exact solution of theoretical equations and approximate solutions of those equations. Very often, practical models treat atmospheric scattering as separate molecular and aerosol scattering mechanisms.

The so-called "exact" solutions for atmospheric scattering are exact only in the sense that closed-form equations have been derived to describe the scattering phenomena. The closed-form solutions are based on assumptions about the state of the atmosphere. One is always uncertain, of course, about the true state of the atmosphere as a result of only being able to measure a finite number of parameters to define that state. As a result, even the "exact" solutions to the scattering equations offer only an approximate solution to the real problem.

Chandrasekhar (1960)[82,83] pioneered the work in exact scattering equations by deriving a set of non-linear equations which could be solved to determine the entire radiation field for a plane-parallel atmosphere illuminated by solar radiation.

Others have refined the equations of Chandrasekhar but the mathematical complexity of the solutions make such exact solutions computationally impractical for real atmospheres.

Several workers have proposed approximations to the exact solutions that are much less complex, although still quite complicated in their own right.[84] One technique involves expanding the scattering phase functions in Legendre polynomials, reducing the radiative transfer equation to an eigenvalue problem. Another procedure discretizes the angular variable of the scattering phase functions, replacing the integration with a summation. Van de Hulst (1957)[64] proposed a simple doubling technique, whereby the atmosphere is layered, each layer having twice the optical thickness of the preceding layer. Computation using this technique is rapid but it cannot be used for vertically inhomogeneous atmospheres. Monte Carlo methods have been used to model scattering on a particle-by-particle basis. A probabilistic description of scattering is developed for the atmosphere to be modeled. Random "radiation particles" are then monitored as they randomly encounter the modeled atmospheric constituents. The Monte Carlo methods have been used to model very complex scattering scenarios but they often require unexceptably long computation time.

Many remote sensing applications do not require a complete scattering calculation. Often the scattered radiation is dominated by radiation that has been scattered only once. Calculation of such single-scattered radiation is relatively simple and straightforward. Assuming plane parallel radiation and a horizontally homogeneous atmosphere, the equations of radiative transfer for single scattering are:

$$L(\tau',-\mu,\phi) = \frac{\omega_0}{4\pi} \int_0^{\tau'} e^{\left[\frac{-\tau' - \tau''}{\mu}\right]} p(\theta) E_\lambda(0,-\mu_0,\phi_0)\, e^{\left[\frac{-\tau''}{\mu}\right]} \frac{d\tau}{\mu} \qquad (1.4\text{-}1)$$

$$L(\tau',+\mu,\phi) = \frac{\omega_0}{4\pi} \int_{\tau'}^{\tau'(0)} e^{\left[\frac{-\tau' - \tau''}{\mu}\right]} p(\theta) E_\lambda(0,+\mu_0,\phi_0)\, e^{\left[\frac{-\tau''}{\mu}\right]} \frac{d\tau'}{\mu} \qquad (1.4\text{-}2)$$

where the top integral describes the solar to scattering point atmospheric path and the bottom integral describes the scattering point to observer path, and

μ = cos(θ)
θ = Zenith Angle
ω_0 = Single Scattering Albedo
ϕ = Azimuth Angle
$E_\lambda(0,-\mu_0,\phi_0)$ = Solar Spectral Irradiance at the top of the Atmosphere from direction (μ_0,ϕ_0)
τ' = Optical Depth of the Atmosphere From Ground To Observer
$p(\theta)$ = Scattering Phase Function
τ'' = Optical Depth of the Total Atmosphere

For a purely molecular atmosphere, $p(\theta)$ is given by the Rayleigh scattering phase function:

$$p(\theta) = \frac{3}{4}\left[1+\cos^2(\theta)\right] \qquad (1.4\text{-}3)$$

For a turbid atmosphere, if the relative amounts of molecular and aerosol scattering are constant, the total scattering phase function can be approximated as the sum of Rayleigh and aerosol contributions:

$$p(\theta) = \frac{\tau_a(0)}{\tau(0)} p_a(\theta) + \frac{\tau_m(0)}{\tau(0)} p_m(\theta) \qquad (1.4\text{-}4)$$

where:

$\tau_a(0)$ = total atmospheric optical depth due to aerosols
$\tau_m(0)$ = total atmospheric optical depth due to molecules
$\tau(0)$ = total atmospheric optical depth
$p_a(\theta)$ = aerosol scattering phase function
$p_m(\theta)$ = molecular scattering phase function

The LOWTRAN 6 atmospheric model includes the single-scattering model of Ridgway *et al*[86] that is very similar to the development presented above.

The research described here requires a method of estimation of the transmittance and line-of-sight path radiance for real atmospheres affected by both Rayleigh and aerosol scattering. The assumption of single scattering to make the modeling tractable should not significantly impact the modeling accuracy since the most useful remotely sensed imagery of water is made on very clear days when little multiple scattering occurs.

The LOWTRAN 6 model itself has been used by many workers in the remote sensing field for some time and has a proven track record for accurately modeling the spectral transmittance and path radiance for a well-characterized atmosphere. Since the LOWTRAN 6 model includes a model for the scattering effects of interest, is assumed to be accurate enough for the research presented here, and is readily available, it is the atmospheric radiation propagation model chosen for this research.

1.5 Atmospheric Radiation Propagation Model: LOWTRAN 6[75,77,81]

Because of the numerical complexity of practical models of radiative transfer and the large database of atmospheric data required to compute atmospheric transmittance and radiance over a wavelength region of interest, very few practical computer codes for computation of atmospheric transmittance and radiance are generally available. Of the few around, the most well known are the LOWTRAN series of atmospheric modelling computer programs. The most up to date version of the code, LOWTRAN 6, as well as its predecessors (LOWTRAN 5, LOWTRAN 4, LOWTRAN 3B, LOWTRAN 3, and LOWTRAN 2) are band models of atmospheric transmittance based on an empirical fit to measured data. Refinements have been made to each of the LOWTRAN models, and the current version, LOWTRAN 6, includes in its model of atmospheric radiation propagation: atmospheric refractive index effects, earth curvature effects, and atmospheric single scattering for both molecular and aerosol scatterers.

The total atmospheric transmittance at a given wavelength is computed as the product of the average transmittance due to molecular band absorption, molecular scattering out of the line-of-sight, and total aerosol extinction. As shown below, each of the above transmittance components is based on a single parameter empirical fit to measured data.

The molecular band absorption model is used to compute the average transmittance from each of the four LOWTRAN atmospheric molecular absorption constituents: water vapor, ozone, nitric acid, and the uniformly mixed gasses (CO_2, N_2O, CH_4, CO, O_2, N_2). The empirical model used is:

$$\tau_{m\lambda} = f\left(C_\lambda k \left[\frac{P(z)}{P(0)} \sqrt{\frac{T(0)}{T(z)}} \right]^n ds \right) \qquad (1.5\text{-}1)$$

where:

$\tau_{m\lambda}$	=atmospheric transmittance due to molecular specie M
C_λ	= LOWTRAN wavelength dependant absorption coefficient
k	= concentration of the absorber species
$P(z)$	= atmospheric pressure at altitude z
$T(z)$	= atmospheric temperature at altitude z
ds	= the length of the atmospheric path
$P(0)$	= 1 atm (Standard Pressure)
$T(0)$	= 273 K (Standard Temperature)

The form of the function and the parameter n are empirically determined for each of the LOWTRAN atmospheric molecular constituents.

Atmospheric transmittance loss caused by molecular scattering out of the line-of-sight is based on Rayleigh scattering theory. The expression used in LOWTRAN 6 is based on a least-squares fit to computed molecular scattering coefficients:

$$\tau_{ms_\lambda} = 1 - \left\{ \frac{\nu^4}{k_1 + k_2 \nu^2} \right\} \qquad (1.5\text{-}2)$$

where:

ν = wavenumber (2π/wavelength) and

$k1$ and $k2$ = least-squares fit coefficients

The least-square coefficients are computed for each molecular absorption component based on its number density as determined from the input atmospheric profile.

The transmittance due to total aerosol extinction is given by:

$$\tau_a = e\left[-EXTV(\nu)hds\right] \qquad (1.5\text{-}3)$$

where:

EXTV(ν)	= normalized extinction coefficient for wavenumber ν of appropriate aerosol model (see below)
h	= LOWTRAN aerosol scaling factor
ds	= length of atmospheric path

To assist in describing the variation of aerosol concentration and composition with altitude, LOWTRAN 6 has divided the atmosphere into four aerosol modelling regions:

1) Boundary Region 0-2KM
2) Upper Troposphere 2-10KM
3) Lower Stratosphere 10-30KM
4) Upper Stratosphere 30-100KM

Additionally, the aerosol composition of the boundary layer is further refined by the choice of one of three aerosol models:

1) Urban aerosol composition
2) Rural aerosol composition
3) Maritime aerosol composition

Versions of LOWTRAN previous to LOWTRAN 6 have treated atmospheric scattering only as a loss mechanism. LOWTRAN 6 includes a single scattering model of atmospheric path radiance. The single scattering function includes only solar or lunar extraterrestrial sources. The single scattering model is:

$$I^{\nu}_{scat} = I^{\nu}_{sun} \int \tau^{(a+m)}_{(e,ps+op)} \left[P^{a}_{\nu} \frac{d\tau^{(a)}_{(s,op)}}{\tau^{(a)}_{(s,op)}} + P^{m}_{\nu} \frac{d\tau^{(m)}_{(s,op)}}{\tau^{(m)}_{(s,op)}} \right] \qquad (1.5\text{-}4)$$

where:

I^{ν}_{sun}	= solar extraterrestrial intensity

$\tau^{(a+m)}_{(e,ps+op)}$ = total atmospheric transmittance along the solar path, ps, and line-of-sight path, op, combined

$\tau^{(a)}_{(s,op)}$ = transmittance due to aerosol scattering out of the line-of-sight path, op

$\tau^{(m)}_{(s,op)}$ = transmittance due to molecular scattering out of the line-of-sight path, op

P^{a}_{v} = aerosol scattering phase function

P^{m}_{v} = molecular scattering phase function

The single scattering model traces two atmospheric paths for each scattering point in the calculation. The extraterrestrial source intensity is first propagated along the source to scattering point path. The molecular and aerosol scattering phase functions determine what fraction of the radiation incident on the scattering point is scattered into the line-of-sight path. This scattered radiation is then propagated to the observer along the line-of-sight path. Because only single scattering is modeled, there is no computation of radiation scattered from the sky dome to the surface and reflected into the line-of-sight. This sky dome downwelling must be computed indirectly from the program.

The LOWTRAN 6 model includes a database of scattering phase functions for each of the LOWTRAN aerosol models. The phase functions were computed using the complex Mie theory for spherical particles. Of course, the spherical particle assumption is not valid for natural, dust-like aerosols, but there is as yet no general method for computing such phase functions for non-spherical particles.

The LOWTRAN 6 model requires as input the geometry of the imaging scenario, an altitude profile of the atmospheric temperature, pressure and water vapor content, and the spectral range of interest. Additionally, the model allows specification of the sun angle, atmospheric aerosol composition and selection of one

of two single scattering atmospheric phase function models. LOWTRAN 6 outputs the estimate of atmospheric spectral transmittance and line-of-sight path spectral radiance for the selected input imaging scenario.

Input to the LOWTRAN 6 model required by this research is found from the LANDSAT TM tape image header for the imaging geometry and sun angle data and from area airport radiosondes for the atmospheric profile data.

Appendix A contains an example of a LOWTRAN 6 calculation.

1.6 The LANDSAT Satellite Series and the Thematic Mapper[87]

The first of the LANDSAT series of satellites, ERTS-1, (later renamed LANDSAT-1) was launched in July of 1972. The satellite carried two multispectral imaging sensors, a Return-Beam Vidicon television system that operated in three spectral bandpasses, and a Multispectral Scanner System (MSS) that operated in four spectral bandpasses. Two more satellite systems, LANDSAT-2 and LANDSAT-3 carried very similar imaging system packages.

With the design of the LANDSAT-4 satellite, a new sensor package was included. This package, called the Thematic Mapper (TM), improved upon the MSS sensor in terms of its ground projected IFOV and choice of spectral bandpasses. Studies have shown that for vegetation vigor studies on developed agricultural fields, the 80-meter IFOV of the MSS system is only marginally adequate. Since vegetation studies are the driving force behind the LANDSAT satellite series, the TM sensor was designed with a smaller nominal ground projected IFOV of 30 meters on a side. The intent of the smaller IFOV is to provide better vegetation discrimination studies requiring less collateral data such as aircraft imagery.

The spectral bandpass channels of the TM were also selected for their utility in vegetation discrimination, but geological and hydrological applications were not ignored. The TM sensor has seven imaging bands vs. the four of the MSS. Each spectral channel of the TM sensor was selected to match some desirable ground feature spectral signature component as follows:

Band 1 0.45-0.52μm: This band corresponds approximately to the peak transmittance of clear, natural waters. The lower limit of 0.45μm was chosen to limit the effects of atmospheric scattering on the image data. The upper limit was chosen so as to be at the upper limit of the blue chlorophyll absorption region.

Band 2 0.52-0.60μm: This band corresponds to the green reflectance peak of healthy vegetation. The spectral region lies between the blue and red chlorophyll absorption bands. The ratio of the blue to green radiance returned from a water body has been correlated with the amount of dissolved organics within that water body.

Band 3 0.63-0.69μm: This band includes the red absorption band of chlorophyll. The upper limit was kept below 0.69μm because vegetation spectral signature crossovers in the 0.69-0.75μm spectral region can confuse spectral signature measurement. Soil boundary and geological boundary determinations can be done using this spectral band. Since atmospheric scattering is less a problem in this band than in the other two visible bands, ground features imaged in this band often have higher contrast giving the impression of an increase in image resolution.

Band 4 0.76-0.90μm: This near-IR band corresponds to the peak reflectance band of healthy vegetation. The combination of bands 4,3, and 2, colored as red, green, and blue, provides satellite imagery that is very similar in appearance to that provided by false-color IR photographic film. This band is even less prone to atmospheric degradation effects than band 3. Clear, natural waters have nearly zero reflectance in this wavelength band.

Band 5 1.55-1.75μm: Because of the very strong absorption by water in this wavelength band, vegetation reflectance is very dependant on vegetative moisture content. Water-land discrimination is easily performed with image data in this band as well as cloud, snow, and ice region delineation.

Band 6 10.4-12.5μm: This band is centered within the long-wave thermal IR wavelength band. The amount of radiant flux from ground features depends on the emissivity and temperature of the feature rather than on reflected solar flux. Data from this band can be used to create ground temperature maps and to locate ground thermal activity.

Band 7 2.08-2.35μm: The primary utility of this band is for geological mapping purposes. Maps of hydrothermally altered rocks can be made using imagery from this wavelength band.

1.6.1 The Thematic Mapper Imaging System:

The basic TM imaging system consists of a large, oscillating mirror in front of an optical system and several arrays of detectors. Both the forward motion of the satellite and the scanning action of the mirror are utilized to form each of the multispectral images. Figure 1.6-1 illustrates the layout of the TM imaging system.

The entire system is mounted in the satellite such that its length is perpendicular to the direction of flight. The electro-optical subsystem consists of a large scan mirror, a cassagrain type telescope consisting of a large, fixed, primary mirror, and a smaller, fixed, secondary mirror, a scan-line corrector system, and a relay optical system that is used to physically separate the detectors for TM Bands 5, 6, and 7 from the remaining detector arrays.

The elliptical scan mirror is made of beryllium, having axes measuring approximately 530 and 410 cm. The scan mirror sweeps in both the west-to-east and east-to-west directions during the nominal north-to-south flight of the satellite. Image data is taken during sweeps in each direction. A scan-line corrector, placed just after the telescope in the optical path, allows usable data to be taken from both scan directions.

The optical system telescope is an f/5.6 Ritchey-Chretien design having a diameter of 410 cm and a focal length of 2.28 meters. The scanning action of the scan mirror assures that off-nadir points in the scene are imaged near the optical axis of the telescope, where the image quality is highest. A motor-driven, two-mirror, scan-line corrector produces scans that are perpendicular to the satellite flight direction. The corrector displaces the line-of-sight by the length of the detector array at the end of each scan. The scan-line corrector moves the scan-line in the aft direction during scanning to compensate for the forward motion of the satellite. Figure 1.6-2 illustrates the TM optical system

A set of relay optics images the focal plane, where the detectors for TM Bands 1, 2, 3, and 4 are located, on an area cooled to 95K where the detectors for TM Bands 5, 6, and 7 are located. The relay optics are fixed and serve only to separate the cooled from the non-cooled detectors.

The detectors for TM Bands 1 through 4 are arranged as four sets of staggered linear arrays, each containing 16 silicon-photodiode detectors. The detectors are staggered to reduce adjacent element crosstalk and to facilitate electronic connections. TM Bands 5 and 7 each contain a 16 element staggered array of indium antimonide detectors. The thermal infrared channel, TM Band 6, has a four element staggered linear array of mercury cadmium telluride detectors. These detectors are each four times as large on a side as the detectors for the other bands, giving a factor of four decrease in the ground projected IFOV for the thermal band.

The point spread function for the entire system is on the order of 10% of an IFOV, the MTF of the imaging system is therefore limited by the detector size rather than by the optical blur. The detector systems provide a noise equivalent reflectance change of less than one percent for the reflected energy bands and a noise equivalent

temperature difference of about 0.5K for TM Band 6, before quantization to 8 bits. System radiometric calibration is accomplished using on-board incandescent lamps for TM Bands 1, 2, 3, 4, 5, and 7 and a ground-controlled blackbody source for TM Band 6.

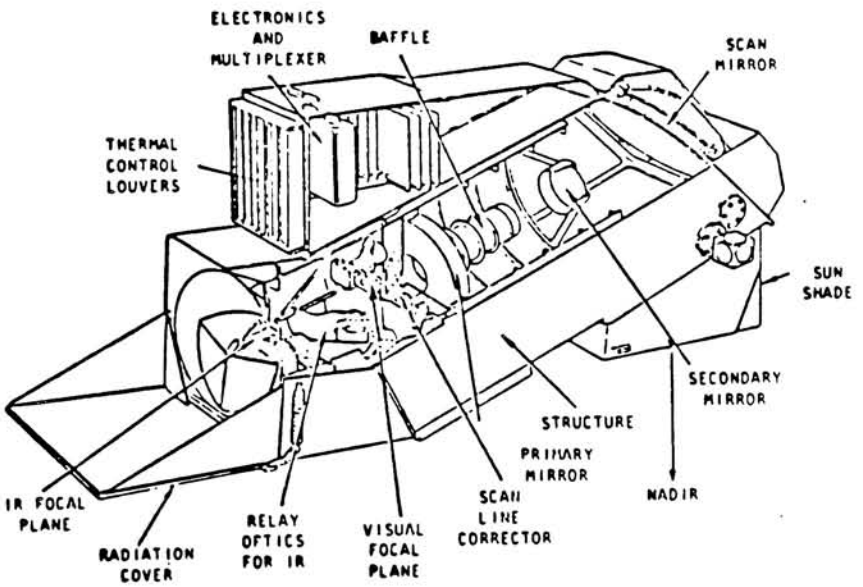

Figure 1.6-1 Layout of the LANDSAT Thematic Mapper (From Slater[87])

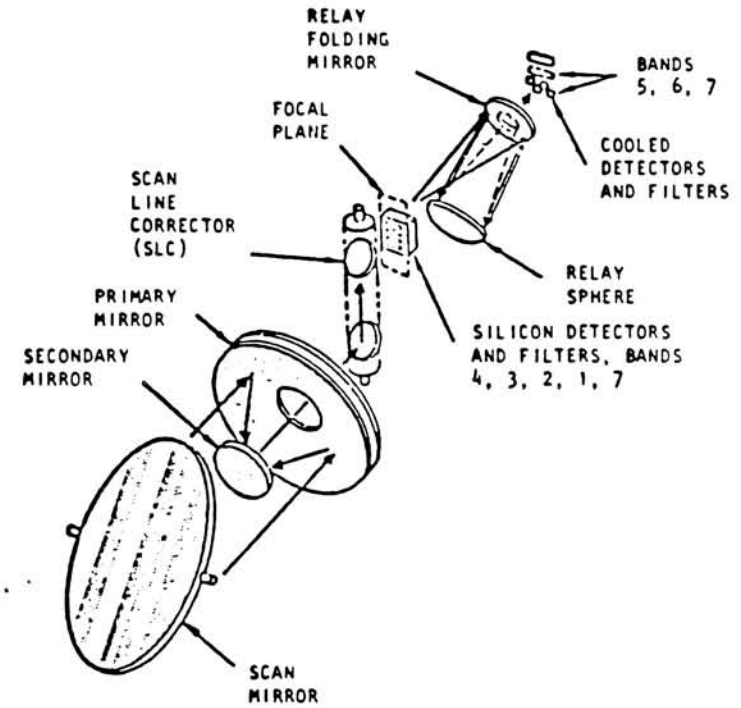

Figure 1.6-2 Thematic Mapper Optical System(From Slater[87])

1.6.2 Processing LANDSAT TM Data

LANDSAT TM image data is telemetered to ground stations in real-time, no on-board recording is involved. The U.S. ground stations then transmit the data to the Goddard Space Flight Center Image Processing Facility for image preprocessing. This preprocessing includes scene framing, basic image radiometric calibration, and geometric resampling to a known map projection. This preprocessed data is then sent to the EROS Data Center Digital Image Processing System (EDIPS). EDIPS reformats the image data onto Computer Compatible Tapes (CCT's) for users along with ancillary information as may be required by the user. EDIPS can also provide users with film output that has had tonal and spatial processing performed on it. Users requiring LANDSAT data can request CCT or film output products from EROS Data Center. The digital image data is shipped to the user on several 1600 BPI tapes or on a single 6250 BPI tape and is formatted as specified in Reference 88 and illustrated in Figure 1.6-3.

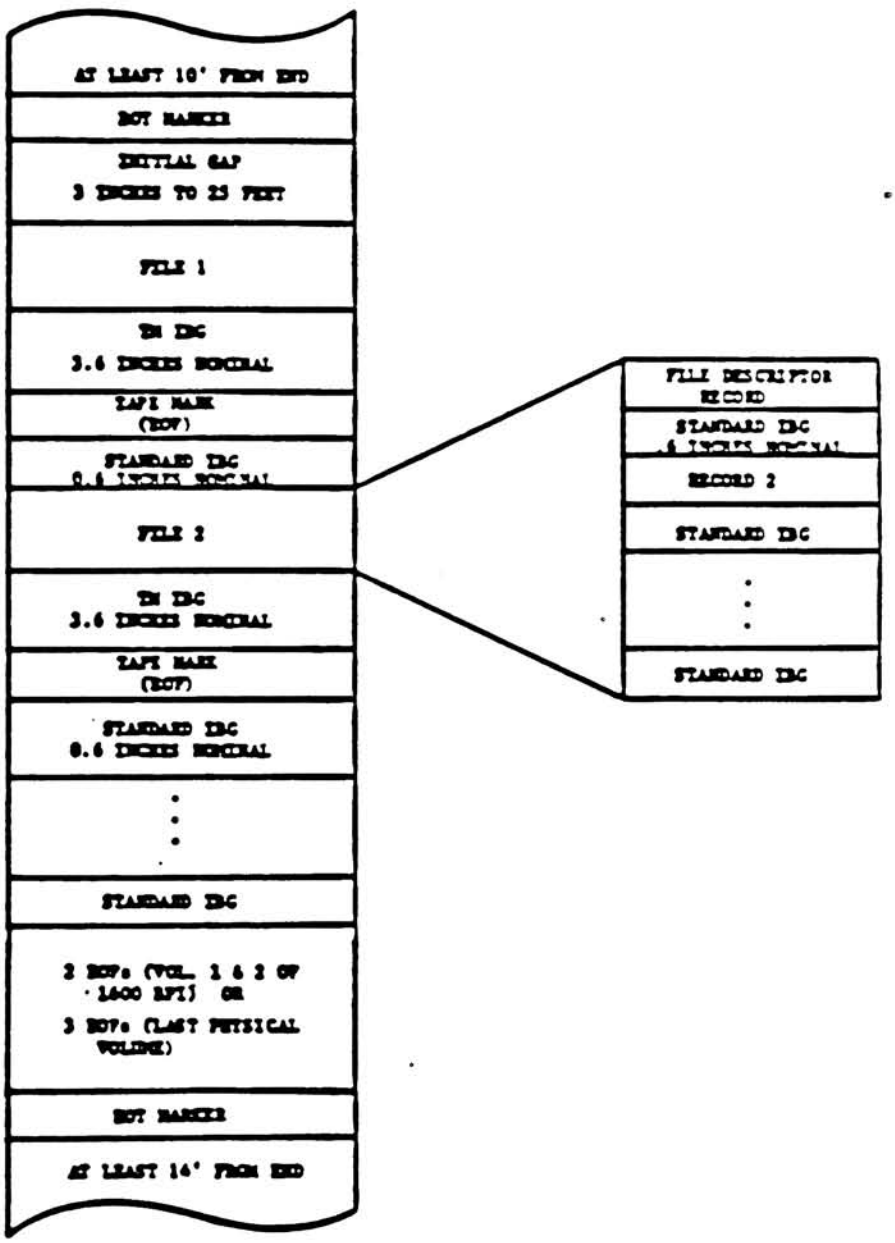

Figure 1.6-3 Layout of a 1600 BPI LANDSAT TM Image CCT (From NASA[88])

2.0 Experimental

All work for this study was performed at the Digital Imaging and Remote Sensing Laboratory (DIRS) at the Rochester Institute of Technology (RIT). Software required for this thesis work was developed in a FORTRAN environment using a Digital Equipment Corporation VAX/VMS 8350 computer system. Image display was done using a Gould/DeAnza IP8500 image array processor using DIRS Laboratory developed software. Hardcopy photographic output was made using a Dunn Instruments Micro Color CRT camera.

2.1 Image Selection

A specific image of Lake Ontario motivated the research of this thesis. A LANDSAT-5 TM image, identification number E-50113-15260, having LANDSAT scene coordinates of Path 030 and Row 017 and imaged on 22 June1984, was used to develop the pixel-by-pixel atmospheric haze reduction technique. The image is multispectral, consisting of seven co-registered image bands as described in Section 1.6. Figure 2.1-1 illustrates a true color representation of the image. The true color image was made by assigning TM Band 1 to the monitor blue channel, TM Band 2 to the monitor green channel, and TM Band 3 to the monitor red channel. Figures 2.1-2 through 2.1-8 present TM Bands 1 through 7 as monochrome images.

This scene was chosen because the TM Band 1 image shows several areas of increased brightness that cannot be attributed to either the lake water or to some atmospheric effect. Probably some type of spatially varying atmospheric correction technique is required if the TM Band 1 image were to be used to analyze the lake water quality.

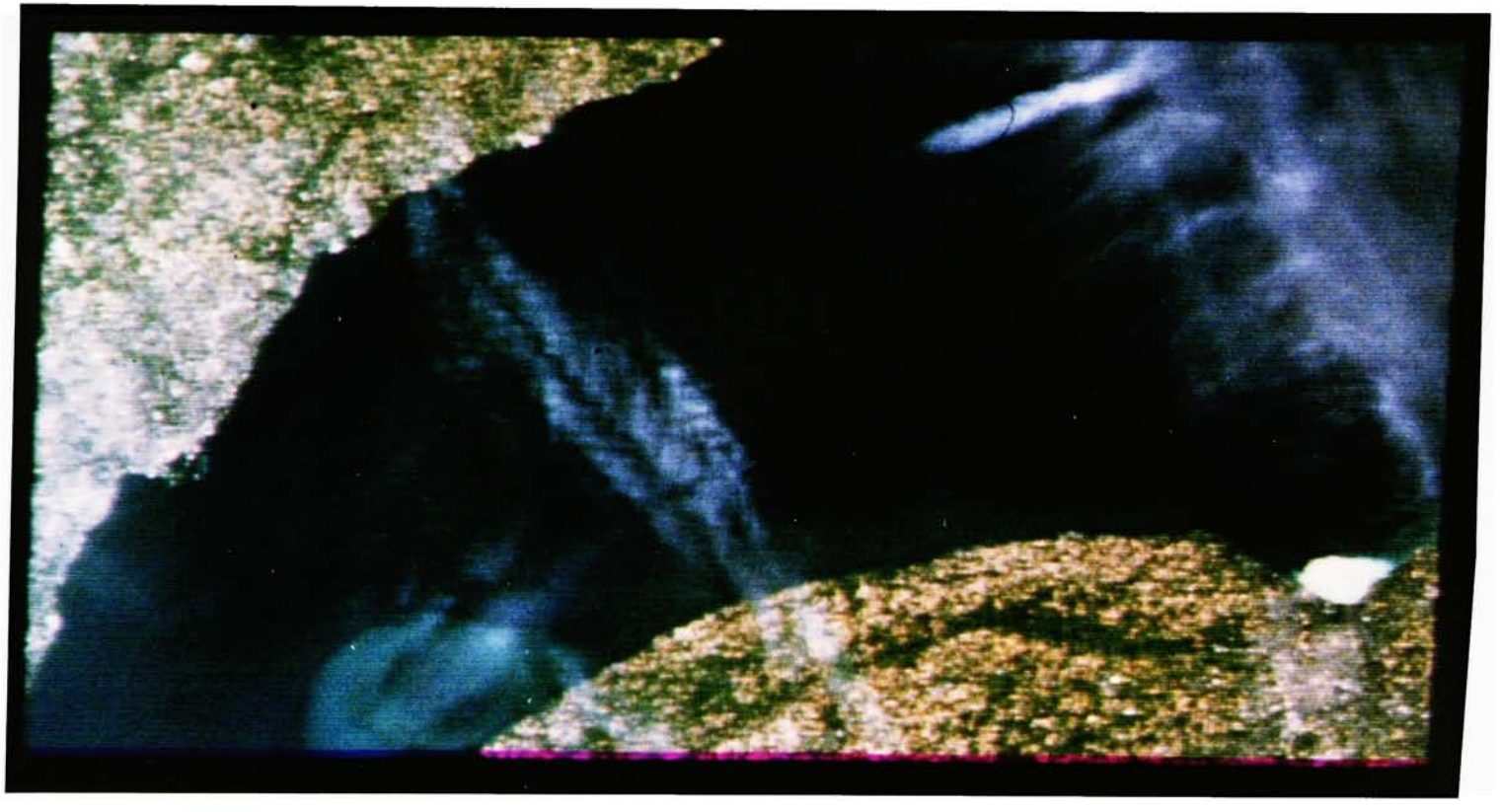

Figure 2.1-1 True Color Image of 22 June 1984 Lake Ontario Scene

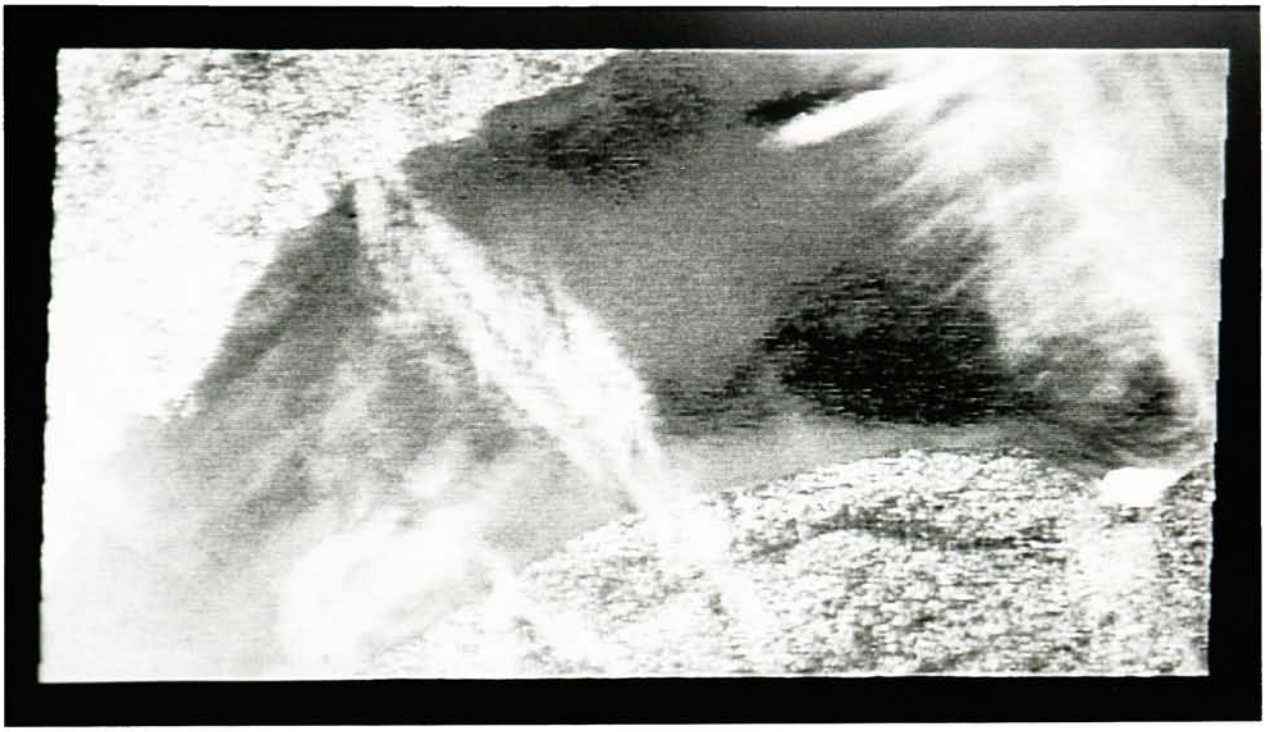

Figure 2.1-2 TM Band 1 Image of the 22 June 1984 Lake Ontario Scene

Figure 2.1-3 TM Band 2 Image of the 22 June 1984 Lake Ontario Scene

Figure 2.1-4 TM Band 3 Image of the 22 June 1984 Lake Ontario Scene

Figure 2.1-5 TM Band 4 Image of the 22 June 1984 Lake Ontario Scene

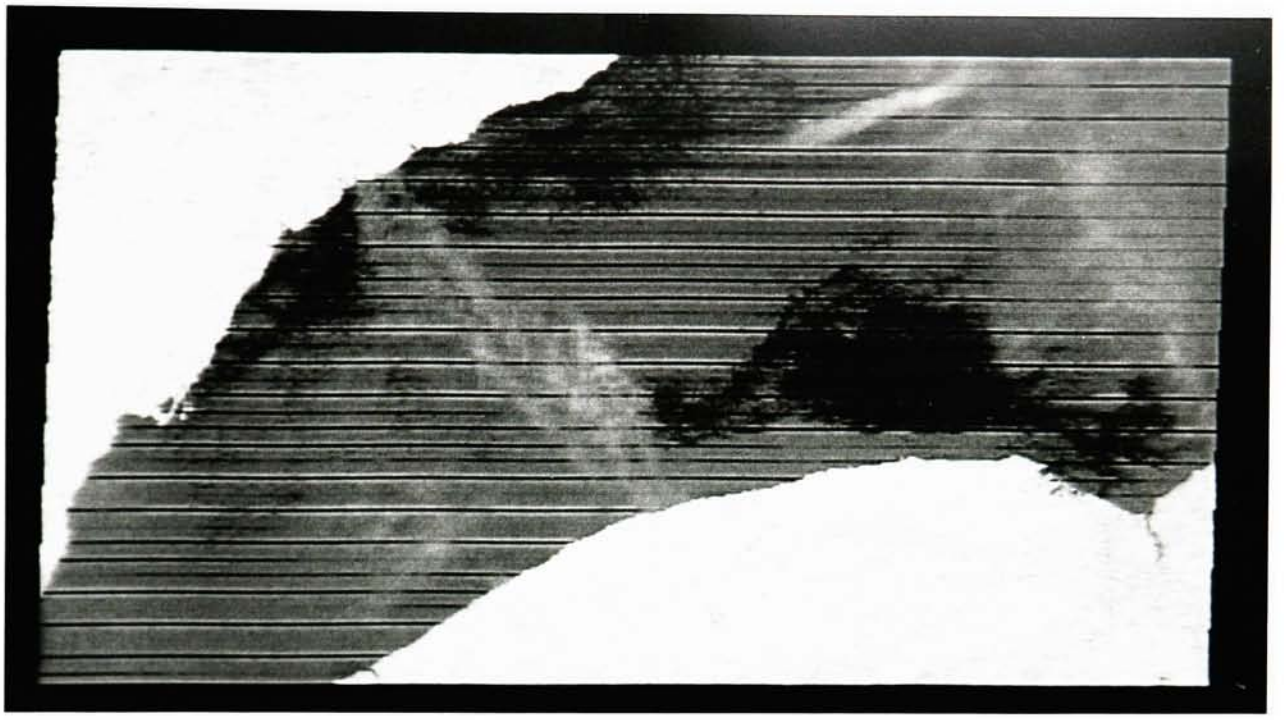

Figure 2.1-6 TM Band 5 Image of the 22 June 1984 Lake Ontario Scene

Figure 2.1-7 TM Band 6 Image of the 22 June 1984 Lake Ontario Scene

Figure 2.1-8 TM Band 7 Image of the 22 June 1984 Lake Ontario Scene

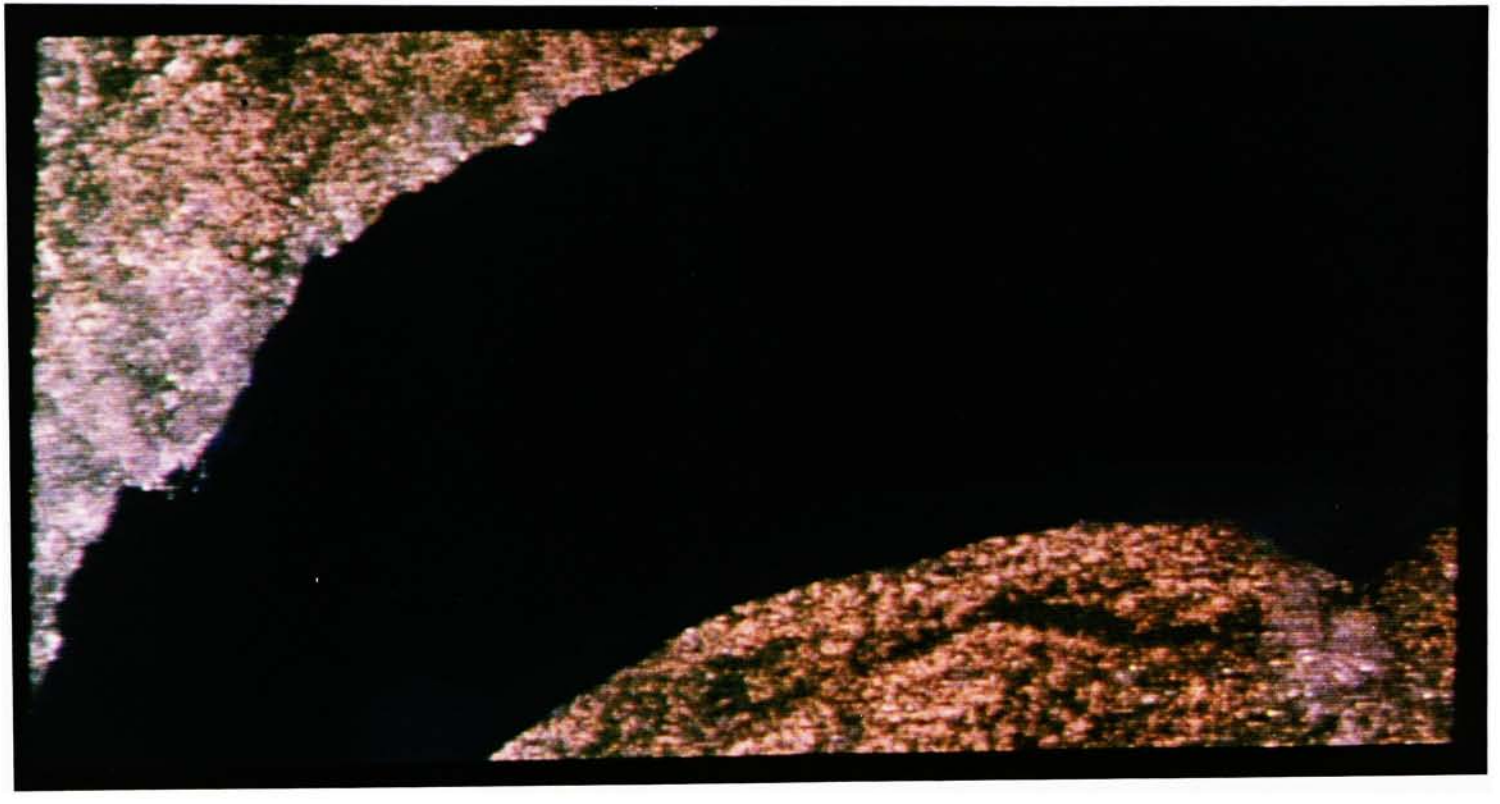

Figure 2.1-9 True Color Image of 25 May 1985 Lake Ontario Scene

Figure 2.1-10 TM Band 1 Image of the 25 May 1985 Lake Ontario Scene

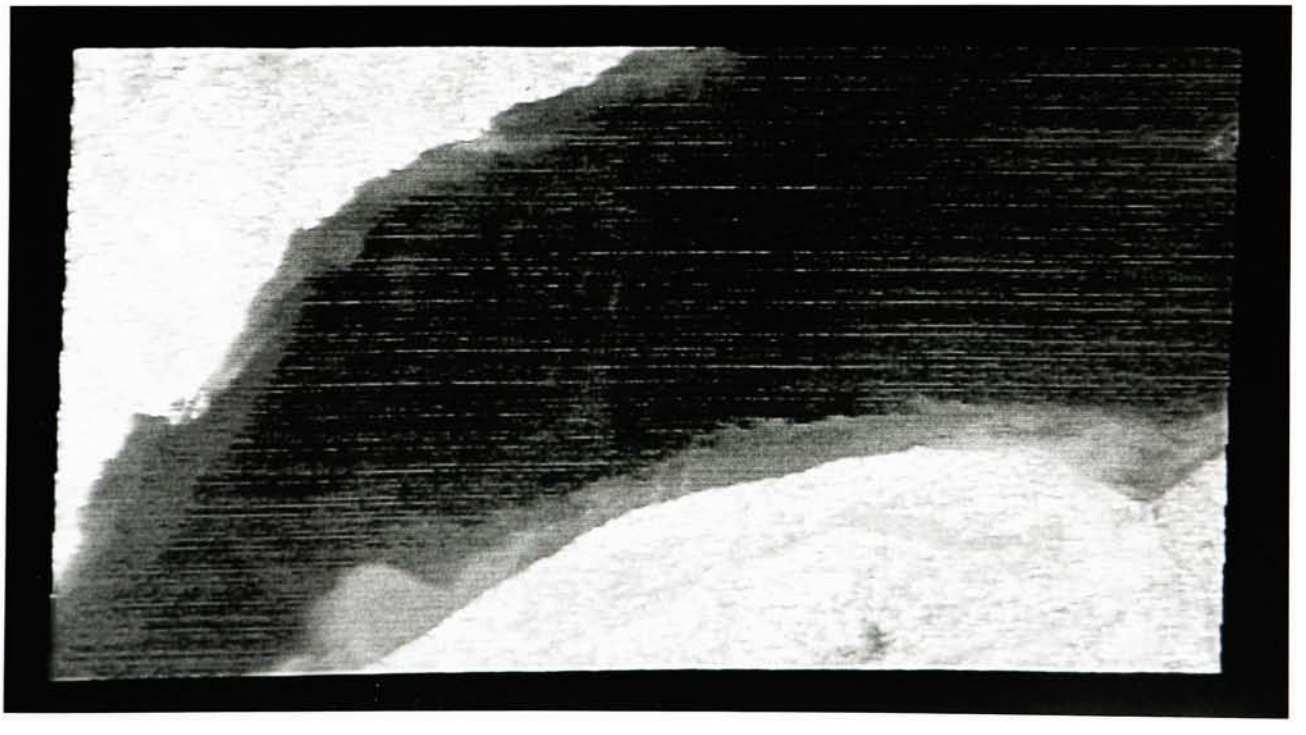

Figure 2.1-11 TM Band 2 Image of the 25 May 1985 Lake Ontario Scene

Figure 2.1-12 TM Band 3 Image of the 25 May 1985 Lake Ontario Scene

Figure 2.1-13 TM Band 4 Image of the 25 May 1985 Lake Ontario Scene

A second scene was chosen for processing using the spatially varying atmospheric correction algorithm developed using the 22 June 1984 scene. This scene, also from the LANDSAT-5 TM sensor, was imaged on 25 May 1985. The second scene was chosen as the most useful from a limited data set of multispectral imagery of water. The scene does not have the areas of increased brightness that the 22 June 1984 scene contains, and is therefore less than ideal for algorithm verification, but it does show a brighter radiance return around the perimeter of the lake near the shoreline. It is very probable that this is indicative of the state of the water and, as such, should not be affected by an atmospheric correction algorithm. It is for this reason that the 25 May 1985 image was included in this work. Figure 2.1-9 is a true color representation of the 25 May 1985 scene and Figures 2.1-10 through 2.1-13 illustrate TM Band 1 through TM Band 4 as monochrome images.

Both of the above LANDSAT-5 TM images were made available from the DIRS Laboratory at RIT. They are archived there on 1600 BPI computer compatible tapes (CCT) in the format illustrated by Figure 1.6-3.

2.1.1 Image Data Reformatting

As is described in Reference 88, each LANDSAT-5 TM image is stored in quadrants on CCT. A full image scene is constructed by reading each quadrant from tape and piecing them together as illustrated in Figure 2.1.1-1. Several computer programs were written to read and reformat the image data as required for this work.

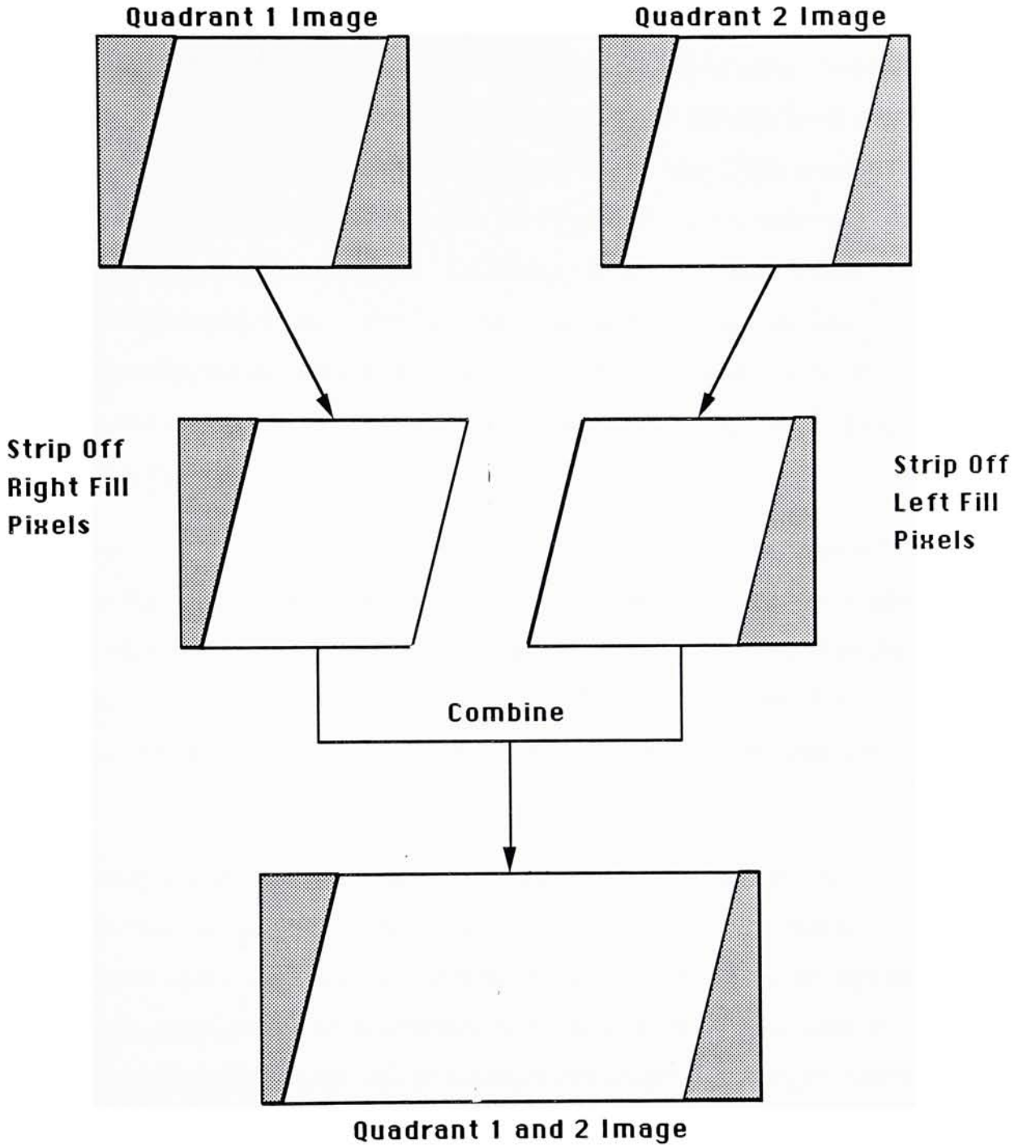

Figure 2.1.1-1 Constuction of Full Scene From Two Quadrant Images

Program READ_TM_TAPE (Appendix C) was used to read an image quadrant from a LANDSAT-5 TM data tape. Lake Ontario only appears in quadrants one and two of the full image so only those quadrants were read from tape. Each quadrant image is rectangular and has 4220 pixels per line and 2983 lines per quadrant. The actual image data occupies a subsection of the above dataset. The image data is skewed during imaging because of the rotation of the earth under the satellite, making the image parallelogram shaped. Zero-count pixels are appended to the beginning and end of each image line to fill out the rectangular image quadrant as illustrated in Figure 2.1.1-1.

Program PATCH (Appendix C) was used to create a single image for each TM band from the two quadrant images. Program PATCH reads in both quadrant images, strips all zero-fill pixels from the end of the quadrant one image lines and from the beginning of the quadrant two image lines. The two quadrant images are then fit together to form a single image that has 8440 pixels per line and 2983 lines per image.

Because of data storage, computer processing time, and image display limitations, the full image data could not be used for the thesis work. Program SUBSAMP (Appendix C) was used to reduce the size of the image data to be used for atmospheric correction algorithm development. Program SUBSAMP was used to subsample the the digital image data by creating a new image using every fourteenth pixel and line of the full image. This subsampling produced an image having 602 pixels per line and 213 lines per image. Only the left-most 512 pixels were retained in the final subsampled images used for the thesis work. All seven bands of the 22 June 1984 scene and TM Band 1 through TM Band 4 of the 25 May 1985 scene were subsampled in this manner.

2.1.2 Ancillary Scene Data Acquisition

Additional scene information required for development of the atmospheric correction algorithm includes knowledge of the imaging geometry, imaging time, and imaging system radiometric calibration parameters. Program TM_CAL_DATA (Appendix D) was used to search the ancillary files on the LANDSAT-5 TM CCTs for the above required scene information. Table 2.1.2-1 summarizes the pertinent geometry and imaging time data, and Table 2.1.2-2 contains the image radiometric calibration data for both the 22 June 1984 and 25 May 1985 scenes.

2.2 LANDSAT-5 TM Image Water Region Segmentation

The algorithm for correcting the spatially varying effects of the atmosphere on multispectral imagery of water takes advantage of the zero reflectivity of water in the infrared spectral region. The algorithm cannot be applied to earth surface features that are not water. An image water region segmentation process was therefore used to create a water region mask to identify image water areas. The water region mask creation is illustrated in Figure 2.2-1 and described here.

The TM Band 7 image of Lake Ontario was displayed using the Gould-DeAnza image array processor system. An interactive image tone processing program was used to binary threshold the TM Band 7 image. The binarization is carried out by setting all image count values that are less than or equal to the selected threshold value to zero. The remaining image pixels are set to the maximum count, 255. Because of the very low radiance return from water in the TM Band 7 spectral region, this simple thresholding technique has been found to be very effective for image

Table 2.1.2-1

Imaging Geometry, Time and Date

22 June 1984 Image:

Scene Center Longitude	43.179 N
Scene Center Latitude	78.588 W
Image Date	06/22/1984
Acquisition Time (GMT)	15:26:01
Nominal Satellite Altitude (Km)	707.959
Sun Elevation (Degrees)	59.0
Sun Azimuth (Degrees)	122.0

25 May 1985 Image:

Scene Center Longitude	43.189 N
Scene Center Latitude	77.102 W
Image Date	05/25/1985
Acquisition Time (GMT)	15:26:31
Nominal Satellite Altitude (Km)	707.875
Sun Elevation (Degrees)	58.0
Sun Azimuth (Degrees)	127.0

Table 2.1.2-2

Image Radiometric Calibration Data

	Gain ([mW/cm2-Sr-μm]/Count)	Offset (mW/cm2-Sr-μm)
22 June 1984 Image:		
TM Band 1:	-0.1500000	0.0602436
TM Band 2:	-0.2804878	0.1175036
TM Band 3:	-0.1194030	0.0805970
TM Band 4:	-0.1500000	0.0814399
25 May 1985 Image:		
TM Band 1:	-0.1500000	0.0602436
TM Band 2:	-0.2804878	0.1175036
TM Band 3:	-0.1194030	0.0805970
TM Band 4:	-0.1500000	0.0814399

water region segmentation.[90] The threshold value was set interactively until the author was satisfied with the quality of the water region segmentation. A threshold value of 11 was selected for the final water region segmentation for both the 22 June 1984 and 25 May 1985 scenes.

The program THRESHOLD_IMAGE (Appendix E) was used to create the water region mask. Similar to the interactive program described above, this program sets all image pixels to zero that have count values less than or equal to the threshold value. All other image counts are set to 255. This program, however, also performs a median filter operation on the binary image using a 5X5 window. The median filter operation removes isolated pixel counts to give a smoother segmentation mask. The program does not use the image array processor hardware and, therefore, can operate on any size image. The water segmentation mask was created using the full TM Band 7 image for both scenes and saved to CCT for future use. Water region masks for the subsampled imagery were constructed using the program SUBSAMP to subsample the full image water region mask down to the size of the subsampled image data. Of course, a separate water region mask had to be created for each lake scene.

The program MASK_PIC (Appendix E) was used to mask image water areas from other image areas for each of the spectral band images of the lake. The program created images that have the original image digital count for image water regions and 255 otherwise.

Histograms of image water region counts values were made from the masked image data. The histogram data for TM Band 1 through TM Band 5 of the 22 June 1984 scene are presented in Figures 2.2-2 through 2.2-6. The histogram data for

Band 1 through TM Band 4 of the 25 May 1985 scene are presented in Figures 2.2-7 through 2.2-10.

The masked image count data from the TM Band 4 image is used as a pixel-by-pixel index into a look-up table designed to correct the spatially varying atmospheric effects on the other spectral band images.

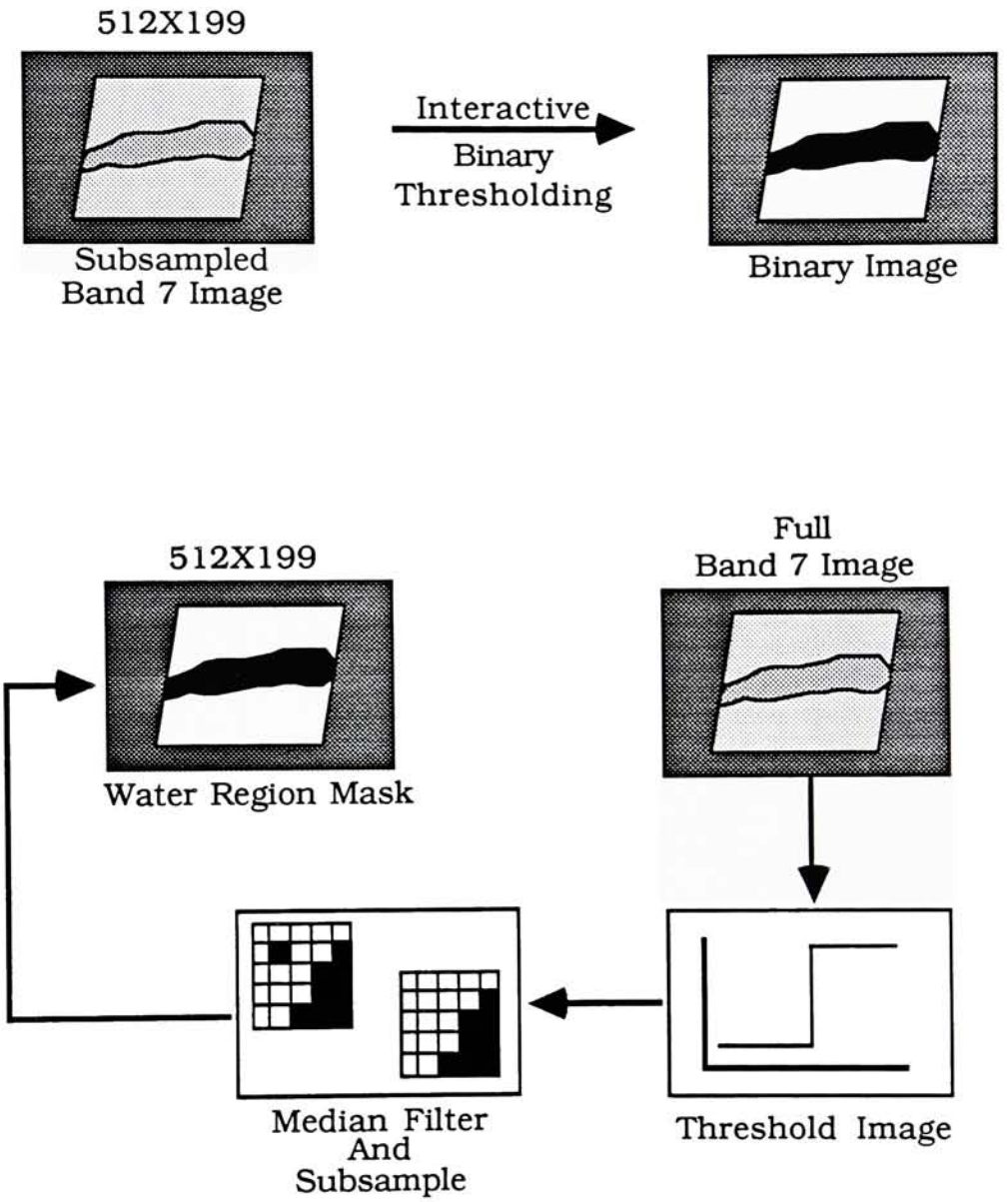

Figure 2.2-1 Water Region Mask Creation

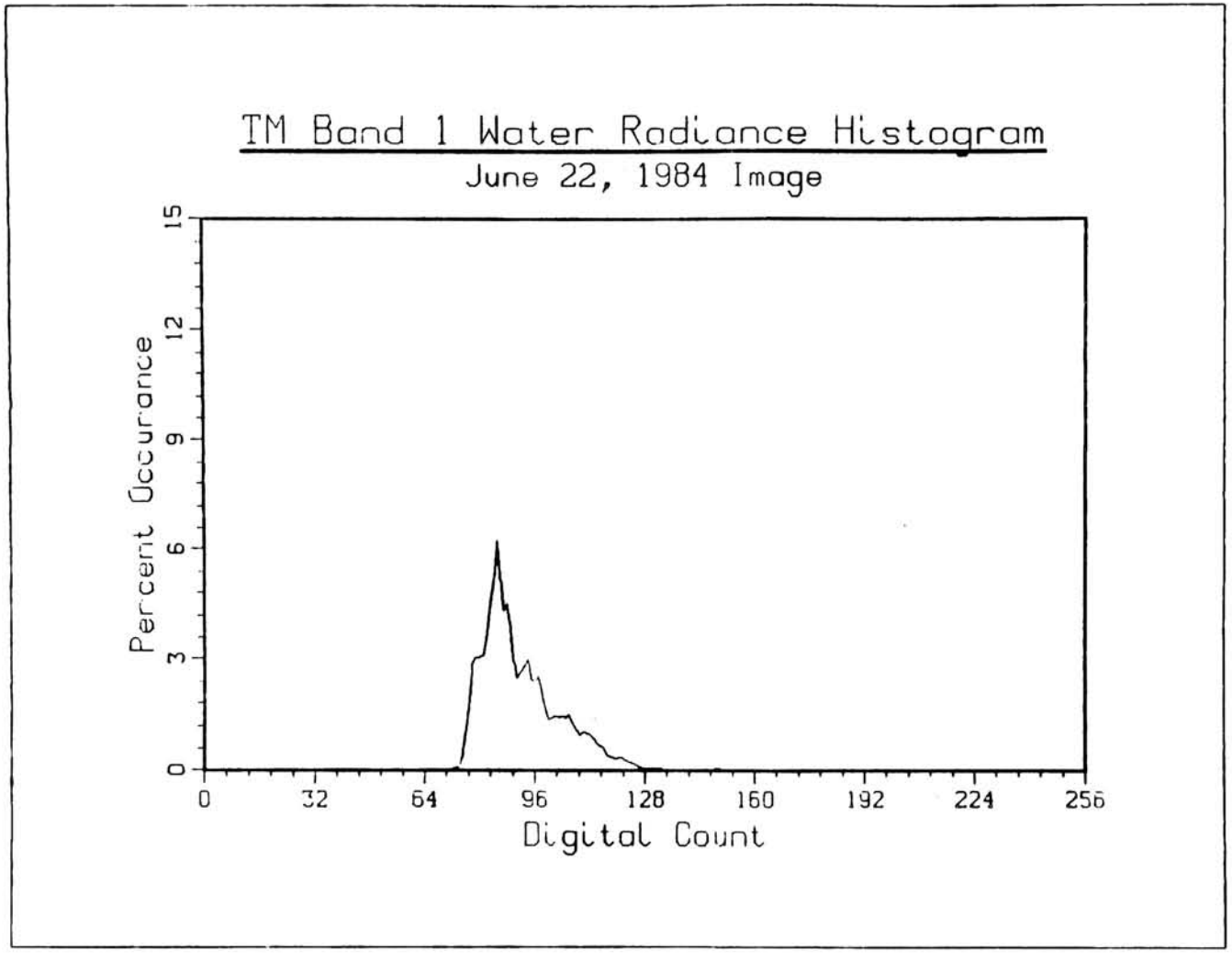

Figure 2.2-2 TM Band 1 Water Radiance Histogram (22 June 1984 Image)

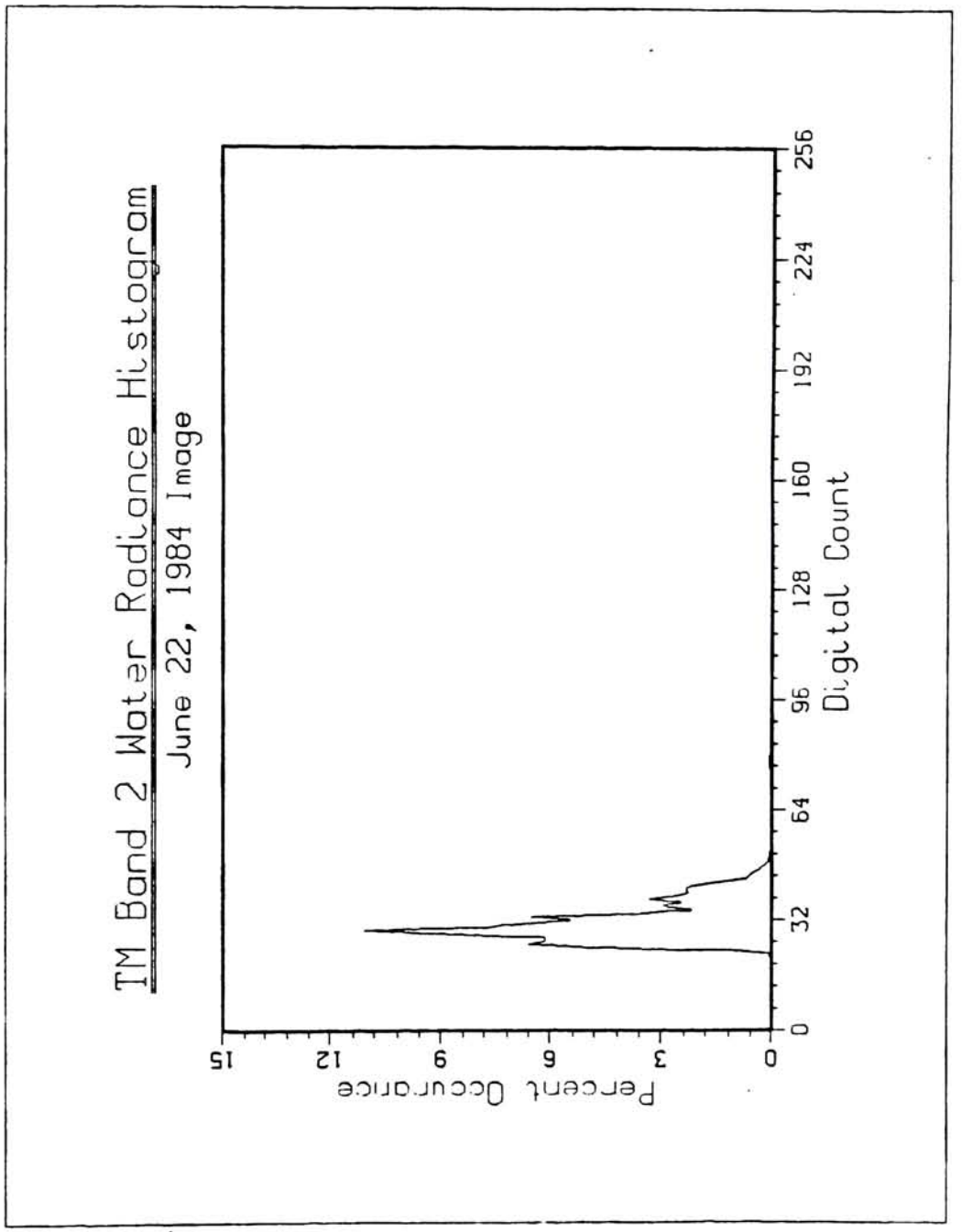

Figure 2.2-3 TM Band 2 Water Radiance Histogram (22 June 1984 Image)

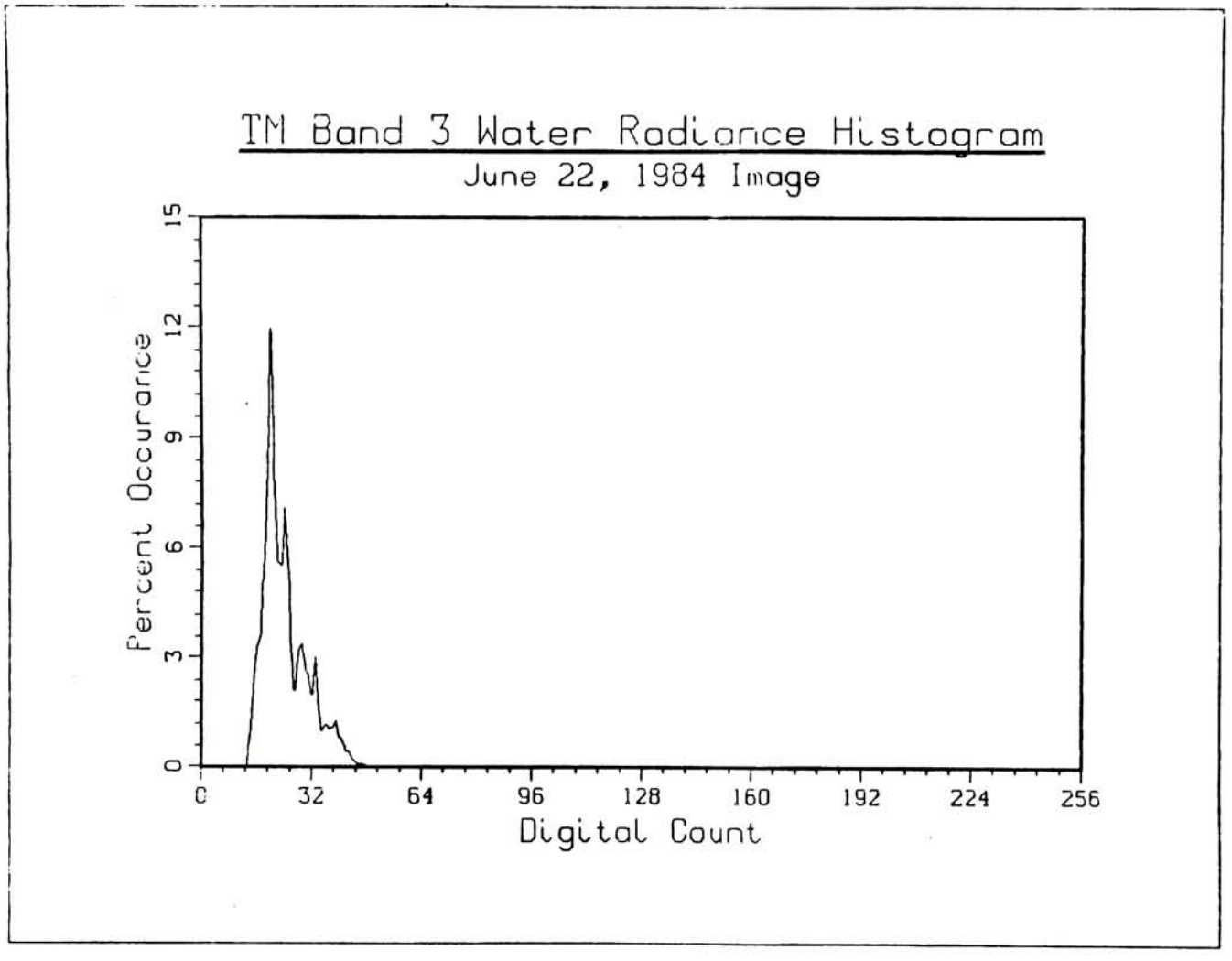

Figure 2.2-4 TM Band 3 Water Radiance Histogram (22 June 1984 Image)

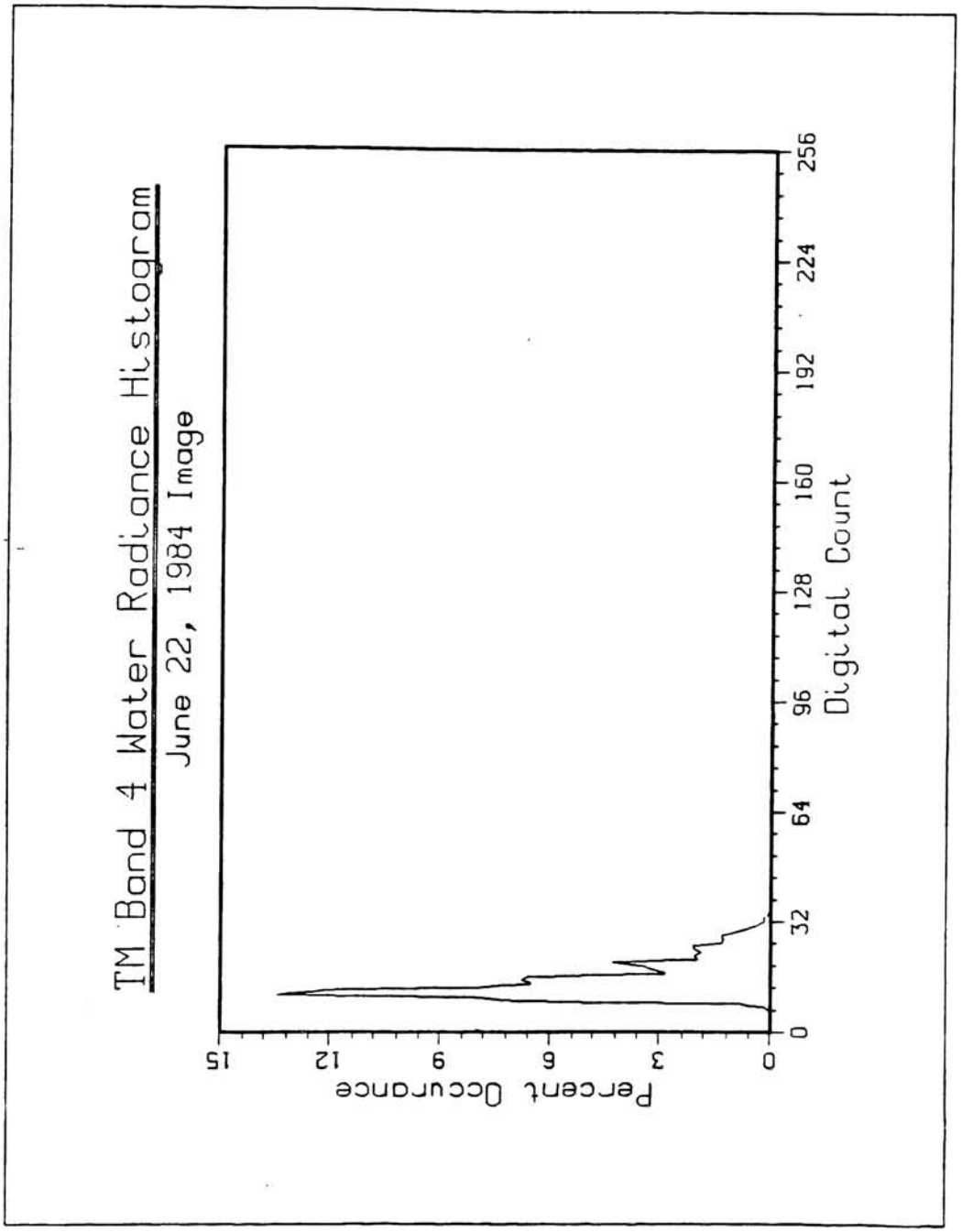

Figure 2.2-5 TM Band 4 Water Radiance Histogram (22 June 1984 Image)

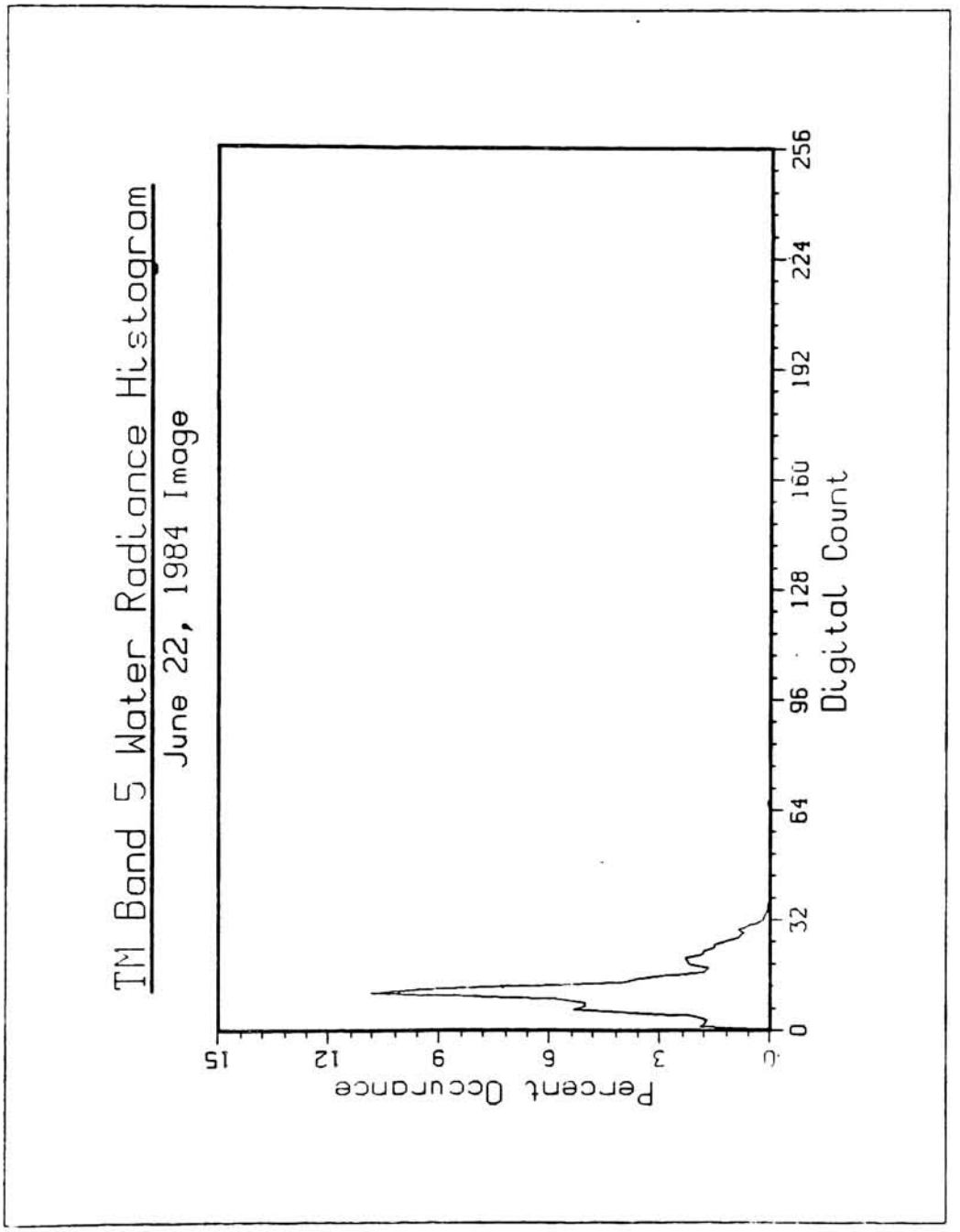

Figure 2.2-6 TM Band 5 Water Radiance Histogram (22 June 1984 Image)

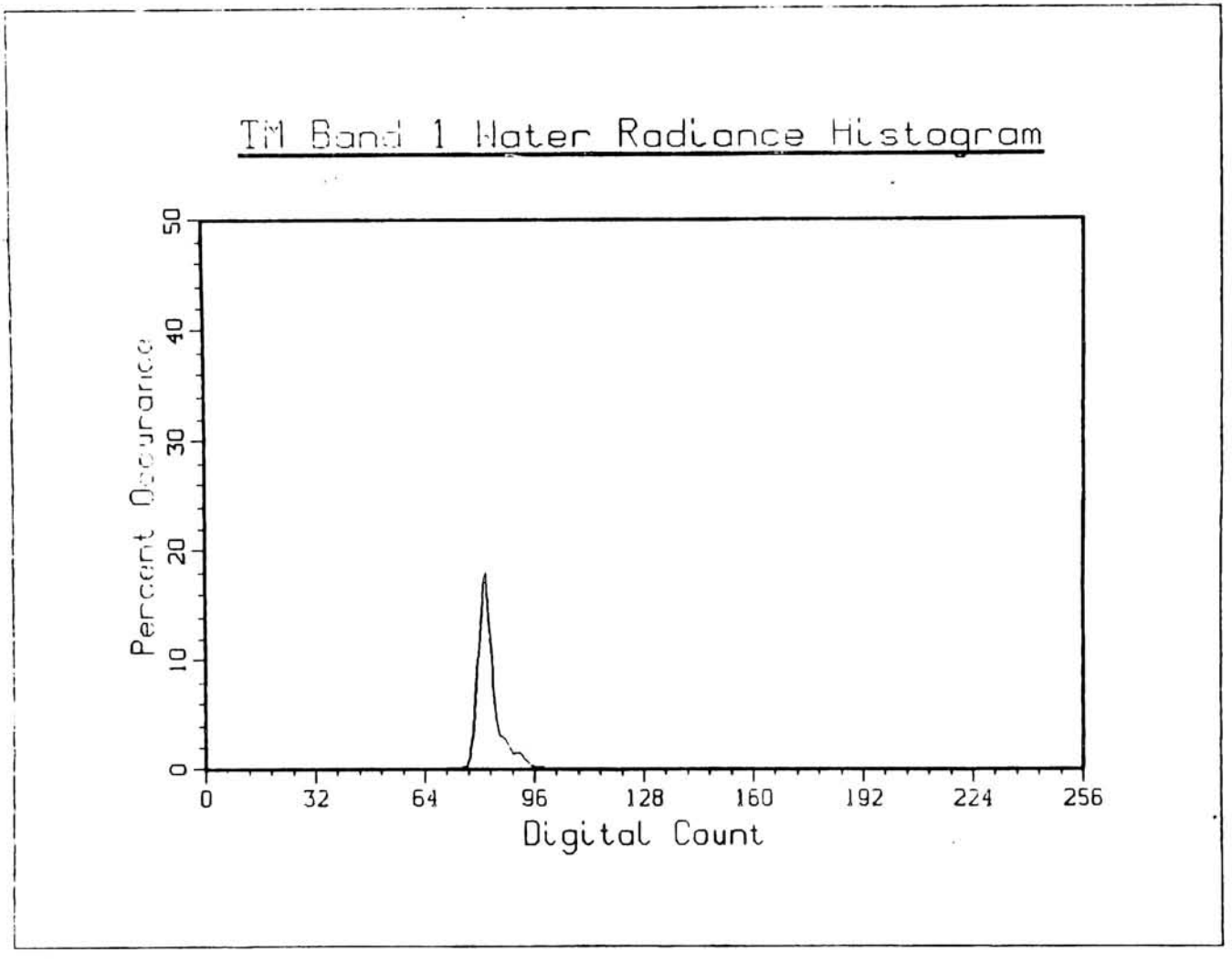

Figure 2.2-7 TM Band 1 Water Radiance Histogram (25 May 1985 Image)

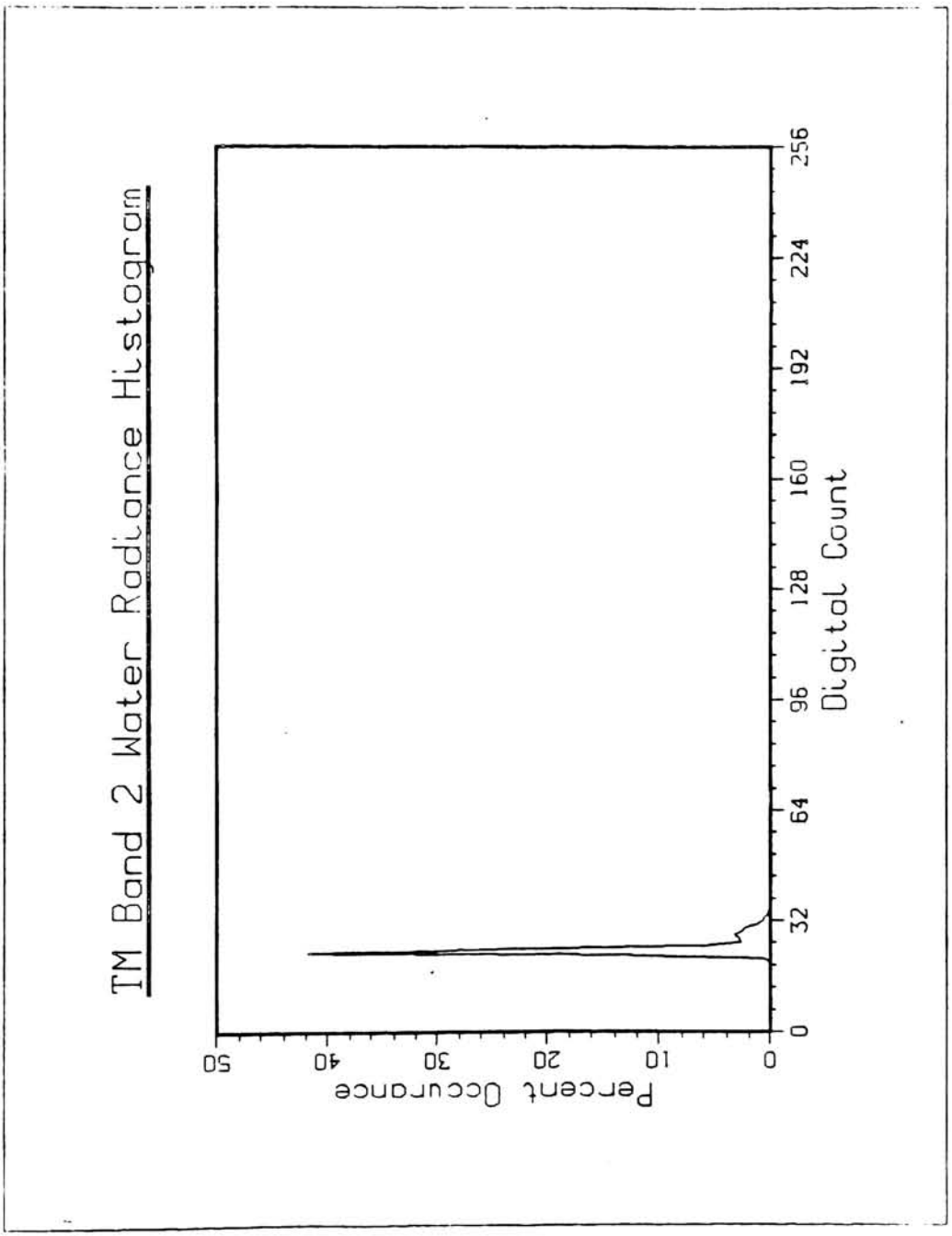

Figure 2.2-8 TM Band 2 Water Radiance Histogram (25 May 1985 Image)

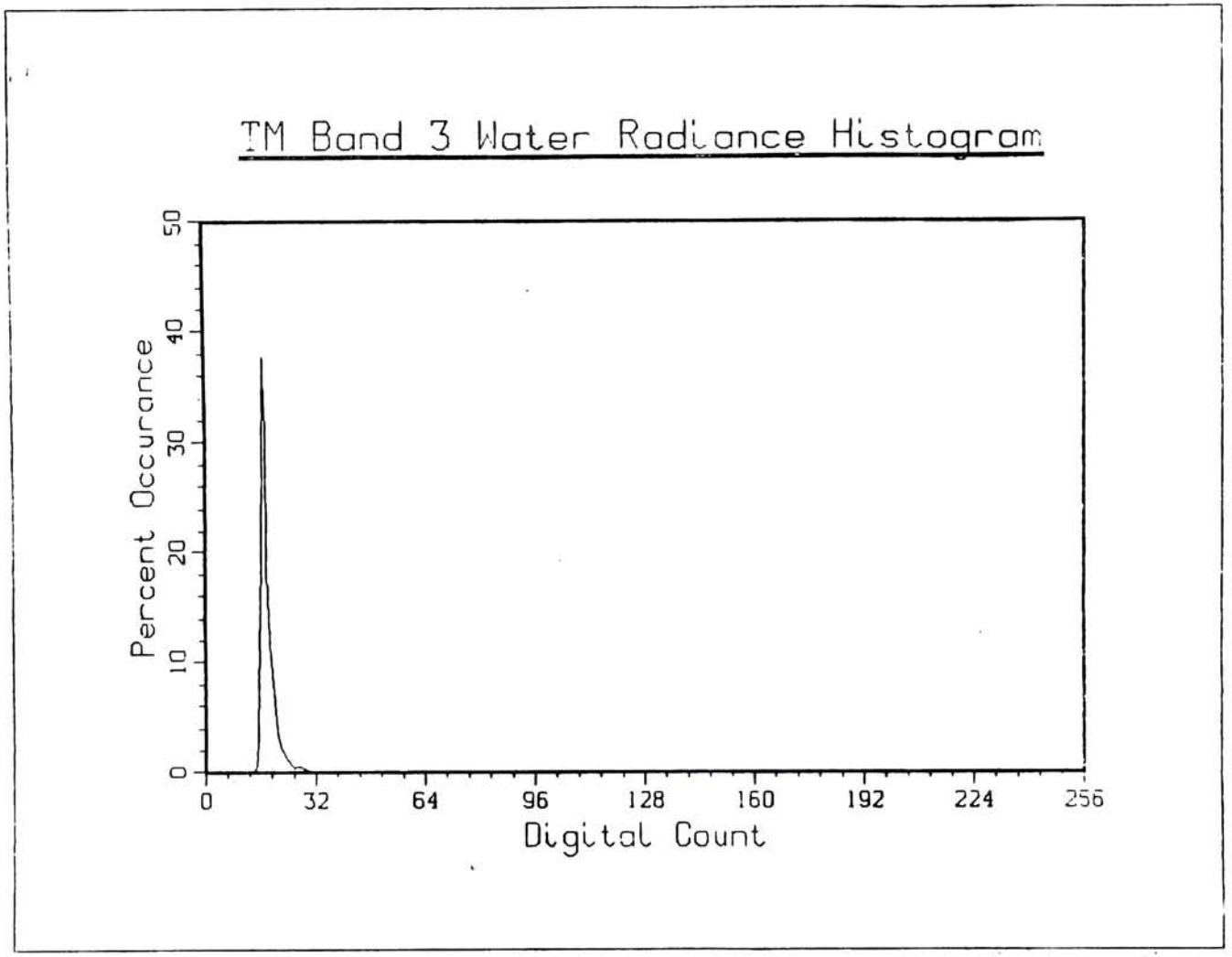

Figure 2.2-9 TM Band 3 Water Radiance Histogram (25 May 1985 Image)

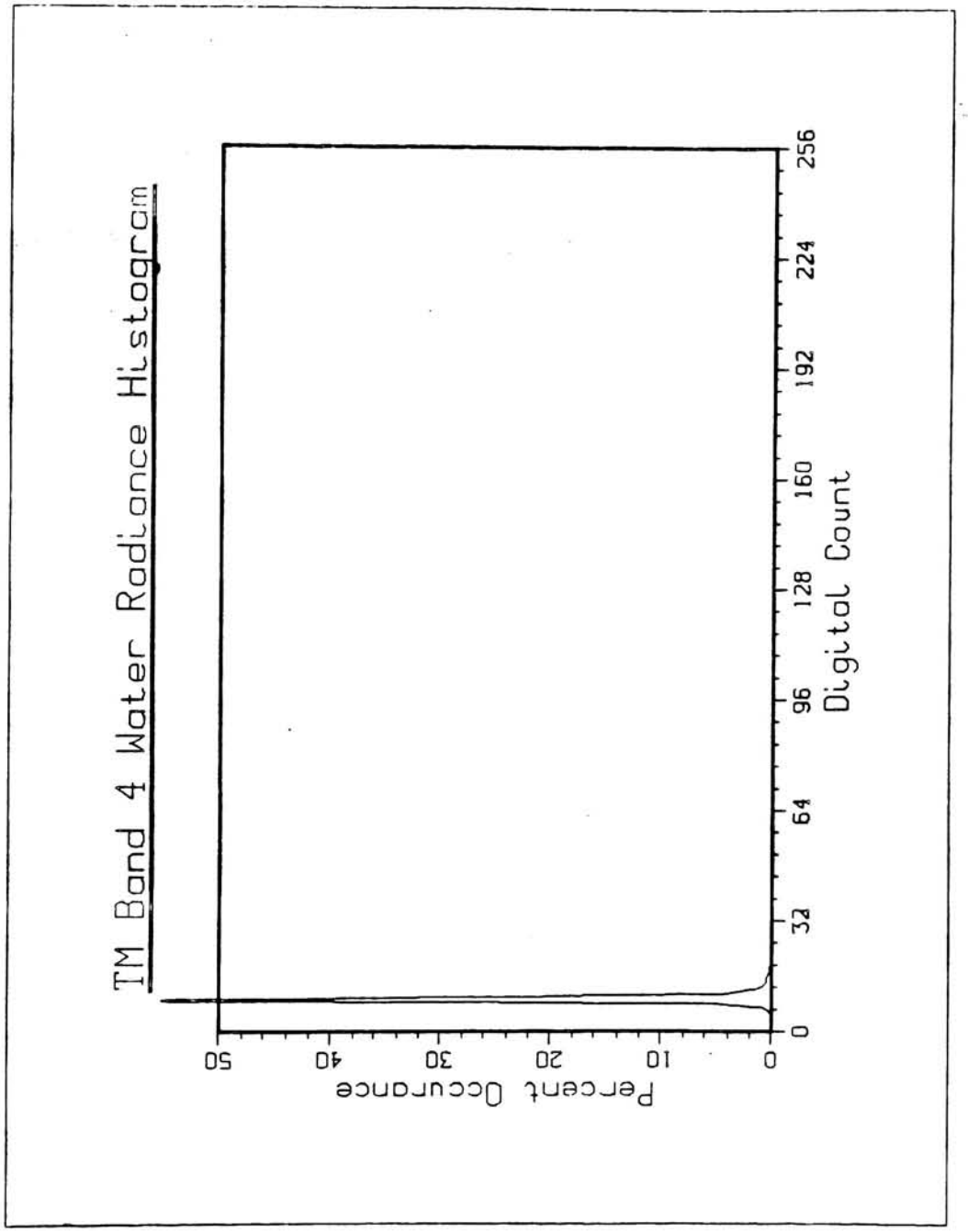

Figure 2.2-10 TM Band 4 Water Radiance Histogram (25 May 1985 Image)

2.3 Modeling of Atmospheric Effects

The radiance-return from water body areas of the TM Band 4 image is used to define the atmosphere for subsequent correction of the remaining spectral band imagery. This is possible because water has a near-zero reflectance in the TM Band 4 spectral region and any return in that band from a water body can be considered to be caused by atmospheric effects alone.

Only those atmospheric effects that are manifested between the water surface and the imaging system, along the line-of-sight of the imaging system, are considered here. Reduction of the image data to a true volume reflectance map of the water surface requires consideration of the effects of the illumination of the water by the sun, sky and Fresnel reflection directed toward the imaging system from the air-water interface. A spatially varying model of each of the above factors would rapidly become intractable. These factors can be assumed to be constant over the entire image with error on the order of just a percent or two, and as such, can be considered to be an additional, uniform effect for the entire scene. The spatially varying atmospheric correction described here will produce a water surface radiance map. Further atmospheric corrections to allow recovery of the volume spectral reflectance have been well documented in the literature and will not be considered here.[92]

2.3.1 Simplification of the Equation of Radiative Transfer

Equation 1.3.1-31, the complete description of the radiative transfer process, can be rewritten in terms of the satellite sensed radiance, $L_{T\lambda}$, and total surface radiance from the water body, $L_{w\lambda}$, as:

$$L_{T\lambda} = \tau_\lambda L_{w\lambda} + L_{u\lambda} \qquad 2.3.1\text{-}1$$

where: $L_{T\lambda} = L_\lambda(\theta,\theta',\phi)$

$\tau_\lambda = e^{-\tau_\lambda' sec(\theta)}$

$L_{u\lambda} = L_{u\lambda}(\theta,\theta',\phi)$

$$L_{w\lambda} = \frac{r_\lambda(\theta,\theta',\phi)}{\pi}\left[E'_{s\lambda}cos(Z)\ e^{-\tau_\lambda' sec(\theta)} + \int_0^{2\pi}\int_0^{\frac{\pi}{2}} L_{d\lambda}(\theta,\phi)cos(\theta)sin(\theta)\,d\theta\,d\phi\right]$$

It should be noted that Equation 2.3.1-1 has fixed the geometry of the imaging scenario. This causes no problems since the image data to be corrected consists of a co-temporal, co-registered, multispectral data set, so all spectral band images have identical imaging geometry. Equation 2.3.1-1 contains the two parameters that are most sensitive to atmospheric spatial variability, τ_λ, and $L_{u\lambda}$. As has been previously stated, the effects of illumination of the water by the sun and sky have been neglected because they induce very small spatially varying atmospheric effects.

For the LANDSAT-5 TM Band 4 image the water reflectance is assumed to be zero, therefore:

$$L_{w\lambda} = 0 \qquad 2.3.1\text{-}2$$

so that

$$L_{T\lambda} = L_{u\lambda} \qquad 2.3.1\text{-}3$$

Therefore, each water pixel count value in the TM Band 4 image can be considered a measure of the upwelling atmospheric radiance in the 0.76-0.90μm spectral region.

The LOWTRAN 6 atmospheric model is used to define the atmospheric conditions that can produce an upwelling atmospheric radiance equal to that

measured from the LANDSAT-5 TM Band 4 image. Those same atmospheric conditions also allow LOWTRAN 6 to provide an estimate of the atmospheric transmittance and upwelling radiance for any other spectral region.

A map of the water surface radiance is made using the LOWTRAN 6 estimates of τ_λ and $L_{u\lambda}$ and by rewriting Equation 2.3.1-1 as:

$$L_{w\lambda} = \frac{L_{T\lambda} - L_{u\lambda}}{\tau_\lambda} \qquad 2.3.1\text{-}4$$

Each of the TM Band 4 water pixels describes the atmospheric conditions present at that point of the scene, therefore, a pixel-by-pixel atmospheric correction can be made.

2.3.2 Preparation of the LOWTRAN 6 Atmospheric Model

The LOWTRAN 6 model has been described in Section 1.5. The LOWTRAN 6 computer code is a FORTRAN program designed to run in batch mode on a large computer system. Input to the program must be made using code values on formatted input "cards". Because of the multitude of LOWTRAN 6 model runs required for this research, the LOWTRAN 6 computer code had to be modified for interactive use and a separate input formatting program had to be developed.

2.3.2.1 Software Development and Modification

A computer program, LOWCNTRL6 (Appendix F) was written to create the formatted, coded data input required by the LOWTRAN 6 computer code. The LOWCNTRL6 program interactively queries the user for selection of the proper

parameter for each of the input values required by the LOWTRAN 6 model. The program substitutes the proper input parameter code value for each input datum and creates a formatted output file that is used as the input file (or cards) for the LOWTRAN 6 program. Appendix A illustrates a formatted input file for the LOWTRAN 6 program.

Each modeling scenario using the LOWTRAN 6 model requires a separate, formatted, input file. Any change at all in the imaging geometry, atmospheric conditions, or spectral region being modeled requires a completely new input file. Because each count value of the TM image requires several runs of the LOWTRAN 6 model to provide a match, the LOWTRAN 6 computer code was modified to allow more than one run per input file and interactive updating of certain modeling parameters. Because the LOWTRAN 6 computer code is very complex, several interactive versions of the program were created to allow modification of specific modeling parameters. Appendix F contains the necessary source code updates for one such interactive version, LOWHGP.

Much of the normal output of the LOWTRAN 6 model had to be eliminated to allow the program to function in an interactive manner. Only that output required to produce a match of the TM Band 4 water count values were retained. Appendix F illustrates the interactive data screen format used by the LOWHGP program and shows the retained output and those model parameters that can be interactively modified.

All of the atmospheric modeling software development and modification was done using Digital Equipment Corporation VAX FORTRAN operating in a VMS environment. Several features of VAX FORTRAN that are not part of the 1977 FORTRAN language standard have been used in the source code. The author is

satisfied that the programs operate properly on the VAX/VMS 8350 computer at the RIT DIRS laboratory. Use of the software modifications on another type of computer system may not produce correct results.

2.3.2.2 Atmospheric Model Control Point

Although the radiance measured from the TM Band 4 image of water is used to define the atmospheric condition at that point in the scene, it alone cannot completely define the atmospheric state. An atmospheric profile describing the vertical temperature, water vapor, and pressure distribution of the atmosphere was used to define a starting point for the atmospheric modeling. Atmospheric radiosondings made at the Greater Buffalo International Airport were used to define the modeling starting point. Buffalo, New York is near the westernmost end of Lake Ontario. This radiosonde is the only one available within the scene so only one scene control point could be set.

Separate radiosondes were obtained for each of the scenes used in this study. The radiosondes were made at 7:00 AM EDT. Both the 22 June 1984 and 25 May 1985 scenes were acquired at approximately 9:30 AM EDT so a small error in the atmospheric profile data may have been present. Additionally, the radiosonde profile data was augmented with a LOWTRAN 6 database vertical profile of midlatitude-summer ozone concentration. It was these profiles that were modified during the interactive LOWTRAN 6 runs to produce the atmospheric corrections. Table 2.3.2.2-1 lists the radiosonde data used for the 22 June 1984 scene. Table 2.3.2.2-2 lists the radiosonde data used for the 25 May 1985 scene.

Table 2.3.2.2-1

22 June 1984 Radiosonde Data
7 AM

Altitude (Km)	Pressure (mb)	Temperature (C)	Dew Point Depression (C)
0.218	994.9	11.70	3.5
0.302	985.0	15.4	8.2
0.827	926.0	16.4	9.6
1.540	850.0	11.0	10.7
2.600	748.0	2.6	10.3
3.137	700.0	3.4	30.0
3.266	689.0	3.6	30.0
4.821	567.0	-5.2	18.6
5.405	526.0	-10.1	18.3
5.794	500.0	-12.8	18.0
6.184	475.0	-15.1	17.2
6.248	471.0	-15.4	10.5
6.508	455.0	-16.6	16.0
7.464	400.0	-23.3	30.0
9.299	309.0	-37.7	12.8
9.502	300.0	-39.2	8.6
9.640	294.0	-39.7	7.7
10.727	250.0	-48.8	7.4
12.131	201.0	-58.2	7.4
12.162	200.0	-57.7	7.4
12.486	190.0	-57.5	7.4
12.622	186.0	-53.4	7.4
12.834	180.0	-51.1	7.4
14.005	150.0	-56.7	7.4
16.542	100.0	-62.5	7.4
18.751	70.0	-60.8	7.4
20.861	50.0	-57.3	7.4
21.824	43.0	-52.9	7.4
24.153	30.0	-51.7	7.4
24.837	27.0	-51.2	7.4
26.813	20.0	-45.5	7.4
27.905	17.0	-42.1	7.4
29.724	13.0	-41.3	7.4
29.724	13.0	-41.3	7.4

Table 2.3.2.2-2

25 May 1985 Radiosonde Data
7 AM

Altitude (Km)	Pressure (mb)	Temperature (C)	Dew Point Depression (C)
0.218	989.7	9.4	4.0
0.249	986.0	10.6	4.9
0.343	975.0	12.7	9.8
0.438	964.0	12.3	10.7
0.660	939.0	15.4	13.6
0.879	915.0	14.8	14.1
1.496	850.0	8.8	9.5
1.862	813.0	5.1	7.4
2.850	719.0	-2.9	14.8
3.063	700.0	-1.5	30.0
4.123	612.0	-6.6	30.0
5.672	500.0	-16.5	30.0
7.306	400.0	-29.8	30.0
8.402	342.0	-38.7	30.0
9.290	300.0	-45.5	100.0
10.483	250.0	-54.0	100.0
10.878	235.0	-56.3	100.0
11.533	212.0	-55.8	100.0
11.903	200.0	-56.9	100.0
12.431	184.0	-57.4	100.0
13.731	150.0	-54.4	100.0
16.306	100.0	-58.1	100.0
18.564	70.0	-55.9	100.0
20.708	50.0	-55.3	100.0
23.972	30.0	-54.8	100.0
26.277	21.0	-50.4	100.0

2.3.3 Theory of Spatially Varying Haze Phenomena

It was presumed that the areas of increased radiance observed in the 22 June 1984 lake scene due to atmospheric effects are caused by localized increases in the concentration of water vapor and aerosols. Both of these atmospheric constituents are modeled in LOWTRAN 6 so no difficulty in successfully modeling the observed effects was anticipated.

Increasing the concentration of water vapor in the model atmosphere was first accomplished by reducing the dew point depression values in the input radiosonde data. Increasing the dew point depression value serves to decrease the water vapor concentration. Atmospheric aerosol concentration is controlled by the VIS input parameter in LOWTRAN 6. VIS is nominally an estimate of the meteorological range at sea level for a given modeling scenario. The LOWTRAN 6 model then fits a curve describing the aerosol concentration as a function of altitude to the sea level value. Adjustments to the VIS parameter, in effect, control the total aerosol concentration in the atmosphere.

No combination of VIS and dew point depression adjustment was found that could produce a matching value for the range of radiance levels observed in the TM Band 4 image of the lake. Increases in the water vapor concentration of the model atmosphere caused the modeled transmittance to approach zero far more rapidly than the upwelled scattered radiance approached the observed values. Similar difficulties were found when adjusting the VIS parameter.

Because the consideration of the water vapor and aerosol concentrations as the cause of the localized atmospheric radiance changes in the water scene is intuitively appealing, the modeling difficulty was assumed to be either a deficiency in

the LOWTRAN 6 model for the spectral regions being investigated or a violation of the requirements of the single-scattering assumptions.

The increased optical thickness of the brighter areas of the water image could have indeed violated the single-scattering assumption. In an attempt to circumvent this possibility, a modification was made to the calculation of the single-scattered radiance. The scattering extinction coefficient in the LOWTRAN 6 single-scattering computation was empirically altered until the modeled value of the upwelling scattered radiance was within the range of the observed values. Even with this increased scattering extinction coefficient, only a small fraction of the range of observed TM Band 4 upwelling radiance could be matched by adjustment of the water vapor concentration and VIS parameters

A careful and very detailed analysis of the LOWTRAN 6 source code was begun to find areas of model weakness or errors in the coding of the model. No such areas were found but it was noted that the aerosol scattering phase function being selected from the database internal to the LOWTRAN 6 model allowed only a very small fraction of the incident sunlight to be scattered toward the satellite. Forced selection of a different aerosol scattering phase function was found to produce modeled values of TM Band 4 upwelling path scattered radiance that were very close to those observed in the image of the lake.

This discovery led to a refinement of the theory behind the cause of the localized radiance increases in the lake scene. It is hypothesized that a localized, large concentration of water vapor would cause the individual water molecules to condense on available nuclei, such as aerosol dust, to form larger water particles. Several individual water molecules condensing on a single nuclei would lead to a water-aerosol or hydrosol formation. Such hydrosols would have particle sizes much

larger than Rayleigh scattering theory can predict. Therefore, an increase in the local concentration of atmospheric water can cause the molecular water vapor concentration to decrease and the aerosol concentration to increase.

The above treatment of the increased localized radiance observed in the TM Band 4 lake image is consistent with the results of the previous LOWTRAN 6 model runs. Increasing the model water vapor concentration gives an increase in the number of water molecules in the atmosphere. Such an increase will significantly increase the atmospheric absorption but only a small increase in the amount of Rayleigh scattering will be found. Decreases in the VIS parameter to increase the model atmosphere aerosol concentration does not provide a sufficient increase in modeled radiance because the LOWTRAN 6 model selects an aerosol scattering phase function representative of dust particles and industrial emissions, not the water particles that are thought to be formed.

Modeling the increase in local radiance in the lake scene as an increase in the number of aerosol water particles having an isotropic scattering phase function leads to a model that is similar to that successfully used by Gordon[55,56] for Coastal Zone Color Scanner imagery.

A rigorous model of the above development was not attempted. Rather, a simplified approximation was developed that is within the capabilities of the LOWTRAN 6 model. The Henyey-Greenstein aerosol scattering phase function modeling option was used in place of the LOWTRAN 6 database of Mie aerosol scattering phase functions This option allows explicit control over the shape of the aerosol scattering phase function. The Henyey-Greenstein phase function is given by:

$$P(\theta) = \frac{1}{4\pi} \frac{1-g^2}{(1-2g\cos\theta+g^2)^{3/2}} \qquad (2.3.3\text{-}1)$$

where: θ is the scattering angle and

g is the asymmetry parameter

The asymmetry parameter, g, controls the shape of the aerosol scattering phase function. A value of g equal to +1 gives complete forward scattering, 0 gives isotropic scattering, and -1 gives complete backward scattering.

No attempt was made to model a decrease in atmospheric molecular water vapor concentration as water particle aerosols are formed. Separate models of dust-like and water particle aerosols were also not included. Inclusion of these factors, although simple in concept, would require major modification to the LOWTRAN 6 model.

Using the Henyey-Greenstein phase function with an asymmetry parameter of zero, and adjusting the input VIS parameter, allowed the modeled atmospheric upwelling path radiance to cover the entire range observed in the TM Band 4 lake image. This approach is essentially that used by Gordon[55] for correction of CZCS image data.

Figure 2.3.3-1 illustrates the aerosol scattering phase function as selected from the LOWTRAN 6 database along with the Henyey-Greenstein phase function for several asymmetry parameters.

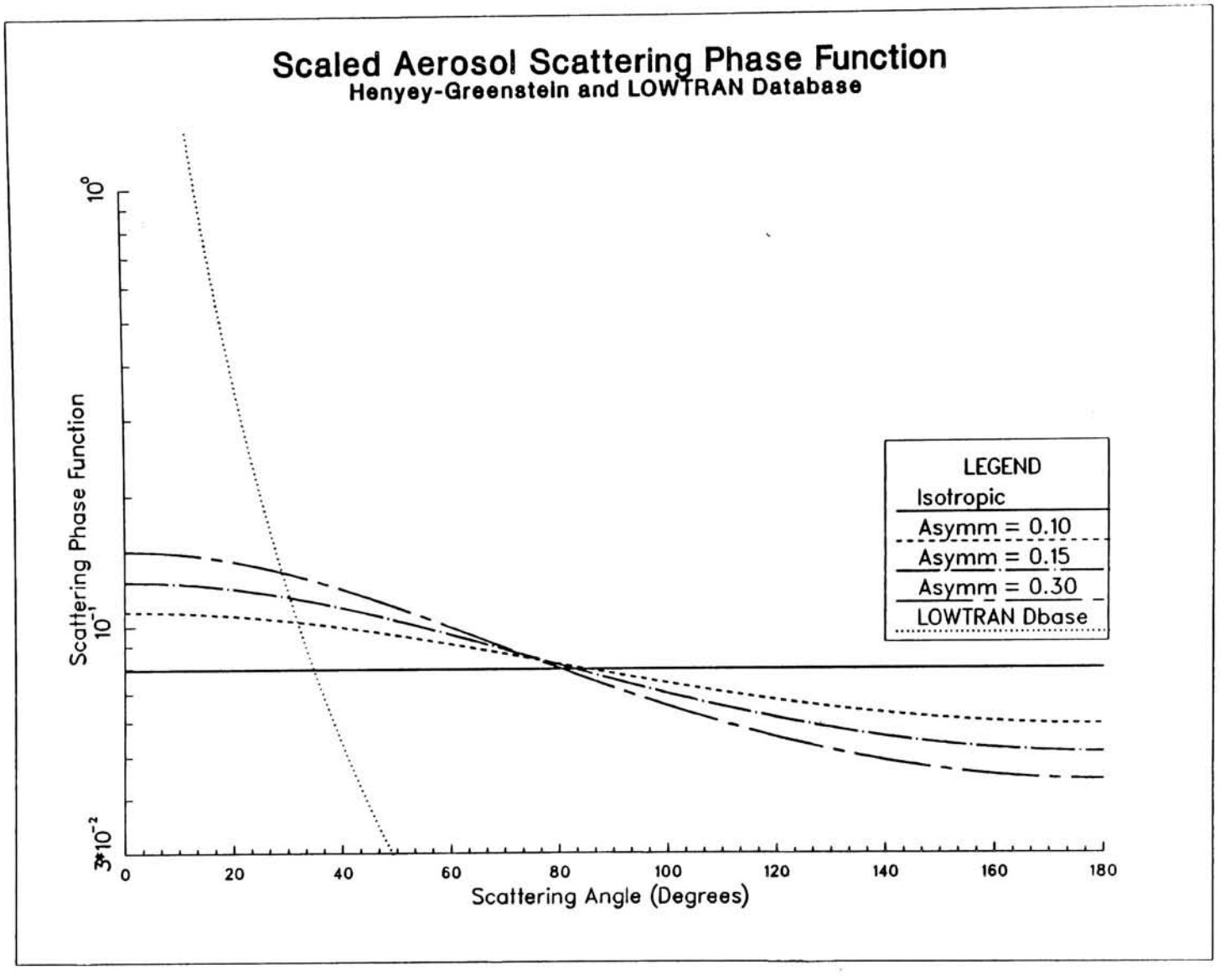

Figure 2.3.3-1 LOWTRAN 6 and Henyey-Greenstein Aerosol Scattering Phase Functions

2.3.4 Creation Of The Atmospheric Correction Look-Up Tables

Look-up tables for the correction of the spatially varying atmospheric effects were created by repeated execution of the program LOWHGP (Appendix F). Figure 2.3.4-1 illustrates the process used to create the atmospheric transmittance and upwelling path radiance correction look-up tables.

A histogram of the water-only areas of the TM Band 4 image was used to define the range of atmospheric upwelling path radiance magnitudes that had to be modeled for the 0.76-0.90μm spectral band region. For each digital count value observed in the water areas a conversion to in-band radiance was made using calibration data and a series of interactive runs of the program LOWHGP had to be made. For each program run, the value of the input VIS parameter was modified. These modifications were repeatedly made until the program produced an output modeled image digital count that matched the observed image digital count under consideration. The largest value of the VIS parameter that produced such a match was the value recorded for later use.

When all of the observed water region digital counts had been assigned a corresponding VIS parameter, modeling of the atmospheric effects for the TM Band 1, 2 and 3 images was done. This modeling consisted of running the program LOWHGP again for each of the spectral regions and each modeled VIS parameter. For each spectral region, a list of modeled values of atmospheric transmittance and upwelling path radiance was made. Each element of the list corresponds to an input value of VIS and to some TM Band 4 observed value of atmospheric upwelling path radiance. Therefore, for each TM Band 4 water region digital count, a modeled value for the atmospheric transmittance and upwelling path radiance was made for all other TM image bands.

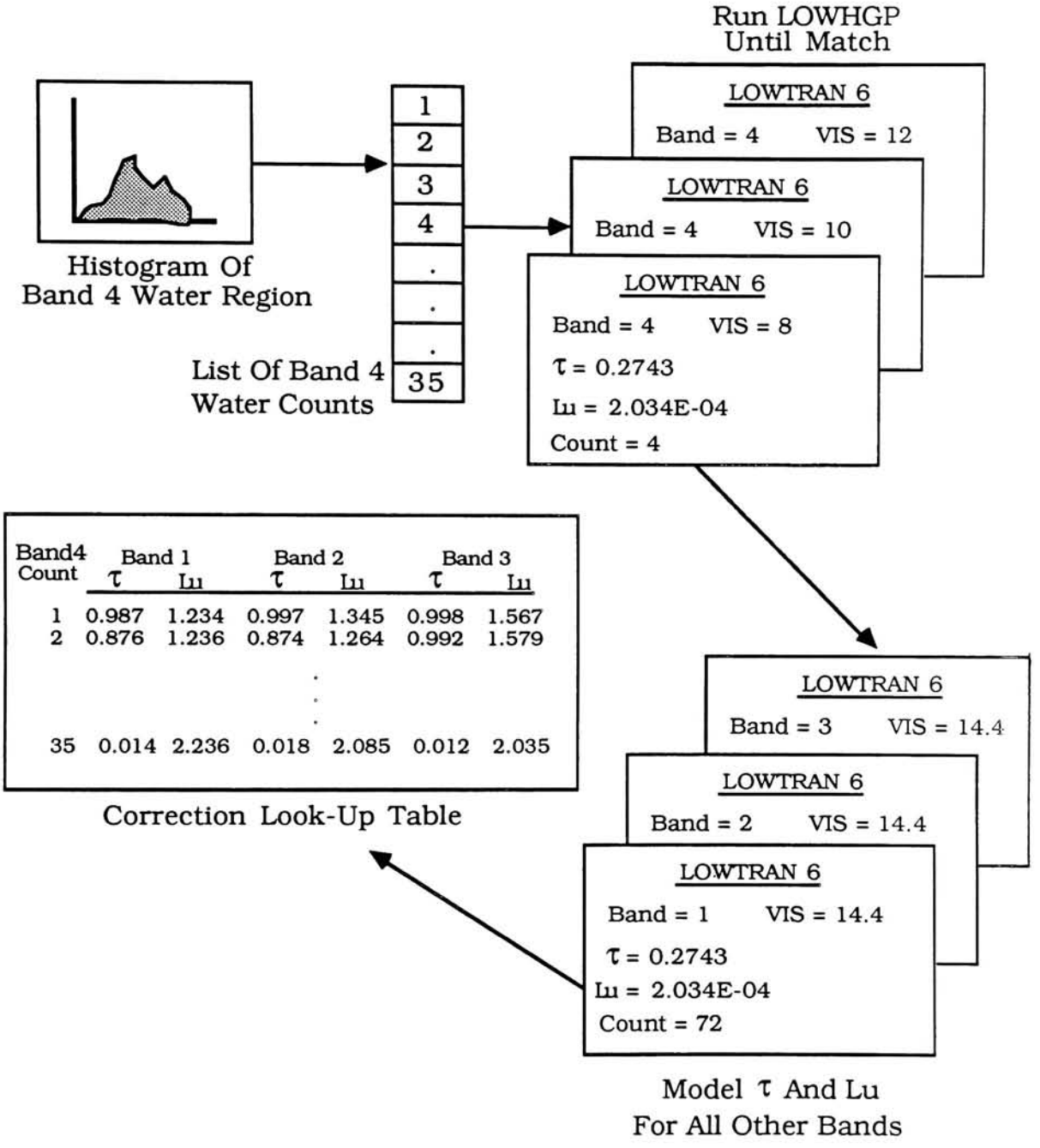

Figure 2.3.4-1

Creation Of Atmospheric Correction
Look-Up Tables

The Henyey-Greenstein asymmetry parameter for the aerosol scattering phase function was kept constant for all of the program runs used to create each atmospheric correction look-up table. Because the best choice for the Henyey-Greenstein asymmetry parameter can not be found deterministically, a series of look-up tables was created using asymmetry parameter values of 0.0, 0.10, 0.15 and 0.20. The choice of best Henyey-Greenstein asymmetry parameter to be used was then made empirically by applying each correction look-up table to all of the images and observing the number of negative water radiance values computed. Computed values of water radiance indicate over-corrected pixels.

2.3.5 Utility Of The TM Band 4 Image For Determining Atmospheric Upwelling Radiance

The efficacy of the atmospheric correction technique described here depends tremendously on the assumption of zero water reflectivity in the TM Band 4 spectral band region (0.76-0.90μm). The use of the TM Band 5 image would lessen concerns about the quality of the zero water reflectivity assumption because radiation in that spectral region (1.55-1.75μm) can only penetrate a few millimeters into the water body and is much less likely to be affected by water contaminants. The TM Band 5 image for the 22 June 1984 Lake Ontario scene, however, suffered from very significant horizontal striping caused by inter-detector miscalibration. This striping rendered the image unusable because the striping artifact would have become imposed on all of the image data using it as an atmospheric reference.

A verification of the zero water reflectivity assumption for the TM Band 4 image was made by computing and comparing pseudoreflectance values computed

from each of the two images. A pseudoreflectance value was determined for each water region pixel in each image by solving Equation 1.3.1-31 for $r(\theta,\theta',\phi)$. Estimates of the solar irradiance at the water surface, atmospheric downwelling sky radiance, atmospheric upwelling path radiance and atmospheric transmittance were computed using the LOWTRAN 6 model using a Henyey-Greenstein asymmetry parameter value of 0.15 and a VIS parameter value of 31.3 km. for the reasons described in Section 3.2-1 The term pseudoreflectance is used because all of the atmospheric modeling parameters were considered to be uniform across the scene for the calculation and no corrections for Fresnel reflection or the TM Band 5 striping were made.

Since the assumption of zero water reflectance is quite good for the TM Band 5 spectral region but is questionable for the TM Band 4 spectral region a comparison of water pseudoreflectance values computed from the TM Band 4 and TM Band 5 images was made. Although the water reflectance calculations are not rigorous, if similar values are computed using both images then the assumption of zero water reflectance for the TM Band 4 spectral region can be considered valid for this particular case. Table 2.3.5-1 lists the atmospheric modeling parameters used to compute the TM Band 4 and TM Band 5 water pseudoreflectance values. The pseudoreflectance calculation results are presented in Section 3.1.

Table 2.3.5-1

TM Band Number	Solar Radiance (W/cm^2-Sr)	Sky Radiance (W/cm^2-Sr)	Upwelling Radiance (W/cm^2-Sr)	Transmittance
4	1.158×10^{-2}	1.107×10^{-4}	9.886×10^{-5}	0.8130
5	4.111×10^{-3}	9.871×10^{-6}	7.086×10^{-6}	0.9134

2.4 Image Processing For Pixel-By-Pixel Atmospheric Haze Reduction

The correction look-up tables described in Section 2.3.5 were applied to the LANDSAT TM image data using the program CORRECT_ATMOS (Appendix G). Figure 2.4-1 illustrates the image processing performed using the correction look-up tables to create the water surface radiance map images.

Program CORRECT_ATMOS applies the correction look-up tables to an image using Equation 2.3.1-4. A TM Band 4 water mask image (Section 2.2) and the image to be corrected are both input into the program. For nonzero pixel count values in the water mask image that are less than 255 (water region pixels) the TM Band 4 pixel count was used as an index into each of the correction look-up table to retrieve the modeled atmospheric upwelling radiance and atmospheric transmittance required to correct the atmosphere at that point in the image.

The pixel count values in the image to be corrected are converted to radiance values based on the LANDSAT TM calibration mapping provided for the particular image. The atmospheric upwelling path radiance selected from the correction look-up table is subtracted from the pixel radiance measure and the result is divided by the selected atmospheric transmittance. The resulting water surface radiance value is then converted to a pixel count value by applying the original calibration mapping. All pixel counts outside the 0-255 range are appropriately clipped to produce an unsigned 8-bit number. The pixel count data is then stored to form a corrected image.

For the pixel values in the TM Band 4 water region mask equal to 255 (non-water areas) no look-up table search was done. Instead, the modeled atmospheric data from look-up table position

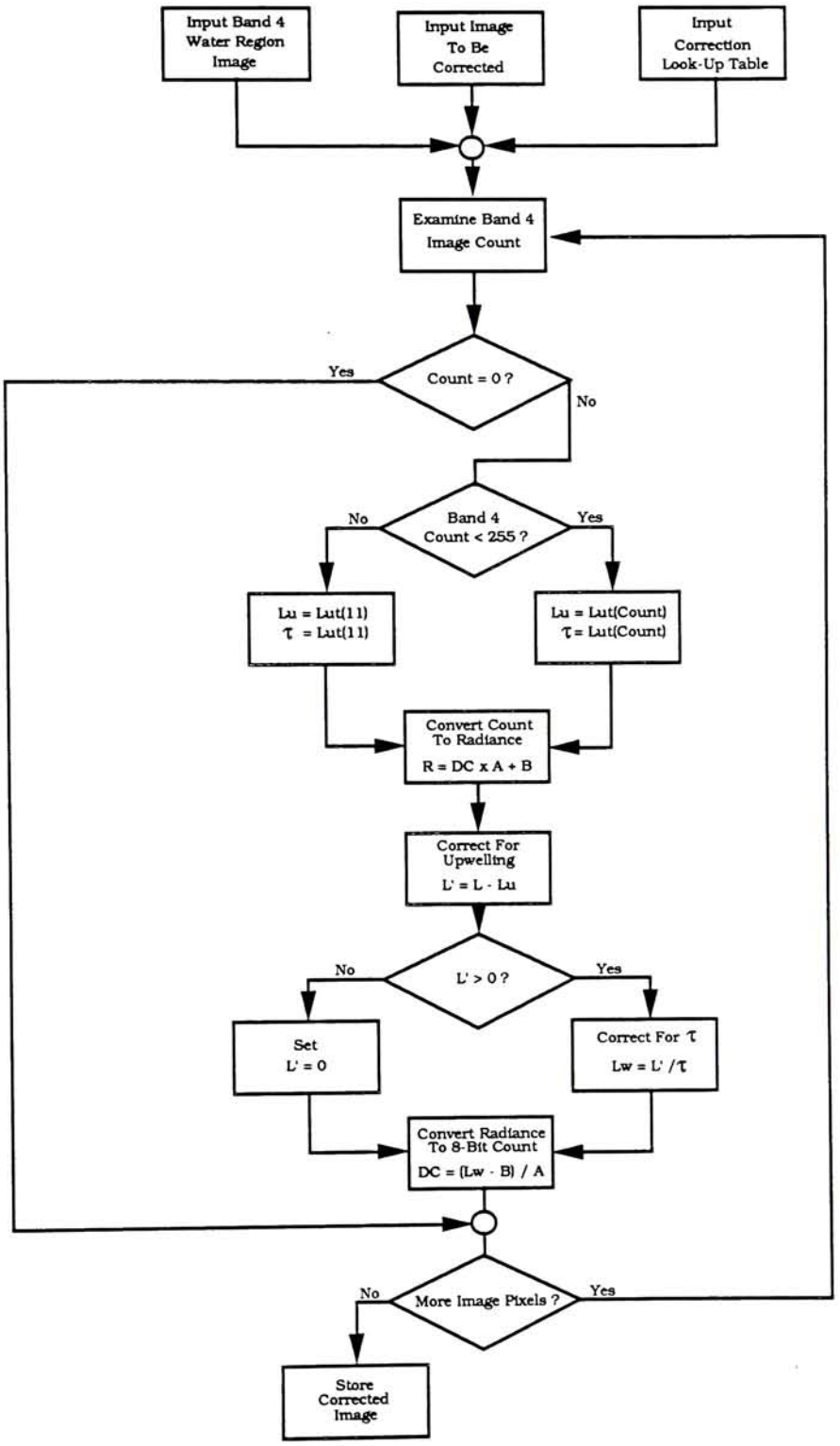

Figure 2.4-1

Flow Chart for the Program CORRECT_ATMOS

11 was used to correct that point in the image. These points correspond to the non-water areas of the image and the uniform atmospheric correction performed on those areas provides a nominal atmospheric correction Look-up table position 11 corresponds to the peak of the histogram of the TM Band 4 water region masked image.

For the pixel values in the TM Band 4 water region mask equal to zero, no correction was performed. TM Band 4 water region mask pixel values of zero are assigned to the fill pixels at the ends of each image line. The zero fill pixels are copied to the same positions in the corrected image.

The above procedure produced an image that has been corrected for atmospheric upwelling path radiance and transmittance everywhere but has had the corrections performed on a pixel-by-pixel basis for all of the image water regions.

If for any point in the image the modeled atmospheric upwelling path radiance value is greater than the observed image radiance that point is assigned a zero radiance value and no atmospheric corrections were applied.

The CORRECT_ATMOS program also computes the image mean, standard deviation, minimum pixel value and maximum pixel value before and after the atmospheric correction has been performed. A report is generated each time the program is run listing the statistics and informing the user of the number of pixel counts that had to be clipped to 0 or 255 after remapping to the 8-bit range.

Imagery for comparison with those processed using the CORRECT_ATMOS program was also created. Because the atmospheric correction process produces imagery having increased contrast, it is difficult to visually compare a processed image with the original. A program, LINFUNC (Appendix G), was written to produce

imagery for comparison with that processed using the pixel-by-pixel atmospheric haze reduction technique. Program LINFUNC performs Equation 2.3.1-4 on an input image using a single value each of atmospheric upwelling path radiance and atmospheric transmittance. Program LINFUNC was used to process the TM Band 1, TM Band 2 and TM Band 3 image data for both the 22 June 1984 scene and the 25 May 1985 scene. Look-up table position 11 values of the modeled atmospheric parameters were again used to produce comparison imagery that has contrast comparable to imagery processed using the CORRECT_ATMOS program.

3.0 Results

Although the goal of this research is to develop a tool that can improve the quantitative utility of remotely sensed imagery of water there are few quantitative measures available that can be used to verify the efficacy of the of the pixel-by-pixel atmospheric correction technique. Because no water surface data is available for the Lake Ontario scenes used for this work, it is necessary to infer the usefulness of the atmospheric correction technique from a combination of qualitative analysis of the processed imagery and the little quantitative data that are available. As the following discussion will illustrate, the inferences made here are indeed convincing enough so that further work, of a planned numerically rigorous nature, is warranted.

3.1 Verification of the Utility of the TM Band 4 Image for Determining Atmospheric Upwelling Radiance

As discussed in Section 2.3.5, the quality of the assumption of zero water reflectance in the TM Band 4 spectral region (0.76-0.90μm) is not assured. The use of the TM Band 5 image to define the atmospheric upwelling path radiance would provide a solid foundation for the zero reflectance assumption because of the shallow penetration of radiation into water in this spectral region (1.55-1.75μm). Use of the TM Band 5 image was not possible for this work because detector miscalibration induced a horizontal streaking artifact into the image data.

Pseudoreflectance values for each water pixel in both the TM Band 4 and TM Band 5 images of the 22 June 1984 Lake Ontario scene were computed as described in Section 2.3.6. The pseudoreflectance data is presented in Figures 3.1-1 and 3.1-2 and shows that, indeed, very similar values of water surface reflectance are computed from each band. Although some of the values of reflectance presented are much greater than the assumed zero value, this can be explained simply as contamination

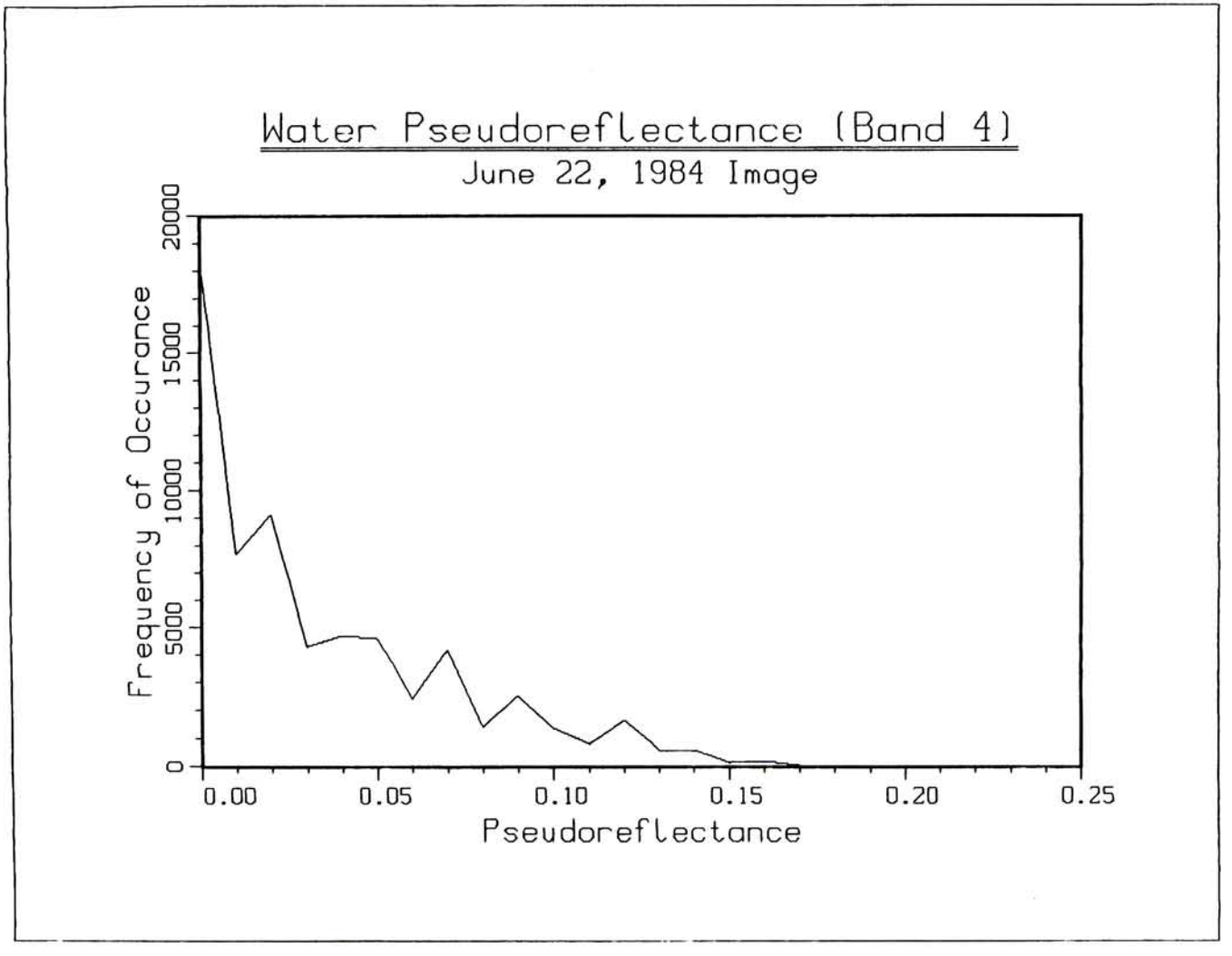

Figure 3.1-1 22 June 1984 TM Band 4 Water Pseudoreflectance Histogram

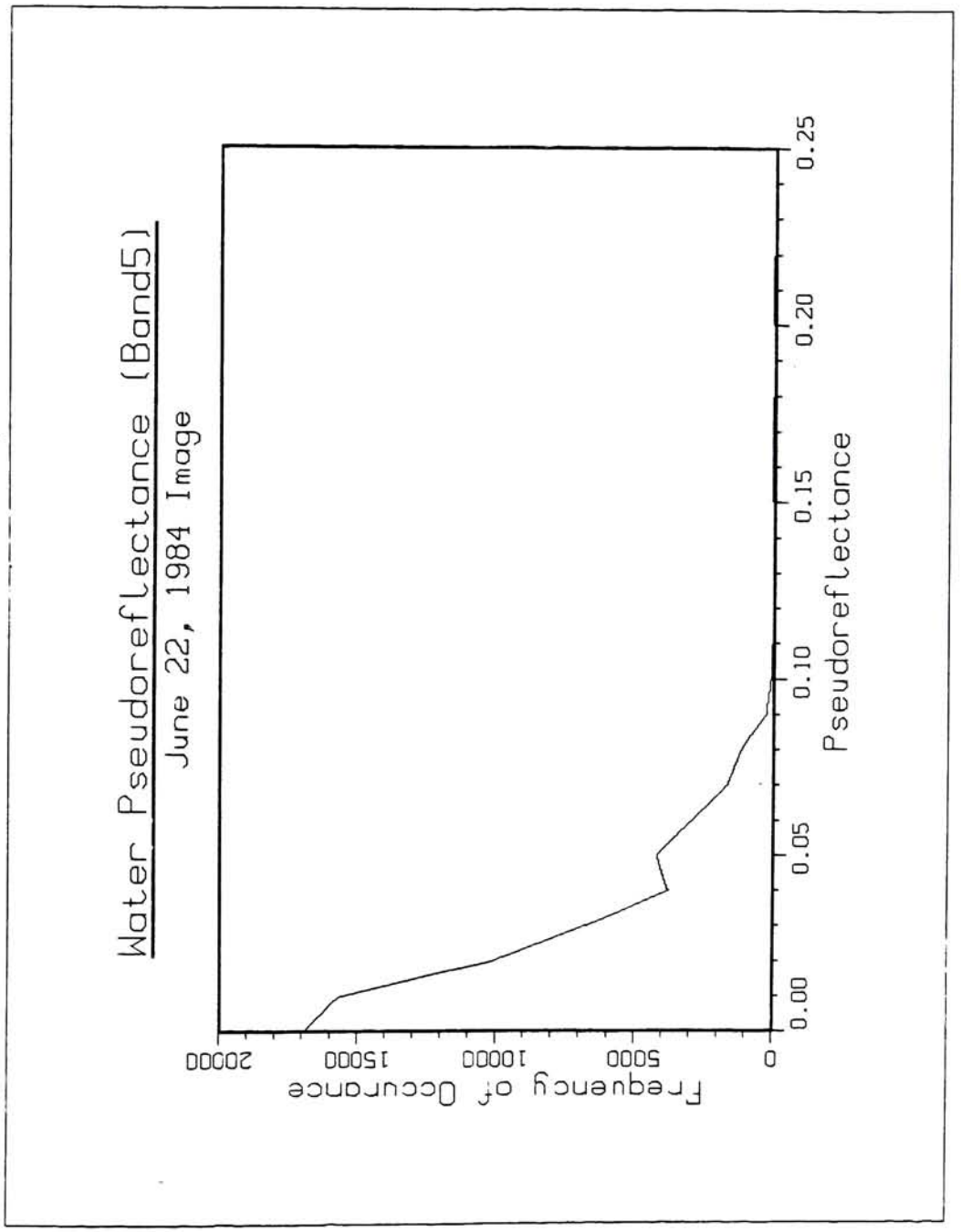

Figure 3.1-2 **22 June 1984 TM Band 5 Water Pseudoreflectance Histogram**

effects caused by the atmosphere. Since only a single, average value of transmittance and path radiance were used for each image, any spatial perturbation of the atmospheric effect would lead to inflated values for water reflectance.

Given that the assumption of zero water reflectance for the TM Band 5 spectral region is valid (Section 1.2.1), all of the radiance values measured from the TM Band 5 water image can be attributed to the radiance of the atmospheric path between the water surface and the LANDSAT satellite.

Water pseudoreflectance values measured from the TM Band 5 image produced a mean reflectance of 0.023 with a standard deviation of 0.025. The mean is not zero because only a nominal atmospheric correction was made to the image.

Water pseudoreflectance values measured from the TM Band 4 image produced a mean reflectance of 0.037 with a standard deviation of 0.052. The increased mean and standard deviation for the TM Band 4 pseudoreflectance simply indicates that the atmosphere has a larger impact on the total signal in that spectral region.

Since the mean water pseudoreflectance calculated from the TM Band 4 image is within just one standard deviation of the mean water pseudoreflectance calculated from the TM Band 5 image the assumption of zero water reflectance for the TM Band 4 spectral region will be considered valid for the work described here.

3.2 Examination of the Corrected Image Data

Several features within the 22 June 1984 Lake Ontario scene suggested that a pixel-by-pixel atmospheric correction technique would produce improved atmospheric correction. Comparison of the TM Band 1 image with the TM Band 4

image from the scene (Figures 2.1-2 and 2.1-5) gives some insight into how well such a correction technique could perform.

The TM Band 1 image displays several features in the water body that are not clearly atmospheric or water characteristics. There is a very large, bright, plume visible in the southwestern portion of the lake that is suspected to be caused by turbid water flowing into the lake from the Niagara River. At the eastern end of the plume, however, is a narrow bright region that extends over both the water and the nearby shore. This narrow region is obviously a semi-transparent cloud or a region of increased haze rather than something in the water. Distinguishing this narrow cloud from the suspected Niagara River plume is difficult, and it is uncertain whether the plume is all or in part an atmospheric rather than a water contribution to the radiance signal.

The Genesse River also appears to cause a small plume of turbid water to be injected into the lake near the southeastern corner of the image. There is also a bright band along the southern shore of the lake that could be either a ring of increased water turbidity or simply an atmospheric effect. The center areas of the TM Band 1 lake image also show localized patches of increased brightness that could be caused by either the atmosphere or the water body.

There are two regions that are obviously cloud areas owing to their texture and opacity. The northeastern corner of the scene appears to be cloud covered although some water may be visible in some areas, and a strip of clouds runs northwest to southeast across the center of the lake and extends over the shoreline at both ends.

Interestingly, the TM Band 4 image shows the same cloud regions and the bright band along the southern shore of the lake but the Genesse River plume is

much less pronounced and the suspected Niagara River plume is not visible at all. The large patches of increased brightness near the center of the lake are also visible in the TM Band 4 image.

Since both plume areas visible in the TM Band 1 image emanate from known river areas, it is very likely that the plumes are both radiance signals from the water and not simply an atmospheric effect. Since the some other areas of increased brightness in the TM Band 1 image do not appear as bright areas in the TM Band 4 image it is reasonable to think that the TM Band 4 image can be successfully used as a guide for correcting the atmospheric effects in the TM Band 1 image.

3.2.1 Comparison of Atmospheric Corrections Using Several Values of the Henyey-Greenstein Asymmetry Parameter

Because the best Henyey-Greenstein asymmetry parameter to use in describing the scattering phase function of the atmospheric hydrosols is not obvious, four different atmospheric correction look-up tables were created using asymmetry parameters of 0.0, 0.10, 0.15, and 0.20. A value of 0.0 for the asymmetry parameter corresponds to isotropic aerosol scattering (See Figure 2.3.3-1) The atmospheric correction look-up tables are presented in Tables 3.2.1-1 through 3.2.1-3.

Using an asymmetry parameter of zero produces a look-up table where the modeled upwelling path radiance was often greater than the radiance observed in the TM Band 1 water image. This indicated that an isotropic aerosol scattering phase function assumption was too simplistic and leads to an exaggeration of the atmospheric effects by the LOWTRAN 6 model.

Although the use of an isotropic aerosol scattering phase function with the LOWTRAN 6 model produces a model that is very similar to Gordon's atmospheric

correction model[55], his model also assumes that the aerosol scattering extinction is spectrally independent. The LOWTRAN 6 model does not and selects a spectral scattering extinction function that increases slightly with decreasing wavelength. This may account for the difference between the results reported here and those reported by Gordon.

Increasing the amount of forward scattering in the model produced data that was more consistent with the observed image data. Use of 0.10 for the asymmetry parameter produced very few cases of modeled upwelling path radiance that were larger than the observed image radiance for the TM Band 1 water image. Figure 3.2.1-1 shows the results of using a value of 0.10 for the asymmetry parameter with the pixel-by-pixel atmospheric correction technique. An image having a uniform atmospheric correction is presented for comparison.

The plumes from both the Niagara River and the Genessee River have been preserved in the pixel-by-pixel corrected image while the patches of increased brightness near the center of the lake have been removed. The narrow cloud near the eastern end of the Niagara River plume was not removed, however. Areas immediately adjacent to the plume do appear to have been corrected using the pixel-by-pixel technique so it is probable that this cloud area is too opaque to allow its removal from the scene. The region of increased brightness along the southern shore of the lake has become darker than the remainder of the water in the corrected image. It is difficult to imagine how the area of the lake closest to shore could be less turbid than the center of the lake, in fact, quite the opposite is more likely to be observed. Given that the region closest to shore is less deep than the center of the lake, the TM Band 1 image would also be more susceptible to bottom effects near the shoreline giving an even greater signal.

Table 3.2.1-1

Atmospheric Correction Look-Up Table
Henyey-Greenstein Asymmetry Parameter = 0.10

Band 4 Count	LOWTRAN 6 Met. Range (Km)	Band 1 Transmittance	Band 1 Upwell (W/cm^2-Sr)	Band 2 Transmittance	Band 2 Upwell (W/cm^2-Sr)	Band 3 Transmittance	Band 3 Upwell (W/cm^2-Sr)	Band 4 Transmittance	Band 4 Upwell (W/cm^2-Sr)
7	158.89	0.7842	2.2786E-04	0.8430	1.4892E-04	0.8969	5.9332E-05	0.8930	5.3181E-05
8	97.89	0.7581	2.4217E-04	0.8196	1.6334E-04	0.8767	6.7982E-05	0.8776	6.4514E-05
9	69.89	0.7319	2.5592E-04	0.7960	1.7738E-04	0.8561	7.6506E-05	0.8618	7.5921E-05
10	53.79	0.7056	2.6917E-04	0.7722	1.9110E-04	0.8353	8.4936E-05	0.8456	8.7349E-05
11	43.39	0.6794	2.8185E-04	0.7482	2.0441E-04	0.8142	9.3219E-05	0.8291	9.8731E-05
12	36.90	0.6565	2.9248E-04	0.7272	2.1573E-04	0.7955	1.0035E-04	0.8122	1.1012E-04
13	30.60	0.6262	3.0584E-04	0.6992	2.3018E-04	0.7706	1.0959E-04	0.7949	1.2153E-04
14	26.49	0.5999	3.1683E-04	0.6747	2.4227E-04	0.7486	1.1744E-04	0.7771	1.3300E-04
15	23.19	0.5734	3.2738E-04	0.6498	2.5409E-04	0.7261	1.2524E-04	0.7589	1.4438E-04
16	20.16	0.5460	3.3808E-04	0.6237	2.6603E-04	0.7021	1.3319E-04	0.7399	1.5573E-04
17	17.25	0.5189	3.4792E-04	0.5977	2.7731E-04	0.6781	1.4084E-04	0.7201	1.6717E-04
18	15.79	0.4929	3.5685E-04	0.5726	2.8773E-04	0.6547	1.4803E-04	0.6998	1.7859E-04
19	13.79	0.4644	3.6603E-04	0.5448	2.9865E-04	0.6285	1.5570E-04	0.6788	1.8997E-04
20	12.47	0.4369	3.7430E-04	0.5176	3.0870E-04	0.6028	1.6291E-04	0.6571	2.0134E-04
21	11.16	0.4091	3.8208E-04	0.4900	3.1837E-04	0.5763	1.6998E-04	0.6345	2.1274E-04
22	19.00	0.5334	3.4267E-04	0.6118	2.7126E-04	0.6912	1.3672E-04	0.6109	2.2414E-04
23	8.85	0.3527	3.9611E-04	0.4328	3.3645E-04	0.5206	1.8365E-04	0.5863	2.3554E-04
24	7.84	0.3240	4.0237E-04	0.4031	3.4486E-04	0.4912	1.9026E-04	0.5603	2.4700E-04
25	6.96	0.2951	4.0806E-04	0.3728	3.5275E-04	0.4607	1.9663E-04	0.5331	2.5838E-04
26	6.18	0.2659	4.1320E-04	0.3417	3.6014E-04	0.4290	2.0279E-04	0.5042	2.6975E-04
27	5.47	0.2358	4.1788E-04	0.3091	3.6713E-04	0.3952	2.0883E-04	0.4734	2.8115E-04
28	4.83	0.2056	4.2196E-04	0.2756	3.7349E-04	0.3598	2.1455E-04	0.4401	2.9256E-04
29	4.24	0.1750	4.2549E-04	0.2408	3.7928E-04	0.3221	2.2000E-04	0.4039	3.0395E-04
30	3.69	0.1440	4.2845E-04	0.2046	3.8442E-04	0.2818	2.2510E-04	0.3634	3.1542E-04
31	3.16	0.1122	4.3089E-04	0.1660	3.8896E-04	0.2374	2.2989E-04	0.3179	3.2680E-04
32	2.63	0.0791	4.3282E-04	0.1239	3.9284E-04	0.1868	2.3434E-04	0.2645	3.3816E-04

Table 3.2.1-2

Atmospheric Correction Look-Up Table
Henyey-Greenstein Asymmetry Parameter = 0.15

Band 4 Count	LOWTRAN 6 Met. Range (Km)	Band 1 Transmittance	Band 1 Upwell (W/cm^2-Sr)	Band 2 Transmittance	Band 2 Upwell (W/cm^2-Sr)	Band 3 Transmittance	Band 3 Upwell (W/cm^2-Sr)	Band 4 Transmittance	Band 4 Upwell (W/cm^2-Sr)
6	298.89	0.8050	2.1217E-04	0.8615	1.3377E-04	0.9129	5.0532E-05	0.9052	4.1730E-05
7	130.78	0.7750	2.2661E-04	0.8348	1.4831E-04	0.8899	5.9224E-05	0.8877	5.3122E-05
8	81.79	0.7451	2.4044E-04	0.8079	1.6244E-04	0.8665	6.7787E-05	0.8698	6.4528E-05
9	58.69	0.7150	2.5366E-04	0.7807	1.7617E-04	0.8428	7.6219E-05	0.8514	7.5926E-05
10	45.19	0.6847	2.6636E-04	0.7531	1.8957E-04	0.8185	8.4572E-05	0.8324	8.7393E-05
11	36.39	0.6543	2.7844E-04	0.7252	2.0254E-04	0.7938	9.2782E-05	0.8132	9.8722E-05
12	30.19	0.6238	2.8990E-04	0.6970	2.1509E-04	0.7686	1.0086E-04	0.7934	1.1013E-04
13	25.59	0.5933	3.0074E-04	0.6684	2.2718E-04	0.7430	1.0878E-04	0.7730	1.2152E-04
14	21.86	0.5625	3.1128E-04	0.6394	2.3899E-04	0.7166	1.1660E-04	0.7517	1.3293E-04
15	18.83	0.5316	3.2128E-04	0.6100	2.5040E-04	0.6895	1.2430E-04	0.7295	1.4436E-04
16	16.34	0.5006	3.3068E-04	0.5801	2.6134E-04	0.6617	1.3183E-04	0.7065	1.5574E-04
17	14.26	0.4693	3.3952E-04	0.5495	2.7187E-04	0.6330	1.3922E-04	0.6826	1.6715E-04
18	12.59	0.4393	3.4737E-04	0.5200	2.8144E-04	0.6051	1.4608E-04	0.6577	1.7855E-04
19	11.90	0.4253	3.5082E-04	0.5061	2.8573E-04	0.5918	1.4920E-04	0.6316	1.8999E-04
20	9.68	0.3734	3.6254E-04	0.4539	3.0070E-04	0.5414	1.6039E-04	0.6044	2.0139E-04
21	8.49	0.3430	3.6863E-04	0.4228	3.0876E-04	0.5108	1.6664E-04	0.5756	2.2182E-04
22	7.33	0.3077	3.7495E-04	0.3861	3.1744E-04	0.4742	1.7356E-04	0.5451	2.2423E-04
23	6.40	0.2745	3.8019E-04	0.3509	3.2493E-04	0.4385	1.7976E-04	0.5129	2.3555E-04
24	5.57	0.2403	3.8488E-04	0.3140	3.3194E-04	0.4003	1.8580E-04	0.4778	2.4703E-04
25	4.83	0.2056	3.8893E-04	0.2756	3.3831E-04	0.3598	1.9154E-04	0.4401	2.5834E-04
26	4.16	0.1707	3.9232E-04	0.2358	3.4397E-04	0.3166	1.9691E-04	0.3980	2.6979E-04
27	3.53	0.1346	3.9510E-04	0.1933	3.4897E-04	0.2690	2.0198E-04	0.3505	2.8123E-04
28	2.92	0.0974	3.9727E-04	0.1474	3.5323E-04	0.2155	2.0665E-04	0.2955	2.9255E-04
29	2.39	0.0645	3.9864E-04	0.1045	3.5620E-04	0.1625	2.1024E-04	0.2266	3.0399E-04

Table 3.2.1-3

Atmospheric Correction Look-Up Table
Henyey-Greenstein Asymmetry Parameter = 0.20

Band 4 Count	LOWTRAN 6 Met. Range Km	Band 1 Transmittance	Band 1 Upwell W/cm^2-Sr	Band 2 Transmittance	Band 2 Upwell W/cm^2-Sr	Band 3 Transmittance	Band 3 Upwell W/cm^2-Sr	Band 4 Transmittance	Band 4 Upwell W/cm^2-Sr
6	239.89	0.7990	2.1123E-04	0.8562	1.3329E-04	0.9083	5.0433E-05	0.9017	4.1723E-05
7	108.89	0.7648	2.2512E-04	0.8257	1.4748E-04	0.8819	5.8996E-05	0.8814	5.3164E-05
8	68.39	0.7300	2.3859E-04	0.7942	1.6148E-04	0.8546	6.7571E-05	0.8606	6.4544E-05
9	49.19	0.6953	2.5124E-04	0.7627	1.7487E-04	0.8270	7.5919E-05	0.8391	7.5966E-05
10	37.89	0.6604	2.6322E-04	0.7308	1.8782E-04	0.7988	8.4132E-05	0.8169	8.7413E-05
11	30.49	0.6256	2.7444E-04	0.6986	2.0022E-04	0.7701	9.2145E-05	0.7942	9.8802E-05
12	25.18	0.5901	2.8511E-04	0.6655	2.1229E-04	0.7403	1.0010E-04	0.7708	1.1014E-04
13	21.04	0.5547	2.9543E-04	0.6321	2.2396E-04	0.7098	1.0789E-04	0.7462	1.2155E-04
14	17.78	0.5193	3.0511E-04	0.5981	2.3514E-04	0.6785	1.1551E-04	0.7204	1.3295E-04
15	15.15	0.4834	3.1415E-04	0.5633	2.4584E-04	0.6460	1.2297E-04	0.6934	1.4437E-04
16	13.90	0.4632	3.1891E-04	0.5436	2.5160E-04	0.6274	1.2706E-04	0.6654	1.5575E-04
17	11.23	0.4107	3.3020E-04	0.4915	2.6567E-04	0.5778	1.3731E-04	0.6358	1.6715E-04
18	9.69	0.3737	3.3724E-04	0.4542	2.7478E-04	0.5416	1.4419E-04	0.6046	1.7856E-04
19	8.25	0.3362	3.4359E-04	0.4157	2.8331E-04	0.5038	1.5084E-04	0.5715	1.8996E-04
20	7.05	0.2982	3.4925E-04	0.3761	2.9122E-04	0.4641	1.5723E-04	0.5361	2.0134E-04
21	6.02	0.2594	3.5423E-04	0.3347	2.9853E-04	0.4218	1.6340E-04	0.4977	2.1279E-04
22	5.13	0.2202	3.5846E-04	0.2919	3.0510E-04	0.3771	1.6922E-04	0.4560	2.2415E-04
23	4.33	0.1799	3.6200E-04	0.2464	3.1097E-04	0.3283	1.7474E-04	0.4093	2.3559E-04
24	3.60	0.1387	3.6480E-04	0.1983	3.1604E-04	0.2747	1.7984E-04	0.3562	2.4698E-04
25	2.90	0.0961	3.6688E-04	0.1458	3.2024E-04	0.2135	1.8449E-04	0.2926	2.5844E-04
26	2.18	0.0519	3.6825E-04	0.0871	3.2346E-04	0.1399	1.8853E-04	0.2114	2.6976E-04
27	1.25	0.0086	3.6920E-04	0.0194	3.2574E-04	0.0407	1.9173E-04	0.0799	2.8115E-04

This tends to indicate that the image may have been over-corrected. This over-correction suspicion is supported by the results observed from the corrected TM Band 2 image (Figure 3.2.1-2). Although the correction appears to be successful, more than 64 percent of the water pixels had to be set to zero count because the modeled upwelling path radiance was greater than the radiance observed in the image.

Changing the asymmetry parameter from 0.10 to 0.15 reduced the number of water pixels in the TM Band 2 image that had to be set to zero count by more than a factor of ten. Results for the TM Band 1 image also appeared to be significantly improved. (See Figures 3.2.1-4 and 3.2.1-5) The bright region along the southern shore of the lake was now corrected to a radiance that is very similar to the other water areas, while both river plumes remain as visible as in the corrected TM Band 1 image that used 0.10 for the asymmetry parameter.

The western end of the original lake scene shows regions of increased haze that is somewhat textured. Both the TM Band 1 and the TM Band 2 corrected images have successfully removed the textured haze, confirming that the increased brightness was, indeed, caused by the atmosphere, and implying that the pixel-by-pixel correction technique appears successful.

The TM Band 3 corrected image results (Figure 3.2.1-6) indicates that the correction may not be as successful as at first hoped. Similar to the TM Band 2 results observed using 0.10 for the asymmetry parameter, the TM Band 3 image had to have 63 percent of the water pixels set to zero count because the modeled values of upwelling path radiance exceeded the observed values in the image. This inconsistency indicated that perhaps again the images had been over-corrected.

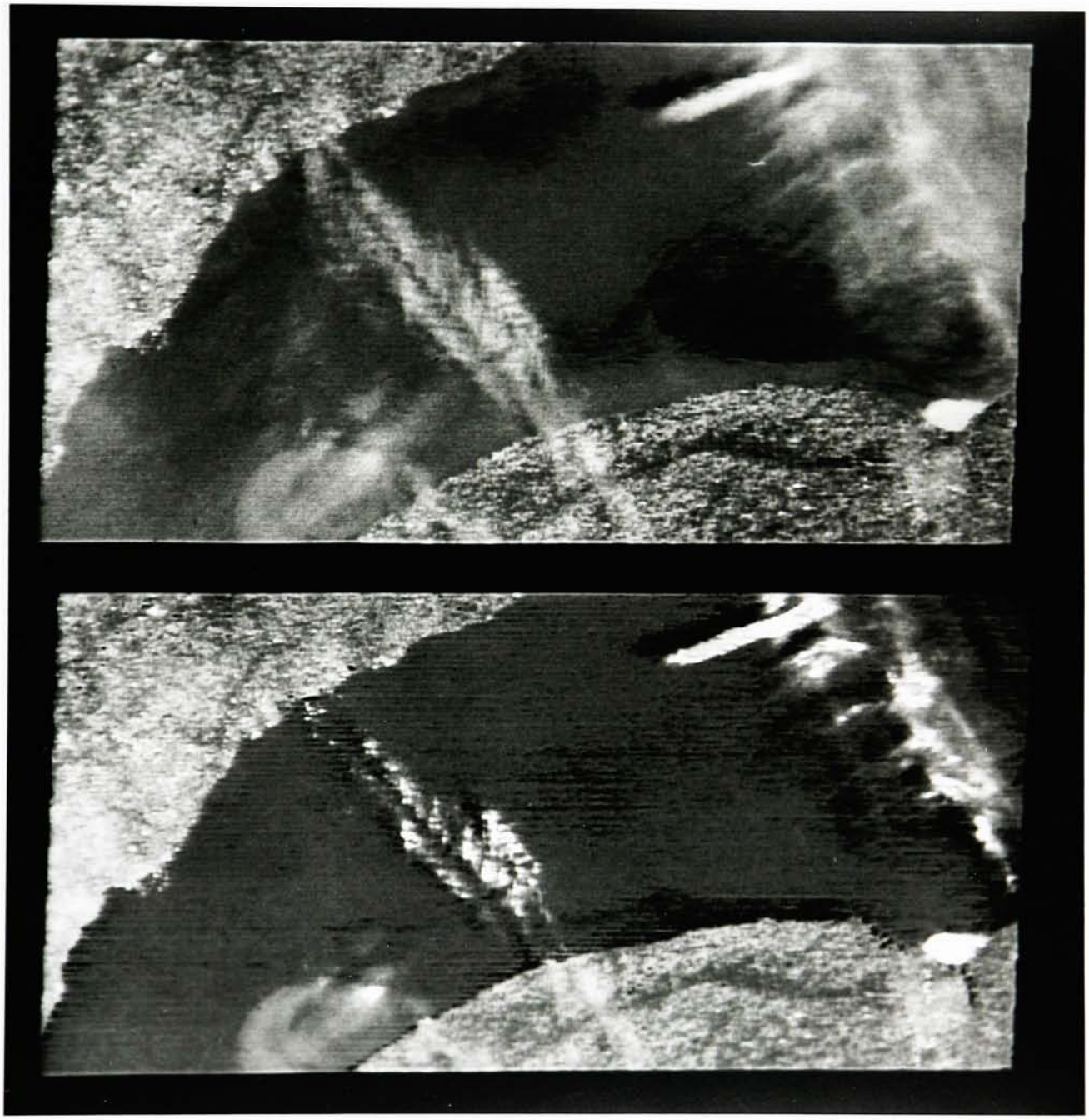

Figure 3.2.1-1 TM Band 1 Image of the June 24, 1984 Lake Ontario Scene Processed Using a Henyey-Greenstein Asymmetry Parameter of 0.010

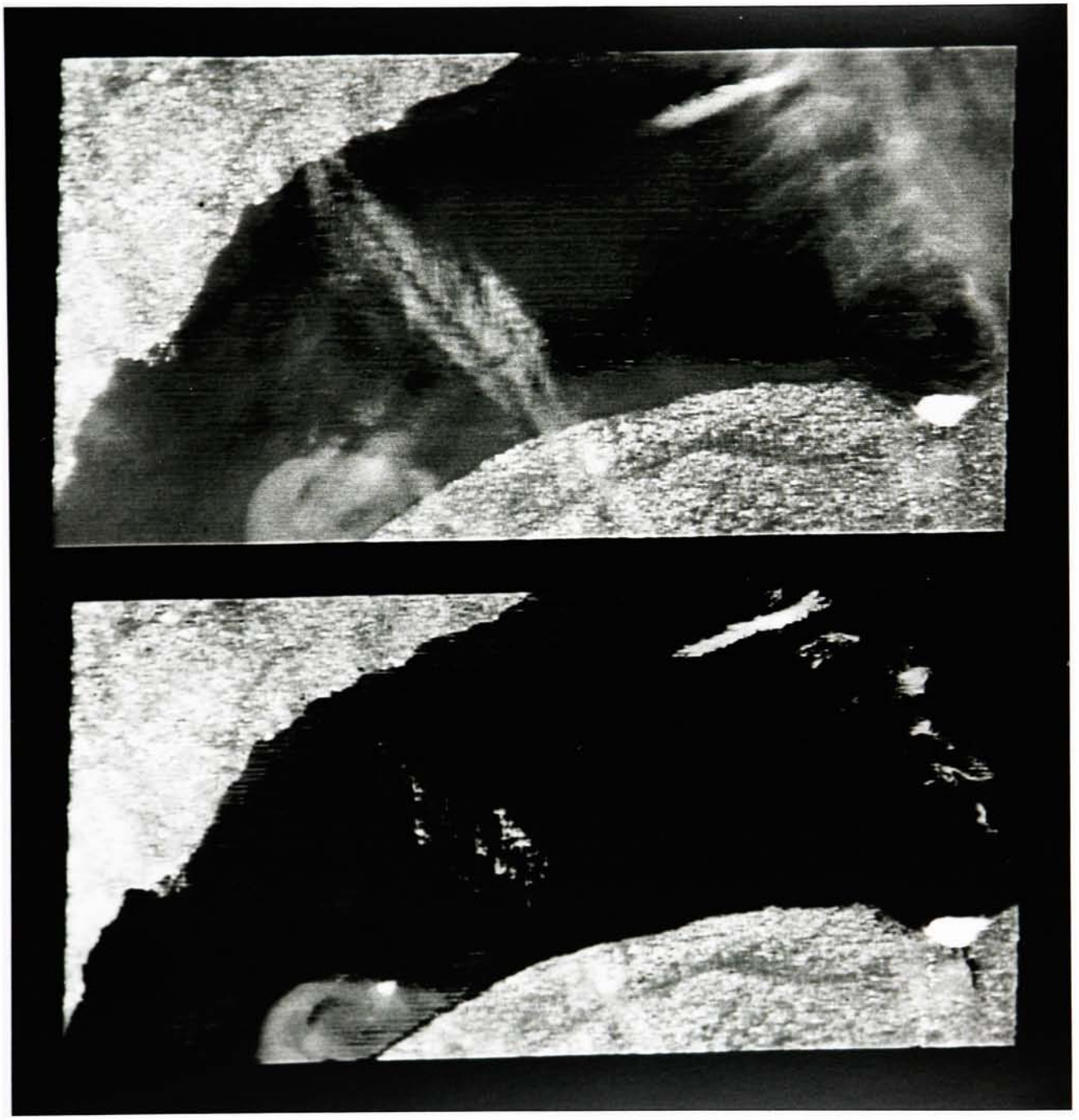

Figure 3.2.1-2 TM Band 2 Image of the June 24, 1984 Lake Ontario Scene Processed Using a Henyey-Greenstein Asymmetry Parameter of 0.10

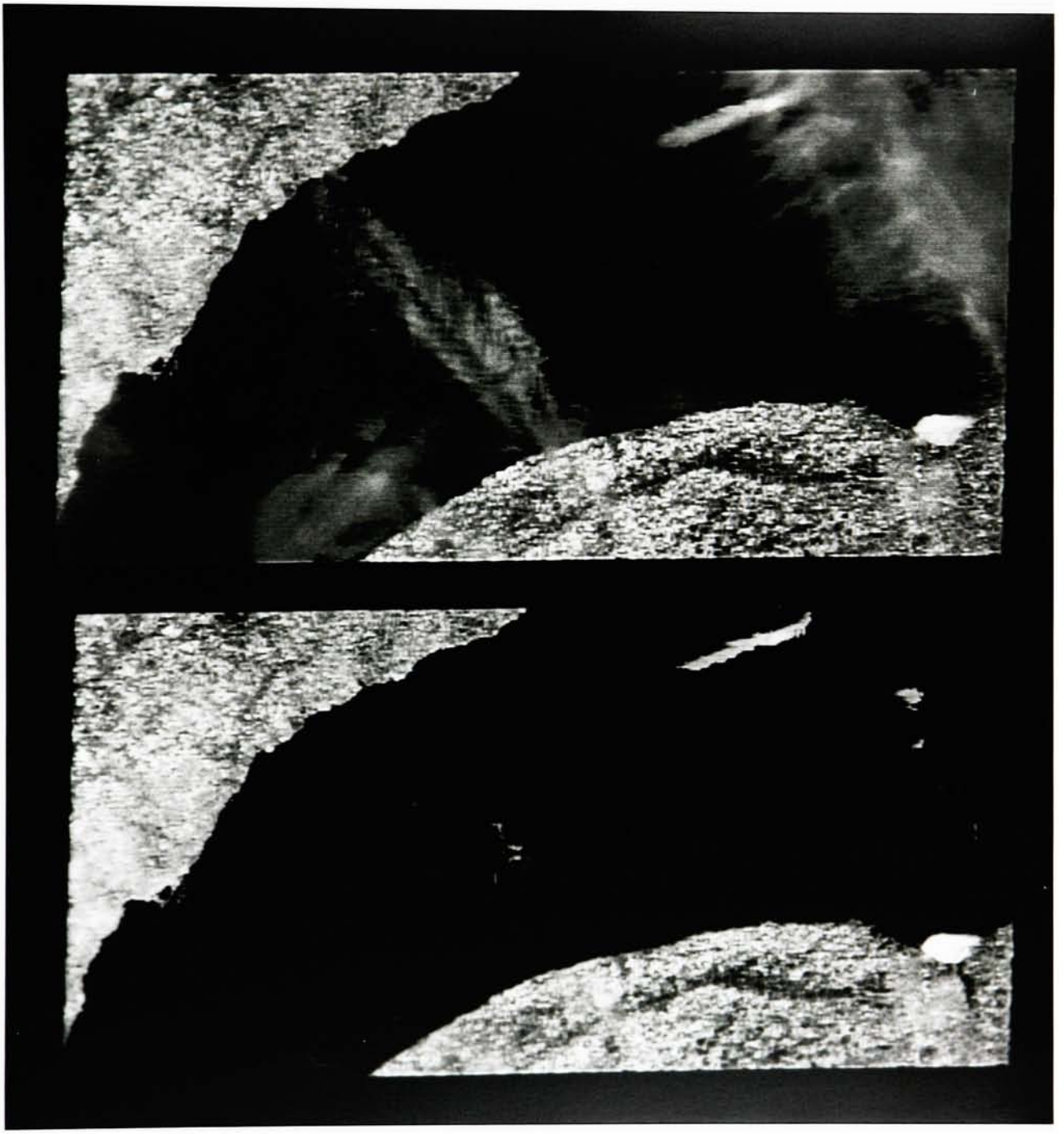

Figure 3.2.1-3 TM Band 3 Image of the June 24, 1984 Lake Ontario Scene Processed Using a Henyey-Greenstein Asymmetry Parameter of 0.10

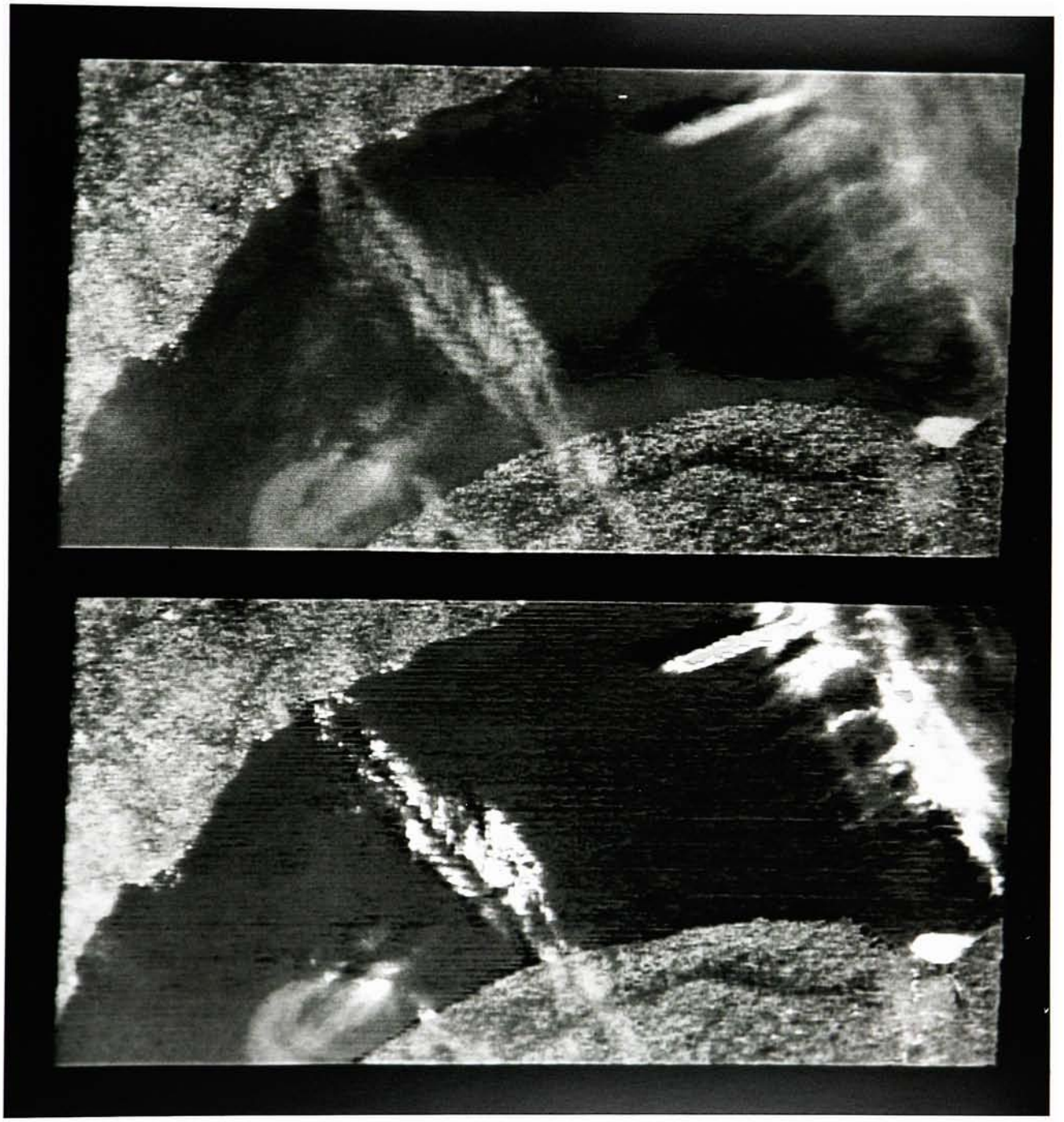

Figure 3.2.1-4 TM Band 1 Image of the June 24, 1984 Lake Ontario Scene Processed Using a Henyey-Greenstein Asymmetry Parameter of 0.15

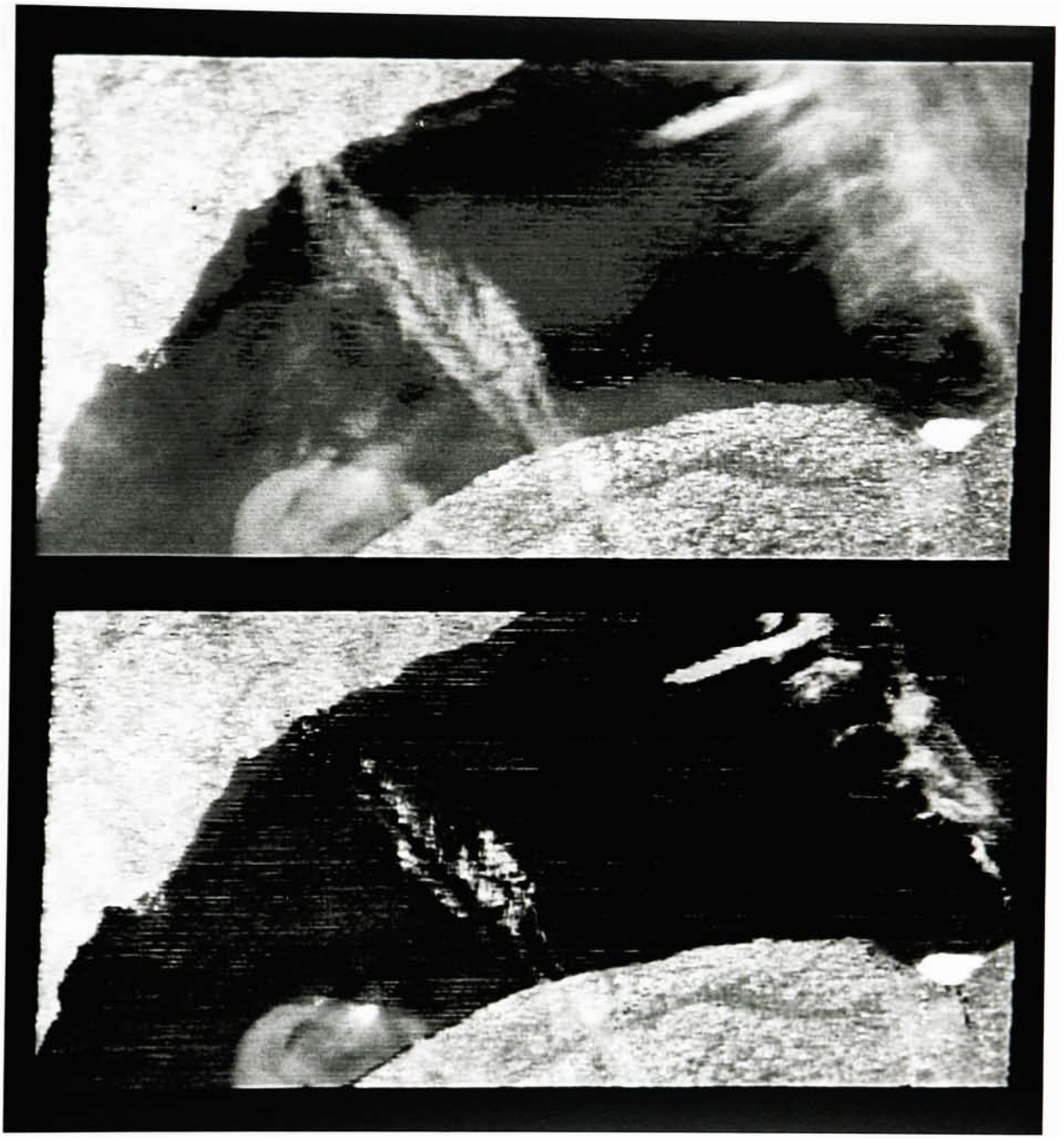

Figure 3.2.1-5 TM Band 2 Image of the June 24, 1984 Lake Ontario Scene Processed Using a Henyey-Greenstein Asymmetry Parameter of 0.15

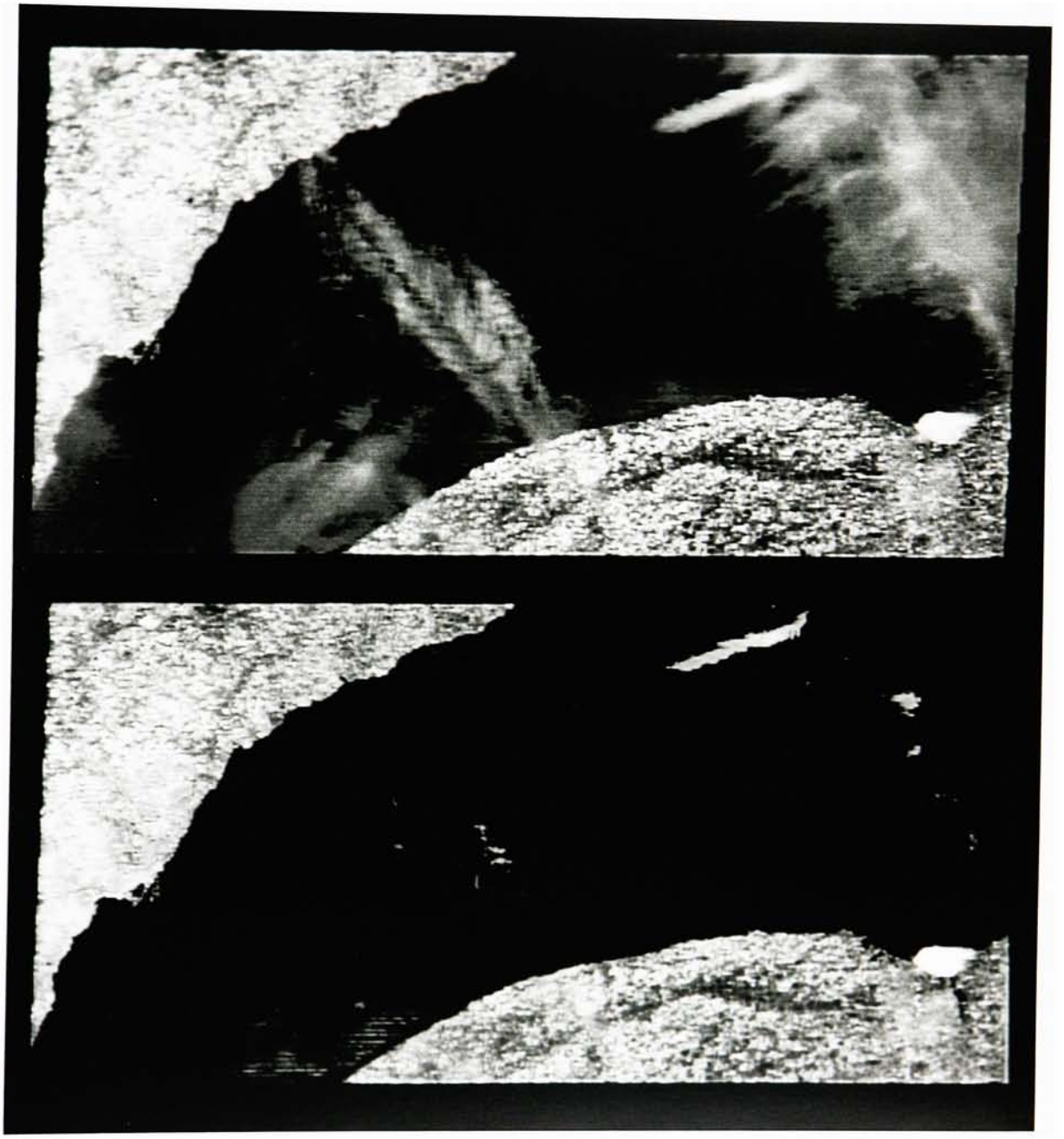

Figure 3.2.1-6 TM Band 3 Image of the June 24, 1984 Lake Ontario Scene Processed Using a Henyey-Greenstein Asymmetry Parameter of 0.15

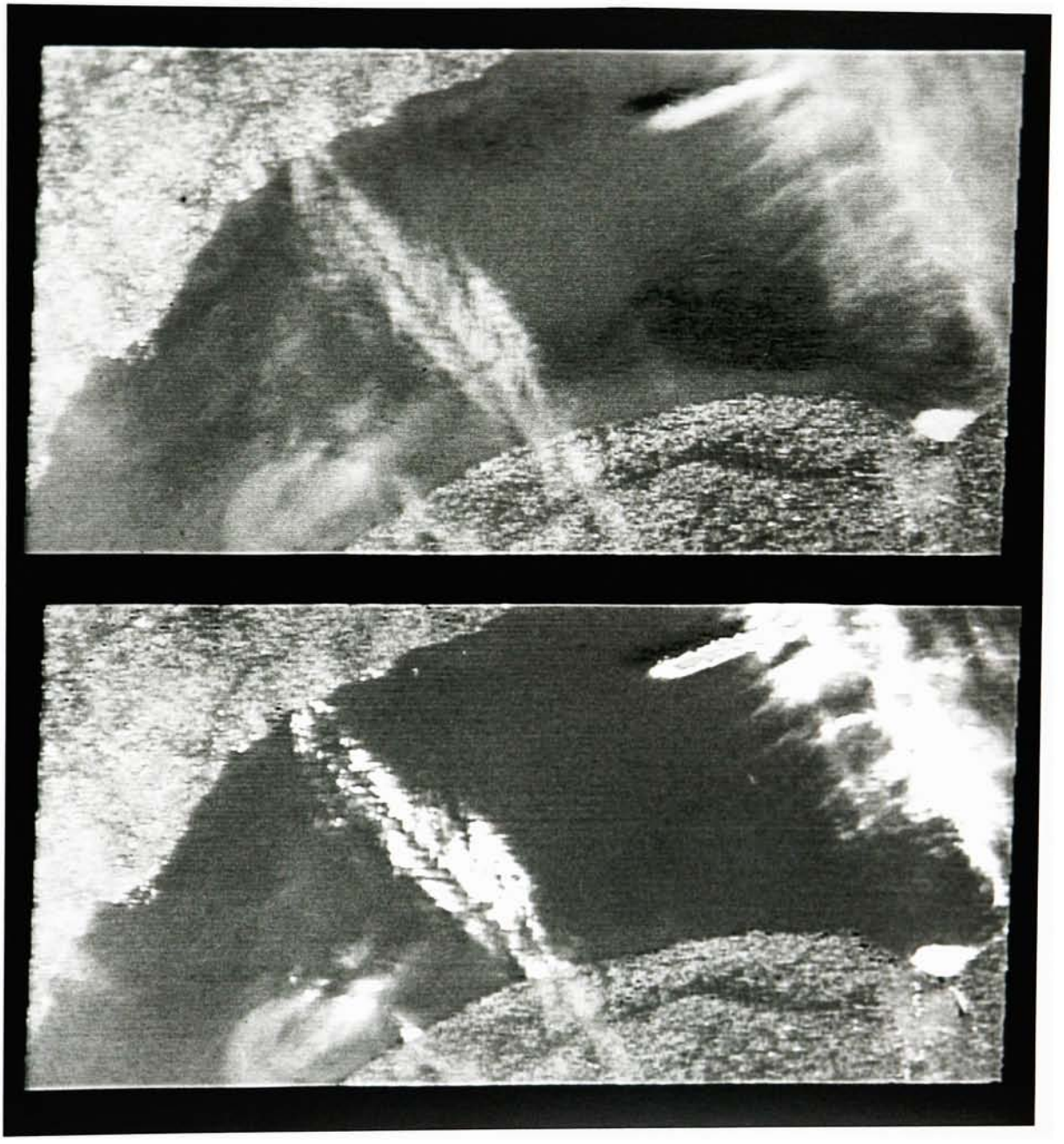

Figure 3.2.1-7 TM Band 1 Image of the June 24, 1984 Lake Ontario Scene Processed Using a Henyey-Greenstein Asymmetry Parameter of 0.20

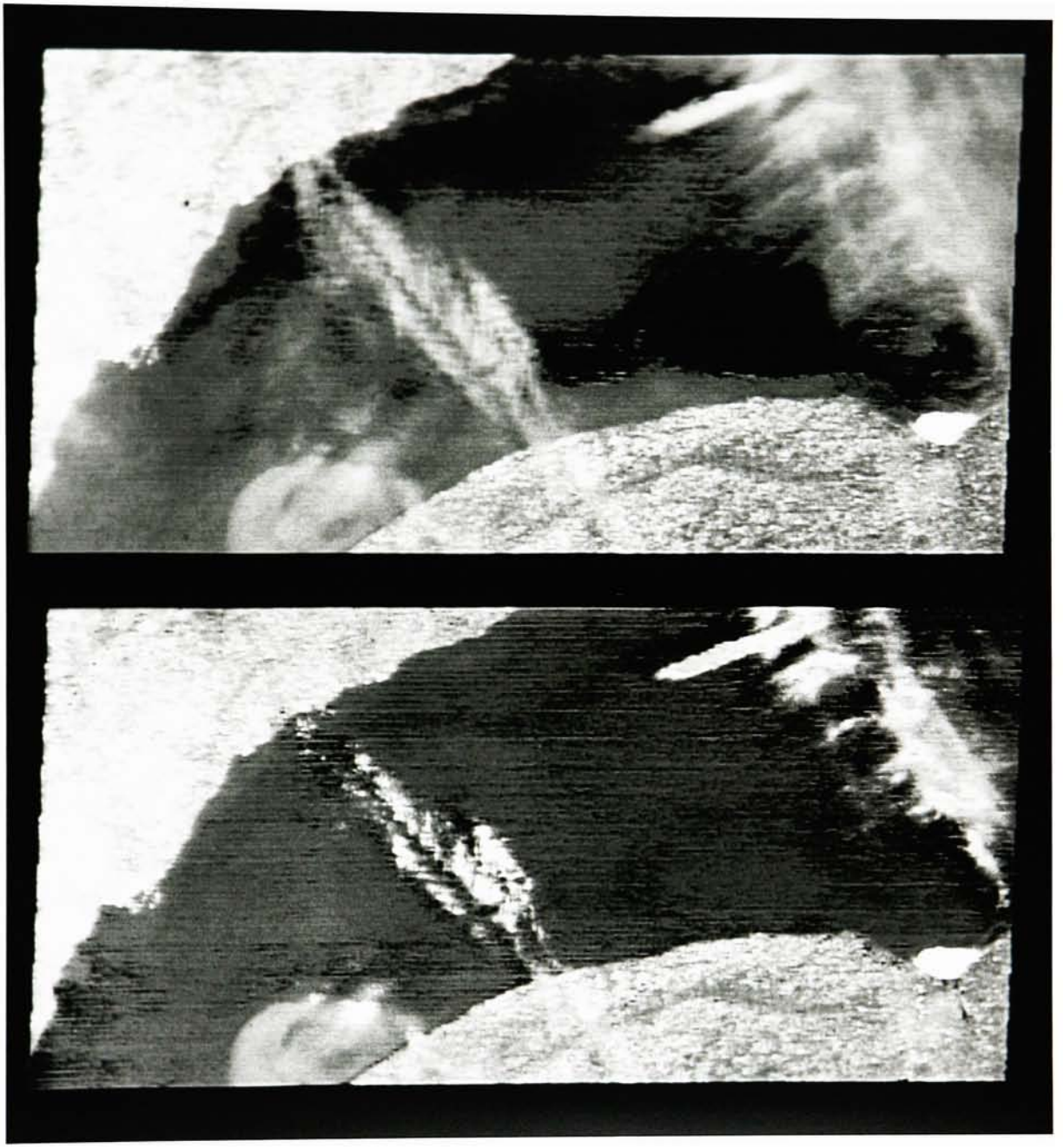

Figure 3.2.1-8 TM Band 2 Image of the June 24, 1984 Lake Ontario Scene Processed Using a Henyey-Greenstein Asymmetry Parameter of 0.20

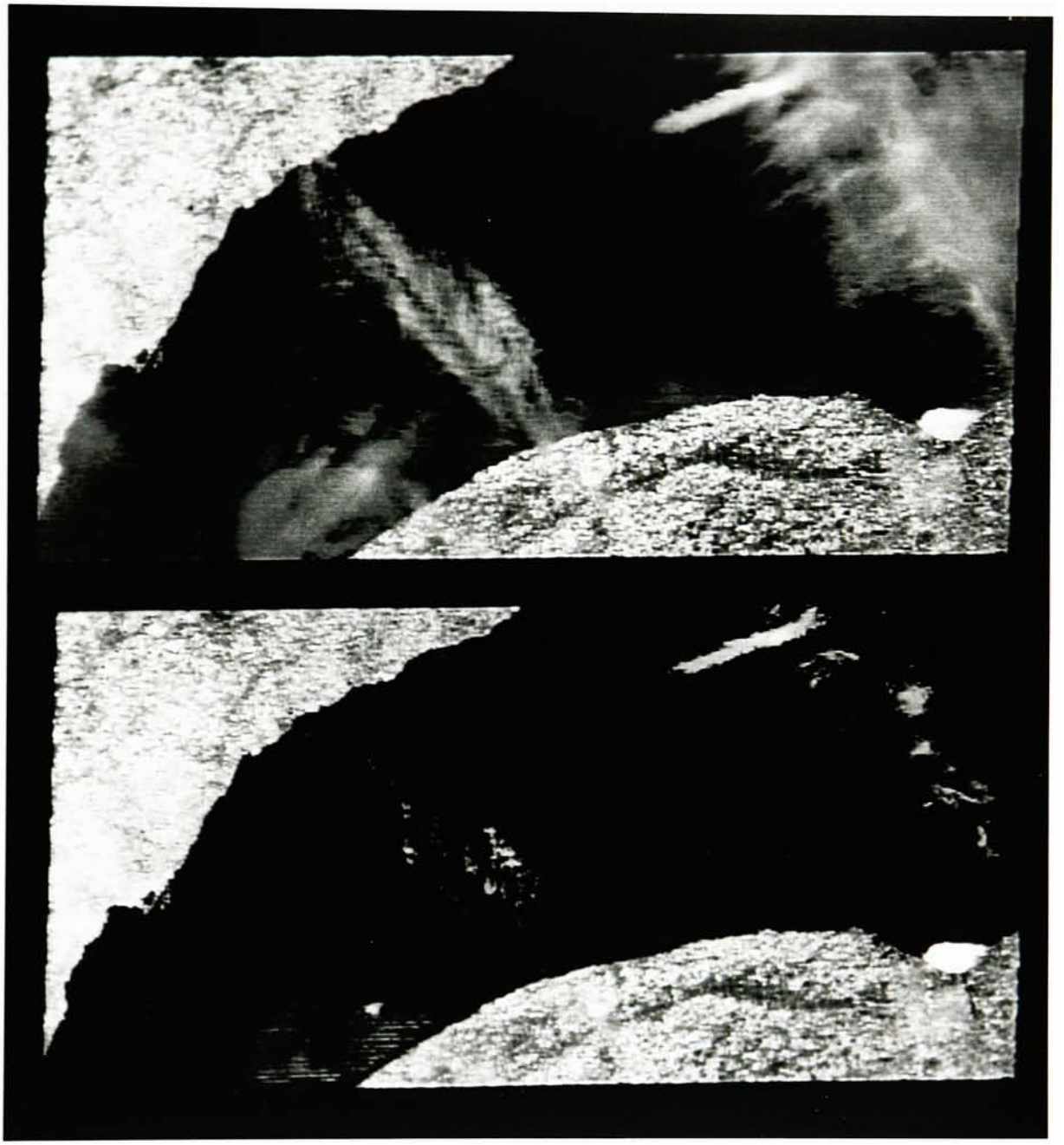

Figure 3.2.1-9 TM Band 3 Image of the June 24, 1984 Lake Ontario Scene Processed Using a Henyey-Greenstein Asymmetry Parameter of 0.20

A new atmospheric correction table using an asymmetry parameter of 0.20 was made and corrected imagery computed. (Figures 3.2.1-7 through 3.2.1-9). The corrections made on the the TM Band 1 and 2 images appeared to be similar to those made using an asymmetry parameter of 0.15 except that the textured atmospheric haze at the Western end of the lake could not be completely removed. The corrections for the TM Band 3 image were not significantly improved using the new correction table. The new corrected TM Band 3 image required just over 60 percent of the water pixels to be set to zero count because of over-estimation of the atmospheric upwelling path radiance.

Because of the very limited improvement in the atmospheric correction observed for the TM Band 3 water image, and the reduction in quality for the atmospheric correction of the TM Band 1 and TM Band 2 water images, a value of 0.15 for the asymmetry parameter was determined to be the most suitable for describing the composite aerosol scattering phase function for use with the pixel-by-pixel atmospheric correction technique.

The inability of the technique to correct the TM Band 3 image without forcing most of the water pixels to be set to zero count could be due to several causes. The technique, as implemented, could simply be overcorrecting all portions of the image in all of the bands but the overcorrection is more obvious in the TM Band 3 image because of the reduced path radiance in that band. Alternatively, the true water reflectance in the TM Band 3 spectral region may be close to zero but the proximity of the TM Band 3 and TM Band 4 spectral regions may be too close for the LOWTRAN 6 model to correctly model the TM Band 3 upwelling radiance. Some insight into the reason may be had through analysis of the results of application of the technique to a second image.

3.2.2 Application of the Pixel-By-Pixel Atmospheric Correction Technique to a Second Image

Because of the difficulty in quantifying the results of the application of the pixel-by-pixel atmospheric correction technique to a real image of water, the technique was applied to a second image of water for comparison. As described in Section 2.1, a second LANDSAT-5 TM image of Lake Ontario was processed using the pixel-by-pixel atmospheric correction technique. This second scene, presented in Figures 2.1-9 through 2.1-13, was imaged on 25 May 1985. This scene does not exhibit any of the confusion between atmospheric and water body contributions to the radiance signal observed in the 22 June 1984 scene. This scene is included here to illustrate the effects of the technique on an image that has little spatial atmospheric variability.

The May scene exhibits increased brightness around the perimeter of the lake, much like that observed in the 22 June 1984 scene, but this brightness is certainly an effect caused by the water body itself, not the atmosphere. This can be stated with confidence because nowhere do the areas of increased brightness extend over land, and these areas are not as uniform as those observed in the June scene.

Some haze areas are visible near the center of the lake and near the eastern edge of the lake image. It was expected that the pixel-by-pixel atmospheric correction technique would remove these haze areas and have little or no effect on the bright perimeter.

The results of the application of the technique to the image are presented in Figures 3.2.2-1 through 3.2.2-3. The corrected images were made using the same procedures developed for the 22 June 1984 scene. A Henyey-Greenstein asymmetry parameter of 0.15 was used for the aerosol scattering phase function and an

atmospheric correction look-up table was developed based on the radiance data from the TM Band 4 water image for the May scene.

As expected, the perimeter remains brighter than the center of the lake and the two areas of localized haze have been removed. Additionally, it should be noted that in the uniform areas of the center of the lake image, the technique introduced no visible processing artifacts.

Examination of the results of the application of the technique to TM Band 3 of the May scene may provide some insight into the efficacy of the technique. The average difference between the observed water radiance and the upwelling path radiance, as modeled by the technique, is 2.6 digital counts with about ten percent of the differences being negative. The average difference for the June scene is -7.1 digital counts with about sixty three percent of the differences being negative. Less than one percent of differences were negative for the TM Band 1 images of both scenes. This indicates that the spectral characteristics of the scattering are being insufficiently modeled. If the Henyey-Greenstein parameters had been selected to provide good corrections for the TM Band 3 image from both scenes then the May TM Band 1 image would have been slightly undercorrected while the June TM Band 1 scene would have exhibited significant undercorrection. This result would be consistent with underestimation of multiply-scattered radiation by using a single-scattering atmospheric model, therefore the lack of multiple scattering capability in the LOWTRAN 6 model is likely to be the cause of the overcorrected TM Band 3 imagery. The use of the technique with an atmospheric model having multiple scattering capability would then be expected to provide significant improvements in the pixel-by-pixel correction results.

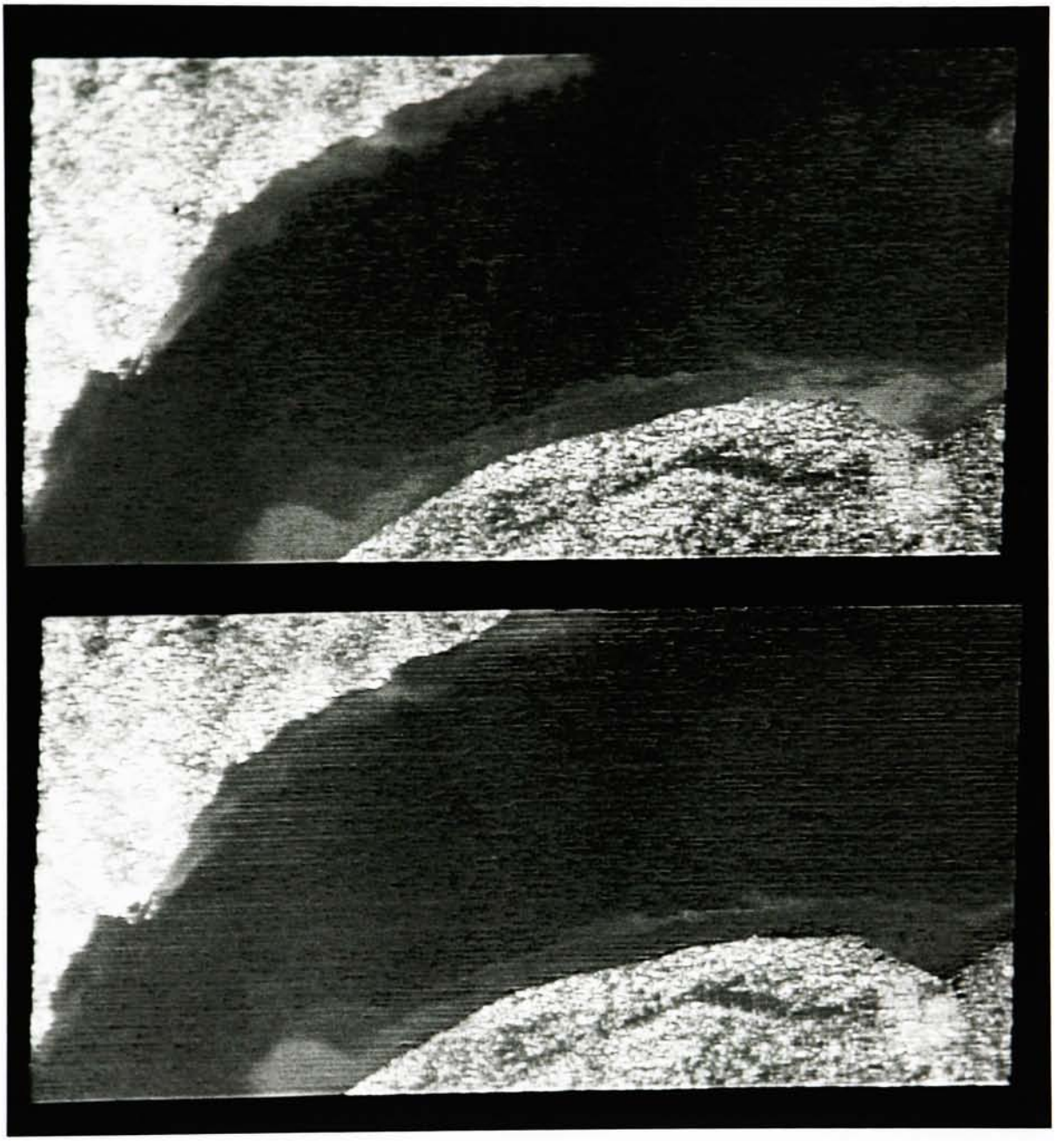

Figure 3.2.2-1 TM Band 1 Image of the 25 May 1985 Lake Ontario Scene Processed Using a Henyey-Greenstein Asymmetry Parameter of 0.15

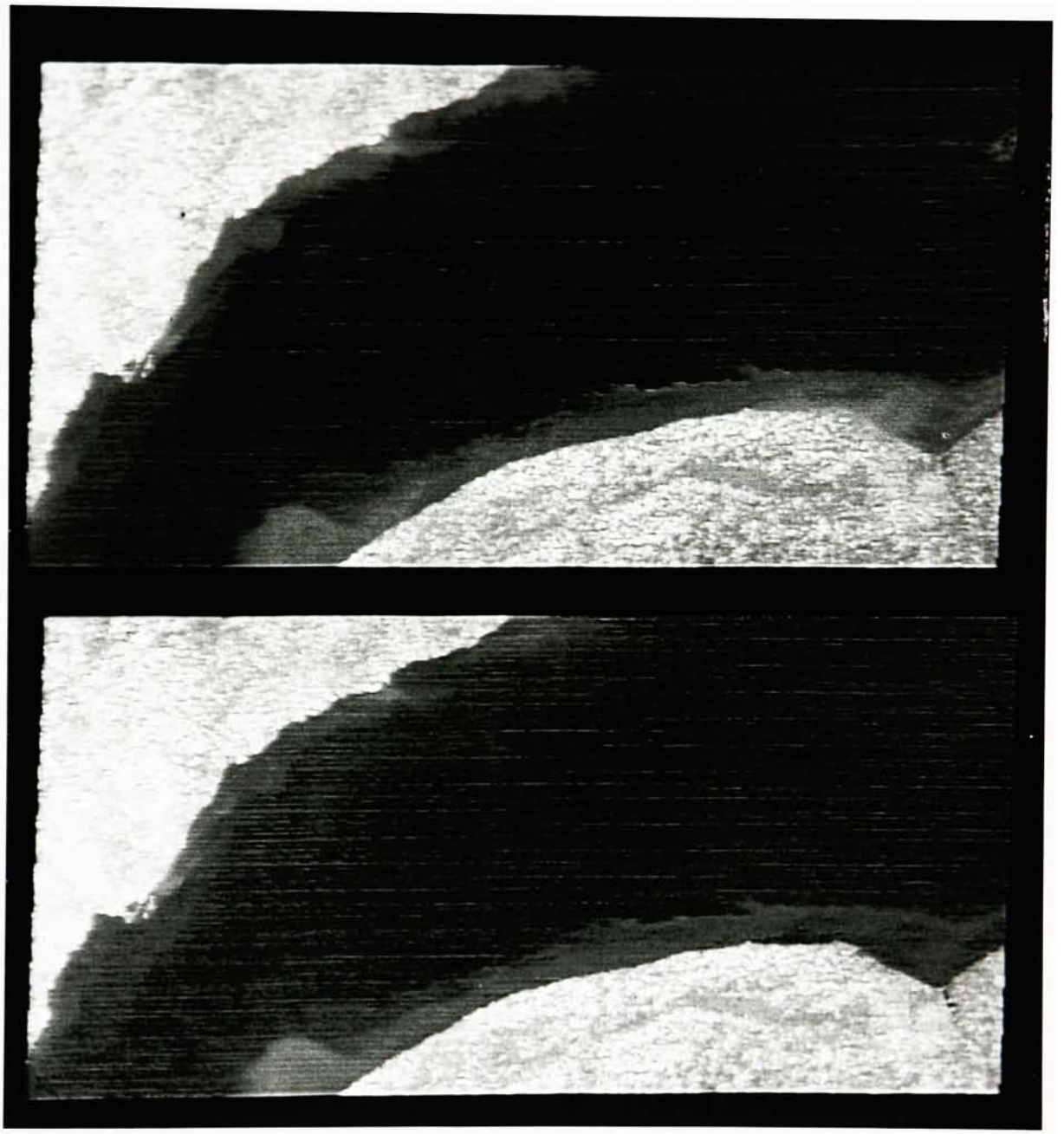

Figure 3.2.2-2 TM Band 2 Image of the 25 May 1985 Lake Ontario Scene Processed Using a Henyey-Greenstein Asymmetry Parameter of 0.15

Figure 3.2.2-3 TM Band 3 Image of the 25 May 1985 Lake Ontario Scene Processed Using a Henyey-Greenstein Asymmetry Parameter of 0.15

3.3 Quantitative Algorithm Performance Analysis

Although no water surface measurements are available for either the 22 June 1984 scene or the 25 May 1985 scene, a quantitative analysis can be made of the algorithm to some extent.

The National Weather Service archives surface weather data for many monitoring stations across the country. Such surface weather data was obtained for three stations within the area of the 22 June 1984 scene. These stations are located at Rochester, Buffalo, and Niagara Falls, New York. Figure 3.3-1 indicates the location of each of the stations within the image.

The surface weather data contains an estimate of the surface visibility at each station. The correlation between the surface visibility obtained from the surface weather data and the LOWTRAN 6 value for the surface meteorological range used to model the atmosphere at a nearby lake region can be used to indicate the veracity of the LOWTRAN 6 model data.

The reflectance of the water as determined using the corrected lake image can also be used to evaluate the quality of the correction algorithm. For a lake as large and as deep as Lake Ontario it is reasonable to assume that the water reflectance computed from the lake image would be close to the nominally clear water reflectance given in Figure 1.2.1-3.

An estimate of the improvement in water reflectance accuracy obtained using the pixel-by-pixel correction technique can be made using the upwelling atmospheric path radiance values determined from the TM Band 4 lake image. Based on the verification of the zero water reflectance assumption as described in Section 3.1, the expected water reflectance error using a uniform atmospheric correction

can be compared to the expected water reflectance error obtained using the pixel-by-pixel technique.

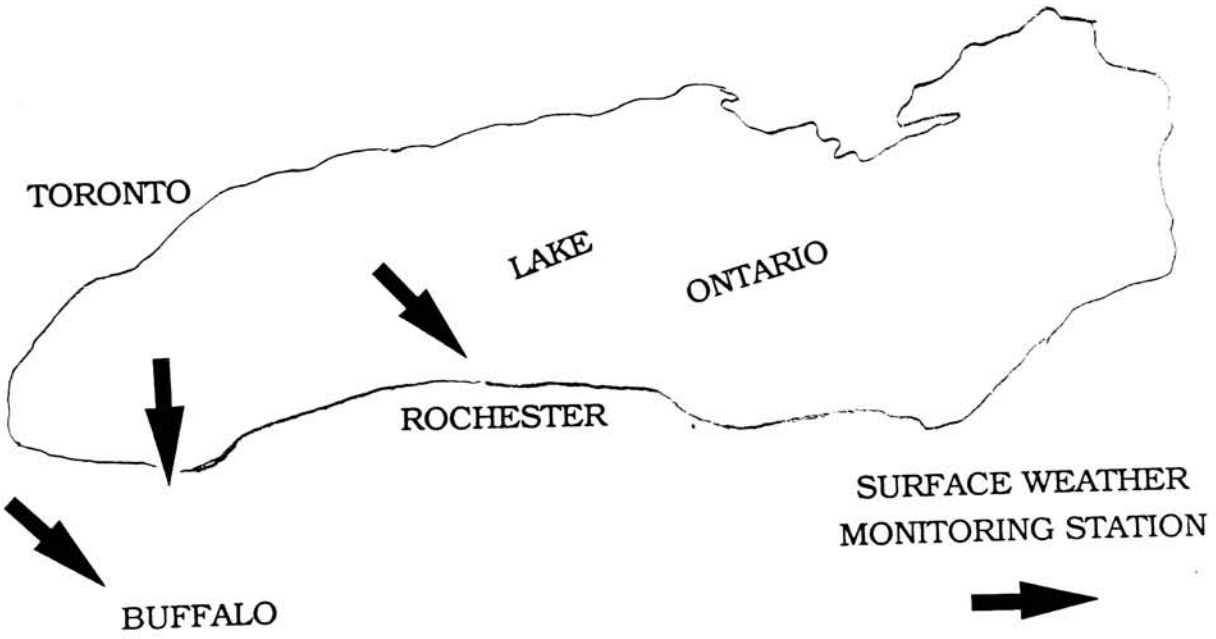

Figure 3.3-1 Locations of Surface Weather Monitoring Stations

3.3.1 Comparison of Surface Measurements of Visibility to LOWTRAN 6 Derived Values of Meteorological Range

The meteorological range values input into the LOWTRAN 6 model to match the TM Band 4 derived upwelling path radiance are used simply to define the total number of aerosol particles in the model atmosphere. The meteorological range values are not estimates of surface visibility but it is known that the surface visibility is very often strongly correlated with the vertical distribution concentration of atmospheric aerosols. This is why the LOWTRAN 6 model is successful in using surface meteorological range to estimate total aerosol concentration.

Surface visibility measurements were obtained from surface weather data measured at Rochester, Buffalo, and Niagara Falls, New York monitoring stations. Image pixel count data were sampled from the lake image near the monitoring stations. Because no region of Lake Ontario is near the Buffalo monitoring station, TM Band 4, quadrant 3 of the 22 June 1984 scene had to be read and pixel count data taken for a region of Lake Erie. Table 3.3-1 lists the surface visibility data (converted to meteorological range), the TM Band 4 image pixel counts, and the LOWTRAN 6 derived meteorological range.

Table 3.3-1

Station	Surface Met. Range	TM Band 4 Counts	LOWTRAN 6 Met. Range
Buffalo	83.7 Km	13	25.5 Km
Rochester	31.4 Km	11	36.3 Km
Niagara Falls	20.9 Km	15	18.8 Km

The Rochester and Niagara Falls station data track very well with the LOWTRAN 6 meteorological range values. The surface weather data indicate that the surface visibility near the Rochester area was about 1.5 time greater than at the Niagara area. The LOWTRAN 6 meteorological range determined from the lake image is 1.9 times greater at the Rochester region than at the Niagara Falls region, and the small discrepancy is well within the uncertainty with which the surface visibility values are measured.

The Buffalo area station does not follow the LOWTRAN 6 derived meteorological range value. The surface visibility data indicates a less turbid atmosphere at the Buffalo area as compared to the Rochester area but the LOWTRAN 6 meteorological range data indicate that the Buffalo area atmosphere is slightly more turbid. This discrepancy is beyond the uncertainty in the surface visibility measurements. It may be caused by using a measurement along a horizontal path near the surface of the earth to compare with an estimate of the vertical aerosol concentration. There are many patches of haze in the Lake Erie scene near the Buffalo area that are probably thin, high-altitude clouds. The pixel count from the image would have the cloud effects included while the surface visibility measurement would not. Considering only the Rochester and Niagara Falls station surface visibility data, the pixel-by-pixel atmospheric correction technique appears to perform quite well in a quantitative sense.

3.3.2 Examination of Computed Water Reflectance

An assessment of the absolute accuracy of the pixel-by-pixel atmospheric correction technique can be made by computing the reflectance of the water body from the corrected image data. Although no water surface measurements of

reflectance are available for the 22 June 1984 scene, expected values for lake water reflectance can be based on Figure 1.2.1-3 and the discussion in Section 3.1. Of course, the accuracy of each pixel correction can not be evaluated but if the average water reflectance value derived from the corrected image data is consistent with Figure 1.2.1-3 then it is reasonable to presume that the technique is performing as expected.

Reflectance determination requires correction for illumination of the water by sun and the sky radiation. Values for these parameters were estimated using the LOWTRAN 6 model with radiosonde profile data, a Henyey-Greenstein asymmetry parameter of 0.15, and a VIS parameter of 36.3. Estimates of the sun and sky illumination of the water for each spectral band are given in Table 3.3.2-1.

Table 3.3.2-1

TM Band Number	Solar Radiance	Sky Radiance
1	2.715×10^{-3} W/cm^2-Sr	2.0122×10^{-4} W/cm^2-Sr
2	3.083×10^{-3} W/cm^2-Sr	1.7482×10^{-4} W/cm^2-Sr
3	2.172×10^{-3} W/cm^2-Sr	9.2784×10^{-5} W/cm^2-Sr

Water body reflectance histograms were computed using imagery corrected with the pixel-by-pixel technique using a Henyey-Greenstein asymmetry parameter of 0.15. The reflectance histograms are presented in Figures 3.3.2-1. through 3.3.2-3 The peak value of each reflectance histogram was used to construct Figure 3.3.2-4, an estimate of the average water spectral signature for the 22 June 1984 Lake Ontario scene.

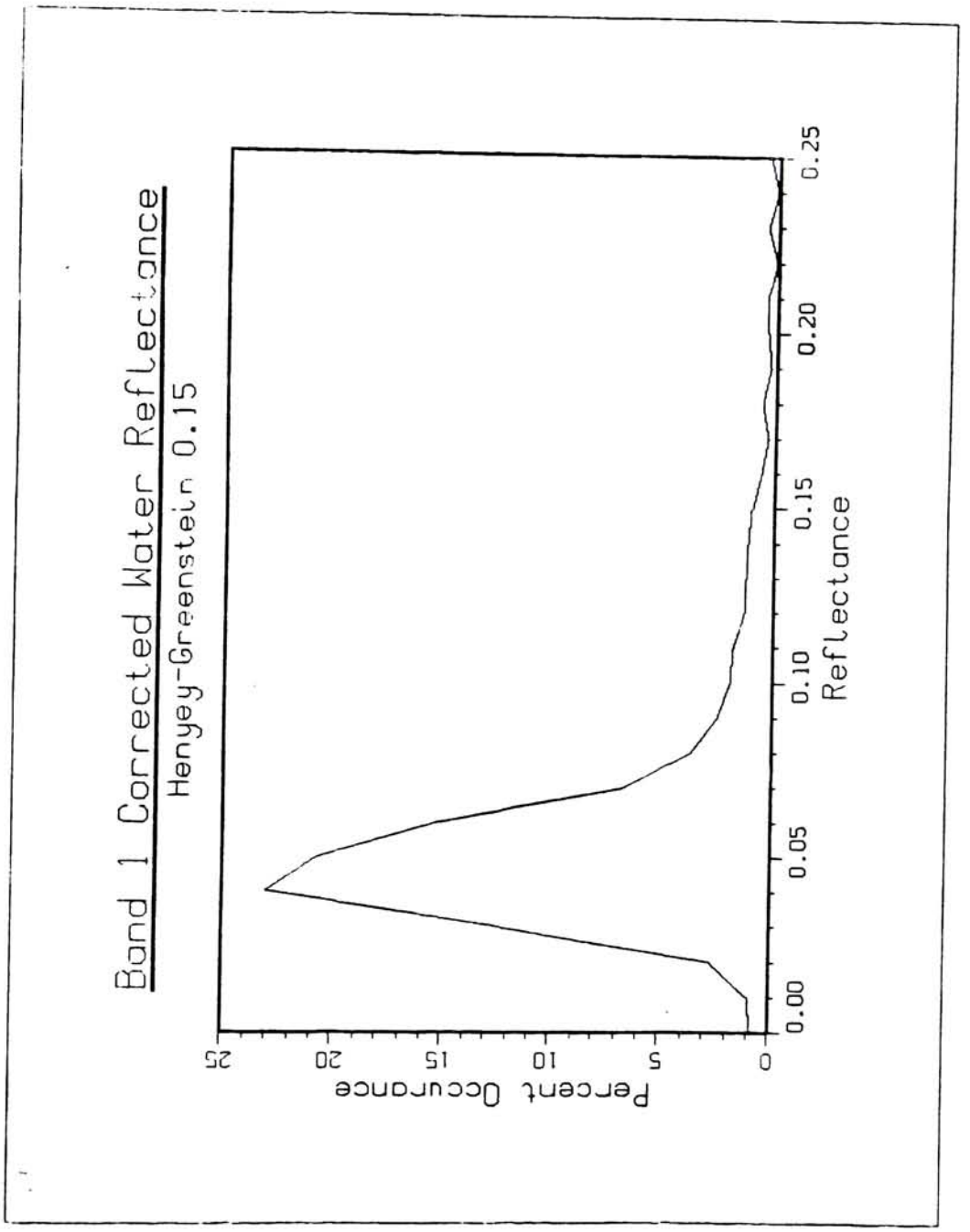

Figure 3.3.2-1 TM Band 1 Corrected Water Reflectance Histogram Using 0.15 for the Henyey-Greenstein Asymmetry Parameter (22 June 1984)

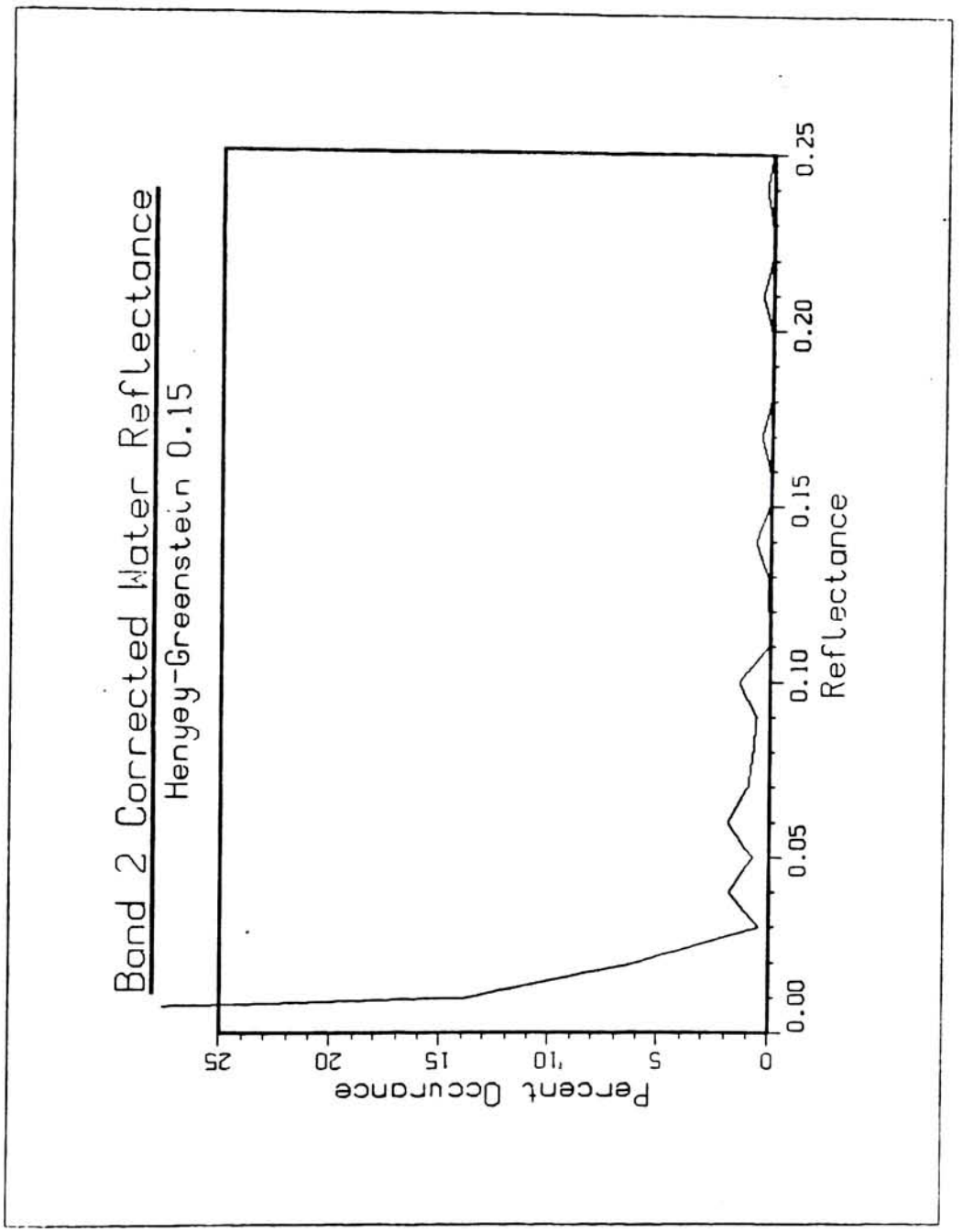

Figure 3.3.2-2 TM Band 2 Corrected Water Reflectance Histogram Using 0.15 for the Henyey-Greenstein Asymmetry Parameter (22 June 1984)

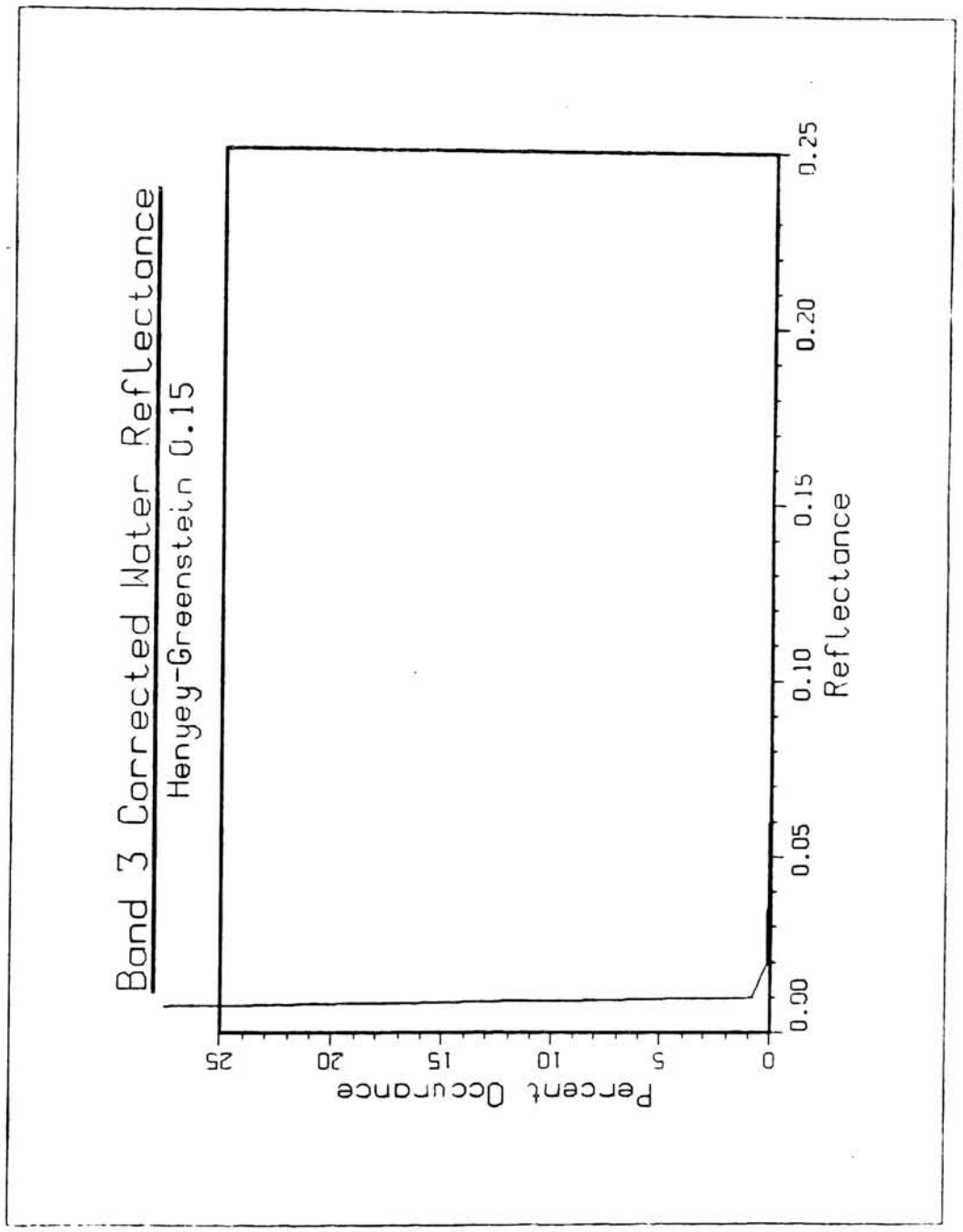

Figure 3.3.2-3 TM Band 3 Corrected Water Reflectance Histogram Using 0.15 for the Henyey-Greenstein Asymmetry Parameter (22 June 1984)

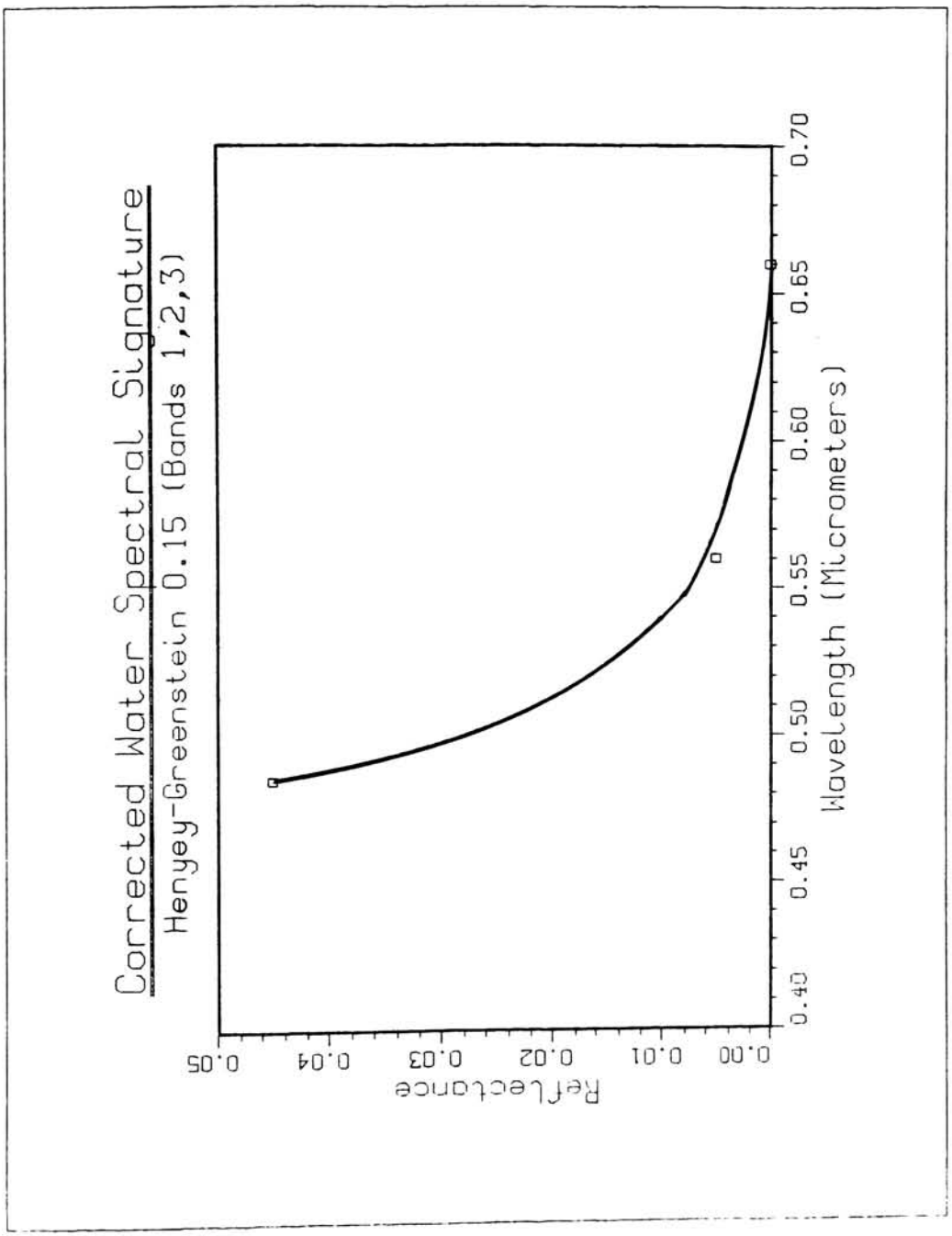

Figure 3.3.2-4 Lake Ontario Spectral Signature

Comparison of Figure 1.2.1-3 with Figure 3.3.2-2 shows that, indeed, an accurate quantitative correction of the atmospheric effects on the lake scene has been achieved.

3.3.3 Reduction of Water Body Reflectance Estimate Error Using the Pixel-By-Pixel Atmospheric Correction Technique

Correction of the spatial variation in the atmospheric effects of the atmosphere on imagery of water can be expected to considerably reduce the water reflectance measurement error. The expected reduction in reflectance measurement error can be determined using the method of Beers[91]. Equation 1.3.1-31, the complete description of the radiative transfer process, can be rewritten as:

$$L_{T\lambda} = r_{w\lambda} (L_{\lambda sun} + L_{\lambda sky}) \tau_{\lambda} + L_{u\lambda} \qquad (3.2.3\text{-}1)$$

where:

$$L_{T\lambda} = L_{\lambda}(\theta, \theta', \phi)$$

$$\tau_{\lambda} = e^{-\tau_{\lambda}' sec(\theta)}$$

$$L_{u\lambda} = L_{u\lambda}(\theta, \theta', \phi)$$

$$L_{\lambda sun} = \frac{1}{\pi} \left[E'_{s\lambda} \cos(Z)\ e^{-\tau_{\lambda}' sec(\theta)} \right]$$

$$L_{\lambda sky} = \int_0^{2\pi} \int_0^{\frac{\pi}{2}} L_{d\lambda}(\theta, \phi) \cos(\theta) \sin(\theta)\, d\theta d\phi$$

Solving Equation (3.2.3-1) for $r_{w\lambda}$ gives:

$$r_{w\lambda} = \frac{L_{T\lambda} - L_{u\lambda}}{\tau_{\lambda} \left(L_{\lambda sun} + L_{\lambda sky} \right)} \qquad (3.2.3\text{-}2)$$

The expected error in reflectance due to atmospheric transmittance and atmospheric upwelling path radiance can be approximated as:

$$\Delta r_{w\lambda}(\tau_\lambda, L_{u\lambda}) = \sqrt{\left[\left(\frac{\delta r_{w\lambda}}{\delta \tau_\lambda}\right) \Delta \tau_\lambda\right]^2 + \left[\left(\frac{\delta r_{w\lambda}}{\delta L_{u\lambda}}\right) \Delta L_{u\lambda}\right]^2} \qquad (3.2.3\text{-}3)$$

where Δ indicates the uncertainty to which the parameter can be measured. This assumes that τ_λ and $L_{u\lambda}$ are statistically independent. Since this is not true, Equation 3.2.3-3 will somewhat overestimate the reflectance error. Reflectance error estimates are presented to provide an indication of the *reduction* in reflectance error provided by the technique, not an estimate of the absolute expected error. Uncertainties due to system calibration errors, image noise ans incorrect atmospherric modeling are not considered.

If a single value of atmospheric transmittance and atmospheric path radiance were each used to correct the 22 June 1984 scene, the uncertainty in the reflectance measured from TM Band 1 would be approximately:

$$\Delta r_{w\lambda}(\tau_\lambda, L_{u\lambda})_1 = \sqrt{[(-0.064061)\ (0.2603)]^2 + [(-685.24)\ (5.420 \times 10^{-5})]^2}$$

$$= 0.0407$$

Where:

$$\frac{\delta r_{w\lambda}}{\delta \tau_\lambda} = \frac{L_{u\lambda}}{(L_{\lambda sun} + L_{\lambda sk})\ \tau_\lambda^2} - \frac{L_{SAT_\lambda}}{(L_{\lambda sun} + L_{\lambda sk})\ \tau_\lambda^2}$$

$$= \frac{3.307 \times 10^{-4}}{(2.714 \times 10^{-3} + 2.012 \times 10^{-4})\ (0.5006)^2} - \frac{3.775 \times 10^{-4}}{(2.714 \times 10^{-3} + 2.012 \times 10^{-4})\ (0.5006)^2}$$

$$= -0.064061$$

$$\frac{\delta r_{w\lambda}}{\delta L_{u\lambda}} = \frac{-1}{(L_{\lambda sun} + L_{\lambda sk})\ \tau_\lambda} = \frac{-1}{(2.714 \times 10^{-3} + 2.012 \times 10^{-4})\ (0.5006)}$$

$$= -685.24$$

And:

$$\Delta\tau_\lambda = 0.2603$$

$$\Delta L_{u\lambda} = 5.420 \times 10^{-5} \text{ W/cm}^2\text{-Sr}$$

The estimates of atmospheric transmittance uncertainty, $\Delta\tau_\lambda$, and atmospheric upwelling path radiance uncertainty, $\Delta L_{u\lambda}$, were made using the atmospheric correction look-up tables having a Henyey-Greenstein asymmetry parameter of 0.15. These estimates were made by computing the difference between the parameter value at look-up table position 16 (the nominal correction value) and the value at look-up table position 24 (the "true" correction value) for each case. These look-up table positions were chosen because the water regions in the 22 June 1984 TM Band 4 image had a mean count value of 15.6 with a standard deviation of 7.8.

The one-sigma uncertainty in reflectance for water, as determined above, is approximately equal to the computed value of the water reflectance. As is evident in the 22 June 1984 scene, very large errors are inherent in the nominal correction process when imagery having non-uniform patches of haze must be employed. Errors of such a magnitude would render the image essentially useless for mapping lake water quality.

The uncertainty in water reflectance when the pixel-by-pixel atmospheric correction technique is used is approximately:

$$\Delta r_{w\lambda}(\tau_\lambda, L_{u\lambda})_1 = \sqrt{[(-0.064061)\ (0.0313)]^2 + [(-685.24)\ (8.840 \times 10^{-6})]^2}$$

$$= 0.0064$$

Here the atmospheric transmittance uncertainty and atmospheric upwelling path radiance uncertainty are estimated using parameter values at adjacent look-up table positions 16 and 17.

Therefore, when considering hazy imagery of water, the pixel-by-pixel atmospheric correction technique may produce significant improvement in water reflectance accuracy over uniform correction techniques. The pixel-by-pixel correction technique could allow determination of water body reflectance using imagery that otherwise could not be used.

4.0 Conclusions and Recommendations

The research described in this thesis has provided a novel technique for the correction of atmospheric effects on multispectral imagery of water. The correction technique accounts for the spatial variations that are often found in wide-expanse satellite imagery. The results of the research indicate:

- Imagery of water made with the LANDSAT-5 TM Band 4 channel can be used to determine the atmospheric upwelling path radiance on a pixel-by-pixel basis.
- Water reflectance computed from hazy imagery of water can be subject to very large errors when spatially uniform atmospheric correction techniques are employed.
- The pixel-by-pixel atmospheric correction technique introduces no processing artifacts into the image to be corrected.
- The correction technique will reduce to a uniform atmospheric correction for extremely clear image data.
- The pixel-by-pixel atmospheric correction technique can significanly improve the subjective interpretability of water imagery.
- A refinement of the pixel-by-pixel atmospheric correction technique may significantly improve the quantitative exploitation of water imagery.

A recommended refinement to the pixel-by-pixel correction technique is the development of a more rigorous (hence more complex) model of the haze phenomena. A more rigorous model would allow direct control of the concentration and scattering phase function for each atmospheric aerosol constituent. The model presented only allows a single, average aerosol effect. Additionally, the results indicate that the atmospheric scattering is not properly modeled for the short

wavelength region. It is anticipated that use of a multiple scattering atmospheric model could reduce the overcorrections observed using the current technique.

More advanced improvements to the technique would include optimization of the imaging spectral window with which the atmosphere is to be measured and extension of the technique to atmospheric correction of non-water imagery using some other material, such as concrete or asphalt, as a reflectance uniformity standard.

Anyone persuing a refinement to the technique should strive to develop more quantitative measures of performance results.

5.0 References

1. P. Pollack, *The Picture History of Photography*, Harry N. Abrams Inc., New York, p. 143, 1969.

2. T. M. Lillesand and R. W. Kiefer, *Remote Sensing and Image Interpretation*, John Wiley and Sons, New York, p. 36, 1979

3. Lillesand and Kiefer, p. 37.

4. W. A. Fischer *et al*, "History of Remote Sensing", in *Manual of Remote Sensing*, R. G. Reeves *et al*, Ed., American Society of Photogrammetry, Falls Church, VA, p. 28, 1975.

5. Fischer, p. 30.

6. Lillesand and Kiefer, p. 37.

7. Fischer, p. 31.

8. Fischer, p. 32.

9. Fischer, p. 33.

10. Lillesand and Kiefer, p. 94.

11. Fischer, p. 34.

12. Fischer, p. 36.

13. Lillesand and Kiefer, p. 55.

14. P. N. Slater, *Remote Sensing, Optics and Optical Systems*, Addison-Wesley, Reading, MA, p. 337, 1980.

15. Fischer, p. 32.

16. Fischer, p. 35.

17. R. N. Colwell, "Determining the Prevalence of Certain Cereal Crop Diseases by Means of Aerial Photography", *Hilgardia, 26*, (1965).

18. Fischer, p. 42.

19. Fischer, p. 43.

20. Fischer, p. 44.

21. Fischer, p. 45.

22. Fischer, p. 46.

23. Fischer, p. 46.

24. Slater, p. 471.

25. Slater, p. 465.

26. D. S. Simonett *et al*, "The Development and Principles of Remote Sensing", in *Manual of Remote Sensing Second Edition*, R. E. Colwell *et al*, Ed., American Society of Photogrammetry, Falls Church, VA, p. 5, 1983.

27. Slater, p. 466.

28. Simonett, p. 6.

29. Slater, p. 497.

30. Slater, p. 499.

31. Slater, p. 498.

32. J. M. Lenorovitz, *Aviation Week and Space Technology*, *124*, 22 (1984).

33. Lenorovitz, p. 21.

34. Slater, p. 511.

35. L. Darden, *The Earth in the Looking Glass*, Anchor Press, Garden City, NY, p. 167, 1974.

36. Darden, p. 168.

37. P. H. Swain and S. M. Davis Ed., *Remote Sensing: The Quantitative Approach*, McGraw-Hill Inc., p. 257, 1970.

38. L. A. Bartolucci, B. F. Robinson, and L. F. Silva, "Field Measurement of the Spectral Response of Natural Waters", *Photogrammetric Engineering and Remote Sensing*, 43, (1977).

39. Swain and Davis, p. 260.

40. R. W. Johnson and R. C. Harris, "Remote Sensing for Water Quality and Biological Measurements in Coastal Waters", *Photogrammetric Engineering and Remote Sensing*, *46*, 77-85, (1980).

41. Johnson and Harris, p. 81.

42. Johnson and Harris, p. 77.

43. R. W. Johnson, G. S. Bahn, and J. T. Thomas, "Synoptic Thermal and Oceanographic Parameter Distributions in the New York Bight Apex", *Photogrammetric Engineering and Remote Sensing*, *48*, 1593-1598, (1981).

44. T. M. Lillesand *et al*, "Use of Landsat Data to Predict the Trophic State of Minnesota Lakes", *Photogrammetric Engineering and Remote Sensing*, *49*, 219, (1983).

45. Lillesand *et al*, p. 229.

46. D. J. Carpenter and S. M. Carpenter, "Modeling Inland Water Quality Using Landsat Data", *Remote Sensing of Environment*, *13*, 352, (1983).

47. Carpenter and Carpenter, p. 348.

48. C. H. Whitlock *et al*, "Criteria for the Use of Regression Analysis for Remote Sensing of Sediment and Pollutants", *Remote Sensing of Environment, 12*, 151, (1982).

49. K. R. Piech and J. R. Schott, "Atmospheric Corrections for Satellite Water Quality Studies", *Proceedings of the SPIE, 51*, 84, (1975).

50. K. R. Piech and J. R. Walker, "Interpretation of Soils", *Photogrammetric Engineering, 40*, 87-97, (1974).

51. Piech and Schott, p. 87.

52. J. C. Munday, "Chromaticity of Path Radiance and Atmospheric Correction of Landsat Data", *Remote Sensing of Environment, 13*, 525-538, (1983).

53. T. Lindell *et al*, "A Further Development of the Chromaticity Technique for Satellite Mapping of Suspended Sediment Load", *Photogrammetric Engineering and Remote Sensing, 52*, 1521-1529, (1986).

54. F. L. Scarpace, K. W. Holmquist, and L. T. Fisher, "Landsat Analysis of Lake Quality", *Photogrammetric Engineering and Remote Sensing, 45*, 623-633, (1979).

55. H. R. Gordon, "Removal of the Atmospheric Effects from Satellite Imagery of the Oceans", *Applied Optics, 17*, 1631-1636, (1978).

56. H. R. Gordon *et al*, "Phytoplankton Pigments from the Nimbus-7 Coastal Zone Color Scanner: Comparisons with Surface Measurements", *Science, 21*, 63-66, (1980).

57. J. P. Verdin, "Monitoring Water Quality Conditions in a Large Western Reservoir with Landsat Imagery", *Photogrammetric Engineering and Remote Sensing, 51*, 343-353, (1985).

58. F. D. Ahern *et al*, "Use of Clear Lakes as Standard Reflectors for Atmospheric Measurements", *Proceedings of the Eleventh International Symposium on Remote Sensing of the Environment, 1*, 731-735, (1977).

59. P. N. Tverskoi, "Physics of the Atmosphere - A Course in Meteorology", *NASA and The National Science Foundation*, Washington D. C., pp. 15-36, 1977.

60. H. D. Holland, *The Chemistry of the Atmosphere and Oceans*, John Wiley and Sons Inc., New York, p. 263, 1978.

61. Holland, p. 267.

62. Holland, p. 297.

63. S. Chandrasekhar, *Radiative Transfer*, Dover Publications, New York, ch. 1, 1960.

64. H. C. Van de Hulst, *Light Scattering by Small Particles*, John Wiley and Sons Inc., New York, p. 3, 1957.

65. J. R. Schott and A. Henderson-Sellers, "Radiation, the Atmosphere, and Satellite Sensors", in *Satellite Sensing of a Cloudy Atmosphere: Observing the Third Planet*, A. Henderson-Sellers Ed., Taylor and Francis Ltd., London, pp. 45-84, 1984.

66. Schott and Henderson-Sellers, p. 61.

67. Slater, p. 244.

68. Slater, p. 211.

69. A. J. LaRocca and R. E. Turner, "Atmospheric Transmittance and Radiance: Methods of Calculation", *IRIA State of the Art Report No. 107600-10-T*, Environmental Research Institute of Michigan, Ann Arbor, p. 20, 1975.

70. Slater, p. 212.

71. LaRocca and Turner, p. 24.

72. LaRocca and Turner, p. 144.

73. LaRocca and Turner, p. 161.

74. LaRocca and Turner, p. 284

75. A. J. LaRocca, "Atmospheric Absorption", in *The Infrared Handbook*, W. L. Wolf and G. J. Zissis Ed., Environmental Research Institute of Michigan, Ann Arbor, p. 5-24, 1978.

76. LaRocca, p. 5-24.

77. F. X. Kneizys *et al*, *Atmospheric Transmittance/Radiance: Computer Code LOWTRAN 5*, Air Force Geophysics Laboratory, AFGL-TR-80-0067, 1980.

78. LaRocca, p. 5-23.

79. LaRocca, p. 5-54.

80. Kneizys *et al*, pp. 15-20.

81. F. X. Kneizys *et al*, *Atmospheric Transmittance/Radiance: Computer Code LOWTRAN 6*, Air Force Geophysics Laboratory, AFGL-TR-83-0187, 1983.

82. B. Herman et al, "Atmospheric Scattering", in *The Infrared Handbook*, W. L. Wolf and G. J. Zissis Ed., Environmental Research Institute of Michigan, Ann Arbor, p. 4-14, 1978.

83. Chandrasekhar, p. 12.

84. Herman *et al*, pp. 4-15 - 4-26.

85. Herman *et al*, p. 4-8.

86. W. L. Ridgway *et al*, "Solar/Lunar Single Scattering Model", in *Atmospheric Transmittance/Radiance: Computer Code LOWTRAN 6*, Air Force Geophysics Laboratory, AFGL-TR-83-0187, pp. 27-41, 1983.

87. Slater, pp. 492-509.

88. NASA, *Interface Control Document Between the NASA-Goddard Space Flight Center and the Department of the Interior EROS Data Center for Landsat-D, Thematic Mapper Computer Compatible Tape*, NASA-Goddard Space Flight Center, Greenbelt, MD, 1983.

89. H. S. Chen, *Space Remote Sensing Systems*, An Introduction, Academic Press, Orlando, Fla., p. 3, 1985.

90. J. D. Biegel and J. R. Schott, "Radiometric Calibration and Image Processing of LANDSAT TM Data to Improve Assessment of Thermal Signatures", *Proceedings of SPIE, Infrared Technology IX, 430* (1984).

91. Y. A. Beers, *Introduction to the Theory of Error*, Addison-Wesley, Reading MA pp. 26-32, 1957.

92. Slater, p 294.

6.0 Appendices

6.1 Appendix A Example LOWTRAN 6 Run

An example run of the LOWTRAN 6 atmospheric model is presented here. The run is based on a spectral band rectangularly shaped, about the LANDSAT TM Band 4 spectral band area. The example calculation models the atmospheric optical effects based on the following ambient conditions:

1. Atmospheric Profile data provided by a Buffalo Area Radiosonde from 22 June1984, 7 AM.
2. The Observer is 100 KM above the Earth surface and is looking straight down.
3. A LOWTRAN standard model of Ozone profile is used.
4. Rural model of aerosol extinction, surface meteorological range assumed to be 23 KM.
5. Spring/Summer Aerosol characteristics
6. Time of day is 15:00 GMT.
7. Program is to calculate atmospheric transmittance and solar scattered path radiance.
8. LOWTRAN database of Mie scattering phase functions are to be used.
9. Ground Area to be modeled is located at 43 degrees north latitude 74 degrees west longitude.
10. Spectral band to be modeled is 0.76um to 0.90μm with a spectral resolution of approx. 0.0015μm.

The formatted input parameter file for the LOWTRAN 6 model is shown in Figure 6.1-1. Section 1 of Figure 6.1-1 contains the LOWTRAN codes for the LOWTRAN atmospheric database items to be used for the model. Section 2 is the radiosonde atmospheric profile to be used, and Section 3 describes the geometry of the model and the spectral region to be used.

The output from the LOWTRAN 6 model is shown in Figure 6.1-2. Section 1 of the output is an echo of the input parameter file, and lists the atmospheric profile

as provided in the input file. Section 2 arranges the atmospheric data as it is required for the modeling, merging both the radiosonde data and its own database atmospheric data. Section 3 continues the echoing of the input parameter file and summarizes the atmospheric and geometrical conditions of the scenario to be modeled. Section 4 lists the atmospheric profile to be used, with atmospheric constituent amount expressed in LOWTRAN concentration units. Section 5 displays the length of the slant path to be modeled. Section 6 shows the calculation of the direction of the refracted atmospheric path from observer to surface. Section 7 displays the calculated absorber amounts for each layer of the atmosphere and prints a summary of the absorber amounts for the entire atmospheric path. Section 8 shows the calculation of the single scattering geometry for the solar scattering model. Section 9 contains the wavelength by wavelength calculation of atmospheric path transmittance and scattered path radiance. Section 10 concludes the modeling run by displaying the atmospheric path transmittance and scattered path radiance integrated over the entire slant path length and integrated over the entire spectral band. The run concludes that for the meteorological and geometrical conditions input, the atmospheric path would have a band transmittance of 0.7387 and a band scattered path radiance of 6.211×10^{-5} Watts/(cm^2 Sr)

```
  7    2    2    0    0    2    1    0      0.000      0.000
  1    1    1    0    0    0   20.000      0.000      0.000      0.000
 34                      dewptl.rsd
   0.218   987.700    23.900  2.0  0.0 0.000E+00 0.000E+00 0.000E+00 0.000000
   0.304   977.000    22.200  1.3  0.0 0.000E+00 0.000E+00 0.000E+00 0.000000
   0.895   912.000    16.200 -0.1  0.0 0.000E+00 0.000E+00 0.000E+00 0.000000
   1.488   850.000    11.000 -1.0  0.0 0.000E+00 0.000E+00 0.000E+00 0.000000
   2.050   794.000     4.800 -2.4  0.0 0.000E+00 0.000E+00 0.000E+00 0.000000
   2.258   774.000     3.200 -2.2  0.0 0.000E+00 0.000E+00 0.000E+00 0.000000
   2.332   767.000     3.100 -5.4  0.0 0.000E+00 0.000E+00 0.000E+00 0.000000
   2.697   733.000     0.100-15.7  0.0 0.000E+00 0.000E+00 0.000E+00 0.000000
   2.974   708.000    -2.400-20.3  0.0 0.000E+00 0.000E+00 0.000E+00 0.000000
   3.064   700.000    -1.500-31.5  0.0 0.000E+00 0.000E+00 0.000E+00 0.000000
   3.225   686.000    -0.800-30.8  0.0 0.000E+00 0.000E+00 0.000E+00 0.000000
   3.862   633.000    -5.000-35.0  0.0 0.000E+00 0.000E+00 0.000E+00 0.000000
   4.438   588.000    -7.700-37.7  0.0 0.000E+00 0.000E+00 0.000E+00 0.000000
   5.679   500.000   -16.300-33.6  0.0 0.000E+00 0.000E+00 0.000E+00 0.000000
   7.316   400.000   -29.000-44.6  0.0 0.000E+00 0.000E+00 0.000E+00 0.000000
   8.662   330.000   -39.500-52.7  0.0 0.000E+00 0.000E+00 0.000E+00 0.000000
   9.307   300.000   -45.100-58.3  0.0 0.000E+00 0.000E+00 0.000E+00 0.000000
  10.501   250.000   -54.100-67.3  0.0 0.000E+00 0.000E+00 0.000E+00 0.000000
  11.284   221.000   -58.500-71.7  0.0 0.000E+00 0.000E+00 0.000E+00 0.000000
  11.758   205.000   -57.400-70.6  0.0 0.000E+00 0.000E+00 0.000E+00 0.000000
  11.914   200.000   -58.100-71.3  0.0 0.000E+00 0.000E+00 0.000E+00 0.000000
  12.617   179.000   -55.300-68.5  0.0 0.000E+00 0.000E+00 0.000E+00 0.000000
  13.022   168.000   -54.600-67.8  0.0 0.000E+00 0.000E+00 0.000E+00 0.000000
  13.414   158.000   -56.300-69.5  0.0 0.000E+00 0.000E+00 0.000E+00 0.000000
  13.744   150.000   -56.100-69.3  0.0 0.000E+00 0.000E+00 0.000E+00 0.000000
  14.699   129.000   -57.800-71.0  0.0 0.000E+00 0.000E+00 0.000E+00 0.000000
  15.482   114.000   -55.900-69.1  0.0 0.000E+00 0.000E+00 0.000E+00 0.000000
  15.884   107.000   -57.100-70.3  0.0 0.000E+00 0.000E+00 0.000E+00 0.000000
  16.313   100.000   -56.900-70.1  0.0 0.000E+00 0.000E+00 0.000E+00 0.000000
  16.771    93.000   -57.900-71.1  0.0 0.000E+00 0.000E+00 0.000E+00 0.000000
  18.565    70.000   -57.300-70.5  0.0 0.000E+00 0.000E+00 0.000E+00 0.000000
  20.705    50.000   -54.800-68.0  0.0 0.000E+00 0.000E+00 0.000E+00 0.000000
  22.452    38.000   -56.900-70.1  0.0 0.000E+00 0.000E+00 0.000E+00 0.000000
  23.957    30.000   -54.600-67.8  0.0 0.000E+00 0.000E+00 0.000E+00 0.000000
  23.957     0.000   171.800      0.000      0.000      0.000     0
  1    2  174    0
  43.179    78.588     0.000      0.000     15.430      0.000      0.000      0.000
11111.12  13157.90    20.000
  1
```

LOWTRAN 6 Input File

```
                    ***** LOWTRAN 6 *****          12-OCT-88  19:50:16

 CARD 1  *****    7    2    2    0    0    2    1    0      0.000      0.000

 CARD 2  *****    1    1    1    0    0    0   20.000      0.000      0.000      0.000

 CARD 2C1*****   34
 MODEL ATMOSPHERE NO. 7
0.218E+00 0.988E+03 0.239E+02  2.0  0.0 0.000E+00 0.000E+00 0.000E+00      0.000  0  0  0
0.304E+00 0.977E+03 0.222E+02  1.3  0.0 0.000E+00 0.000E+00 0.000E+00      0.000  0  0  0
0.895E+00 0.912E+03 0.162E+02 -0.1  0.0 0.000E+00 0.000E+00 0.000E+00      0.000  0  0  0
0.149E+01 0.850E+03 0.110E+02 -1.0  0.0 0.000E+00 0.000E+00 0.000E+00      0.000  0  0  0
0.205E+01 0.794E+03 0.480E+01 -2.4  0.0 0.000E+00 0.000E+00 0.000E+00      0.000  0  0  0
0.226E+01 0.774E+03 0.320E+01 -2.2  0.0 0.000E+00 0.000E+00 0.000E+00      0.000  0  0  0
0.233E+01 0.767E+03 0.310E+01 -5.4  0.0 0.000E+00 0.000E+00 0.000E+00      0.000  0  0  0
0.270E+01 0.733E+03 0.100E+00-15.7  0.0 0.000E+00 0.000E+00 0.000E+00      0.000  0  0  0
0.297E+01 0.708E+03-0.240E+01-20.3  0.0 0.000E+00 0.000E+00 0.000E+00      0.000  0  0  0
0.306E+01 0.700E+03-0.150E+01-31.5  0.0 0.000E+00 0.000E+00 0.000E+00      0.000  0  0  0
0.322E+01 0.686E+03-0.800E+00-30.8  0.0 0.000E+00 0.000E+00 0.000E+00      0.000  0  0  0
0.386E+01 0.633E+03-0.500E+01-35.0  0.0 0.000E+00 0.000E+00 0.000E+00      0.000  0  0  0
0.444E+01 0.588E+03-0.770E+01-37.7  0.0 0.000E+00 0.000E+00 0.000E+00      0.000  0  0  0
0.568E+01 0.500E+03-0.163E+02-33.6  0.0 0.000E+00 0.000E+00 0.000E+00      0.000  0  0  0
0.732E+01 0.400E+03-0.290E+02-44.6  0.0 0.000E+00 0.000E+00 0.000E+00      0.000  0  0  0
0.866E+01 0.330E+03-0.395E+02-52.7  0.0 0.000E+00 0.000E+00 0.000E+00      0.000  0  0  0
0.931E+01 0.300E+03-0.451E+02-58.3  0.0 0.000E+00 0.000E+00 0.000E+00      0.000  0  0  0
0.105E+02 0.250E+03-0.541E+02-67.3  0.0 0.000E+00 0.000E+00 0.000E+00      0.000  0  0  0
0.113E+02 0.221E+03-0.585E+02-71.7  0.0 0.000E+00 0.000E+00 0.000E+00      0.000  0  0  0
0.118E+02 0.205E+03-0.574E+02-70.6  0.0 0.000E+00 0.000E+00 0.000E+00      0.000  0  0  0
0.119E+02 0.200E+03-0.581E+02-71.3  0.0 0.000E+00 0.000E+00 0.000E+00      0.000  0  0  0
0.126E+02 0.179E+03-0.553E+02-68.5  0.0 0.000E+00 0.000E+00 0.000E+00      0.000  0  0  0
0.130E+02 0.168E+03-0.546E+02-67.8  0.0 0.000E+00 0.000E+00 0.000E+00      0.000  0  0  0
0.134E+02 0.158E+03-0.563E+02-69.5  0.0 0.000E+00 0.000E+00 0.000E+00      0.000  0  0  0
0.137E+02 0.150E+03-0.561E+02-69.3  0.0 0.000E+00 0.000E+00 0.000E+00      0.000  0  0  0
0.147E+02 0.129E+03-0.578E+02-71.0  0.0 0.000E+00 0.000E+00 0.000E+00      0.000  0  0  0
0.155E+02 0.114E+03-0.559E+02-69.1  0.0 0.000E+00 0.000E+00 0.000E+00      0.000  0  0  0
0.159E+02 0.107E+03-0.571E+02-70.3  0.0 0.000E+00 0.000E+00 0.000E+00      0.000  0  0  0
0.163E+02 0.100E+03-0.569E+02-70.1  0.0 0.000E+00 0.000E+00 0.000E+00      0.000  0  0  0
0.168E+02 0.930E+02-0.579E+02-71.1  0.0 0.000E+00 0.000E+00 0.000E+00      0.000  0  0  0
0.186E+02 0.700E+02-0.573E+02-70.5  0.0 0.000E+00 0.000E+00 0.000E+00      0.000  0  0  0
0.207E+02 0.500E+02-0.548E+02-68.0  0.0 0.000E+00 0.000E+00 0.000E+00      0.000  0  0  0
0.225E+02 0.380E+02-0.569E+02-70.1  0.0 0.000E+00 0.000E+00 0.000E+00      0.000  0  0  0
0.240E+02 0.300E+02-0.546E+02-67.8  0.0 0.000E+00 0.000E+00 0.000E+00      0.000  0  0  0
```

LOWTRAN 6 Model Output

Z (KM)	P (MB)	T (K)	REL H (%)	H20 (GM M-3)	O3 (GM M-3)	TYPE	AEROSOL PROFILE	SEASON
0.218	987.700	297.05	23.78	5.147E+00	6.000E-05	RURAL	RURAL	
0.304	977.000	295.35	25.07	4.924E+00	6.000E-05	RURAL	RURAL	
0.895	912.000	289.35	32.95	4.542E+00	6.000E-05	RURAL	RURAL	
1.488	850.000	284.15	43.29	4.331E+00	6.000E-05	RURAL	RURAL	
2.050	794.000	277.95	59.58	3.994E+00	6.010E-05	TROPOSPHERIC	TROPOSPHERIC	SPRING-SUMMER
2.258	774.000	276.35	67.66	4.077E+00	6.051E-05	TROPOSPHERIC	TROPOSPHERIC	SPRING-SUMMER
2.332	767.000	276.25	53.61	3.209E+00	6.066E-05	TROPOSPHERIC	TROPOSPHERIC	SPRING-SUMMER
2.697	733.000	273.25	29.34	1.432E+00	6.139E-05	TROPOSPHERIC	TROPOSPHERIC	SPRING-SUMMER
2.974	708.000	270.75	23.88	9.790E-01	6.195E-05	TROPOSPHERIC	TROPOSPHERIC	SPRING-SUMMER
3.064	700.000	271.65	8.06	3.522E-01	6.213E-05	TROPOSPHERIC	TROPOSPHERIC	SPRING-SUMMER
3.225	686.000	272.35	8.19	3.756E-01	6.244E-05	TROPOSPHERIC	TROPOSPHERIC	SPRING-SUMMER
3.862	633.000	268.15	7.45	2.538E-01	6.372E-05	TROPOSPHERIC	TROPOSPHERIC	SPRING-SUMMER
4.438	588.000	265.45	6.99	1.955E-01	6.487E-05	TROPOSPHERIC	TROPOSPHERIC	SPRING-SUMMER
5.679	500.000	256.85	20.98	3.040E-01	6.802E-05	TROPOSPHERIC	TROPOSPHERIC	SPRING-SUMMER
7.316	400.000	244.15	20.74	1.030E-01	7.624E-05	TROPOSPHERIC	TROPOSPHERIC	SPRING-SUMMER
8.662	330.000	233.65	23.26	4.298E-02	8.357E-05	TROPOSPHERIC	TROPOSPHERIC	SPRING-SUMMER
9.307	300.000	228.05	21.35	2.229E-02	8.721E-05	TROPOSPHERIC	TROPOSPHERIC	SPRING-SUMMER
10.501	250.000	219.05	18.30	7.103E-03	9.952E-05	BACKGROUND STRATO	BACKGROUND STRATO	SPRING-SUMMER
11.284	221.000	214.65	16.83	3.887E-03	1.128E-04	BACKGROUND STRATO	BACKGROUND STRATO	SPRING-SUMMER
11.758	205.000	215.75	17.20	4.533E-03	1.175E-04	BACKGROUND STRATO	BACKGROUND STRATO	SPRING-SUMMER
11.914	200.000	215.05	16.97	4.111E-03	1.191E-04	BACKGROUND STRATO	BACKGROUND STRATO	SPRING-SUMMER
12.617	179.000	217.85	17.90	6.045E-03	1.377E-04	BACKGROUND STRATO	BACKGROUND STRATO	SPRING-SUMMER
13.022	168.000	218.55	18.13	6.643E-03	1.506E-04	BACKGROUND STRATO	BACKGROUND STRATO	SPRING-SUMMER
13.414	158.000	216.85	17.57	5.275E-03	1.618E-04	BACKGROUND STRATO	BACKGROUND STRATO	SPRING-SUMMER
13.744	150.000	217.05	17.63	5.421E-03	1.718E-04	BACKGROUND STRATO	BACKGROUND STRATO	SPRING-SUMMER
14.699	129.000	215.35	17.06	4.287E-03	1.869E-04	BACKGROUND STRATO	BACKGROUND STRATO	SPRING-SUMMER
15.482	114.000	217.25	17.70	5.571E-03	1.994E-04	BACKGROUND STRATO	BACKGROUND STRATO	SPRING-SUMMER
15.884	107.000	216.05	17.30	4.725E-03	2.076E-04	BACKGROUND STRATO	BACKGROUND STRATO	SPRING-SUMMER
16.313	100.000	216.25	17.36	4.857E-03	2.190E-04	BACKGROUND STRATO	BACKGROUND STRATO	SPRING-SUMMER
16.771	93.000	215.25	17.03	4.228E-03	2.328E-04	BACKGROUND STRATO	BACKGROUND STRATO	SPRING-SUMMER
18.565	70.000	215.85	17.23	4.596E-03	3.019E-04	BACKGROUND STRATO	BACKGROUND STRATO	SPRING-SUMMER
20.705	50.000	218.35	18.07	6.467E-03	3.540E-04	BACKGROUND STRATO	BACKGROUND STRATO	SPRING-SUMMER
22.452	38.000	216.25	17.36	4.857E-03	3.508E-04	BACKGROUND STRATO	BACKGROUND STRATO	SPRING-SUMMER
23.957	30.000	218.55	18.13	6.643E-03	3.208E-04	BACKGROUND STRATO	BACKGROUND STRATO	SPRING-SUMMER

```
CARD 3  *****     23.957      0.000    171.800      0.000      0.000      0.000    0

CARD 3A1*****     1    2  174    0

CARD 3A2*****     43.179     78.588      0.000      0.000     15.430      0.000      0.000      0.000

CARD 4  ***** 11111.120 13157.900    20.000

PROGRAM WILL COMPUTE RADIANCE+SOLAR SCATTERNG

ATMOSPHERIC MODEL
        TEMPERATURE =     7
        WATER VAPOR =     7
        OZONE       =     2     MIDLATITUDE SUMMER

SLANT PATH, H1 TO H2
        H1     =      23.957 KM
        H2     =       0.000 KM
        ANGLE  =     171.800 DEG
        RANGE  =       0.000 KM
        BETA   =       0.000 DEG
```

```
        LEN   =      0

SINGLE SCATTERING CONTROL PARAMETERS SUMMARY

        OBSERVER LATITUDE =          43.18 DEG NORTH OF EQUATOR
        OBSERVER LONGITUDE =         78.59 DEG WEST OF GREENWICH
        SUBSOLAR LATITUDE =          23.39 NORTH OF EQUATOR
        SUBSOLAR LONGITUDE =         50.99 WEST OF GREENWICH
        TIME ((0 IS UNDEF)=         15.430 GREENWICH TIME
        PATH AZIMUTH =               0.000 DEG EAST OF NORTH
        DAY OF YEAR =                  174

EXTRATERRESTIAL SOURCE IS THE SUN

PHASE FUNCTION FROM MIE DATA BASE

FREQUENCY RANGE
         V1 =      11110.0 CM-1  (      0.90 MICROMETERS)
         V2 =      13155.0 CM-1  (      0.76 MICROMETERS)
         DV =         20.0 CM-1
```

ATMOSPHERIC PROFILES

I	Z (KM)	P (MB)	T (K)	H20	CO2+ (SCALED LOWTRAN UNITS)	O3	N2	CNTMSLF (MOL/CM2 KM)	MOL SCAT (-)	N-1 (-)	O3 (UV) (ATM CM/KM)
1	0.22	987.700	297.0	4.844E-01	8.521E-01	2.725E-03	6.703E-01	1.194E+20	8.964E-01	2.596E-04	2.800E-03
2	0.30	977.000	295.4	4.600E-01	8.427E-01	2.717E-03	6.615E-01	1.093E+20	8.917E-01	2.583E-04	2.800E-03
3	0.89	912.000	289.4	4.026E-01	7.684E-01	2.654E-03	5.944E-01	9.299E+19	8.497E-01	2.461E-04	2.800E-03
4	1.49	850.000	284.1	3.633E-01	6.965E-01	2.589E-03	5.306E-01	8.456E+19	8.064E-01	2.336E-04	2.800E-03
5	2.05	794.000	277.9	3.182E-01	6.372E-01	2.535E-03	4.786E-01	7.190E+19	7.701E-01	2.231E-04	2.805E-03
6	2.26	774.000	276.4	3.183E-01	6.142E-01	2.529E-03	4.587E-01	7.492E+19	7.550E-01	2.187E-04	2.824E-03
7	2.33	767.000	276.3	2.485E-01	6.049E-01	2.527E-03	4.507E-01	4.641E+19	7.485E-01	2.169E-04	2.831E-03
8	2.70	733.000	273.3	1.070E-01	5.672E-01	2.517E-03	4.184E-01	9.243E+18	7.232E-01	2.096E-04	2.865E-03
9	2.97	708.000	270.8	7.119E-02	5.405E-01	2.509E-03	3.958E-01	4.320E+18	7.049E-01	2.044E-04	2.891E-03
10	3.06	700.000	271.6	2.531E-02	5.275E-01	2.503E-03	3.850E-01	5.592E+17	6.947E-01	2.014E-04	2.899E-03
11	3.22	686.000	272.4	2.647E-02	5.074E-01	2.495E-03	3.683E-01	6.358E+17	6.790E-01	1.969E-04	2.914E-03
12	3.86	633.000	268.1	1.676E-02	4.503E-01	2.473E-03	3.210E-01	2.903E+17	6.364E-01	1.845E-04	2.974E-03
13	4.44	588.000	265.4	1.214E-02	4.013E-01	2.449E-03	2.812E-01	1.723E+17	5.971E-01	1.732E-04	3.027E-03
14	5.68	500.000	256.9	1.655E-02	3.162E-01	2.423E-03	2.136E-01	4.166E+17	5.248E-01	1.522E-04	3.174E-03
15	7.32	400.000	244.1	4.691E-03	2.294E-01	2.509E-03	1.475E-01	4.778E+16	4.417E-01	1.281E-04	3.558E-03
16	8.66	330.000	233.6	1.680E-03	1.740E-01	2.569E-03	1.073E-01	8.325E+15	3.807E-01	1.104E-04	3.900E-03
17	9.31	300.000	228.1	8.084E-04	1.523E-01	2.593E-03	9.193E-02	2.239E+15	3.546E-01	1.028E-04	4.070E-03
18	10.50	250.000	219.1	2.226E-04	1.170E-01	2.773E-03	6.781E-02	2.274E+14	3.077E-01	8.922E-05	4.644E-03
19	11.28	221.000	214.6	1.100E-04	9.696E-02	3.003E-03	5.463E-02	6.810E+13	2.776E-01	8.049E-05	5.262E-03
20	11.76	205.000	215.8	1.196E-04	8.442E-02	3.034E-03	4.665E-02	9.260E+13	2.561E-01	7.428E-05	5.483E-03
21	11.91	200.000	215.1	1.063E-04	8.121E-02	3.047E-03	4.462E-02	7.619E+13	2.507E-01	7.270E-05	5.558E-03
22	12.62	179.000	217.8	1.406E-04	6.570E-02	3.361E-03	3.505E-02	1.647E+14	2.215E-01	6.423E-05	6.427E-03
23	13.02	168.000	218.6	1.457E-04	5.854E-02	3.581E-03	3.073E-02	1.989E+14	2.072E-01	6.009E-05	7.028E-03
24	13.41	158.000	216.8	1.099E-04	5.315E-02	3.759E-03	2.750E-02	1.254E+14	1.964E-01	5.696E-05	7.549E-03
25	13.74	150.000	217.1	1.077E-04	4.847E-02	3.910E-03	2.475E-02	1.325E+14	1.863E-01	5.402E-05	8.017E-03
26	14.70	129.000	215.3	7.465E-05	3.763E-02	4.011E-03	1.852E-02	8.285E+13	1.615E-01	4.683E-05	8.724E-03
27	15.48	114.000	217.3	8.645E-05	2.994E-02	4.065E-03	1.428E-02	1.399E+14	1.415E-01	4.102E-05	9.305E-03
28	15.88	107.000	216.1	6.943E-05	2.701E-02	4.131E-03	1.268E-02	1.006E+14	1.335E-01	3.872E-05	9.687E-03
29	16.31	100.000	216.3	6.713E-05	2.396E-02	4.240E-03	1.106E-02	1.063E+14	1.247E-01	3.615E-05	1.022E-02
30	16.77	93.000	215.3	5.485E-05	2.124E-02	4.383E-03	9.634E-03	8.057E+13	1.165E-01	3.378E-05	1.086E-02
31	18.57	70.000	215.8	4.611E-05	1.287E-02	5.071E-03	5.435E-03	9.520E+13	8.742E-02	2.535E-05	1.409E-02
32	20.70	50.000	218.3	4.769E-05	7.029E-03	5.185E-03	2.726E-03	1.885E+14	6.173E-02	1.790E-05	1.652E-02
33	22.45	38.000	216.3	2.810E-05	4.407E-03	4.613E-03	1.597E-03	1.063E+14	4.737E-02	1.374E-05	1.637E-02
34	23.96	30.000	218.6	3.092E-05	2.872E-03	3.830E-03	9.799E-04	1.989E+14	3.700E-02	1.073E-05	1.497E-02

ATMOSPHERIC PROFILES

I	Z (KM)	P (MB)	T (K)	CNTMFRN MOL/CM2 KM	HNO3 ATM CM/KM	AEROSOL 1 (-)	AEROSOL 2 (-)	AEROSOL 3 (-)	AEROSOL 4 (-)	AER1*RH (-)	CIRRUS (-)	RH (PERCNT)
1	0.22	987.700	297.0	1.659E+22	0.000E+00	1.706E-01	0.000E+00	0.000E+00	0.000E+00	4.058E+00	0.000E+00	2.378E+01
2	0.30	977.000	295.4	1.580E+22	0.000E+00	1.658E-01	0.000E+00	0.000E+00	0.000E+00	4.157E+00	0.000E+00	2.507E+01
3	0.89	912.000	289.4	1.389E+22	0.000E+00	1.361E-01	0.000E+00	0.000E+00	0.000E+00	4.484E+00	0.000E+00	3.295E+01
4	1.49	850.000	284.1	1.257E+22	0.000E+00	9.115E-02	0.000E+00	0.000E+00	0.000E+00	3.946E+00	0.000E+00	4.329E+01
5	2.05	794.000	277.9	1.107E+22	0.000E+00	0.000E+00	6.031E-02	0.000E+00	0.000E+00	0.000E+00	0.000E+00	0.000E+00
6	2.26	774.000	276.4	1.108E+22	0.000E+00	0.000E+00	5.340E-02	0.000E+00	0.000E+00	0.000E+00	0.000E+00	0.000E+00
7	2.33	767.000	276.3	8.654E+21	0.000E+00	0.000E+00	5.114E-02	0.000E+00	0.000E+00	0.000E+00	0.000E+00	0.000E+00
8	2.70	733.000	273.3	3.742E+21	0.000E+00	0.000E+00	4.131E-02	0.000E+00	0.000E+00	0.000E+00	0.000E+00	0.000E+00
9	2.97	708.000	270.8	2.496E+21	0.000E+00	0.000E+00	3.513E-02	0.000E+00	0.000E+00	0.000E+00	0.000E+00	0.000E+00
10	3.06	700.000	271.6	8.858E+20	0.000E+00	0.000E+00	3.324E-02	0.000E+00	0.000E+00	0.000E+00	0.000E+00	0.000E+00
11	3.22	686.000	272.4	9.232E+20	0.000E+00	0.000E+00	3.005E-02	0.000E+00	0.000E+00	0.000E+00	0.000E+00	0.000E+00
12	3.86	633.000	268.1	5.847E+20	0.000E+00	0.000E+00	2.017E-02	0.000E+00	0.000E+00	0.000E+00	0.000E+00	0.000E+00
13	4.44	588.000	265.4	4.228E+20	0.000E+00	0.000E+00	1.369E-02	0.000E+00	0.000E+00	0.000E+00	0.000E+00	0.000E+00
14	5.68	500.000	256.9	5.776E+20	0.000E+00	0.000E+00	8.191E-03	0.000E+00	0.000E+00	0.000E+00	0.000E+00	0.000E+00
15	7.32	400.000	244.1	1.647E+20	0.000E+00	0.000E+00	5.131E-03	0.000E+00	0.000E+00	0.000E+00	0.000E+00	0.000E+00
16	8.66	330.000	233.6	5.927E+19	6.007E-16	0.000E+00	2.241E-03	0.000E+00	0.000E+00	0.000E+00	0.000E+00	0.000E+00
17	9.31	300.000	228.1	2.863E+19	5.116E-06	0.000E+00	7.775E-04	0.000E+00	0.000E+00	0.000E+00	0.000E+00	0.000E+00
18	10.50	250.000	219.1	7.917E+18	1.582E-05	0.000E+00	0.000E+00	3.024E-04	0.000E+00	0.000E+00	0.000E+00	0.000E+00
19	11.28	221.000	214.6	3.908E+18	2.491E-05	0.000E+00	0.000E+00	7.505E-04	0.000E+00	0.000E+00	0.000E+00	0.000E+00
20	11.76	205.000	215.8	4.206E+18	2.786E-05	0.000E+00	0.000E+00	6.761E-04	0.000E+00	0.000E+00	0.000E+00	0.000E+00
21	11.91	200.000	215.1	3.734E+18	2.905E-05	0.000E+00	0.000E+00	6.533E-04	0.000E+00	0.000E+00	0.000E+00	0.000E+00
22	12.62	179.000	217.8	4.850E+18	2.923E-05	0.000E+00	0.000E+00	5.614E-04	0.000E+00	0.000E+00	0.000E+00	0.000E+00
23	13.02	168.000	218.6	4.987E+18	2.910E-05	0.000E+00	0.000E+00	5.152E-04	0.000E+00	0.000E+00	0.000E+00	0.000E+00
24	13.41	158.000	216.8	3.753E+18	2.906E-05	0.000E+00	0.000E+00	4.845E-04	0.000E+00	0.000E+00	0.000E+00	0.000E+00
25	13.74	150.000	217.1	3.659E+18	2.881E-05	0.000E+00	0.000E+00	4.601E-04	0.000E+00	0.000E+00	0.000E+00	0.000E+00
26	14.70	129.000	215.3	2.508E+18	2.805E-05	0.000E+00	0.000E+00	4.086E-04	0.000E+00	0.000E+00	0.000E+00	0.000E+00
27	15.48	114.000	217.3	2.855E+18	2.613E-05	0.000E+00	0.000E+00	3.887E-04	0.000E+00	0.000E+00	0.000E+00	0.000E+00
28	15.88	107.000	216.1	2.285E+18	2.521E-05	0.000E+00	0.000E+00	3.835E-04	0.000E+00	0.000E+00	0.000E+00	0.000E+00
29	16.31	100.000	216.3	2.193E+18	2.407E-05	0.000E+00	0.000E+00	3.950E-04	0.000E+00	0.000E+00	0.000E+00	0.000E+00
30	16.77	93.000	215.3	1.784E+18	2.302E-05	0.000E+00	0.000E+00	4.147E-04	0.000E+00	0.000E+00	0.000E+00	0.000E+00
31	18.57	70.000	215.8	1.455E+18	1.933E-05	0.000E+00	0.000E+00	5.536E-04	0.000E+00	0.000E+00	0.000E+00	0.000E+00
32	20.70	50.000	218.3	1.446E+18	2.147E-05	0.000E+00	0.000E+00	5.262E-04	0.000E+00	0.000E+00	0.000E+00	0.000E+00
33	22.45	38.000	216.3	8.334E+17	2.191E-05	0.000E+00	0.000E+00	3.607E-04	0.000E+00	0.000E+00	0.000E+00	0.000E+00
34	23.96	30.000	218.6	8.903E+17	2.207E-05	0.000E+00	0.000E+00	2.016E-04	0.000E+00	0.000E+00	0.000E+00	0.000E+00

CASE 2A: GIVEN H1, H2, ANGLE

EITHER A SHORT PATH (LEN=0) OR A LONG PATH THROUGH A TANGENT HEIGHT (LEN=1) IS POSSIBLE: LEN = 0

SLANT PATH PARAMETERS IN STANDARD FORM

H1	=	23.957 KM
H2	=	0.000 KM
ANGLE	=	171.800 DEG
PHI	=	8.229 DEG
HMIN	=	0.000 KM
LEN	=	0

ATMOSPHERIC PROFILES

I	Z (KM)	P (MB)	T (K)	CNTMFRN MOL/CM2 KM	HNO3 ATM CM/KM	AEROSOL 1 (-)	AEROSOL 2 (-)	AEROSOL 3 (-)	AEROSOL 4 (-)	AER1*RH (-)	CIRRUS (-)	RH (PERCNT)
1	0.22	987.700	297.0	1.659E+22	0.000E+00	1.706E-01	0.000E+00	0.000E+00	0.000E+00	4.058E+00	0.000E+00	2.378E+01
2	0.30	977.000	295.4	1.580E+22	0.000E+00	1.658E-01	0.000E+00	0.000E+00	0.000E+00	4.157E+00	0.000E+00	2.507E+01
3	0.89	912.000	289.4	1.389E+22	0.000E+00	1.361E-01	0.000E+00	0.000E+00	0.000E+00	4.484E+00	0.000E+00	3.295E+01
4	1.49	850.000	284.1	1.257E+22	0.000E+00	9.115E-02	0.000E+00	0.000E+00	0.000E+00	3.946E+00	0.000E+00	4.329E+01
5	2.05	794.000	277.9	1.107E+22	0.000E+00	0.000E+00	6.031E-02	0.000E+00	0.000E+00	0.000E+00	0.000E+00	0.000E+00
6	2.26	774.000	276.4	1.108E+22	0.000E+00	0.000E+00	5.340E-02	0.000E+00	0.000E+00	0.000E+00	0.000E+00	0.000E+00
7	2.33	767.000	276.3	8.654E+21	0.000E+00	0.000E+00	5.114E-02	0.000E+00	0.000E+00	0.000E+00	0.000E+00	0.000E+00
8	2.70	733.000	273.3	3.742E+21	0.000E+00	0.000E+00	4.131E-02	0.000E+00	0.000E+00	0.000E+00	0.000E+00	0.000E+00
9	2.97	708.000	270.8	2.496E+21	0.000E+00	0.000E+00	3.513E-02	0.000E+00	0.000E+00	0.000E+00	0.000E+00	0.000E+00
10	3.06	700.000	271.6	8.858E+20	0.000E+00	0.000E+00	3.324E-02	0.000E+00	0.000E+00	0.000E+00	0.000E+00	0.000E+00
11	3.22	686.000	272.4	9.232E+20	0.000E+00	0.000E+00	3.005E-02	0.000E+00	0.000E+00	0.000E+00	0.000E+00	0.000E+00
12	3.86	633.000	268.1	5.847E+20	0.000E+00	0.000E+00	2.017E-02	0.000E+00	0.000E+00	0.000E+00	0.000E+00	0.000E+00
13	4.44	588.000	265.4	4.228E+20	0.000E+00	0.000E+00	1.369E-02	0.000E+00	0.000E+00	0.000E+00	0.000E+00	0.000E+00
14	5.68	500.000	256.9	5.776E+20	0.000E+00	0.000E+00	8.191E-03	0.000E+00	0.000E+00	0.000E+00	0.000E+00	0.000E+00
15	7.32	400.000	244.1	1.647E+20	0.000E+00	0.000E+00	5.131E-03	0.000E+00	0.000E+00	0.000E+00	0.000E+00	0.000E+00
16	8.66	330.000	233.6	5.927E+19	6.007E-16	0.000E+00	2.241E-03	0.000E+00	0.000E+00	0.000E+00	0.000E+00	0.000E+00
17	9.31	300.000	228.1	2.863E+19	5.116E-06	0.000E+00	7.775E-04	0.000E+00	0.000E+00	0.000E+00	0.000E+00	0.000E+00
18	10.50	250.000	219.1	7.917E+18	1.582E-05	0.000E+00	0.000E+00	3.024E-04	0.000E+00	0.000E+00	0.000E+00	0.000E+00
19	11.28	221.000	214.6	3.908E+18	2.491E-05	0.000E+00	0.000E+00	7.505E-04	0.000E+00	0.000E+00	0.000E+00	0.000E+00
20	11.76	205.000	215.8	4.206E+18	2.786E-05	0.000E+00	0.000E+00	6.761E-04	0.000E+00	0.000E+00	0.000E+00	0.000E+00
21	11.91	200.000	215.1	3.734E+18	2.905E-05	0.000E+00	0.000E+00	6.533E-04	0.000E+00	0.000E+00	0.000E+00	0.000E+00
22	12.62	179.000	217.8	4.850E+18	2.923E-05	0.000E+00	0.000E+00	5.614E-04	0.000E+00	0.000E+00	0.000E+00	0.000E+00
23	13.02	168.000	218.6	4.987E+18	2.910E-05	0.000E+00	0.000E+00	5.152E-04	0.000E+00	0.000E+00	0.000E+00	0.000E+00
24	13.41	158.000	216.8	3.753E+18	2.906E-05	0.000E+00	0.000E+00	4.845E-04	0.000E+00	0.000E+00	0.000E+00	0.000E+00
25	13.74	150.000	217.1	3.659E+18	2.881E-05	0.000E+00	0.000E+00	4.601E-04	0.000E+00	0.000E+00	0.000E+00	0.000E+00
26	14.70	129.000	215.3	2.508E+18	2.805E-05	0.000E+00	0.000E+00	4.086E-04	0.000E+00	0.000E+00	0.000E+00	0.000E+00
27	15.48	114.000	217.3	2.855E+18	2.613E-05	0.000E+00	0.000E+00	3.887E-04	0.000E+00	0.000E+00	0.000E+00	0.000E+00
28	15.88	107.000	216.1	2.285E+18	2.521E-05	0.000E+00	0.000E+00	3.835E-04	0.000E+00	0.000E+00	0.000E+00	0.000E+00
29	16.31	100.000	216.3	2.193E+18	2.407E-05	0.000E+00	0.000E+00	3.950E-04	0.000E+00	0.000E+00	0.000E+00	0.000E+00
30	16.77	93.000	215.3	1.784E+18	2.302E-05	0.000E+00	0.000E+00	4.147E-04	0.000E+00	0.000E+00	0.000E+00	0.000E+00
31	18.57	70.000	215.8	1.455E+18	1.933E-05	0.000E+00	0.000E+00	5.536E-04	0.000E+00	0.000E+00	0.000E+00	0.000E+00
32	20.70	50.000	218.3	1.446E+18	2.147E-05	0.000E+00	0.000E+00	5.262E-04	0.000E+00	0.000E+00	0.000E+00	0.000E+00
33	22.45	38.000	216.3	8.334E+17	2.191E-05	0.000E+00	0.000E+00	3.607E-04	0.000E+00	0.000E+00	0.000E+00	0.000E+00
34	23.96	30.000	218.6	8.903E+17	2.207E-05	0.000E+00	0.000E+00	2.016E-04	0.000E+00	0.000E+00	0.000E+00	0.000E+00

CASE 2A: GIVEN H1, H2, ANGLE

EITHER A SHORT PATH (LEN=0) OR A LONG PATH THROUGH A TANGENT HEIGHT (LEN=1) IS POSSIBLE: LEN = 0

SLANT PATH PARAMETERS IN STANDARD FORM

H1	=	23.957 KM
H2	=	0.000 KM
ANGLE	=	171.800 DEG
PHI	=	8.229 DEG
HMIN	=	0.000 KM
LEN	=	0

9	13.744	216.22	5.429E-04	1.675E-01	4.718E-02	2.350E-04	1.368E-01	1.278E+15	1.278E+15	1.732E+19
10	13.414	216.95	5.792E-04	1.844E-01	4.846E-02	2.446E-04	1.394E-01	1.321E+15	1.321E+15	1.856E+19
11	13.022	217.71	6.295E-04	2.065E-01	4.992E-02	2.561E-04	1.423E-01	1.384E+15	1.384E+15	2.028E+19
12	12.617	218.20	6.880E-04	2.319E-01	5.133E-02	2.680E-04	1.450E-01	1.458E+15	1.458E+15	2.229E+19
13	11.914	216.42	7.758E-04	2.839E-01	5.361E-02	2.888E-04	1.493E-01	1.544E+15	1.544E+15	2.534E+19
14	11.758	215.40	7.936E-04	2.970E-01	5.409E-02	2.933E-04	1.502E-01	1.557E+15	1.557E+15	2.597E+19
15	11.284	215.19	8.485E-04	3.403E-01	5.554E-02	3.059E-04	1.527E-01	1.595E+15	1.595E+15	2.791E+19
16	10.501	216.88	9.749E-04	4.247E-01	5.782E-02	3.220E-04	1.567E-01	1.700E+15	1.700E+15	3.240E+19
17	9.307	223.63	1.523E-03	5.862E-01	6.106E-02	3.346E-04	1.619E-01	2.761E+15	2.761E+15	5.184E+19
18	8.662	230.87	2.299E-03	6.923E-01	6.274E-02	3.363E-04	1.645E-01	5.780E+15	5.780E+15	7.927E+19
19	7.316	238.99	6.288E-03	9.650E-01	6.619E-02	3.363E-04	1.696E-01	3.649E+16	3.649E+16	2.196E+20
20	5.679	250.63	2.185E-02	1.412E+00	7.027E-02	3.363E-04	1.751E-01	3.182E+17	3.182E+17	7.638E+20
21	4.438	261.22	3.983E-02	1.860E+00	7.333E-02	3.363E-04	1.790E-01	6.874E+17	6.749E+17	1.391E+21
22	3.862	266.81	4.817E-02	2.108E+00	7.476E-02	3.363E-04	1.808E-01	8.191E+17	7.817E+17	1.682E+21
23	3.225	270.27	6.185E-02	2.415E+00	7.636E-02	3.363E-04	1.827E-01	1.103E+18	9.845E+17	2.159E+21
24	3.064	272.00	6.606E-02	2.500E+00	7.676E-02	3.363E-04	1.831E-01	1.200E+18	1.049E+18	2.306E+21
25	2.974	271.20	7.009E-02	2.548E+00	7.699E-02	3.363E-04	1.834E-01	1.367E+18	1.164E+18	2.447E+21
26	2.697	272.00	9.469E-02	2.703E+00	7.769E-02	3.363E-04	1.842E-01	3.179E+18	2.372E+18	3.308E+21
27	2.332	274.76	1.567E-01	2.919E+00	7.862E-02	3.363E-04	1.853E-01	1.168E+19	7.389E+18	5.471E+21
28	2.258	276.30	1.777E-01	2.965E+00	7.881E-02	3.363E-04	1.855E-01	1.611E+19	9.815E+18	6.202E+21
29	2.050	277.15	2.447E-01	3.096E+00	7.935E-02	3.363E-04	1.861E-01	3.157E+19	1.791E+19	8.533E+21
30	1.488	281.06	4.379E-01	3.475E+00	8.080E-02	3.363E-04	1.877E-01	7.589E+19	3.630E+19	1.524E+22
31	0.895	286.76	6.670E-01	3.913E+00	8.237E-02	3.363E-04	1.893E-01	1.290E+20	4.992E+19	2.315E+22
32	0.304	292.36	9.242E-01	4.394E+00	8.397E-02	3.363E-04	1.910E-01	1.893E+20	5.601E+19	3.200E+22
33	0.218	296.20	9.653E-01	4.468E+00	8.421E-02	3.363E-04	1.913E-01	1.992E+20	5.601E+19	3.341E+22
34	0.000	299.20	1.079E+00	4.658E+00	8.481E-02	3.363E-04	1.919E-01	2.287E+20	5.601E+19	3.730E+22

J	Z (KM)	N2 CONT	MOL SCAT	AER 1	AER 2	AER 3	AER 4	CIRRUS
1	22.452	1.921E-03	6.382E-02	0.000E+00	0.000E+00	4.158E-04	0.000E+00	0.000E+00
2	20.705	5.648E-03	1.596E-01	0.000E+00	0.000E+00	1.189E-03	0.000E+00	0.000E+00
3	18.565	1.414E-02	3.192E-01	0.000E+00	0.000E+00	2.357E-03	0.000E+00	0.000E+00
4	16.771	2.743E-02	5.027E-01	0.000E+00	0.000E+00	3.234E-03	0.000E+00	0.000E+00
5	16.313	3.221E-02	5.585E-01	0.000E+00	0.000E+00	3.422E-03	0.000E+00	0.000E+00
6	15.884	3.736E-02	6.145E-01	0.000E+00	0.000E+00	3.591E-03	0.000E+00	0.000E+00
7	15.482	4.282E-02	6.702E-01	0.000E+00	0.000E+00	3.747E-03	0.000E+00	0.000E+00
8	14.699	5.571E-02	7.898E-01	0.000E+00	0.000E+00	4.062E-03	0.000E+00	0.000E+00
9	13.744	7.646E-02	9.574E-01	0.000E+00	0.000E+00	4.481E-03	0.000E+00	0.000E+00
10	13.414	8.516E-02	1.021E+00	0.000E+00	0.000E+00	4.638E-03	0.000E+00	0.000E+00
11	13.022	9.667E-02	1.101E+00	0.000E+00	0.000E+00	4.836E-03	0.000E+00	0.000E+00
12	12.617	1.101E-01	1.189E+00	0.000E+00	0.000E+00	5.056E-03	0.000E+00	0.000E+00
13	11.914	1.383E-01	1.356E+00	0.000E+00	0.000E+00	5.487E-03	0.000E+00	0.000E+00
14	11.758	1.455E-01	1.396E+00	0.000E+00	0.000E+00	5.592E-03	0.000E+00	0.000E+00
15	11.284	1.697E-01	1.524E+00	0.000E+00	0.000E+00	5.933E-03	0.000E+00	0.000E+00
16	10.501	2.179E-01	1.755E+00	0.000E+00	0.000E+00	6.350E-03	0.000E+00	0.000E+00
17	9.307	3.135E-01	2.154E+00	0.000E+00	4.690E-04	6.532E-03	0.000E+00	0.000E+00
18	8.662	3.783E-01	2.393E+00	0.000E+00	1.370E-03	6.532E-03	0.000E+00	0.000E+00
19	7.316	5.501E-01	2.952E+00	0.000E+00	6.115E-03	6.532E-03	0.000E+00	0.000E+00
20	5.679	8.455E-01	3.749E+00	0.000E+00	1.694E-02	6.532E-03	0.000E+00	0.000E+00
21	4.438	1.154E+00	4.451E+00	0.000E+00	3.036E-02	6.532E-03	0.000E+00	0.000E+00
22	3.862	1.329E+00	4.810E+00	0.000E+00	4.010E-02	6.532E-03	0.000E+00	0.000E+00
23	3.225	1.550E+00	5.234E+00	0.000E+00	5.605E-02	6.532E-03	0.000E+00	0.000E+00
24	3.064	1.612E+00	5.345E+00	0.000E+00	6.119E-02	6.532E-03	0.000E+00	0.000E+00
25	2.974	1.647E+00	5.409E+00	0.000E+00	6.429E-02	6.532E-03	0.000E+00	0.000E+00
26	2.697	1.761E+00	5.609E+00	0.000E+00	7.497E-02	6.532E-03	0.000E+00	0.000E+00
27	2.332	1.921E+00	5.880E+00	0.000E+00	9.197E-02	6.532E-03	0.000E+00	0.000E+00
28	2.258	1.955E+00	5.936E+00	0.000E+00	9.586E-02	6.532E-03	0.000E+00	0.000E+00

29	2.050	2.054E+00	6.097E+00	0.000E+00	1.078E-01	6.532E-03	0.000E+00	0.000E+00
30	1.488	2.340E+00	6.544E+00	2.588E-02	1.249E-01	6.532E-03	0.000E+00	0.000E+00
31	0.895	2.676E+00	7.040E+00	9.302E-02	1.249E-01	6.532E-03	0.000E+00	0.000E+00
32	0.304	3.051E+00	7.560E+00	1.829E-01	1.249E-01	6.532E-03	0.000E+00	0.000E+00
33	0.218	3.109E+00	7.638E+00	1.975E-01	1.249E-01	6.532E-03	0.000E+00	0.000E+00
34	0.000	3.259E+00	7.836E+00	2.365E-01	1.249E-01	6.532E-03	0.000E+00	0.000E+00

SUMMARY OF THE GEOMETRY CALCULATION

H1	=	23.957 KM
H2	=	0.000 KM
ANGLE	=	171.800 DEG
RANGE	=	24.206 KM
BETA	=	0.031 DEG
PHI	=	8.229 DEG
HMIN	=	0.000 KM
BENDING	=	0.002 DEG
LEN	=	0

EQUIVALENT SEA LEVEL TOTAL ABSORBER AMOUNTS

H2O	CO2+	O3	HNO3	O3 UV	CNTMSLF1	CNTMSLF2	CNTMFRN
(SCALED LOWTRAN UNITS)			(ATM CM)	(ATM CM)	(MOL CM-2)	(MOL CM-2)	(MOL CM-2)
1.079E+00	4.658E+00	8.481E-02	3.363E-04	1.919E-01	2.287E+20	5.601E+19	3.730E+22

N2 CONT	MOL SCAT	AER 1	AER 2	AER 3	AER 4	CIRRUS	MEAN RH (PRCNT)
3.259E+00	7.836E+00	2.365E-01	1.249E-01	6.532E-03	0.000E+00	0.000E+00	31.48

SINGLE SCATTERING POINT TO SOURCE PATHS

SCTTR POINT	SCTTR ALT	SUBTENDED ANGLE	SOLAR ZENITH	PATH ZENITH	RELATIVE AZIMUTH	SCTTR ANGLE	MOLECULAR PHASE F
1	0.00	0.00	30.14	171.80	122.13	153.39	0.106E+00
2	22.45	0.00	30.14	171.80	122.13	153.39	0.106E+00
3	20.70	0.00	30.14	171.80	122.14	153.39	0.106E+00
4	18.57	0.01	30.14	171.79	122.14	153.39	0.106E+00
5	16.77	0.01	30.14	171.79	122.14	153.39	0.106E+00
6	16.31	0.01	30.14	171.79	122.15	153.39	0.106E+00
7	15.88	0.01	30.14	171.79	122.15	153.39	0.106E+00
8	15.48	0.01	30.14	171.79	122.15	153.39	0.106E+00
9	14.70	0.01	30.14	171.79	122.15	153.39	0.106E+00
10	13.74	0.01	30.14	171.79	122.15	153.39	0.106E+00
11	13.41	0.01	30.15	171.79	122.15	153.39	0.106E+00
12	13.02	0.01	30.15	171.79	122.15	153.39	0.106E+00
13	12.62	0.01	30.15	171.79	122.15	153.39	0.106E+00
14	11.91	0.02	30.15	171.78	122.15	153.39	0.106E+00
15	11.76	0.02	30.15	171.78	122.15	153.39	0.106E+00
16	11.28	0.02	30.15	171.78	122.15	153.39	0.106E+00
17	10.50	0.02	30.15	171.78	122.16	153.39	0.106E+00
18	9.31	0.02	30.15	171.78	122.16	153.39	0.106E+00

19	8.66	0.02	30.15	171.78	122.16	153.39	0.106E+00
20	7.32	0.02	30.15	171.78	122.16	153.39	0.106E+00
21	5.68	0.02	30.15	171.78	122.17	153.39	0.106E+00
22	4.44	0.03	30.15	171.78	122.17	153.39	0.106E+00
23	3.86	0.03	30.15	171.78	122.17	153.39	0.106E+00
24	3.22	0.03	30.15	171.77	122.17	153.39	0.106E+00
25	3.06	0.03	30.15	171.77	122.17	153.39	0.106E+00
26	2.97	0.03	30.15	171.77	122.17	153.39	0.106E+00
27	2.70	0.03	30.15	171.77	122.17	153.39	0.106E+00
28	2.33	0.03	30.15	171.77	122.17	153.39	0.106E+00
29	2.26	0.03	30.15	171.77	122.17	153.39	0.106E+00
30	2.05	0.03	30.15	171.77	122.17	153.39	0.106E+00
31	1.49	0.03	30.15	171.77	122.17	153.39	0.106E+00
32	0.89	0.03	30.15	171.77	122.17	153.39	0.106E+00
33	0.30	0.03	30.15	171.77	122.18	153.39	0.106E+00
34	0.22	0.03	30.15	171.77	122.18	153.39	0.106E+00
35	0.00	0.03	30.15	171.77	122.18	153.39	0.106E+00

RADIANCE(WATTS/CM2-STER-XXX)

FREQ (CM-1)	WAVLEN (MICRN)	ATMOS RADIANCE (CM-1)	(MICRN)	PATH SCATTERED (CM-1)	(MICRN)	GROUND REFLECTED (CM-1)	(MICRN)	TOTAL (CM-1)	(MICRN)	INTEGRAL (CM-1)	TOTAL TRANS
11110.	0.900	2.09E-25	2.58E-21	2.41E-08	2.97E-04	0.00E+00	0.00E+00	2.41E-08	2.97E-04	2.41E-07	0.6920
11130.	0.898	1.94E-25	2.40E-21	2.40E-08	2.97E-04	0.00E+00	0.00E+00	2.40E-08	2.97E-04	7.21E-07	0.6849
11150.	0.897	1.77E-25	2.20E-21	2.41E-08	2.99E-04	0.00E+00	0.00E+00	2.41E-08	2.99E-04	1.20E-06	0.6833
11170.	0.895	1.24E-25	1.55E-21	2.50E-08	3.12E-04	0.00E+00	0.00E+00	2.50E-08	3.12E-04	1.70E-06	0.7215
11190.	0.894	8.62E-26	1.08E-21	2.59E-08	3.24E-04	0.00E+00	0.00E+00	2.59E-08	3.24E-04	2.22E-06	0.7545
11210.	0.892	4.52E-26	5.69E-22	2.67E-08	3.36E-04	0.00E+00	0.00E+00	2.67E-08	3.36E-04	2.75E-06	0.7881
11230.	0.890	3.40E-26	4.29E-22	2.69E-08	3.39E-04	0.00E+00	0.00E+00	2.69E-08	3.39E-04	3.29E-06	0.7937
11250.	0.889	2.80E-26	3.55E-22	2.71E-08	3.43E-04	0.00E+00	0.00E+00	2.71E-08	3.43E-04	3.83E-06	0.7963
11270.	0.887	2.44E-26	3.10E-22	2.72E-08	3.45E-04	0.00E+00	0.00E+00	2.72E-08	3.45E-04	4.38E-06	0.7967
11290.	0.886	2.31E-26	2.94E-22	2.73E-08	3.48E-04	0.00E+00	0.00E+00	2.73E-08	3.48E-04	4.92E-06	0.7955
11310.	0.884	1.99E-26	2.54E-22	2.74E-08	3.50E-04	0.00E+00	0.00E+00	2.74E-08	3.50E-04	5.47E-06	0.7962
11330.	0.883	1.84E-26	2.37E-22	2.75E-08	3.52E-04	0.00E+00	0.00E+00	2.75E-08	3.52E-04	6.02E-06	0.7949
11350.	0.881	1.64E-26	2.12E-22	2.76E-08	3.55E-04	0.00E+00	0.00E+00	2.76E-08	3.55E-04	6.57E-06	0.7952
11370.	0.880	1.50E-26	1.94E-22	2.77E-08	3.58E-04	0.00E+00	0.00E+00	2.77E-08	3.58E-04	7.13E-06	0.7947
11390.	0.878	1.36E-26	1.76E-22	2.78E-08	3.60E-04	0.00E+00	0.00E+00	2.78E-08	3.60E-04	7.68E-06	0.7943
11410.	0.876	1.21E-26	1.57E-22	2.79E-08	3.63E-04	0.00E+00	0.00E+00	2.79E-08	3.63E-04	8.24E-06	0.7944
11430.	0.875	1.09E-26	1.43E-22	2.80E-08	3.66E-04	0.00E+00	0.00E+00	2.80E-08	3.66E-04	8.80E-06	0.7940
11450.	0.873	9.94E-27	1.30E-22	2.81E-08	3.68E-04	0.00E+00	0.00E+00	2.81E-08	3.68E-04	9.36E-06	0.7935
11470.	0.872	9.04E-27	1.19E-22	2.82E-08	3.71E-04	0.00E+00	0.00E+00	2.82E-08	3.71E-04	9.92E-06	0.7931
11490.	0.870	8.23E-27	1.09E-22	2.83E-08	3.74E-04	0.00E+00	0.00E+00	2.83E-08	3.74E-04	1.05E-05	0.7926
11510.	0.869	7.49E-27	9.93E-23	2.84E-08	3.76E-04	0.00E+00	0.00E+00	2.84E-08	3.76E-04	1.11E-05	0.7921
11530.	0.867	6.82E-27	9.07E-23	2.85E-08	3.79E-04	0.00E+00	0.00E+00	2.85E-08	3.79E-04	1.16E-05	0.7916
11550.	0.866	6.21E-27	8.28E-23	2.86E-08	3.82E-04	0.00E+00	0.00E+00	2.86E-08	3.82E-04	1.22E-05	0.7911
11570.	0.864	5.65E-27	7.56E-23	2.87E-08	3.84E-04	0.00E+00	0.00E+00	2.87E-08	3.84E-04	1.28E-05	0.7906
11590.	0.863	5.14E-27	6.91E-23	2.88E-08	3.87E-04	0.00E+00	0.00E+00	2.88E-08	3.87E-04	1.33E-05	0.7902
11610.	0.861	4.68E-27	6.31E-23	2.89E-08	3.90E-04	0.00E+00	0.00E+00	2.89E-08	3.90E-04	1.39E-05	0.7897
11630.	0.860	4.26E-27	5.77E-23	2.90E-08	3.92E-04	0.00E+00	0.00E+00	2.90E-08	3.92E-04	1.45E-05	0.7892
11650.	0.858	3.88E-27	5.27E-23	2.91E-08	3.95E-04	0.00E+00	0.00E+00	2.91E-08	3.95E-04	1.51E-05	0.7887
11670.	0.857	3.54E-27	4.82E-23	2.92E-08	3.98E-04	0.00E+00	0.00E+00	2.92E-08	3.98E-04	1.57E-05	0.7882
11690.	0.855	3.22E-27	4.40E-23	2.93E-08	4.00E-04	0.00E+00	0.00E+00	2.93E-08	4.00E-04	1.63E-05	0.7877
11710.	0.854	2.94E-27	4.02E-23	2.94E-08	4.03E-04	0.00E+00	0.00E+00	2.94E-08	4.03E-04	1.68E-05	0.7872
11730.	0.853	2.67E-27	3.68E-23	2.95E-08	4.06E-04	0.00E+00	0.00E+00	2.95E-08	4.06E-04	1.74E-05	0.7868
11750.	0.851	2.44E-27	3.37E-23	2.96E-08	4.09E-04	0.00E+00	0.00E+00	2.96E-08	4.09E-04	1.80E-05	0.7862
11770.	0.850	2.24E-27	3.10E-23	2.97E-08	4.11E-04	0.00E+00	0.00E+00	2.97E-08	4.11E-04	1.86E-05	0.7856
11790.	0.848	2.08E-27	2.89E-23	2.98E-08	4.14E-04	0.00E+00	0.00E+00	2.98E-08	4.14E-04	1.92E-05	0.7846
11810.	0.847	2.05E-27	2.85E-23	2.99E-08	4.16E-04	0.00E+00	0.00E+00	2.99E-08	4.16E-04	1.98E-05	0.7824
11830.	0.845	1.87E-27	2.62E-23	3.00E-08	4.19E-04	0.00E+00	0.00E+00	3.00E-08	4.19E-04	2.04E-05	0.7817
11850.	0.844	1.87E-27	2.63E-23	3.00E-08	4.21E-04	0.00E+00	0.00E+00	3.00E-08	4.21E-04	2.10E-05	0.7787
11870.	0.842	1.82E-27	2.56E-23	3.00E-08	4.23E-04	0.00E+00	0.00E+00	3.00E-08	4.23E-04	2.16E-05	0.7758
11890.	0.841	1.86E-27	2.64E-23	3.01E-08	4.25E-04	0.00E+00	0.00E+00	3.01E-08	4.25E-04	2.22E-05	0.7718
11910.	0.840	1.73E-27	2.45E-23	3.01E-08	4.27E-04	0.00E+00	0.00E+00	3.01E-08	4.27E-04	2.28E-05	0.7700
11930.	0.838	2.21E-27	3.15E-23	2.98E-08	4.24E-04	0.00E+00	0.00E+00	2.98E-08	4.24E-04	2.34E-05	0.7524
11950.	0.837	1.95E-27	2.79E-23	3.00E-08	4.28E-04	0.00E+00	0.00E+00	3.00E-08	4.28E-04	2.40E-05	0.7546
11970.	0.835	2.02E-27	2.89E-23	2.98E-08	4.27E-04	0.00E+00	0.00E+00	2.98E-08	4.27E-04	2.46E-05	0.7444
11990.	0.834	2.12E-27	3.05E-23	2.96E-08	4.26E-04	0.00E+00	0.00E+00	2.96E-08	4.26E-04	2.52E-05	0.7319
12010.	0.833	2.12E-27	3.05E-23	2.94E-08	4.24E-04	0.00E+00	0.00E+00	2.94E-08	4.24E-04	2.58E-05	0.7186
12030.	0.831	1.89E-27	2.74E-23	2.97E-08	4.30E-04	0.00E+00	0.00E+00	2.97E-08	4.30E-04	2.64E-05	0.7262
12050.	0.830	1.58E-27	2.30E-23	2.99E-08	4.35E-04	0.00E+00	0.00E+00	2.99E-08	4.35E-04	2.70E-05	0.7314
12070.	0.829	1.44E-27	2.10E-23	3.00E-08	4.38E-04	0.00E+00	0.00E+00	3.00E-08	4.38E-04	2.76E-05	0.7309
12090.	0.827	1.09E-27	1.60E-23	3.05E-08	4.46E-04	0.00E+00	0.00E+00	3.05E-08	4.46E-04	2.82E-05	0.7460

RADIANCE(WATTS/CM2-STER-XXX)

FREQ (CM-1)	WAVLEN (MICRN)	ATMOS RADIANCE (CM-1)	ATMOS RADIANCE (MICRN)	PATH SCATTERED (CM-1)	PATH SCATTERED (MICRN)	GROUND REFLECTED (CM-1)	GROUND REFLECTED (MICRN)	TOTAL (CM-1)	TOTAL (MICRN)	INTEGRAL (CM-1)	TOTAL TRANS
12110.	0.826	9.77E-28	1.43E-23	3.07E-08	4.50E-04	0.00E+00	0.00E+00	3.07E-08	4.50E-04	2.88E-05	0.7474
12130.	0.824	9.95E-28	1.46E-23	3.05E-08	4.49E-04	0.00E+00	0.00E+00	3.05E-08	4.49E-04	2.94E-05	0.7376
12150.	0.823	1.91E-27	2.82E-23	2.80E-08	4.14E-04	0.00E+00	0.00E+00	2.80E-08	4.14E-04	3.00E-05	0.6362
12170.	0.822	6.27E-28	9.28E-24	3.12E-08	4.62E-04	0.00E+00	0.00E+00	3.12E-08	4.62E-04	3.06E-05	0.7548
12190.	0.820	6.89E-28	1.02E-23	3.10E-08	4.61E-04	0.00E+00	0.00E+00	3.10E-08	4.61E-04	3.12E-05	0.7438
12210.	0.819	8.43E-28	1.26E-23	3.04E-08	4.53E-04	0.00E+00	0.00E+00	3.04E-08	4.53E-04	3.18E-05	0.7145
12230.	0.818	9.16E-28	1.37E-23	3.00E-08	4.48E-04	0.00E+00	0.00E+00	3.00E-08	4.48E-04	3.24E-05	0.6934
12250.	0.816	9.74E-28	1.46E-23	2.95E-08	4.43E-04	0.00E+00	0.00E+00	2.95E-08	4.43E-04	3.30E-05	0.6728
12270.	0.815	8.08E-28	1.22E-23	2.99E-08	4.50E-04	0.00E+00	0.00E+00	2.99E-08	4.50E-04	3.36E-05	0.6820
12290.	0.814	6.98E-28	1.05E-23	3.03E-08	4.57E-04	0.00E+00	0.00E+00	3.03E-08	4.57E-04	3.42E-05	0.6915
12310.	0.812	4.09E-28	6.20E-24	3.16E-08	4.79E-04	0.00E+00	0.00E+00	3.16E-08	4.79E-04	3.49E-05	0.7385
12330.	0.811	3.45E-28	5.25E-24	3.18E-08	4.83E-04	0.00E+00	0.00E+00	3.18E-08	4.83E-04	3.55E-05	0.7423
12350.	0.810	2.22E-28	3.38E-24	3.23E-08	4.93E-04	0.00E+00	0.00E+00	3.23E-08	4.93E-04	3.61E-05	0.7583
12370.	0.808	1.73E-28	2.64E-24	3.26E-08	4.99E-04	0.00E+00	0.00E+00	3.26E-08	4.99E-04	3.68E-05	0.7651
12390.	0.807	1.40E-28	2.15E-24	3.28E-08	5.04E-04	0.00E+00	0.00E+00	3.28E-08	5.04E-04	3.75E-05	0.7682
12410.	0.806	1.26E-28	1.95E-24	3.29E-08	5.07E-04	0.00E+00	0.00E+00	3.29E-08	5.07E-04	3.81E-05	0.7679
12430.	0.805	1.25E-28	1.93E-24	3.29E-08	5.09E-04	0.00E+00	0.00E+00	3.29E-08	5.09E-04	3.88E-05	0.7651
12450.	0.803	1.19E-28	1.84E-24	3.30E-08	5.12E-04	0.00E+00	0.00E+00	3.30E-08	5.12E-04	3.94E-05	0.7635
12470.	0.802	1.07E-28	1.66E-24	3.31E-08	5.15E-04	0.00E+00	0.00E+00	3.31E-08	5.15E-04	4.01E-05	0.7634
12490.	0.801	9.46E-29	1.48E-24	3.32E-08	5.18E-04	0.00E+00	0.00E+00	3.32E-08	5.18E-04	4.08E-05	0.7636
12510.	0.799	8.13E-29	1.27E-24	3.34E-08	5.22E-04	0.00E+00	0.00E+00	3.34E-08	5.22E-04	4.14E-05	0.7648
12530.	0.798	7.80E-29	1.22E-24	3.34E-08	5.25E-04	0.00E+00	0.00E+00	3.34E-08	5.25E-04	4.21E-05	0.7631
12550.	0.797	8.18E-29	1.29E-24	3.34E-08	5.27E-04	0.00E+00	0.00E+00	3.34E-08	5.27E-04	4.28E-05	0.7590
12570.	0.796	5.77E-29	9.12E-25	3.37E-08	5.33E-04	0.00E+00	0.00E+00	3.37E-08	5.33E-04	4.34E-05	0.7654
12590.	0.794	4.97E-29	7.87E-25	3.39E-08	5.37E-04	0.00E+00	0.00E+00	3.39E-08	5.37E-04	4.41E-05	0.7664
12610.	0.793	4.81E-29	7.66E-25	3.39E-08	5.39E-04	0.00E+00	0.00E+00	3.39E-08	5.39E-04	4.48E-05	0.7641
12630.	0.792	4.49E-29	7.16E-25	3.40E-08	5.42E-04	0.00E+00	0.00E+00	3.40E-08	5.42E-04	4.55E-05	0.7631
12650.	0.791	4.22E-29	6.75E-25	3.41E-08	5.45E-04	0.00E+00	0.00E+00	3.41E-08	5.45E-04	4.62E-05	0.7617
12670.	0.789	4.24E-29	6.80E-25	3.41E-08	5.47E-04	0.00E+00	0.00E+00	3.41E-08	5.47E-04	4.68E-05	0.7585
12690.	0.788	3.50E-29	5.63E-25	3.43E-08	5.52E-04	0.00E+00	0.00E+00	3.43E-08	5.52E-04	4.75E-05	0.7608
12710.	0.787	3.15E-29	5.09E-25	3.44E-08	5.55E-04	0.00E+00	0.00E+00	3.44E-08	5.55E-04	4.82E-05	0.7608
12730.	0.786	2.55E-29	4.13E-25	3.46E-08	5.60E-04	0.00E+00	0.00E+00	3.46E-08	5.60E-04	4.89E-05	0.7631
12750.	0.784	2.36E-29	3.84E-25	3.46E-08	5.63E-04	0.00E+00	0.00E+00	3.46E-08	5.63E-04	4.96E-05	0.7624
12770.	0.783	2.00E-29	3.27E-25	3.48E-08	5.67E-04	0.00E+00	0.00E+00	3.48E-08	5.67E-04	5.03E-05	0.7636
12790.	0.782	1.81E-29	2.96E-25	3.49E-08	5.71E-04	0.00E+00	0.00E+00	3.49E-08	5.71E-04	5.10E-05	0.7633
12810.	0.781	1.65E-29	2.71E-25	3.50E-08	5.74E-04	0.00E+00	0.00E+00	3.50E-08	5.74E-04	5.17E-05	0.7628
12830.	0.779	1.50E-29	2.47E-25	3.51E-08	5.78E-04	0.00E+00	0.00E+00	3.51E-08	5.78E-04	5.24E-05	0.7624
12850.	0.778	1.37E-29	2.25E-25	3.52E-08	5.81E-04	0.00E+00	0.00E+00	3.52E-08	5.81E-04	5.31E-05	0.7620
12870.	0.777	1.24E-29	2.06E-25	3.53E-08	5.84E-04	0.00E+00	0.00E+00	3.53E-08	5.84E-04	5.38E-05	0.7616
12890.	0.776	1.13E-29	1.88E-25	3.54E-08	5.88E-04	0.00E+00	0.00E+00	3.54E-08	5.88E-04	5.45E-05	0.7612
12910.	0.775	1.03E-29	1.72E-25	3.55E-08	5.91E-04	0.00E+00	0.00E+00	3.55E-08	5.91E-04	5.52E-05	0.7607
12930.	0.773	9.37E-30	1.57E-25	3.56E-08	5.95E-04	0.00E+00	0.00E+00	3.56E-08	5.95E-04	5.59E-05	0.7603
12950.	0.772	8.52E-30	1.43E-25	3.57E-08	5.98E-04	0.00E+00	0.00E+00	3.57E-08	5.98E-04	5.66E-05	0.7599
12970.	0.771	7.76E-30	1.30E-25	3.58E-08	6.02E-04	0.00E+00	0.00E+00	3.58E-08	6.02E-04	5.74E-05	0.7595
12990.	0.770	8.26E-30	1.39E-25	3.55E-08	5.98E-04	0.00E+00	0.00E+00	3.55E-08	5.98E-04	5.81E-05	0.7506
13010.	0.769	9.24E-30	1.56E-25	3.45E-08	5.83E-04	0.00E+00	0.00E+00	3.45E-08	5.83E-04	5.88E-05	0.7279
13030.	0.767	1.09E-29	1.86E-25	3.24E-08	5.50E-04	0.00E+00	0.00E+00	3.24E-08	5.50E-04	5.94E-05	0.6812
13050.	0.766	1.38E-29	2.34E-25	2.92E-08	4.97E-04	0.00E+00	0.00E+00	2.92E-08	4.97E-04	6.00E-05	0.6123
13070.	0.765	1.67E-29	2.86E-25	2.41E-08	4.11E-04	0.00E+00	0.00E+00	2.41E-08	4.11E-04	6.05E-05	0.4996
13090.	0.764	1.85E-29	3.18E-25	1.88E-08	3.22E-04	0.00E+00	0.00E+00	1.88E-08	3.22E-04	6.08E-05	0.3749

RADIANCE(WATTS/CM2-STER-XXX)

FREQ (CM-1)	WAVLEN (MICRN)	ATMOS RADIANCE (CM-1)	ATMOS RADIANCE (MICRN)	PATH SCATTERED (CM-1)	PATH SCATTERED (MICRN)	GROUND REFLECTED (CM-1)	GROUND REFLECTED (MICRN)	TOTAL (CM-1)	TOTAL (MICRN)	INTEGRAL (CM-1)	TOTAL TRANS
13110.	0.763	1.69E-29	2.91E-25	1.94E-08	3.33E-04	0.00E+00	0.00E+00	1.94E-08	3.33E-04	6.12E-05	0.3881
13130.	0.762	1.51E-29	2.61E-25	1.87E-08	3.23E-04	0.00E+00	0.00E+00	1.87E-08	3.23E-04	6.16E-05	0.3713
13150.	0.760	1.31E-29	2.26E-25	1.05E-08	1.81E-04	0.00E+00	0.00E+00	1.05E-08	1.81E-04	6.18E-05	0.1823
13170.	0.759	7.86E-30	1.36E-25	2.96E-08	5.13E-04	0.00E+00	0.00E+00	2.96E-08	5.13E-04	6.21E-05	0.6084

INTEGRATED ABSORPTION FROM11110 TO13170 CM-1 = 538.35 CM-1
AVERAGE TRANSMITTANCE =0.7387

INTEGRATED RADIANCE = 6.211E-05 WATTS CM-2 STER-1
MINIMUM RADIANCE = 1.045E-08 WATTS CM-2 STER-1 (CM-1)-1 AT 13150.0 CM-1
MAXIMUM RADIANCE = 3.579E-08 WATTS CM-2 STER-1 (CM-1)-1 AT 12970.0 CM-1
BOUNDARY TEMPERATURE = 0.00 K
BOUNDARY EMISSIVITY = 1.000

CARD 5 ***** 1

6.2 Appendix B Spectral Response of the LANDSAT-4 TM and LANDSAT-5 TM Reflected Energy Sensors

The relative spectral response characteristics of the LANDSAT 4 and 5 Thematic Mapper sensors were determines by Markham and Barker[89]. They designated the TM-4 sensors the "protoflight" model and the TM sensors the "flight" model. The relative spectral response characteristics for the two sensors are presented on the following pages.

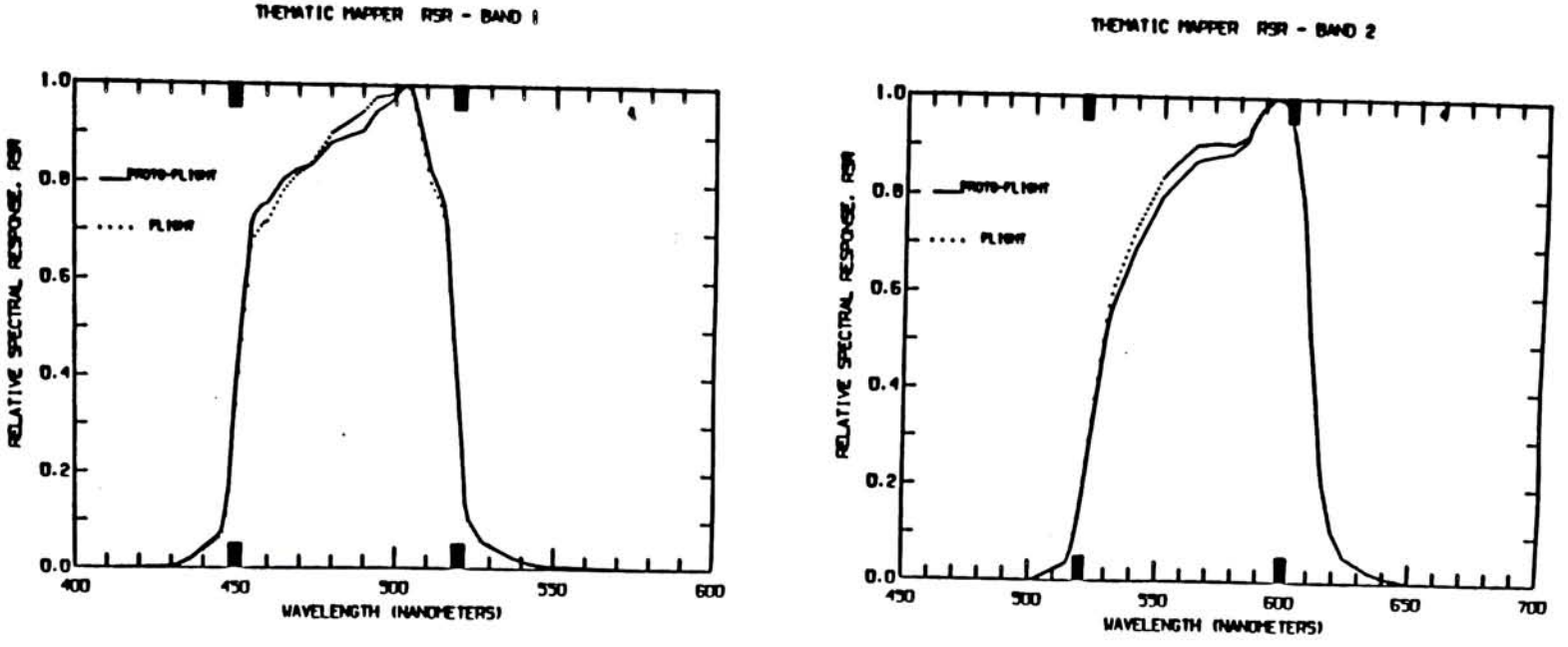

Figure 6.2-1 LANDSAT TM Spectral Response Band 1 and Band 2

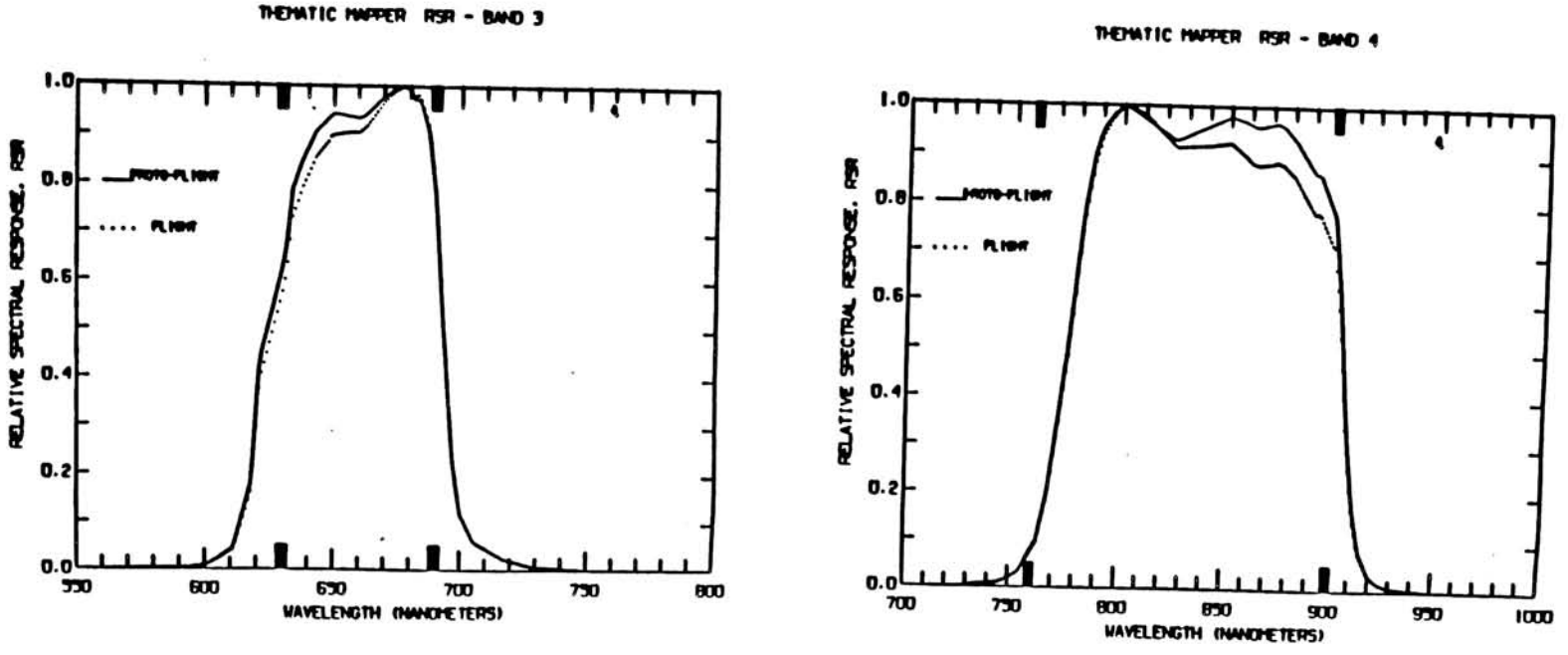

Figure 6.2-2 LANDSAT TM Spectral Response Band 3 and Band 4

6.3 Appendix C LANDSAT TM Tape Reading and Format Programs

Programs: READ_TM_TAPE
PATCH
SUBSAMP

```
*****************************************************************
*
*       program read_tm_tape
*
*  This program will read an EROS Data Center LANDSAT TM P-format tape
*
*  The program assumes that the tape is loaded on drive MUA0:
*   Three disk files are output:
*              1) LANDSAT.PIC  -> The image quadrant
*               2) LANDSAT_LRFILL.DAT -> Fill pixel data
*
*   Author: John Francis
*
*****************************************************************
*
      integer*4   line_num,left_fill,right_fill
      character*50  lognam,outnam
      character*12  docnum
      character*4   datbuff,skip_file
      character*1   charbuff(4500),char
      byte  bytebuff(4500),  itb

*****************************************************************
*
*  Set up some equivalences for reading image information
*
*****************************************************************
      equivalence  ( charbuff(1),  bytebuff(1) )
      equivalence  (bytebuff(1),  irecnum)
      equivalence  (bytebuff(5),  irecod)
      equivalence  (bytebuff(9),  ireclen)

*****************************************************************
*
*     Allocate and mount the tape and skip to the desired file
*
*****************************************************************
      lognam='mua0:'
c
      type61
  61  format(' Number of tape files to skip?> ')
      accept13,  skip_file
  13  format(a)
      call lib$spawn('ALLOC MUA0:')
      call lib$spawn('MOUNT/FOR/BLOCKSIZE=4320/RECORDSIZE=4320 MUA0:')
      call  lib$spawn('SET  MAG/SKIP=FILES:'//skip_file//'  mua0:')
c
      open(3,file=lognam,form='unformatted',blocksize=4320,
     +     recordtype='fixed',access='sequential',
     +     status='old',recl=4320/4)
      outnam='landsat.pic'
```

```
*****************************************************************
*
*    Determine the number of lines and pixels in the image quadrant
*
*****************************************************************
      read(3)  (bytebuff(i),  i=1,4320)
      datbuff=charbuff(253)//charbuff(254)//charbuff(255)//charbuff(256)
      read(datbuff,*)  npixels
      datbuff=charbuff(241)//charbuff(242)//charbuff(243)//charbuff(244)
      read(datbuff,*)  nlines
c
      type*,'  npixels,nlines=',npixels,nlines

*****************************************************************
*
*                Open the output files
*
*****************************************************************

      open(1,file=outnam,form='unformatted',
     +     recordtype='fixed',access='sequential',
     +     status='new',recl=4220/4)
c
      type*, 'Hit <ret> to continue'
      accept13,char
      open(2,file='landsat_lrfill.dat',form='unformatted',
     +     recordtype='fixed',access='sequential',
     +     status='new',recl=3)

*****************************************************************
*
*       Read an image data line and save the image and fill data
*
*****************************************************************
      do k=1,nlines
         read(3)  (bytebuff(i),  i=1,4320)
         call  byte_to_i4(bytebuff(13),line_num)
         call  byte_to_i4(bytebuff(25),left_fill)
         call  byte_to_i4(bytebuff(29),right_fill)
         write(1)  (bytebuff(i),  i=33,4252)
         write(2)  line_num,left_fill,right_fill
      end do
  999 stop
      end
```

```
*
*****************************************************************
C
      subroutine  byte_to_i4(jbyte,i4val)
*
*  subroutine to reverse the order of bytes in binary imtegers for VAX
*
*****************************************************************
      integer*4  i4val,itemp
      byte  ibyte(4),  jbyte(4),  itbyt
C
      equivalence  ( itemp,  ibyte(1) )
C
C  copy 4 bytes into temp vector
C
      do  i=1,4
          ibyte(i)=jbyte(i)
      enddo
C
C swap the bytes around --> 1 2 3 4  to  4 3 2 1
C
          itbyt=ibyte(1)
          ibyte(1)=ibyte(4)
          ibyte(4)=itbyt
          itbyt=ibyte(3)
          ibyte(3)=ibyte(2)
          ibyte(2)=itbyt
C
      i4val=itemp   ! for the return
      return
      end
```

```
*****************************************************************
*
*       program patch
*
*   Program to create a single image from quadrant 1 and quadrant 2 of a
*                    LANDSAT TM image
*   The program expects the image quadrant data and fill pixel data that
*    is output from the program READ_TM_TAPE
*
*   The program creates a single image called b%q12.pic
*    where % indicates the TM image band number
*
*   Author:  John Francis
*
*****************************************************************

        implicit  integer*4  (a-z)
c
        byte  q1buff(4220),  q2buff(4220),  outvec(8440)
        character*1 band

*****************************************************************
*
*     Set up and open the input image quadrant and fill pixel data files
*
*****************************************************************
        type118
  118   format(' Which Band Number? ',$)
        accept13,band
   13   format(a1)
        open(1,file='b'//band//'q1.pic',form='unformatted',
     +          status='old',recordtype='fixed',recl=4220/4)
        open(2,file='b'//band//'q2.pic',form='unformatted',
     +          status='old',recordtype='fixed',recl=4220/4)
        open(3,file='b'//band//'q1_lrfill.dat',
     +          form='unformatted',status='old',recordtype='fixed',recl=3)
        open(4,file='b'//band//'q2_lrfill.dat',
     +          form='unformatted',status='old',recordtype='fixed',recl=3)

*****************************************************************
*
*     Assume that a full resolution image of quads 1 & 2 will be created
*
*****************************************************************
        nlines=2983
        outrec=8440
c
        open(9,file='band'//band//'q12.pic',
     +        form='unformatted',status='new',
     +          recordtype='fixed',recl=outrec/4)
c
```

```
**********************************************************************
*
*    Read a line of data from each image quadrant and fill pixel file
*
**********************************************************************
       do  i=1,nlines
           write(*,469)  i
 469       format('+Line  ',i5)
           read(1)  (q1buff(j),  j=1,4220)
           read(2)  (q2buff(j),  j=1,4220)
           read(3)  iline,q1_lft,q1_rt
           read(4)  iline,q2_lft,q2_rt

**********************************************************************
*
*      Strip left fill pixels from quad 1 right fill pixels from quad 2
*       Fit the two resulting lines together to form one image line
*
**********************************************************************
          l=0
           do  k=1,4220-q1_rt
           l=l+1
            outvec(l)=q1buff(k)
         end do !k
           do  k=1+q2_lft,4220
           l=l+1
            outvec(l)=q2buff(k)
         end do !k

**********************************************************************
*
*                 Save the resulting image
*
**********************************************************************
            write(9)  (outvec(l),l=1,outrec)
c
       end do !i
       end
```

```
*****************************************************************
*
*       program subsamp
*
*  This program produces a subsampled version of an input image file
*
*  The program assumes that the input image is a LANDSAT TM two quadrant
*   image data file created by program PATCH
*
*  Author:  John Francis
*
*****************************************************************
      byte  inbuff(8440),  outvec(8440)
      character*80  infile,outfile,lbuff
      integer outrec

*****************************************************************
*
*           Assume a two qudrant TM image input file
*
*****************************************************************
      nlines=2983
      outrec=8440
      npixels=outrec

*****************************************************************
*
*         Get image filenames and determine output file size
*
*****************************************************************
      type1
 1    format(/' Input image file> ',$)
      accept13,  infile
      type2
 2    format(/' Output image file> ',$)
      accept13,  outfile
 13   format(a)
      type3
 3    format(/' Increment for subsampling> ',$)
      accept*,inc

      newrec=outrec/inc
      newlin=nlines/inc
```

```
*****************************************************************
*
*       Adjust the size of the output image, if necessary
*
*****************************************************************
      type4, newrec,newlin
  4   format(/' Output pixels,lines= ',i5,1x,i5,'> ',$)
      accept14, len,lbuff
 14   format(q,a)
      if (len .ne. 0) then
          read(lbuff,*) newrec,newlin
         type4, newrec,newlin
      end if

*****************************************************************
*
*             Open the image data files
*
*****************************************************************
      open(1,file=infile,
     +       form='unformatted',status='old',
     +        recordtype='fixed',recl=outrec/4)
c
c
      open(2,file=outfile,
     +       form='unformatted',status='new',
     +        recordtype='fixed',recl=newrec/4)
c
*****************************************************************
*
*           Read an input image line and subsample
*
*****************************************************************
      do  i=1,newlin*inc,inc
        type91,i
 91      format('+Line ',i5)

         read(1)  (inbuff(j),j=1,outrec)

        k=0
        do j=1,npixels,inc
          k=k+1
            outvec(k)=inbuff(j)
        end do

         write(2)  (outvec(k),  k=1,newrec)

        do l=1,inc-1
          read(1)              ! skip some image lines
        end do

      end do
```

```
*****************************************************************
*
*       Zero the output array to fill output image to 512 lines
*
*****************************************************************
      do i=1,newrec
        outvec(i)=0
      enddo

      do  i=newlin+1,512
         write(2)  (outvec(k),  k=1,newrec)
      enddo

      end
```

6.4 Appendix D LANDSAT TM ANCILLARY SCENE DATA ACQUISITION PROGRAM

Program TM_CAL_DATA

```
*****************************************************************
*
*  Program to get radiometric calibration data from LANDSAT TM-4 tapes
*
*  The program assumes that the tapes are 1600 BPI and contain two images each
*
*  Author:  John Francis
*
*****************************************************************

      byte  inbuff(4320)
      character*4320  cbuff
c
      equivalence  (  inbuff(1),cbuff  )

*****************************************************************
*
*     Mount tape on drive MUA0:, and skip to first image calibration record
*
*****************************************************************
      type1
   1  format(' Tape loaded, allocated and ready to go? ',$)
      accept*
      type2
   2  format(' $ MOUNT/FOREIGN/BLOCKSIZE=4320/RECORDSIZE=4320 MUA0:')
      call lib$spawn('MOU/FOR/BLOCK=4320/RECORD=4320 MUA0:')
c
      write(7,381)
 381  format('1 *** LANDSAT TM-4 DATA READING PROGRAM ***'////)

*****************************************************************
*
*              Skip over the volume descriptor file
*
*****************************************************************
      type3
   3  format(' $ SET MAG/SKIP=FILES:1 MUA0:')
      call lib$spawn('SET MAG/SKIP=FILES:1 MUA0:')
c
      open(1,file='MUA0:',status='old',access='sequential',
     +          form='unformatted',recordtype='fixed',recl=4320/4)

*****************************************************************
*
*             Skip over leader file descriptor record
*
*****************************************************************
      read(1)  (inbuff(i),  i=1,4320)
```

```
*****************************************************************
*
*            Read the scene header record
*
*****************************************************************
      read(1)  (inbuff(i),  i=1,4320)

*****************************************************************
*
*        Get necessary data from the scene header record
*
*****************************************************************
      write(7,111)   cbuff(21:21),cbuff(22:22),cbuff(23:23),cbuff(24:26),
     +               cbuff(27:29),cbuff(30:31),cbuff(32:34),cbuff(35:36)
  111 format(/' Sensor Type ',a1/' Mission ',a1,/' Quadrant Number ',
     +        a1,/' Path Number ',a3,/' Row Number ',a3,/
     +        ' Year ',a2,/' Day of year ',a3,//
     +        ' Corrections code ',a2/)

*****************************************************************
*
* Get full scene center longitude and lattitude, center line number and pixel
*
*****************************************************************
      read(cbuff(53:68),222)  alatit
      read(cbuff(69:84),222)  alongit
      read(cbuff(85:100),222)  cline
      read(cbuff(101:116),222)  cpix
  222 format(f16.7)
c
      write(7,333)  alatit,alongit,cline,cpix
  333 format(/' Scene Center Longitude:',f16.7,/
     +        ' Full scene center latitude:',f16.7/
     +        ' Line number at full scene center:',f16.7/
     +        ' Pixel number at full scene center:',f16.7/)

*****************************************************************
*
*        Get the time and date the image was recorded
*
*****************************************************************
      write(7,444)   cbuff(121:122),cbuff(123:124),cbuff(117:120),
     +               cbuff(125:126),cbuff(127:128),cbuff(129:130)
  444 format(' Image Date MM/DD/YYYY: ',a2,'/',a2,'/',a4,/
     +        ' Aquisition Time [GMT]: ',a2,':',a2,':',a2)
```

```
*****************************************************************
*
*           Get the type of resampling done on image
*
*****************************************************************
      if(cbuff(1541:1542) .eq. 'CC') then
          write(7,555)
  555   format(/' Map Resampling Done: CUBIC CONVOLUTION')
      else if(cbuff(1541:1542) .eq. 'NN') then
          write(7,666)
  666   format(/' Map Resampling Done: NEAREST NEIGHBOR')
      else
          write(7,777)
  777   format(/' Map Resampling Done: NONE')
      endif

*****************************************************************
*
*              Read map projection ancillary record
*
*****************************************************************
      read(1) (inbuff(i), i=1,4320)
      write(7,781) cbuff(493:508),cbuff(557:572),
     &             cbuff(605:620),cbuff(621:636)
  781 format(/' Nominal Satellite Altitude [KM]:      ',a16,/
     &       ' Cross Track Field Of View [Degrees]: ',a16,/
     &       ' Sun Elevation [Degrees]:             ',a16,/
     &       ' Sun Azimuth [Degrees]:               ',a16,/)

*****************************************************************
*
*           Get the radiometric conversion data
*
*****************************************************************
      read(1) (inbuff(i), i=1,4320)
      read(cbuff(13:16),755) iband
  755 format(i4)
      write(7,372)
  372 format(//70('*')/)
      write(7,888) iband
  888 format(//' *** Radiometric Conversions for Band',i2,' ***'/)
      read(cbuff(17:20),755) lolim
      read(cbuff(21:24),755) ihilim
  766 format(f16.7)
      write(7,999) lolim,ihilim
  999 format(' Lower Reflectance Limit ??[MW/CM**2-SR]??: ',i4/,
     +       ' Upper Reflectance Limit ??[MW/CM**2-SR]??: ',i4/)
      read(cbuff(32:48),*) a0
      read(cbuff(52:68),*) a1
      write(7,991) a0,a1
  991 format(' Radiance = Digital Count X Gain + Offset'//,
     +       ' A0  ??Gain Coefficient??: ',f16.7,/,
     +       ' A1  ??Offset Coefficient??: ',f16.7)
```

```
*****************************************************************
*
*       Skip to the leader file of the next image on tape
*
*****************************************************************
      type4
  4   format(' $ SET MAG/SKIP=FILES:3 MUA0:')
      call lib$spawn('SET MAG/SKIP=FILES:3 MUA0:')

*****************************************************************
*
*              Skip the first 3 records
*
*****************************************************************
      read(1)       ! skip leader file descriptor record
      read(1)       ! skip scene header record

*****************************************************************
*
*            Read map projection ancillary record
*
*****************************************************************
      read(1)  (inbuff(i),  i=1,4320)
      write(7,781)  cbuff(493:508),cbuff(557:572),
     &              cbuff(605:620),cbuff(621:636)

*****************************************************************
*
*          And read the radiometric data for this band
*
*****************************************************************
      read(1)  (inbuff(i),  i=1,4320)
c
      write(7,372)
      read(cbuff(13:16),755)  iband
      write(7,888)  iband
      read(cbuff(17:20),755)  lolim
      read(cbuff(21:24),755)  ihilim
      write(7,999)  lolim,ihilim
      read(cbuff(32:48),*)  a0
      read(cbuff(52:68),*)  a1
      write(7,991)  a0,a1
      stop
      end
```

6.5 APPENDIX E Image Thresholding and Masking Programs

Programs: THRESHOLD_IMAGE
MASK_PIC

```
************************************************************************
*
*       Program threshold_image
*
*  Program to binarize an image based on on an input threshold value
*
*  The binary image data is then median filtered to remove any isolated pixels
*  The program assumes that the image is a two quadrant TM image as created
*   by program PATCH
*
*  Author:  John Francis
*
************************************************************************
      integer*4     itemp
      byte          image(8440,3),lut(256),ibyte(4)
      character*60          infile,outfile
c
      equivalence   (  itemp,ibyte(1)  )

************************************************************************
*
*    Assume a two-quadrant image, get and open input and output filenames
*
************************************************************************
      nlines=2983
      npixels=8440
c
      type1
  1   format(//25x,'Threshold And Median Filter An Image File'//,
     &       ' Enter Input Image Filename: ',$)
      accept13,infile
 13   format(a)

      open(1,file=infile,status='old',form='unformatted',
     &       recordtype='fixed',recl=8440/4)

      type2
  2   format(' Enter Output Image Filename: ',$)
      accept13,outfile

      open(2,file=outfile,status='new',form='unformatted',
     &       recordtype='fixed',recl=8440/4)
************************************************************************
*
*          Get the threshold value and make a look-up table
*
************************************************************************
      type3
  3   format(/' Enter Threshold Value [0...threshold -> 0]: ',$)
      accept*,  ithresh

      do  i=1,ithresh
         lut(i)=0
      enddo
```

```
      do  i=ithresh+1,256
          lut(i)=-1
      end do

      type*

*****************************************************************
*
*     Read and threshold the first 3 lines of the image
*
*****************************************************************
      do  i=1,3
          read(1)  (image(j,i),  j=1,npixels)
        do j=1,npixels
           ibyte(1)=image(j,i)
           image(j,i)=lut(itemp+1)
       end do
      end do
*****************************************************************
*
*     First line is a special case, threshold, filter and write it
*
*  Perform a 3x3 median filter to remove spurious zeros on first line
*
*           Exclude the end pixels on the line
*
*****************************************************************
        i=1                              ! image line 1
        do  j=2,npixels-1

         n0=0
         n255=0
         do kk=0,1
           do jj=0,1
              if( image(j+jj,1+kk) .eq. 0) then
              n0=n0+1
           else
                 n255=n255+1
              end if
          end do     ! jj
        end do     ! kk

         if(n255 .gt. n0) then
            image(j,1)=-1
        else
            image(j,1)=0
        end if

       end do     ! j
```

```
*****************************************************************
*
*         Take care of the end pixels on the line
*
*****************************************************************
      if ( image(1,1) .ne. image(2,1) ) image(1,1)=image(1,2)
      if ( image(npixels,1) .ne. image(npixels-1,1) )
     &                    image(npixels,1)=image(npixels-1,1)

*****************************************************************
*
*             Write out the first image line
*
*****************************************************************
      write(2)  (image(j,1),  j=1,npixels)
      type*,'Writing  First  Line'

*****************************************************************
*
*             Now filter lines 2 thru nlines-1
*
*****************************************************************
      do  iline=2,nlines-1
        do  j=2,npixels-1

         n0=0
         n255=0
         do kk=-1,1
           do jj=-1,1

              if( image(j+jj,2+kk) .eq. 0) then
              n0=n0+1
           else
                n255=n255+1
              end if

           end do    ! jj
         end do    ! kk

          if(n255 .gt. n0) then
             image(j,2)=-1
         else
            image(j,2)=0
         end if

        end do    ! j
*****************************************************************
*
*         Take care of the end pixels on the line
*
*****************************************************************
      if ( image(1,2) .ne. image(2,2) ) image(1,2)=image(2,2)
      if ( image(npixels,2) .ne. image(npixels-1,2) )
```

```
     &                    image(npixels,2)=image(npixels-1,2)
*****************************************************************
*
*              Write out the image line
*
*****************************************************************
        write(2)  (image(j,2),  j=1,npixels)
        type61,  iline
   61   format('+Writing  Line:  ',i4)
*****************************************************************
*
*       Copy line 2 into buffer 1 and line 3 into buffer 2
*
*****************************************************************
        do  i=1,2
          do j=1,npixels
              image(j,i)=image(j,i+1)
           end do  ! j
        end do  ! i
*****************************************************************
*
*       Read the next image line into buffer 3 and threshold
*
*****************************************************************
        read(1,end=997)  (image(j,3),  j=1,npixels)

        do  j=1,npixels
            ibyte(1)=image(j,3)
            image(j,3)=lut(itemp+1)
        end do

        end do  ! iline
*****************************************************************
*
*     Last line is a special case, threshold, filter and write it
*
*****************************************************************
   997  continue
*****************************************************************
*
*   Perform a 3x3 median filter to remove spurious zeros on last line
*             Exclude the end pixels on the line
*
*****************************************************************
           do  j=2,npixels-1

            n0=0
            n255=0
            do kk=0,1
```

```
            do jj=0,1
                if( image(j-jj,3-kk) .eq. 0) then
                n0=n0+1
            else
                    n255=n255+1
                end if
            end do    ! jj
          end do    ! kk

           if(n255 .gt. n0) then
              image(j,3)=-1
          else
              image(j,3)=0
          end if

        end do    ! j

*****************************************************************
*
*          Take care of the end pixels on the line
*
*****************************************************************
       if ( image(1,3) .ne. image(2,3) )
    &              image(1,3)=image(2,3)
       if ( image(npixels,3) .ne. image(npixels-1,3) )
    &               image(npixels,3)=image(npixels-1,3)

*****************************************************************
*
*              Write out the last image line
*
*****************************************************************
       write(2)  (image(j,3),  j=1,npixels)
       type*,'Writing  Last  Line'

       stop 'Threshold  Completed'
       end
```

```
************************************************************************
*
*       Program mask_pic
*
*  Program to mask out unwanted areas of an input image
*  A mask image is used to set the unwanted areas to a count of 255
*   the mask image indicates the unwanted areas by a count of 255
*   all other counts in the mask image are zero
*
*  Author:  John Francis
*
************************************************************************
      byte   inbuff(8440),mskbuff(8440)
      character*80  infile1,infile2,outfile

************************************************************************
*
*       Get name of image to be masked and make sure its ok
*
************************************************************************
      type1
   1  format(/' Input image file to be masked> ',$)
      accept13,  infile1
  13  format(a)
c
      inquire(file=infile1,recl=irec1)

      type*
      type*,'Image Has ',irec1,' Pixels Per Line'
      type*

************************************************************************
*
*           Get name of mask file and make sure its ok
*
************************************************************************
      type2
   2  format(/' Input mask file name> ',$)
      accept13,  infile2
c
      inquire(file=infile2,recl=irec2)

      type*
      type*,'Image Has ',irec2,' Pixels Per Line'
      type*

************************************************************************
*
*              The two had better be the same size
*
************************************************************************
      if (irec1 .ne. irec2) then
        type*
        type*,'***** ERROR *****  Mask and Image are different sizes'
```

```
        type*
        stop
       end if

*****************************************************************
*
*   Set up for an output file assume that all the images are two-quadrant
*
*****************************************************************
       type3
   3   format(/' Input output file name> ',$)
       accept13, outfile
c
       ipoint=0
       nlines=2983
       npixels=irec1

       open(1,file=infile1,
     +      form='unformatted',status='old',
     +       recordtype='fixed',recl=irec1/4,readonly)
c
       open(2,file=infile2,
     +      form='unformatted',status='old',
     +       recordtype='fixed',recl=irec1/4,readonly)
c
       open(3,file=outfile,
     +      form='unformatted',status='new',
     +       recordtype='fixed',recl=irec1/4)


*****************************************************************
*
*             Read an image line from each file
*
*****************************************************************
       do  i=1,nlines
           read(1,end=991)  (inbuff(j),j=1,npixels)
           read(2)  (mskbuff(j),j=1,npixels)

         type91,i
   91     format('+Line  ',i5)
```

```
*****************************************************************
*
*   Set output image to 255 if mask is 255, otherwise copy inage to output
*
*****************************************************************
        do j=1,npixels
            if(mskbuff(j) .eq. -1) inbuff(j)=-1
        end do

           write(3)  (inbuff(j),j=1,npixels)
       end do

  991  stop 'MASK_PIC Completed'
       end
```

6.6 APPENDIX F Atmospheric Modeling Programs

Programs: LOWCNTRL6

LOWTRAN 6 Modifications for LOWHGP

LOWHGP Interactive Screen

```
*****************************************************************
*
*       Program  lowcntrl6
*
*   program to created a formatted input file for use with
*              LOWTRAN 6 type programs
*
*   the formatted input file that is created is called FOR001.DAT
*
*   Author:  John Francis
*
*****************************************************************
*
*   common block declarations for each card-subroutine
*
        common  /card01/  model,itype,iemsct,m1,m2,m3,im,noprt,
     +                    tbound,salb
        common  /card02/  ihaze,iseasn,ivulcn,icstl,icir,ivsa,vis,
     +                    wss,whh,rainrt
        common  /card2a/  cthik,calt,iseed
        common  /card2b/  zcvsa,ztvsa,zinvsa
        common  /card2c/  z,p,t,dp,rh,wh,wo,ahaze,vis1,iha1,isea1,ivul1
        common  /card2d/  dummy,extc,absc
        common  /card03/  h1,h2,angle,range,beta,ro,len
        common  /card3a/  iparm,iph,iday,isourc,parm1,parm2,parm3,
     +                    parm4,time,psipo,anglem,g
        common  /card3b/  nangls,angf,f
        common  /card04/  v1,v2,dv
        common  /card05/  irpt
*
*****************************************************************
*
*   main program to call subroutine for each input card
*
        imode=0
        call  card1(imode)
        call  card2(imode)
        call  card3(imode)
        call  card4(imode)
    1   call  card5(imode,icall5)
        if (icall5 .ne. 1) stop 'End of Lowcntrl6 Run'
        goto 1
        end
*****************************************************************
* * *
c
        subroutine  card1(imode)
c
c   subroutine to format the "card1" data for input into lowtran6
c
*****************************************************************
*
*   common block declarations for each card-subroutine
```

```
*
      common  /card01/  model,itype,iemsct,m1,m2,m3,im,noprt,
     +                  tbound,salb
      common  /card02/  ihaze,iseasn,ivulcn,icstl,icir,ivsa,vis,
     +                  wss,whh,rainrt
      common  /card2a/  cthik,calt,iseed
      common  /card2b/  zcvsa,ztvsa,zinvsa
      common  /card2c/  z,p,t,dp,rh,wh,wo,ahaze,vis1,iha1,isea1,ivul1
      common  /card2d/  dummy,extc,absc
      common  /card03/  h1,h2,angle,range,beta,ro,len
      common  /card3a/  iparm,iph,iday,isourc,parm1,parm2,parm3,
     +                  parm4,time,psipo,anglem,g
      common  /card3b/  nangls,angf,f
      common  /card04/  v1,v2,dv
      common  /card05/  irpt
*
*****************************************************************
*
c
      type7
    7 format(///,15x,'***  CARD  1  ***'//)
      if (imode .eq. 1) then                ! imode=1 is fast mode
        type1
    1   format(' MODEL,ITYPE,IEMSCT,M1,M2,M3,IM,NOPRT,TBOUND,SALB'/)
        type2
    2   format(' CARD 1: ',$)
        accept*,  model,itype,iemsct,m1,m2,m3,im,noprt,tbound,salb
      else                                  ! or use prompt mode
*
*****************************************************************
*
*         get the model atmosphere type
*
        type87
   87     format(///1x,78('*'),/)
        type4
    4   format(' Input Atmospheric Model Type',//,
     +         ' Model= 0  If meteorological data are specified '
     +          '(Horizontal Path Only)',/
     +         '       1  Tropical Atmosphere',/
     +         '       2  Mid-latitude Summer',/
     +         '       3  Mid-latitude Winter',/
     +         '       4  Sub-arctic Summer',/
     +         '       5  Sub-arctic Winter',/
     +         '       6  1962 U.S. Standard Atmosphere',/
     +         '       7  New Model Atmosphere '
     +          '(or Radiosonde Data)'/)
  111   type5
    5   format(' Choose a Model Number: ',$)
        accept*, model
        if (model .lt. 0 .or. model .gt. 7) goto 111
        if (model .eq. 7) then
          type71
   71     format(/' Is input Radiosonde Data? [Y/N] ',$)
```

```
          accept13, ans
           if (ans .eq. 'Y' .or. ans .eq. 'y') im=1
         end if          ! initial radiosonde input
*
*************************************************************************
* *
*
*          get the type of atmospheric path
*
         type87
         type6
   6      format(//' Input the Type of Atmospheric Path'/)
         type47
  47      format(' ITYPE= 1  For a horizontal (constant pressure) path',/
     +          '       2  Vertical or slant path between two '
     +          'altitiudes',/
     +          '       3  Vertical path to space'//)
 222     type8
   8     format(' Choose a Path: ',$)
         accept*, itype
         if (itype .lt. 1 .or. itype .gt. 3) goto 222
*
*************************************************************************
*
*
*        execution in transmittance, radiance, or scattering mode
*
         type87
         type9
   9      format(//,' Program Execution Mode',/)
         type10
  10     format(' IEMSCT= 0   Program Execution in Transmittance Mode',/
     +          '       1   Program Execution in Radiance Mode',/
     +          '       2   Program Execution in Radiance Mode',/
     +          '                with Solar/Lunar Scattered Radiance',/)
 333     type11
  11     format(' Enter Execution Mode: ',$)
         accept*, iemsct
         if (iemsct .lt. 0 .or. iemsct .gt. 2) goto 333
c
*************************************************************************
*
*  modify or supplement the altitude profiles of temp, water vapor, ozone
*
         type87
c
c  temperature and pressure profiles
c
         type12
  12     format(' Do you want to modify the default altitude profiles '
     +          'of temperature and pressure?')
         accept13, ans
  13      format(a)
         if (ans .eq. 'Y' .or. ans .eq. 'y') then
```

```
          type14
  14      format(/'       M1= 1  Tropical temperature and'
     +        ' pressure profile'/
     +          '          2  Mid-latitude summer'/
     +          '          3  Mid-latitude winter'/
     +          '          4  Sub-arctic summer'/
     +          '          5  sub-arctic winter'/
     +          '          6  U.S. 1962 Standard'/)
  444     type15
  15      format(' Choose an option: ',$)
          accept*, m1
          if (m1 .lt. 1 .or. m1 .gt. 6) goto 444
        else
          m1=0
        end if          ! end of option m1
c
c   water vapor profiles
c
        type16
  16    format(/' Do you want to modify the default altitude profiles '
     +          'of water vapor?')
        accept13, ans
        if (ans .eq. 'Y' .or. ans .eq. 'y') then
          type17
  17      format(/'       M2= 1  Tropical water vapor profile'/
     +          '          2  Mid-latitude summer'/
     +          '          3  Mid-latitude winter'/
     +          '          4  Sub-arctic summer'/
     +          '          5  sub-arctic winter'/
     +          '          6  U.S. 1962 Standard'/)
  555     type18
  18      format(' Choose an option: ',$)
          accept*, m2
          if (m2 .lt. 1 .or. m2 .gt. 6) goto 555
        else
          m2=0
        end if          ! end of option m2
c
c   ozone profiles
c
        type19
  19    format(/' Do you want to modify the default altitude profiles '
     +          'of ozone?')
        accept13, ans
        if (ans .eq. 'Y' .or. ans .eq. 'y') then
          type20
  20      format(/'       M3= 1  Tropical ozone profile'/
     +          '          2  Mid-latitude summer'/
     +          '          3  Mid-latitude winter'/
     +          '          4  Sub-arctic summer'/
     +          '          5  sub-arctic winter'/
     +          '          6  U.S. 1962 Standard'/)
  666     type21
  21      format(' Choose an option: ',$)
```

```
            accept*, m3
             if (m3 .lt. 1 .or. m3 .gt. 6) goto 666
          else
            m3=0
          end if          ! end of option m3
*
*************************************************************************
***********
*
*   do we print the radiance table?
*
          type87
          type22
   22      format(/' Do you want to print the atmospheric profiles?')
          accept13, ans
          if (ans .eq. 'Y' .or. ans .eq. 'y') then
            type23
   23       format(' ARE YOU SURE YOU WANT TO?')
            accept13, ans
          end if
          if (ans .eq. 'Y' .or. ans .eq.'y') then
            noprt=0
          else
            noprt=1
          end if
*
*************************************************************************
*
*          get the temperature of the earth
*
          type87
          type25
   25      format(/' What is the temperature of the earth?  (Kelvin)'/
    +              '    (0.0 uses the first radiosonde reading)')
          accept*, tbound
*
*************************************************************************
*
*            get the surface albedo
*
          type87
          type24
   24      format(/' Enter the surface albedo (0=Blackbody) ',$)
          accept*, salb
        end if   ! end of fast or slow mode
c
c   write the formatted record to the unit 1 file
c
        write(1,99)  model,itype,iemsct,m1,m2,m3,im,noprt,tbound,salb
   99   format(8i5,2f10.3)
c
        return
        end
c
```

```
      subroutine card2(imode)
c
c   subroutine to format "card2" data for input into Lowtran6
c
*****************************************************************
*
*   common block declarations for each card-subroutine
*
      common /card01/ model,itype,iemsct,m1,m2,m3,im,noprt,
     +               tbound,salb
      common /card02/ ihaze,iseasn,ivulcn,icstl,icir,ivsa,vis,
     +               wss,whh,rainrt
      common /card2a/ cthik,calt,iseed
      common /card2b/ zcvsa,ztvsa,zinvsa
      common /card2c/ z,p,t,dp,rh,wh,wo,ahaze,vis1,iha1,isea1,ivul1
      common /card2d/ dummy,extc,absc
      common /card03/ h1,h2,angle,range,beta,ro,len
      common /card3a/ iparm,iph,iday,isourc,parm1,parm2,parm3,
     +               parm4,time,psipo,anglem,g
      common /card3b/ nangls,angf,f
      common /card04/ v1,v2,dv
      common /card05/ irpt
*
*****************************************************************
*
c
c
c
      type1
1     format(/////15x,'***  CARD  2  ***'//)
      if(imode .eq. 1) then  ! mode=1 is fast mode
        type2
2       format(' IHAZE,ISEASN,IVULCN,ICSTL,ICIR,IVSA,VIS,WSS,'
     +       'WHH,RAINRT'/)
        type3
3       format(' CARD 2: ',$)
          accept*, ihaze,iseasn,ivulcn,icstl,icir,ivsa,vis,wss,whh,rainrt
      else    ! do prompt mode
*
*****************************************************************
*
*   select a type of aerosol extinction and visibility
*
        type87
87        format(//1x,75('*')/)
        type104
104     format(/' Input an Aerosol Extinction')
        type4
4       format(/'  IHAZE= 0  No Aerosol Attenuation'/
     +          '         1  Rural Extinction,  23-KM Vis.'/
     +          '         2  Rural Extinction,   5-KM Vis.'/
     +          '         3  Navy Maritime Extinction, sets own Vis.'/
     +          '         4  Maritime Extinction, 23-KM Vis.'/
     +          '         5  Urban Extinction, 5-KM Vis.'/
```

```
     +            '        6  Tropospheric Extinction, 50-KM Vis.'/
     +            '       7  User Defined (Ten Cards)'/
     +            '        8  Advection Fog Extinction, 0.2-KM Vis.'/
     +            '        9  Radiation Fog Extinction, 0.5-KM Vis.'/)
   111     type5
    5      format(' Choose an extinction: ',$)
          accept*, ihaze
          if (ihaze .lt. 0 .or. ihaze .gt. 9) goto 111
*
*****************************************************************
* *
*
*              select a season
*
          type87
          type106
   106    format(/' Select a Season')
          type6
    6     format(/' ISEASN= 0  Default Season for model'/
     +            '              (Summer for models 0,1,2,4,6,7)'/
     +            '             (Winter for models 3,5)'/
     +          '       1  Spring-Summer'/
     +          '        2  Fall-Winter'/)
   222    type7
    7     format(' Choose a season: ',$)
          accept*, iseasn
          if(iseasn .lt. 0 .or. iseasn .gt. 2) goto 222
*
*****************************************************************
*
*
*       select a volcanic aerosol extinction
*
          type87
          type108
   108    format(/' Select a Volcanic Aerosol Extinction')
          type8
    8     format(/' IVULCN= 0  Default to Stratospheric Background'/
     +          '       1  Stratospheric Background'/
     +    '       2  Aged Volcanic Type/Moderate Volcanic Profile'/
     +    '       3  Fresh Volcanic Type/High Volcanic Profile'/
     +    '       4  Aged Volcanic Type/High Volcanic Profile'/
     +    '       5  Fresh Volcanic Type/Moderate Volcanic Profile'/)
   333    type9
    9     format(' Choose a Volcanic Extinction: ',$)
          accept*, ivulcn
          if(ivulcn .lt. 0 .or. ivulcn .gt. 5) goto 333
*
*****************************************************************
*
*
*   if ihaze=3 then ask about icstl,wss,whh
*
          if (ihaze .eq. 3) then
```

```
            type87
            type110
  110        format(/' Navy Maritime Extinction Requires Air Mass'
     +      ' Character, and Wind Speed Information')
            type10
   10       format(/' ICSTL=1   Open Ocean Air Mass Character'/
     +           '      ./
     +           '      ./
     +           '      ./
     +            '      10   Strong Continental Influence'/)
  444       type11
   11       format(' Choose an Air Mass Character: ',$)
            accept*, icstl
             if(icstl .lt. 0 .or. icstl .gt. 10) goto 444
            type87
            type12
   12        format(/' Current Wind Speed is: [M/S] ',$)
            accept*, wss
            type13
   13        format(/' 24 Hour Average Wind Speed is: [M/S] ',$)
            accept*, whh
          end if                  ! end of special input for ihaze=3
*
          type87
          type15
   15     format(/' Do you want to include Cirrus Cloud Attenuation? ',$)
          accept16, ans
   16      format(a)
          if (ans .eq. 'Y' .or. ans .eq. 'y') icir=1       ! use cirrus profile
          type87
          type17
   17     format(/' Do you want to use the Army Vertical Structure '
     +       'Algorithm'/' for aerosols in the boundary layer? ',$)
          accept16, ans
          if (ans .eq. 'Y' .or. ans .eq. 'y') ivsa=1       ! incl Vert Struc Algor
          type87
          type18
   18     format(/' Do you want to override the default visibility? ',$)
          accept16, ans
          if (ans .eq. 'Y' .or. ans .eq. 'y') then
            type19
   19         format(' Visibility [KM] ',$)
            accept*, vis
          end if
          type87
          type14
   14     format(/' What is the Rain Rate? [MM/HR] ',$)
          accept*, rainrt
        end if  ! end of "imode" if
*
*****************************************************************
*
*    write out the card 2 line to unit 1 file
*
```

```
      write(1,987) ihaze,iseasn,ivulcn,icstl,icir,ivsa,vis,wss,whh,rainrt
  987 format(6i5,4f10.3)
*
*****************************************************************
*
*    do we need to write card2a or card2b or card2c???????
*
      if(icir .eq. 1) call card2a(imode)
      if(ivsa .eq. 1) call card2b(imode)
      if(im .eq. 1 .and. model .eq. 7) call card2c(imode)
      if(ihaze .eq. 7) call card2d
      return
      end
      subroutine card2a(imode)
c
c   subroutine to write card2a data for input into lowtran6
c
*****************************************************************
*
*   common block declarations for each card-subroutine
*
      common /card01/ model,itype,iemsct,m1,m2,m3,im,noprt,
     +               tbound,salb
      common /card02/ ihaze,iseasn,ivulcn,icstl,icir,ivsa,vis,
     +               wss,whh,rainrt
      common /card2a/ cthik,calt,iseed
      common /card2b/ zcvsa,ztvsa,zinvsa
      common /card2c/ z,p,t,dp,rh,wh,wo,ahaze,vis1,iha1,isea1,ivul1
      common /card2d/ dummy,extc,absc
      common /card03/ h1,h2,angle,range,beta,ro,len
      common /card3a/ iparm,iph,iday,isourc,parm1,parm2,parm3,
     +               parm4,time,psipo,anglem,g
      common /card3b/ nangls,angf,f
      common /card04/ v1,v2,dv
      common /card05/ irpt
*
      equivalence (seed,iseed)
*
*****************************************************************
*
c
      type1
    1 format(///15x,'***  CARD  2A  ***',5x,
     +     'Cirrus Cloud Model Included'//)
      if (imode .eq. 1) then                ! imode = 1 is fast mode
        type3
    3    format(/' CHTHIK,CALT')
        type2
    2    format(/' CARD2A: ',$)
        accept*, chthik,calt
      else
        type87
   87      format(/1x,76('*')/)
        type4
```

```
   4       format(/' Input Cirrus Cloud Thickness  '
    +              '(0=Calculate Thickness)  ',$)
           accept*,chthik
           type5
   5       format(/' Input Cirrus Base Altitude'
    +           ' (0=Calculate Base) ',$)
           accept*,calt
         end if
c
c
c
       seed=secnds(0.0)        ! seed random number generator
         write(1,987)  cthik,calt,iseed/25
  987    format(2f10.0,i10)
         return
         end
         subroutine  card2b(imode)
c
c   optional card used when Army Vertical Structure Algorithm
c  is selected
*****************************************************************
*
*   common block declarations for each card-subroutine
*
         common  /card01/  model,itype,iemsct,m1,m2,m3,im,noprt,
    +                tbound,salb
         common  /card02/  ihaze,iseasn,ivulcn,icstl,icir,ivsa,vis,
    +                wss,whh,rainrt
         common /card2a/  cthik,calt,iseed
         common /card2b/  zcvsa,ztvsa,zinvsa
         common  /card2c/  z,p,t,dp,rh,wh,wo,ahaze,vis1,iha1,isea1,ivul1
         common /card2d/  dummy,extc,absc
         common  /card03/  h1,h2,angle,range,beta,ro,len
         common  /card3a/  iparm,iph,iday,isourc,parm1,parm2,parm3,
    +                parm4,time,psipo,anglem,g
         common /card3b/  nangls,angf,f
         common  /card04/  v1,v2,dv
         common  /card05/  irpt
*
*****************************************************************
*
c
         type87
  87     format(/1x,78('*')//)
         type1
   1     format(//15x,'***  Card  2B  ***',10x,'Army  Vertical  Structure',/
    +           40x,'Algoritm Selected'//)
         if (imode .eq. 1) then
           type2
   2       format(5x,'ZCVSA,ZTVSA,ZINVSA'/)
           type3
   3       format(1x,'Card 2 B: ',$)
           accept*,zcvsa,ztvsa,zinvsa
         else
```

```
            type4
    4       format(' ZCVSA= Cloud Ceiling Height [KM]'/
     +         '      Less than 0 = No Cloud Ceiling'/
     +              '      Greater than 0 = Cloud Ceiling Height'/
     +         '      Equal to 0 = Calculate Cloud Ceiling'//)
            type5
    5       format(' Enter Cloud Ceiling Height: ',$)
            accept*, zcvsa
            type87
            type6
    6       format(' ZTVSA= Thickness of Cloud or Fog [KM]'/
     +              '      0 = Default to 200 Meters'/)
            type7
    7       format(' Enter the Cloud Thickness: ',$)
            accept*, ztvsa
            type87
            type8
    8       format(' ZINVSA= Height of the inversion [KM]'/
     +              '      0 = Default to 100 Meters'/
     +         '      Less than 0 = No inversion'//)
            type9
    9       format(' Enter the Height of the Inversion Layer: ',$)
            accept*, zinvsa
          end if
c
c
c
          write(1,123)  zcvsa,ztvsa,zinvsa
      123 format(3f10.3)
          return
          end
          subroutine  card2c(imode)
c
c   subroutine to input data for a user defined atmosphere
c   ...right now ONLY Buffalo style radiosonde data is allowed
*************************************************************************
*
*    common block declarations for each card-subroutine
*
          common  /card01/  model,itype,iemsct,m1,m2,m3,im,noprt,
     +                  tbound,salb
          common  /card02/  ihaze,iseasn,ivulcn,icstl,icir,ivsa,vis,
     +                  wss,whh,rainrt
          common /card2a/  cthik,calt,iseed
          common /card2b/  zcvsa,ztvsa,zinvsa
          common  /card2c/  z,p,t,dp,rh,wh,wo,ahaze,vis1,iha1,isea1,ivul1
          common /card2d/  dummy,extc,absc
          common  /card03/  h1,h2,angle,range,beta,ro,len
          common  /card3a/  iparm,iph,iday,isourc,parm1,parm2,parm3,
     +                  parm4,time,psipo,anglem,g
          common /card3b/  nangls,angf,f
          common  /card04/  v1,v2,dv
          common  /card05/  irpt
*
```

```
*****************************************************************
*
c
      real   z(34),p(34),t(34),dp(34)
      character*50  filnam
c
      type1
   1  format(///15x,'*** CARD 2C ***',10x,'Initial Radiosonde Input'//)
      type2
   2  format(/' What File Contains the Radiosonde Data? ',$)
      accept3, filnam
   3  format(a)
c
c  open radiosonde data file and read into Z,P,T, and, DP
c   ...all others remain zero
c
      open(2,file=filnam,status='old')
      do 19 i=1,34 ! 34 levels of radiosonde allowed
           read(2,*,end=991,err=992)  z(i),p(i),t(i),dp(i)
c
          z(i)=z(i)/1000.0 ! change altitude from meters to KM
          dp(i)=t(i)-dp(i)  ! change dew point depression to dew point
c
  19  continue
 991  k1=i-1                ! # of levels of radiosonde
c
c  write out the radiosonde data
c
      write(1,111)  k1,filnam     ! # levels and radiosonde description
 111  format(i5,a72)
      do 20 j=1,k1
           write(1,222)  z(j),p(j),t(j),dp(j),            ! real data
     +      rh,wh,wo,ahaze,vis1,iha1,isea1,ivul1         ! dummy data all 0
 222      format(3f10.3,2f5.1,3e10.3,f7.3,3i1)
  20  continue
      return
c
c   error in reading the radiosonde input file
c
 992  type6
   6  format(//' %%% ERROR %%%  Can"t Read Radiosonde Data File'//)
      write(1,333)
 333  format(' ***'/'  34 Blank Lines Left for Radiosonde Input',32(/))
      return
      end
      subroutine card2d(imode)
*****************************************************************
*
*   common block declarations for each card-subroutine
*
      common /card01/ model,itype,iemsct,m1,m2,m3,im,noprt,
     +               tbound,salb
      common /card02/ ihaze,iseasn,ivulcn,icstl,icir,ivsa,vis,
     +               wss,whh,rainrt
```

```
      common /card2a/ cthik,calt,iseed
      common /card2b/ zcvsa,ztvsa,zinvsa
      common /card2c/ z,p,t,dp,rh,wh,wo,ahaze,vis1,iha1,isea1,ivul1
      common /card2d/ dummy,extc,absc
      common /card03/ h1,h2,angle,range,beta,ro,len
      common /card3a/ iparm,iph,iday,isourc,parm1,parm2,parm3,
     +                parm4,time,psipo,anglem,g
      common /card3b/ nangls,angf,f
      common /card04/ v1,v2,dv
      common /card05/ irpt
*
*****************************************************************
*
      end
      subroutine card3(imode)
c
c  subroutine to format the geometrical path input parameters
c  for a given lowtran run
*****************************************************************
*
*  common block declarations for each card-subroutine
*
      common /card01/ model,itype,iemsct,m1,m2,m3,im,noprt,
     +               tbound,salb
      common /card02/ ihaze,iseasn,ivulcn,icstl,icir,ivsa,vis,
     +               wss,whh,rainrt
      common /card2a/ cthik,calt,iseed
      common /card2b/ zcvsa,ztvsa,zinvsa
      common /card2c/ z,p,t,dp,rh,wh,wo,ahaze,vis1,iha1,isea1,ivul1
      common /card2d/ dummy,extc,absc
      common /card03/ h1,h2,angle,range,beta,ro,len
      common /card3a/ iparm,iph,iday,isourc,parm1,parm2,parm3,
     +               parm4,time,psipo,anglem,g
      common /card3b/ nangls,angf,f
      common /card04/ v1,v2,dv
      common /card05/ irpt
*
*****************************************************************
*
c
      type87
 87   format(//1x,76('*')//)
      type1
 1    format(15x,'***  Card  3  ***'//)
      if (imode .eq. 1) then
        type2
 2      format(' H1,H2,ANGLE,RANGE,BETA,RO,LEN'//,' CARD 3: ',$)
        accept*, h1,h2,angle,range,beta,ro,len
      else
        type87
        type3
 3       format(' H1= Initial Altitude [KM] (Observer Position)'//,
     1         ' Input H1: ',$)
        accept*, h1
```

```
            type87
            type4
    4        format(/' H2= Final Altitude [KM]'//' Input H2: ',$)
            accept*, h2
            type87
            type5
    5       format(/' ANGLE= Initial Zenith Angle [Degrees] as Measured ',
     1              'from H1'//' Input the Zenith Angle: ',$)
            accept*, angle
            type87
            type6
    6        format(/' RANGE= Path Length [KM]'//' Input the Range: ' ,$)
            accept*, range
            type87
            type7
    7       format(/' BETA= Earth Center Angle Subtended by H1 and H2 ',
     1              '[Degrees]'//' Input Earth Center Angle: ',$)
            accept*, beta
            type87
            type8
    8        format(/' Do you want to override the default ',
     1                  'Earth Radius? ',$)
            accept13, ans
   13        format(a)
            if ( ans .eq. 'Y' .or. ans .eq. 'y') then
              type9
    9           format(/' Earth Radius is: ',$)
              accept*, ro
            end if
            len=0
         type*,'iemsct=',iemsct
            type10
   10        format(/' Using the short path from H1 to H2 , ok? [Y] ',$)
            accept13, ans
            if (ans .eq. 'N' .or. ans .eq. 'n') len=1
         end if
c
c
         write(1,22)  h1,h2,angle,range,beta,ro,len
   22    format(6f10.3,i5)
c
c  do we need to get data for card3a???
c
         if (iemsct .eq. 2) call card3a(imode)        ! solar/lunar MIE scatter
c
         return
         end
         subroutine  card3a(imode)
c
c  subroutine to define phase functions when iemsct=2
c
         character ans
c
*****************************************************************
```

```
*
*   common block declarations for each card-subroutine
*
      common  /card01/  model,itype,iemsct,m1,m2,m3,im,noprt,
     +                  tbound,salb
      common  /card02/  ihaze,iseasn,ivulcn,icstl,icir,ivsa,vis,
     +                  wss,whh,rainrt
      common /card2a/ cthik,calt,iseed
      common /card2b/ zcvsa,ztvsa,zinvsa
      common  /card2c/  z,p,t,dp,rh,wh,wo,ahaze,vis1,iha1,isea1,ivul1
      common /card2d/ dummy,extc,absc
      common  /card03/  h1,h2,angle,range,beta,ro,len
      common  /card3a/  iparm,iph,iday,isourc,parm1,parm2,parm3,
     +                  parm4,time,psipo,anglem,g
      common /card3b/ nangls,angf,f
      common /card04/ v1,v2,dv
      common /card05/ irpt
*
*****************************************************************
*
      type87
   87 format(///1x,78('*')///)
      type1
    1 format(/15x,'***  Card  3A  ***'//)
      if (imode .eq. 1 ) then
        type2
    2    format(/' IPARM,IPH,IDAY,ISOURC',//,' CARD 3A1: ',$)
         accept*,  iparm,iph,iday,isourc
        type3
    3    format(/' PARM1,PARM2,PARM3,PARM4,TIME,PSIPO,ANGLEM,G',//,
     +          ' CARD 3A2: ',$)
         accept*,  parm1,parm2,parm3,parm4,time,psipo,anglem,g
      else
        type4
    4   format(/' IPH= 0  Use Henyey-Greenstein aerosol phase functions',
     +      /'     1  User Supplied Phase Functions [NOT ALLOWED YET]',
     +       /'     2  Lowtran Database Phase Functions'/)
   81     type5
    5     format(' Choose a Phase Function Type: ',$)
          accept*,iph
          if (iph .lt. 0 .or. iph .gt. 2) goto 81
          type6
    6     format(//' IDAY= Number of the day of the year (1 to 365)'/)
          type7
    7     format(' Enter the day number: ',$)
          accept*, iday
          type8
    8     format(//' Is the source the sun? [Y] ',$)
          accept13, ans
   13     format(a)
          if (ans .eq. 'N' .or. ans .eq. 'n') then
             isourc=1           ! source is the moon
          else
             isourc=0           ! source is the sun
```

```
          end if
c
c   this is the end of input for card 3a1,   go right on to card3a2
c
          type87
          type9
    9      format(//10x,'Specify the Geometry of the Observation'//)
          type10
   10     format(' IPARM= 0  Specify Longitude and Latitude of Observer'
     +           ' and Source'/,
     +           '       1  Specify Longitude and Latitude of Observer'
     +           ' and Time of Day'/,
     +           '       2  Specify Sun Zenith and Azimuth Angles'/)
   82     type11
   11     format(' Choose a Type of Geometry Specification: ',$)
          accept*, iparm
          if (iparm .lt. 0 .or. iparm .gt. 2) goto 82
c
c  select the inputs based on IPARM
c
          if(iparm .eq. 0) then
            type12
   12         format(/' Observer Latitude (-90 to 90): ',$)
            accept*, parm1
            type14
   14         format(/' Observer Longitude (0 to 360): ',$)
            accept*, parm2
            type15
   15         format(/' Source Latitude (-90 to 90): ',$)
            accept*, parm3
            type16
   16         format(/' Source Longitude (0 to 360): ',$)
            accept*, parm4
            type23
   23         format(/' Path Azimuth as degrees East of North: ',$)
            accept*, psipo
          else if(iparm .eq. 1) then
            type17
   17         format(/' Observer Latitude (-90 to 90): ',$)
            accept*, parm2
            type18
   18         format(/' Observer Longitude (0 to 360): ',$)
            accept*, parm1
            type19
   19         format(/' Time of Day in decimal hours: ',$)
            accept*, time
            type22
   22         format(/' Path Azimuth as degrees East of North: ',$)
            accept*, psipo
          else if (iparm .eq. 2) then
            type20
   20   format(/' Azimuthal angle between observer"s line of sight '
     +           'and the Observer-to-Sun path'/' measured from the '
     +           'line of sight, positive east of north (-180 to 180)')
```

```
            accept*, parm1
            type21
   21        format(/' Sun Zenith Angle: ',$)
            accept*, parm2
          end if
c
c
c
          if (isourc .eq. 1) then        ! if the source is the moon
            type24
   24        format(/' Phase Angle of the moon: ',$)
            accept*, anglem
          end if
          if (iph .eq. 0) then           ! when using Henyey-Greenstein
            type25
   25         format(/' Henyey-Greenstein Phase Asymmetry factor: ',$)
            accept*, g
          end if
        end if          ! mode if
c
c
c
        write(1,412)  iparm,iph,iday,isourc
  412   format(4i5)
        write(1,413)  parm1,parm2,parm3,parm4,time,psipo,anglem,g
  413   format(8f10.3)
        return
        end
        subroutine  card4(imode)
c
c  subroutine to input the wavelength range for the Lowtran 6 run
c
        character*6  units
c
*****************************************************************
*
*   common block declarations for each card-subroutine
*
        common  /card01/  model,itype,iemsct,m1,m2,m3,im,noprt,
     +                    tbound,salb
        common  /card02/  ihaze,iseasn,ivulcn,icstl,icir,ivsa,vis,
     +                    wss,whh,rainrt
        common /card2a/  cthik,calt,iseed
        common /card2b/  zcvsa,ztvsa,zinvsa
        common  /card2c/  z,p,t,dp,rh,wh,wo,ahaze,vis1,iha1,isea1,ivul1
        common /card2d/  dummy,extc,absc
        common  /card03/  h1,h2,angle,range,beta,ro,len
        common  /card3a/  iparm,iph,iday,isourc,parm1,parm2,parm3,
     +                    parm4,time,psipo,anglem,g
        common /card3b/  nangls,angf,f
        common /card04/  v1,v2,dv
        common /card05/  irpt
*
*****************************************************************
```

```
*
      type1
    1 format(///15x,'***  Card  4  ***'///)
    7 type2
    2 format(' What units are you using for wavelength? [Microns]  ',$)
      accept3, len,units
    3 format(q,a)
      if(len .eq. 0) then
         anum=1.0e-4
      else if(units .eq. 'MICRON' .or. units .eq. 'Micron' .or.
     +    units .eq. 'micron') then
         anum=1.0e-4
      else if(units .eq. 'NANOME' .or. units .eq. 'Nanome' .or.
     +    units .eq. 'nanome') then
         anum=1.0e-7
      else
        type4, units
    4   format(/' Undefined unit [',a6,']')
        goto 7
      endif
c
c
      type5
    5 format(//' Input Initial Wavelength, Final Wavelength, Increment')
      accept*, v1,v2,dv
      a=(v2-v1)/dv
      v1=1.0/(anum*v1)
      v2=1.0/(anum*v2)
      dv=(v1-v2)/a
c
c
      write(1,10)  v2,v1,dv
   10 format(3f10.3)
      return
      end
      subroutine  card5(imode,icall5)
c
c   subroutine to write "repeat" card for lowtran6 run
c   this subroutine takes control from the main program
c   and calls all of the necessary subroutines to format
c   data for the repeat running of lowtran6
*************************************************************************
*
*   common block declarations for each card-subroutine
*
      common  /card01/  model,itype,iemsct,m1,m2,m3,im,noprt,
     +                  tbound,salb
      common  /card02/  ihaze,iseasn,ivulcn,icstl,icir,ivsa,vis,
     +                  wss,whh,rainrt
      common /card2a/ cthik,calt,iseed
      common /card2b/ zcvsa,ztvsa,zinvsa
      common  /card2c/  z,p,t,dp,rh,wh,wo,ahaze,vis1,iha1,isea1,ivul1
      common /card2d/ dummy,extc,absc
      common  /card03/  h1,h2,angle,range,beta,ro,len
```

```
      common  /card3a/  iparm,iph,iday,isourc,parm1,parm2,parm3,
     +                  parm4,time,psipo,anglem,g
      common /card3b/ nangls,angf,f
      common  /card04/  v1,v2,dv
      common  /card05/  irpt
*
**********************************************************************
*
c
      type87
   87 format(/1x,78('*'))
      type1
    1 format(///,15x,'***  Card  5  ***'///)
c
      if (imode .eq. 1) then
   11   type2
    2    format(/' IRPT: ',$)
         accept*, irpt
         if( (irpt .ne. 0) .and. (irpt .ne. 1) .and. (irpt .ne. 3) .and.
     +       (irpt .ne. 4) ) goto 11
      else
        type3
    3    format(/' IRPT= 0 To End Lowtran 6 Run'/
     +          '     1 To Read All Data Cards Again'/
     +          '     3 To Read Only Card 3 Again (Geometry Data)'/
     +          '     4 To Read Only Card 4 Again (Wavelength Range)')
   12   type4
    4    format(/' Select IRPT: ',$)
         accept*,irpt
         if( (irpt .ne. 0) .and. (irpt .ne. 1) .and. (irpt .ne. 3) .and.
     +       (irpt .ne. 4) ) goto 12
      end if
c
      write(1,99)  irpt
   99 format(i5)
c
      icall5=0
      if (irpt .eq. 0) return
c
      if (irpt .eq. 1) then
        call card1(imode)
        call card2(imode)
        call card3(imode)
        call card4(imode)
      else if (irpt .eq. 3) then
        call card3(imode)
      else if (irpt .eq. 4) then
        call card4(imode)
      end if
      icall5=1       ! when icall5=1 need to call card 5 again
      return
      end
```

LOWTRAN 6 Modifications for LOWHGP:

```
*
**********************************************************************
*
    In routine LOWTR6:

    common /acntrl/ interactive,rh_mean                                  lwt 2781
    common /dpdep/chngh2o,deltadp,deltadpnew                             lwt 2782
    common /qlamda/newlam,wave1,wave2                                    lwt 2783
    common /radiom/gain,offset,delta                                     lwt 2784
    common /aerfac/scat,newscat,g                                        lwt2784A
    common /reflect/chngalbedo,albedo                                    lwt2784B
    character*1 esc                                                      lwt 2796
    logical interactive,chngvis,chngh2o,newlam,chngalbedo,newscat        lwt 2797

    interactive =.true.                                                  lwt 2801
    chngvis =.false.                                                     lwt 2802
    chngh2o=.false.                                                      lwt 2803
    newlam=.false.                                                       lwt 2804
    chngalbedo=.false.                                                   lwt2804A
    newscat=.false.                                                      lwt2804B

    gain=0.1e+10                                                         lwt2804C
    offset=-1.0                                                          lwt2804D
    delta=1.0                                                            lwt2804E
    scat=0.0                                                             lwt2804F
    facmol=1.0                                                           lwt2804G

    if(interactive) then                                                 lwt2804H

    write(*,7761)                                                        lwt2804I
    7761 format('Assigning Data Files'//                                 lwt2804J
    &' Assigning NEWLOW.INP As Input File'/                              lwt2804K
    &' Assigning Unit 7 To Throw Away Tapefile'/)                        lwt2804L

    open(7,file='nl:',status='old')                                      lwt2804M
    end if                                                               lwt2804N

    100 CONTINUE                                                         LWT 2970

    if(interactive) then                                                 lwt 2981
    esc=char(27)                                                         lwt 2982
    write(ipr,1001) esc,esc                                              lwt 2983
    1001 format(1x,a1,'[2J',a1,'[H',$)                                   lwt 2984
    WRITE(IPR,1011) HDATE,HTIME                                          lwt2984A
    1011 FORMAT(10X,'***** INTERACTIVE LOWTRAN 6 *****',10X,A9,2X,A8)
                                                                         lwt2984B
    ELSE                                                                 lwt2984C
    end if                                                               lwt 2991

    if( chngalbedo ) salb=albedo                                         lwt 3016
```

```
if( .not. interactive) then                                          lwt 3021
end if                                                               lwt 3031

if(chngvis) vis=anewvis                                              lwt 3061

if( .not. interactive) then                                          lwt 3062
end if                                                               lwt 3071

if( .not. interactive) then                                          lwt 3121
end if                                                               lwt 3131

if( .not. interactive) then                                          lwt 3191
end if                                                               lwt 3201

if( .not. interactive) then                                          lwt 3226
end if                                                               lwt 3236

IF(IFLGT.EQ.0 .and. .not. interactive) WRITE(IPR,1221) CTHIK         LWT 3240

IF(IFLGT.EQ.1 .and. .not. interactive) WRITE(IPR,1222) CTHIK         LWT 3255

IF(IFLGT.EQ.2 .and. .not. interactive) WRITE(IPR,1223) CTHIK         LWT 3265

IF(IFLGA.EQ.0 .and. .not. interactive) WRITE(IPR,1224)CALT           LWT 3280

IF(IFLGA.EQ.1 .and. .not. interactive) WRITE(IPR,1225) CALT          LWT 3295

IF(IFLGA.EQ.2 .and. .not. interactive) WRITE(IPR,1226) CALT          LWT 3310

if( .not. interactive) then                                          lwt 3321
end if                                                               lwt 3336

if( .not. interactive) then                                          lwt 3376
end if                                                               lwt 2286

if( .not. interactive) then                                          lwt 3446
end if                                                               lwt 3456

if( .not. interactive) then                                          lwt 3506
end if                                                               lwt 3516

if( .not. interactive) then                                          lwt 3676
end if                                                               lwt 3686

if( .not. interactive) then                                          lwt 3711
end if                                                               lwt 3721

if( .not. interactive) then                                          lwt 3881
end if                                                               lwt 3891

if (newscat) g=scat                                                  lwt 3916

if( .not. interactive) then                                          lwt 3917
end if                                                               lwt 3926
```

```
if( .not. interactive) then                                          lwt 3971
end if                                                               lwt 3981

if( .not. interactive) then                                          lwt 4006
end if                                                               lwt 4016

if(newlam) then                                                      lwt 4066

v1=1.e+4/wave1                                                       lwt 4067

v2=1.e+4/wave2                                                       lwt 4068
end if                                                               lwt 4069

if( .not. interactive) then                                          lwt4069A
end if                                                               lwt 4076

if( .not. interactive) then                                          lwt 4086
end if                                                               lwt 4096

if( .not. interactive) then                                          lwt 4141
end if                                                               lwt 4151

if( .not. interactive) then                                          lwt 4211
end if                                                               lwt 4236

IF(ITYPE.EQ.1 .and. .not. interactive) WRITE(IPR,1515) H1,RANGE      LWT 4280

IF(ITYPE.EQ.2 .and. .not. interactive) WRITE(IPR,1516) H1,H2,
X   ANGLE,RANGE,BETA,LEN                                             LWT 4295

IF(ITYPE.EQ.3 .and. .not. interactive) WRITE(IPR,1517)H1,H2,ANGLE    LWT 4320

if (.not. interactive) WRITE (IPR,1530)                              LWT 4375

IF(IPARM.NE.2 .and. .not. interactive) then                          lwt 4381
WRITE(IPR,1532) PARM1,PARM2,PARM3,PARM4,TIME,PSIPO                   LWT 4385
end if                                                               lwt 4391

IF (IPARM.EQ.2 .and. .not. interactive)
&      WRITE (IPR,1534)PARM1,PARM2,TIME,PSIPO,IDAY                   LWT 4430

IF (ISOURC.EQ.0 .and. .not. interactive) WRITE (IPR,1535)            LWT 4460

IF (ISOURC.EQ.1 .and. .not. interactive) WRITE (IPR,1536) ANGLEM     LWT 4470

IF (IPH.EQ.0 .and. .not. interactive) WRITE (IPR,1538) G             LWT 4485

IF (IPH.EQ.1 .and. .not. interactive) WRITE (IPR,1540)               LWT 4495

IF (IPH.EQ.2 .and. .not. interactive) WRITE (IPR,1542)               LWT 4505

if (.not. interactive) then                                          lwt 4546
end if                                                               lwt 4551
```

```
      if( .not. interactive) then                                    lwt 4856
      end if                                                         lwt 4866

      CALL DATE(HDATE)                                               lwt 4876
      CALL GTIME(HTIME)                                              lwt 4877

      if (irpt .eq. 1 .and. interactive) rewind(5)                   lwt 4878

      if (interactive) call update(anewvis,chngvis)                  lwt 4879

      900 STOP                                                       LWT 4885
*
*****************************************************************
*
      NEW Routine UPDATE:

      subroutine update(anewvis,chngvis)                             upd 1000
      common  /ifil/ird,ipr,ipu,npr                                  upd 1005
      common /dpdep/chngh2o,deltadp,deltadpnew                       upd 1010
      common /qlamda/newlam,wave1,wave2                              upd 1015
      common /radiom/gain,offset,delta                               upd 1020
      common /aerfac/scat,newscat,g                                  upd 1025
      common /reflect/chngalbedo,albedo                              upd 1030
      common /molscat/mscatfac,facmol                                upd 1035

      character*80 char                                              upd 1040
      logical chngvis,chngh2o,newlam,chngalbedo,newscat,mscatfac     upd 1045

      write(*,1)                                                     upd 1050
      1   format(/'New Visibility: ',$)                              upd 1055
      read(*,13,end=991) len,char                                    upd 1060
      13  format(q,a)                                                upd 1065
      if(len .gt. 0) then                                            upd 1070
      read(char,*) anewvis                                           upd 1075

      chngvis=.true.                                                 upd 1080
      end if                                                         upd 1085

      write(*,2)                                                     upd 1090
      2     format(/'Molecular Scatter Factor: ',$)                  upd 1095
      read(*,13,end=991) len,char                                    upd 2000

      if(len .gt. 0) then                                            upd 2010
      read(char,*) facmol                                            upd 2015
      mscatfac=.true.                                                upd 2020
      else                                                           upd 2025
      deltadp=0.0                                                    upd 2030
      end if                                                         upd 2035

      write(*,3)                                                     upd 2040
      3     format(/'New Lower Wavelength Limit: ',$)                upd 2045
      read(*,13,end=991) len,char                                    upd 2050
```

```
if(len.gt.0.and.char(1:1).ne.'B'.and.char(1:1).ne.'b')then          upd 2055
   gain=0.1e+10                                                     upd 2060
   offset=1.0                                                       upd 2065
   delta=1.0                                                        upd 2070
   read(char,*) wave2                                               upd 2075
   newlam=.true.                                                    upd 2080
   write(*,4)                                                       upd 2085
4     format(/' New Upper Wavelength Limit: ',$)                    upd 2090
   read(*,*) wave1                                                  upd 2095
end if                                                              upd 3000

if(len.gt.0.and.(char(1:1).eq.'B'.or.char(1:1).eq.'b'))then         upd 3005

if(char(2:2) .eq. '1') then                                         upd 3010
   gain=0.0602436                                                   upd 3015
   offset=0.15                                                      upd 3020
   wave2=0.45                                                       upd 3025
   wave1=0.52                                                       upd 3030
   delta=wave1-wave2                                                upd 3035
   newlam=.true.                                                    upd 3040
end if                                                              upd 3045


if(char(2:2) .eq. '2') then                                         upd 3050
   gain=0.1175036                                                   upd 3055
   offset=0.2804878                                                 upd 3060
   wave2=0.52                                                       upd 3065
   wave1=0.60                                                       upd 3070
   delta=wave1-wave2                                                upd 3075
   newlam=.true.                                                    upd 3080
end if                                                              upd 3085


if(char(2:2) .eq. '3') then                                         upd 3090
   gain=0.0805970                                                   upd 3095
   offset=-0.1194030                                                upd 3100
   wave2=0.63                                                       upd 3105
   wave1=0.69                                                       upd 3110
   delta=wave1-wave2                                                upd 3115
   newlam=.true.                                                    upd 3120
end if                                                              upd 3125


if(char(2:2) .eq. '4') then                                         upd 3130
   gain=0.0814399                                                   upd 3135
   offset=0.15                                                      upd 3140
   wave2=0.76                                                       upd 3145
   wave1=0.90                                                       upd 3150
   delta=wave1-wave2                                                upd 3155
   newlam=.true.                                                    upd 3160
end if                                                              upd 3165


if(char(2:2) .eq. '5') then                                         upd 3170
```

```
      gain=0.0108074                                                upd 3175
      offset=0.0370046                                              upd 3180
      wave2=1.55                                                    upd 3185
      wave1=1.75                                                    upd 3190
      delta=wave1-wave2                                             upd 3195
      newlam=.true.                                                 upd 3200
    end if                                                          upd 3205

    end if                                                          upd 3210

    write(*,5)                                                      upd 3215
    5     format(/'New H-G Phase Function G: ',$)                   upd 3220
    read(*,13,end=991)  len,char                                    upd 3225
    if(len .gt. 0) then                                             upd 3230
    read(char,*)  scat                                              upd 3235
    newscat=.true.                                                  upd 3240
    end if                                                          upd 3245

    write(*,6)                                                      upd 3250
    6     format(/'New Surface Albedo: ',$)                         upd 3255
    read(*,13,end=991)  len,char                                    upd 3260
    if(len .gt. 0) then                                             upd 3265
    read(char,*)  albedo                                            upd 3270
    chngalbedo=.true.                                               upd 3275
    end if                                                          upd 3280

    return                                                          upd 3285

    991     stop ' Interactive LOWTRAN Completed'                   upd 3290
    end                                                             upd 3295

*
*************************************************************************
*
    In Routine NSMDL:

    common  /acntrl/interactive,rh_mean                             nsm 216
    common /dpdep/chngh2o,deltadp                                   nsm 217
    logical chngh2o                                                 nsm 226

    IF (M.NE.0 .and. .not. interactive) WRITE(IPR,100)              NSM 340

    IF(M.EQ.0  .and..not.interactive)WRITE(IPR,90)H1,P(1,7),TMP,DP,RH,
                                                                    nsm 416
    X       WH(K,7),WO(K,7),RANGE                                   NSM 420

    if(chngh2o) then                                                nsm 441
    dp=dp+deltadp                                                   nsm 442
    end if                                                          nsm 443

    if( .not. interactive) then                                     nsm 446
    end if                                                          nsm 456

    IF(ML.LT.20 .and. .not. interactive) WRITE (IPR,903)            NSM 985
```

```
      IF(ML.GE.20 .and. .not. interactive) WRITE (IPR,900)                NSM 995

      if( .not. interactive) then                                         nsm 1001
      end if                                                              nsm 1006

      if( .not. interactive) then                                         nsm 1114
      WRITE(IPR,915)Z(KK),P(KK,7),T(KK,7),RELHUM(KK),WH(KK,7),WO(KK,7),
                                                                          NSM 1115
      end if                                                              nsm 1121

      IF(MODEL.EQ.0 .and. .not. interactive) WRITE(IPR,903)               NSM 1160

*
*****************************************************************
*
      In Routine STDMDL:

      common  /acntrl/interactive,rh_mean                                 std 196

      if( .not. interactive) then                                         std 656
      end if                                                              std 711

*
*****************************************************************
*
      In Routine DRYSTR:

      common  /acntrl/interactive,rh_mean                                 dry 166

      if( .not. interactive) then                                         dry 186
      end if                                                              dry 191

*
*****************************************************************
*
      In Routine GEO:

      common  /acntrl/interactive,rh_mean                                 geo 241

      if( .not. interactive) then                                         geo 431
      end if                                                              geo 436

      if( .not. interactive) then                                         geo 881
      end if                                                              geo 886

      IF(NPR.NE.1 .and. .not.interactive)WRITE(IPR,44)J,ZP(LZ),TBBY(J),
     X        (WPATH(J,KMOL(K)),K=1,8)                                    GEO 965

      IF(NPR.NE.1 .and. .not. interactive) WRITE(IPR,46)                  GEO 980

      IF(NPR.NE.1 .and. .not. interactive) WRITE(IPR,48) J,ZP(LZ),        geo 1026
     X        (WPATH(J,KMOL(K)),K=9,15)                                   GEO 1030

      if( .not. interactive) then                                         geo 1051
```

```
      end if                                                          geo 1056

      rh_mean=w(15)                                                   geo 1106

      if( .not. interactive) then                                     geo 1116
      end if                                                          geo 1121

*
*****************************************************************
*
      In Routine GEOINP:

      common  /acntrl/interactive,rh_mean                             gin 196

      IF(NPR.NE.1 .and. .not. interactive) WRITE(IPR,10)              GIN 235

      IF(NPR.NE.1 .and. .not. interactive) WRITE(IPR,12)              GIN 275

      IF(NPR.NE.1 .and. .not. interactive) WRITE(IPR,16)              GIN 340

      IF(H2.LT.H1.AND.ANGLE.GT.90.0.AND.NPR.NE.1.and. .not. interactive)
     X       WRITE(IPR,15) LEN                                        GIN 360

      IF(NPR.NE.1 .and. .not. interactive) WRITE(IPR,18)              GIN 440

      IF(NPR.NE.1 .and. .not. interactive) WRITE(IPR,17) RANGE        GIN 495

      IF(NPR.NE.1 .and. .not. interactive) WRITE(IPR,19)              GIN 560

      IF(NPR.NE.1 .and. .not. interactive) WRITE(IPR,20)
      H1,H2,ANGLE,
     X      PHI,HMIN,LEN                                             GIN 670

*
*****************************************************************
*
      In Routine REDUCE:

      common  /acntrl/interactive,rh_mean                             rdu 166

      if( .not. interactive) then                                     rdu 236
      end if                                                          rdu 241

*
*****************************************************************
*
      In Routine FDBETA:

      common  /acntrl/interactive,rh_mean                             bet 141

      IF(NPR.NE.1 .and. .not. interactive) WRITE(IPR,24)              BET 290

      IF(NPR.NE.1 .and. .not. interactive) WRITE(IPR,26)ITER,ANGLE1,
     X BETA1,DBETA,RANGE,HMIN,PHI,BENDNG                             BET 360
```

```
      IF(NPR.NE.1 .and. .not. interactive) WRITE(IPR,26)ITER,ANGLE2,
     X BETA2,DBETA,RANGE,HMIN,PHI,BENDNG                          BET 445

      IF(NPR.NE.1 .and. .not. interactive) WRITE(IPR,26)ITER,ANGLE3,
     X BETA3,DBETA,RANGE,HMIN,PHI,BENDNG                          BET 520

      IF(NPR.NE.1 .and. .not. interactive) WRITE(IPR,45)           BET 645

      IF(NPR.NE.1 .and. .not. interactive) WRITE(IPR,46)H1,H2,BETA,ITER,
     1     ANGLE1,BETA1,ANGLE2,BETA2,ANGLE3,BETA3                  BET 680

*
*****************************************************************
*
      In Routine FNDHMN:

      common  /acntrl/interactive,rh_mean                          hmn 186
      IF(ISSGEO.NE.1 .and. .not. interactive) WRITE(IPR,22) H1,ANGLE   HMN 515

*
*****************************************************************
*
      In Routine RFPATH:

      common  /acntrl/interactive,rh_mean                          pth 196

      IF(IAMT.EQ.1 .AND. NPR.NE.1 .and. .not. interactive)WRITE(IPR,20)  PTH 280

      IF(IAMT.EQ.1 .AND. NPR.NE.1 .and. .not. interactive) then    pth 471
      WRITE(IPR,24)  HLOW(IHLOW)                                   PTH 475
      end if                                                       pth 476

      IF(IAMT.EQ.1 .AND. NPR.NE.1 .and. .not. interactive) then    pth 571
      WRITE(IPR,22)   J,ZP(J),ZP(J+1),                             PTH 575
      end if                                                       pth 581

      IF(IAMT.EQ.1 .AND. NPR.NE.1 .and. .not. interactive) then    pth 641
      WRITE(IPR,26) S,BETA,BENDNG                                  PTH 645
      end if                                                       pth 646

      IF(IAMT.EQ.1 .AND. NPR.NE.1 .and. .not. interactive) then    pth 786
      WRITE(IPR,28)  HLOW(IHLOW),                                  PTH 790
      end if                                                       pth 796

      IF(IAMT.EQ.1 .AND. NPR.NE.1 .and. .not. interactive) then    pth 871
      WRITE(IPR,22)   J,ZP(J),ZP(J+1),                             PTH 875
      end if                                                       pth 881

*
*****************************************************************
*
      IN ROUTINE TRANS:
```

```
      common  /acntrl/interactive,rh_mean                              tra 302
      common /dpdep/chngh2o,deltadp,deltadpnew                         tra 303
      common  /radiom/gain,offset,delta                                tra 304
      common  /aerfac/scat,newscat,g                                   tra 304A
      common  /molscat/mscatfac,facmol                                 tra 304B

      if( .not. interactive) then                                      tra 556
      end if                                                           tra 576

      sum=sum-tx(6)                                                    tra 1016
      tx(6)=tx(6)*facmol                                               tra 1017
      sum=sum+tx(6)                                                    tra 1018

c
cc    if (ipath .eq. 3) then                                           tra 1046
cc
      tx(7)=tx(10)+(   tx(7)-tx(10)   )*scat                           tra 1047
cc    end if                                                           tra 1048
c
      if( .not. interactive) then                                      tra 1241
      end if                                                           tra 1246

      if( .not. interactive) then                                      tra 1306
      end if                                                           tra 1311

      if( .not. interactive) then                                      tra 1426
      end if                                                           tra 1436

      if( .not. interactive) then                                      tra 1496
      end if                                                           tra 1501

      if( .not. interactive) then                                      tra 1581
      else                                                             tra 1586
      write(ipr,742)   1.0e+4/iv2,1.0e+4/iv1                           tra 1587
      742       format(' Wavelength Region: ',f8.4,' to ',f8.4,' Microns'//)  tra 1588
      WRITE(IPR,741)  vis,rh_mean,AB,facmol                            tra 1589
      end if                                                           tra1589A

      if( .not. interactive) then                                      tra 1591
      else                                                             tra 1596

      radsum2=radsum*1.2464-1.537e-5                                   tra 1597

      WRITE(IPR,751)  RADSUM,nint((radsum*1000./delta-offset)/gain),   tra 1598
      &          RADSUM2,nint((radsum2*1000./delta-offset)/gain),     tra 1599
      &    g                                                           tra1599A
      end if                                                           tra1599B

      741  FORMAT(/' Visibility=',f10.4,10X,'Average Humidity %=',f10.4/ tra 1811
      1       ' Average Transmittance =',F6.4,                         tra 1812
      2         8x,'Last Molecular Scatter Factor=',f10.4)              tra 1813
      751 FORMAT(' Integrated radiance = ',1PE10.3,                    tra 1836
      X         'Watts CM-2 Ster-1',/,' TM Counts = ',i4/,             tra 1837
      X       'Rescaled Integrated radiance = ',1PE10.3,               tra 1838
```

```
      X        'Watts CM-2 Ster-1',/,' TM Counts = ',i4,                tra 1839
      X      5x,'Last H-G Phase G: ',0pf6.2)                            tra1839A

*
*****************************************************************
*
      In Routine SSGEO:

      common  /acntrl/interactive,rh_mean                              ssg 226

      if( .not. interactive) then                                      ssg 336
      end if                                                           ssg 341

      if( .not. interactive) then                                      ssg 381
      end if                                                           ssg 386

      if( .not. interactive) then                                      ssg 416
      end if                                                           ssg 421

      if( .not. interactive) then                                      ssg 616
      end if                                                           ssg 626

      if( .not. interactive) then                                      ssg 831
      end if                                                           ssg 841

      if( .not. interactive) then                                      ssg 906
      end if                                                           ssg 916

      if( .not. interactive) then                                      ssg 1136
      end if                                                           ssg 1146

*
*****************************************************************
*
      In Routine RDNSM:

      common  /acntrl/interactive,rh_mean                              rdm 126
      if( .not. interactive) then                                      rdm 136
      end if                                                           rdm 141
```

LOWHGP Interactive Screen:

```
      ***** INTERACTIVE LOWTRAN 6 *****          24-SEP-88  10:13:47

Wavelength Region:  0.4500 to  0.5200 Microns


Visibility=  25.0000          Average Humidity %=  31.5097
Average Transmittance =0.5886         Last Molecular Scatter Factor=    1.0000
Integrated radiance =  3.023E-04   Watts CM-2 Ster-1
TM Counts =  74
Rescaled Integrated radiance =  3.615E-04   Watts CM-2 Ster-1
TM Counts =  88    Last H-G Phase G:  0.15
BOUNDARY TEMPERATURE =     0.00 K
BOUNDARY EMISSIVITY =     1.000

New  Visibility: 24.3

Molecular Scatter Factor:  1

New Lower Wavelength Limit:  B4

New H-G Phase Function G:

New Surface Albedo:


 Interactive LOWTRAN Completed
```

6.7 APPENDIX G Atmospheric Correction Programs

Programs: CORRECT_ATMOS
LINFUNC

```
*****************************************************************
*
*       Program correct_atmos
*
*       Program to apply the atmospheric correction look-up tables that
*       are created using the LOWHGP program
*
*       The program requires the following as input:
*       1) The input image to be corrected
*       2) The TM band number of the input image
*       3) The Band 4 Water region mask image
*       4) The atmospheric correction look-up table
*       5) A file name for the corrected image
*
*       Author:         John Francis
*
*****************************************************************
      real*4   tmpvec(8440),gain(4),offset(4),delta(4)
      real*4   tau(256),lu(256),multiplier
      integer*4  itemp,outrec
      byte   inbuff(8440),b4buff(8440),   outvec(8440),it(4)
      character*80   infile,outfile,lbuff,lutfile,refile

      equivalence ( itemp,it(1) )

*****************************************************************
*
*       Conversion Gain Factors for each band 6/22/84
*
*****************************************************************
      gain(1)=0.0602436         !0.15
      gain(2)=0.1175036         !0.2804878
      gain(3)=0.0805970         !0.1194030
      gain(4)=0.0814399         !0.15

*****************************************************************
*
*       Conversion Offset Values for each band 6/22/84
*
*****************************************************************
      offset(1)=-0.150000               !0.0602436
      offset(2)=-0.2804878              !0.1175036
      offset(3)=-0.1194030              !0.0805970
      offset(4)=-0.1500000              !0.0814399

*****************************************************************
*
*       Bandpass Widths for the TM Channels
*
*****************************************************************
      delta(1)=0.52-0.45
      delta(2)=0.60-0.52
      delta(3)=0.69-0.63
      delta(4)=0.90-0.76
```

```
*****************************************************************
*
*       Get input information
*
*****************************************************************
      type441
      441   format(/' *** Apply LOWTRAN 6 Corrections to LANDSAT-5 TM ***'/)
      type1
      1     format(/' Input image file to be corrected> ',$)
      accept13, lenin,infile
*
      inquire(file=infile,recl=outrec)
      type81, outrec
      81    format(/10x,'This Image Has ',i4,' Pixels Per Line')

      type11
      11    format(5x,'Image Band Number> ',$)
      accept*, iband

      type71
      71    format(/' Atmospheric reference image file> ',$)
      accept13, lenref,refile

      inquire(file=refile,recl=outrec)
      type81, outrec


      type2
      2     format(/' Output image file> ',$)
      accept13, lenout,outfile
      13    format(q,a)

      type3
      3     format(/' Atmospheric Look-Up Table File> ',$)
      accept13, lenlut,lutfile

*****************************************************************
*
*       Open the image files
*
*****************************************************************
      open(1,file=infile,
     +           form='unformatted',status='old',
     +           recordtype='fixed',recl=outrec/4)
*
      open(2,file=outfile,
     +           form='unformatted',status='new',
     +           recordtype='fixed',recl=outrec/4)
*
      open(4,file='scratchfile.tmp',form='unformatted',status='new',
     +           recordtype='fixed',recl=outrec/4,disp='delete')
*
      open(3,file=lutfile,status='old')
```

```
*
      open(7,file='correct_atmos.out',status='new')
*
      open(8,file=refile,
     +            form='unformatted',status='old',
     +            recordtype='fixed',recl=outrec/4)
*****************************************************************
*
*     Read in the atmospheric look-up data
*
*****************************************************************
      do i=1,255
            read(3,*,end=990)  lu(i),tau(i)
      enddo
      990   lutsize=i-1
*****************************************************************
*
*     Fill out the look-up table to 255 with the last value
*
*****************************************************************
      do i=lutsize+1,255
            tau(i)=tau(lutsize)
            lu(i)=lu(lutsize)
      enddo
*****************************************************************
*
*     Apply the atmospheric correction look-up table
*
*****************************************************************
      sum1=0.0
      sum2=0.0
      sumsq1=0.0
      sumsq2=0.0
      pts=0.0
      ineg=0

      do i=1,3000
            if (mod(i,100) .eq. 0) then
            type91,i
      91          format('+Line  ',i5)
            end if

            read(1,end=991)  (inbuff(j),j=1,outrec)
            read(8,end=991)  (b4buff(j),j=1,outrec)

            do j=1,outrec
*****************************************************************
*
*     Convert from byte pixel counts to real*4 radiance units
*
*****************************************************************
```

```
            it(1)=b4buff(j)     ! DC for reference image
            ipoint=itemp  !     convert to pointer for atmospheric LUT
            itemp=0

            it(1)=inbuff(j)     ! DC for image to correct

*****************************************************************
*
*       Ignore pixels in water map image set to 255
*
*****************************************************************
            if (itemp .ne. 0) then              ! ignore fill pixels

            if(ipoint .ne. 255) then

*****************************************************************
*
*       Over water - correct pixel radiance for atmosphere
*
*****************************************************************
            atemp=(float(itemp)*gain(iband)+offset(iband))
      &     /1000.0*delta(iband)
            tmpvec(j)=atemp-lu(ipoint)

            if( tmpvec(j) .lt. 0.0 ) then
            tmpvec(j)=0.0
            ineg=ineg+1
            end if

            tmpvec(j)=tmpvec(j)/tau(ipoint)

            else

*****************************************************************
*
*       Over land - replace pixel with the original value
*
*****************************************************************
            tmpvec(j)=(float(itemp)*gain(iband)+offset(iband))
      &     /1000.0*delta(iband)

            end if

*****************************************************************
*
*       Compute some statistics on the original and corrected images
*
*****************************************************************
            sum1=sum1+atemp
            sumsq1=sumsq1+atemp**2
            sum2=sum2+tmpvec(j)
            sumsq2=sumsq2+tmpvec(j)**2
            pts=pts+1.0
```

```
            end if
            end do

*****************************************************************
*
*       Save record in a temporary file for now, just in case it's very big
*
*****************************************************************
            write(4)  (tmpvec(k),  k=1,outrec/4)
            write(4)  (tmpvec(k),  k=outrec/4+1,outrec/2)
            write(4)  (tmpvec(k),  k=outrec/2+1,outrec*3/4)
            write(4)  (tmpvec(k),  k=outrec*3/4+1,outrec)

      end do

*****************************************************************
*
*       Compute the before and after statistics
*
*****************************************************************
      991   nlines=i-1

      avg1=sum1/pts
      std1=sqrt(  (pts*sumsq1-sum1*sum1)/(pts*(pts-1.0))  )
      avg2=sum2/pts
      std2=sqrt(  (pts*sumsq2-sum2*sum2)/(pts*(pts-1.0))  )

      adder=avg1-avg2
      if(std2  .gt.  0.0)  multiplier=std1/std2

*****************************************************************
*
*       Make a report to the user of the stats etc.
*
*****************************************************************
      write(7,770)  infile(1:lenin),outfile(1:lenout),
      &     refile(1:lenref),lutfile(1:lenlut)
      770   format(20x,'*****************************'/
      &     20X,'*** CORRECT_ATMOS OUTPUT ***'/
      &     20x,'*****************************'//
      &     /10x,'Image To Be Corrected:        ',a<lenin>/
      &     10x,'Output Image:   ',a<lenout>/
      &     10x,'Reference Image:        ',a<lenref>/
      &     10x,'Atmospheric Look-Up Table File: ',a<lenlut>//)

      write(7,773)  avg1,std1,avg2,std2,adder,multiplier,ineg,ifix(pts)
      773   format(/' Old and New Image Radiance Statistics'//
      &     ' Old Image Mean:      ',1pe12.4/
      &     ' Old Image Std Deviation:     ',1pe12.4//
      &     ' New Image Mean:     ',1pe12.4/
      &     ' New Image Standard Deviation:      ',1pe12.4//
      &     ' Difference in Means [Old-New]:     ',1pe12.4/
      &     ' Ratio of Std Deviations [Old/New]: ',0pf10.4//
      &     ' Negative Radiance Pixels [New]:     ',i8/
```

```
      &      ' Number Of Points:  ',i8//)
*****************************************************************
*
*     Read the entire corrected image from the temporary file
*
*****************************************************************
      ihi=0
      ilow=0
      iok=0

      rewind(4)

      do i=1,nlines
            read(4)  (tmpvec(k),  k=1,outrec/4)
            read(4)  (tmpvec(k),  k=outrec/4+1,outrec/2)
            read(4)  (tmpvec(k),  k=outrec/2+1,outrec*3/4)
            read(4)  (tmpvec(k),  k=outrec*3/4+1,outrec)
*****************************************************************
*
*     Remap radiance to 8-bit pixels using the TM calibration data
*
*****************************************************************
            do j=1,outrec
            itemp=(tmpvec(j)*1000./delta(iband)-offset(iband))/gain(iband)
*****************************************************************
*
*     Clip pixel counts to values between 0 and 255
*
*****************************************************************
            if( itemp .gt. 255) then
            outvec(j)=-1
            ihi=ihi+1
            else if (itemp .lt. 0) then
            outvec(j)=0
            ilow=ilow+1
            else
            outvec(j)=it(1)
            iok=iok+1
            end if

            end do
            write(2)  (outvec(k),  k=1,outrec)
      end do
*****************************************************************
*
*     Report on the number of pixels that had to be clipped
*
*****************************************************************
      type*
      type*,'Pixels  >255',ihi
```

```
      type*,'Pixels  <0       ',ilow
      type*,'Pixels  Ok       ',iok
      type*
*****************************************************************
*
*     Fill out to a 512x512 image for display
*
*****************************************************************
      do  j=1,outrec
            outvec(j)=0
      enddo

      do  i=nlines+1,512
            write(2)  (outvec(k),  k=1,outrec)
      enddo

            stop
      end
```

```
*****************************************************************
*
*       Program linfunc
*
*   Program to correct an input image for atmospheric transmittance
*    and path radiance, uniform over the entire image
*
*   The program expects a fractional transmittance value and an
*    upwelling path radiance value in digital count units appropriate
*    for the TM image band of interest
*
*   Author: John Francis
*
*****************************************************************
      integer*4  lu(256),itemp,outrec
      byte  inbuff(8440),b4buff(8440),  outvec(8440),it(4)
      character*80  infile,outfile,lbuff,lutfile,refile

      equivalence ( itemp,it(1) )

*****************************************************************
*
*        Get the input and output image file names and verify
*
*****************************************************************
      type1
  1   format(/' Input image file to be corrected> ',$)
      accept13,  lenin,infile
c
      inquire(file=infile,recl=outrec)
      type81, outrec
 81   format(/10x,'This Image Has ',i4,' Pixels Per Line')
c


      type2
  2   format(/' Output image file> ',$)
      accept13,  lenout,outfile
 13   format(q,a)

*****************************************************************
*
*        Get the transmittance and upwelling values to apply
*
*****************************************************************
      type3
  3   format(/' Atmospheric Upwell, Transmittance> ',$)
      accept*,  upwell,trans
```

```
*****************************************************************
*
*                  Open the image files
*
*****************************************************************
      open(1,file=infile,
     +       form='unformatted',status='old',
     +        recordtype='fixed',recl=outrec/4)
c
c
      open(2,file=outfile,
     +       form='unformatted',status='new',
     +        recordtype='fixed',recl=outrec/4)

*****************************************************************
*
*          Read a line of data from the input image file
*
*****************************************************************
      do  i=1,3000
        if (mod(i,100) .eq. 0) then
          type91,i
 91       format('+Line ',i5)
        end if

          read(1,end=991)  (inbuff(j),j=1,outrec)

*****************************************************************
*
*            Cycle through the pixels in the image line
*
*****************************************************************
        do j=1,outrec
c
          itemp=0
            it(1)=inbuff(j)    ! DC for image to correct

*****************************************************************
*
*       Correct each image pixel for transmittance and path radiance
*            Ignore pixels in water map image set to 255
*
*****************************************************************
          if (itemp .ne. 0) then              ! ignore fill pixels

              itemp=nint( (float(itemp)-upwell)/trans )
```

```
*****************************************************************
*
*              Clip results to fall within 0 to 255 range
*
*****************************************************************
              if (itemp .gt. 255) then
                inbuff(j)=-1
              else if (itemp .lt. 0) then
                inbuff(j)=0
            else
                 inbuff(j)=it(1)
             end if
            end if

          end do
*****************************************************************
*
*     Write out the corrected image line, and go get the next image line
*
*****************************************************************
            write(2)  (inbuff(k),  k=1,outrec)

         end do

  991           stop
         end
```